STATE SPACE MODELLING AND MULTIVARIABLE STOCHASTIC CONTROL OF A PILOT PLANT PACKED-BED REACTOR

STATE SPACE MODELLING AND MULTIVARIABLE STOCHASTIC CONTROL OF A PILOT PLANT PACKED-BED REACTOR

By

ARTHUR JUTAN, B.Sc. (Eng.), M.Eng.

A Thesis

Submitted to the Faculty of Graduate Studies

in Partial Fulfilment of the Requirments

for the Degree

Doctor of Philosophy

McMaster University

October, 1976

DOCTOR OF PHILOSOPHY
(Chemical Engineering)

McMASTER UNIVERSITY
Hamilton, Ontario

TITLE: State Space Modelling and Multivariable Stochastic Control of a Pilot Plant Packed-Bed Reactor

AUTHOR: Arthur Jutan B.Sc. (Eng.) (University of Witwatersrand)
M.Eng. (McMaster Univeristy)

SUPERVISORS: Dr. J.F. MacGregor, Dr. J.D. Wright

NUMBER OF PAGES: xvi, 243

ABSTRACT

This study is concerned with the multivariable stochastic regulatory control of a pilot plant fixed bed reactor which is interfaced to a minicomputer. The reactor is non-adiabatic with a highly exothermic, gaseous catalytic reaction, involving several independent species. A low order state space model for the reactor is developed starting from the partial differential equations describing the system. A parameter estimation method is developed to fit the model to experimental data. Noise disturbances present in the system are identified using two methods, and two alternative dynamic-stochastic state space models are obtained. Multivariable stochastic feedback control algorithms are derived from these models and are implemented on the reactor in a series of DDC control studies. The control algorithms are compared with each other and with a single loop controller. The best of the multivariable control algorithms is used to regulate the exit concentrations of the various species from the reactor and the results are compared to data.

ACKNOWLEDGEMENTS

The author wishes to thank all those who contributed to this work.

He is particularly indebted to:

His research directors, Drs. J.F. MacGregor and J.D. Wright for their encouragement and moral support throughout the course of this work.

His research colleague, Mr. J.P. Tremblay for his support on the experimental aspects of this work, as well as his help on the many mini-computer real time programming problems encountered.

All members of the Control Group at McMaster for their lively discussions and happy faces.

Mrs. Lillian Mogensen for her care and patience in typing this thesis.

McMaster University for providing financial assistance.

TO

Cheryll Rose

- My Best Friend
- My Lover
- My Wife

TABLE OF CONTENTS

LIST OF FIGURES

LIST OF TABLES

NOMENCLATURE

a	heat transfer area for catalyst, cm^2/g catalyst
$A_{ij}^{(n)}$	collocation weights for 1st derivative
$a_i(z,t)$	collocation trial function coefficents
A	nxn dynamic state matrix (5-20)
$\underline{a}(t)$	white noise sequence (5-34)
$\dot{\underline{a}}(\ )$	canonical white noise sequence (5-43)
B_i	Biot number $(\frac{h_w R}{\lambda_{er}})$
$B_{ij}^{(n)}$	collocation weights for Laplacian
$\bar{B}_{ij}$	derived collocation weights
B	backward shift operator (5-16)
B	control matrix (5-20)
C^i	concentration of species i, g moles/cc
$\bar{C}^i$	radial average concentration of species i, g moles/cc
$C_j^{\ i}$	concentration of species i at radial collocation point j
C_{P_s}	specific heat of solid, cal/(g°K)
C_{P_g}	specific heat of gas, cal/(g°K)
$\bar{C}$	specific heat term $[C_{P_s}\rho_B + C_{P_g}\rho_g\varepsilon]$, Equation (3-6)
D_{er}	effective radial diffusivity (based on empty reactor volume), cm^2/s
d_p	catalyst particle diameter, cm
$D_{ij}^{(n)}$	collocation weights, Equation (4-45)
E	reaction activation energy, cal/g mole
ex	subscript-exit conditions for reactor
$E[\cdot]$	expectation operator (5-13)

F	matrix for discrete state space model, Equation (4-56)
G_m	mass flow rate based on area of empty reactor, g /(cm^2. s)
G_o	superficial gas velocity, cm^3 gas/(cm^2 reactor. s)
G	control matrix, Equation (4-56)
h	heat transfer coefficient particle to fluid, cal/(cm^2°K s)
h_w	heat transfer coefficient at reactor wall, cal/(cm^2°K s)
H	mxn measurement matrix (5-20)
i	subscript-most commonly used for species number
I_m	m^{th} order unity matrix
K_∞	steady state Kalman gain matrix (6-14)
k	discrete time lag
L	reactor length, cm
L	mxm matrix for canonical non-singular transformation (Section 5.5.1)
L_∞	optimal steady state feedback gain matrix (6-8)
$N_{Pe_{m,r}}$	Peclet number for radial mass transfer $(\frac{G_m d_p}{\rho D_{er}})$
$N_{Pe_{m,z}}$	Peclet number for axial mass transfer $(\frac{G_m d_p}{\rho D_{ez}})$
$N_{Pe_{h,r}}$	Peclet number for radial heat transfer $(\frac{G_m C_p d_p}{\lambda_{er}})$
N_{Re}	Reynolds number for particles $(\frac{G_m d_p}{\mu})$
(n), n	order of collocation approximation
n'	order of state space model, $(n' = n + 1)$ (4-51)
$\underline{N}(t)$	residual noise vector (5-6)
$\dot{\underline{N}}(t)$	canonical noise vector (5-43)
$\hat{\dot{N}}(t,1)$	one step ahead forecast for canonical noise vector (5-37)

o	subscript indicating centre axial conditions
$P_i(r^2)$	orthogonal polynomial symmetric in r
$P(\cdot)$	conditional covariance matrix (6-15)
r	radial distance in reactor (normalised)
r_j	radial collocation point j
R	radius of reactor bed, cm
R^i	net reaction rate for species i, moles i/(g catalyst s)
R_i	reaction rate for reaction i, moles i/(g catalyst s)
Rw	variance covariance matrix for $\underline{w}(t)$ (5-13)
Rv	variance covariance matrix for $\underline{v}(t)$ (5-13)
$\underline{s}(t)$	state variable (5-21)
T	homogeneous gas/solid temperature, Equation (3-5), °K
T_j	temperature at radial collocation point j °K
T_o	temperature along centre axis of reactor, °K
T_w	temperature of reactor wall, °K
T_g	gas temperature, Equation (3-3), °K
T_s	solid (catalyst) temperature, Equation (3-4), °K
t	time: continuous (sec); discrete (minutes)
$\underline{u}$	vector of manipulated variables
v_T	thermal wave velocity $\frac{G_o C_{P_g} \rho_g}{L\bar{C}}$, cm/(s.cm)
v_C	concentration wave velocity $\frac{G_o}{\varepsilon L}$, cm/(s.cm)
$\underline{v}(t)$	white measurement noise sequence (5-12)
$V[\cdot]$	variance operator (5-37)

$w_i^{(n)}$	collocation quadrature weights
$\underline{w}(t)$	white generating noise sequence (5-11)
$\underline{x}(t)$	state vector at sample time t
$\dot{\underline{x}}$	time derivative of state vector (continuous)
$\hat{\underline{x}}(t/t)$	state estimate (simultaneous) of $\underline{x}$
$\underline{y}$	vector of output variables
z	axial distance along reactor (normalised)
λ_{er}	effective radial thermal conductivity,cal/(cm°K s)
ρ_B	bulk density of catalyst,g/cc
ρ_g	gas density,g/cc
Δh_i	heat of reaction for reaction i,cal/g mole
ε	void fraction,cm^3 gas in voids/cm^3 empty reactor
∇^2	Laplacian operator
β_{ij}	derived collocation weights
β	parameter vector
Δ	prefix for deviation variable about steady state or operating point.example, $\Delta C_o = C_o - C_o$(steady state)
∇^d	d^{th} difference operator
ϕ	mxm autoregressive matrix of parameters (5-19)
$\sum$	mxm variance-covariance matrix of $\underline{a}(t)$ (5-27)
$\Gamma(k)$	auto covariance matrix at lag k (5-28)
$\Gamma_x(0)$	auto covarinace of x at lag 0
λ	generalised eigenvalue (5-38)
μ	generalised eigenvalue (5-39)
Λ	ratio of generalised variances (5-48)

χ^2_{2m}	Chi-squared distribution with 2m degrees of freedom (5-49)
σ	standard deviation
∞	subscript infinity refers to steady steady value
$'$	denotes transpose of matrix or vector, e.g., $\underline{a}'(t)$
$-$	denotes vector, e.g., $\underline{N}(t)$
$\hat{}$	denotes estimate, e.g., $\hat{D}(\underline{\beta})$
$\cdot$	denotes derivative with respect to time, e.g., $\dot{\underline{x}}$; denotes canonical variate, e.g., $\dot{\underline{N}}(t)$

CHAPTER 1

OBJECTIVES OF THIS STUDY

There are very few reported practical implementations of modern multivariable control theory to complex chemical processes. Most studies appear to be confined to systems such as distillation columns, evaporators, boilers, paper machines, etc., which are generally easily modelled. Applications to tubular reactors have been largely by-passed due to modelling complexities, particularly because these reactors often require partial differential equations to adequately describe their dynamics. Indeed, to this author's knowledge, no experimental applications of multivariable control theory to these reactors have been published. Because of a lack of practical application studies, a large gap exists between modern control theory and its use in the complex control problems often found in industry. The objective of this study is to narrow this gap, by developing and implementing a multivariable stochastic control scheme on a pilot plant, non-adiabatic, packed-bed catalytic reactor. A low order state space model suitable for on-line control of the reactor is developed. This model is then fitted to experimental dynamic data using a parameter estimation method. Stochastic feedback controllers are derived from the fitted model and implemented on the reactor in a series of direct digital control (DDC) studies using a minicomputer.

The reaction (hydrogenolysis of butane over a nickel catalyst)

is a complex series-parallel type, involving several species and is highly exothermic. The equations describing the dynamics of the reactor are highly non-linear and represent a considerable challenge in developing a model suitable for control.

In Chapter 2, some of the overall gaps in the application of modern control theory to chemical processes are discussed with reference to leading workers in the field. A review of the present state of the art in the modelling of fixed bed reactors is given.

In Chapter 3, a mathematical model for the fixed bed reactor is developed. This forms the basis for the simpler models that are eventually used for on-line control.

In Chapter 4, the mathematical model is simplified in two stages. First, a high order state space model for simulation studies is developed, followed by a low order state space model, suitable for on-line DDC studies.

In Chapter 5, we discuss the problems of fitting this low order state model to dynamic data, obtained from the reactor.

In Chapter 6, multivariable stochastic control algorithms are derived from the state model. These algorithms are implemented on the reactor in a series of control studies.

Chapter 7 discusses the significance of this work and possible extensions of it.

This study is intended to provide the ground work for a series of future application studies on the reactor with a view to encourage the application of modern control theory to industrial reactor control problems.

CHAPTER 2

INTRODUCTION AND LITERATURE REVIEW

2.1 Control of Chemical Processes

Many workers in the area of process control readily acknowledge that there is a wide gap between the theory of process control and its application to the chemical industry. Some contend that the theoreticians are far ahead of those who apply the theories and it is simply a question of catching up.

Recently there have been some strong comments on the state of modern control theory. Two leading groups of workers in the field were selected for their especially enlightening remarks and their suggestions for new directions in modern control theory.

(1) Foss

(2) Weekman and Lee.

(1) Foss

Foss (F8) in a critique of chemical process control theory presents a strong case against modern control theory and contends that it still has some rugged terrain to cover before it can be of some use in solving the complex control problems often found in the chemical process industry.

Foss begins by emphasising the complex non-linear interactions present in a typical reaction system. Often it is not possible or

economical to measure all the relevant variables of the system and even if we could, all measurements would be subject to random and systematic errors. The crucial step, Foss proposes, is the design of a control configuration. From our complex interacting system, we should determine what inputs should be manipulated, which variables should be measured and what connection should be made between these two sets of variables - a difficult problem, which has been tackled almost wholly qualitatively in the past with heavy reliance on previously successful configurations.

Information needed for design of a control system concerns both static and dynamic characteristics of the system. Some control systems have been designed using only static information; however, for rational design, dynamic characteristics are required. The problem occurs in the quantitative characterisation of chemical process dynamics. This is often extremely difficult and time consuming. It is also true that for the purposes of control, a detailed description of the dynamics is impractical and unnecessary and only the dominant dynamic characteristics need be included in process control models. What Foss fails to emphasise though, is the fact that it is almost impossible, a priori, to decide what constitutes "dominant dynamics". Obviously we require the "bare bones" equations that constitute our simple model, but then we begin the process of adding terms to our model; terms which we feel describe or give rise to significant dynamic effects. Even for a particular process, there are no guidelines as to whether the inclusion of an extra dynamic effect (if this can be done without overly complicating the model) will, in fact, significantly improve the quality of control.

In other words, the question: "can we improve the quality of control by improving our models?" remains unanswered.

Foss proceeds to discuss briefly the success (or lack of it) of various control theories in the process control industry. In spite of all the research effort put into multivariable control theory over the past decade or so, most processes today are still controlled by more or less isolated single loops and occasionally cascade loops even though the systems are inherently multivariable.

Single loop methods are nevertheless inadequate for the treatment of dynamically interacting multivariable systems. A theory of non interacting control (Gould (G1)) was proposed; it attempted to reduce the multivariable control problem to a set of single loop controls. Here inputs are manipulated in such a way as to affect only one output at a time. This technique, borrowed from the aerospace literature has seen limited success. If the system under control is weakly interacting in nature (as in the control of an aircraft) then this technique has some success. However, most chemical processes are highly interactive and it is, in a sense, unnatural to force the control model to be non-interactive, simply because it is difficult to design interactive control schemes. Rather than eliminating interaction, it should be exploited to achieve better control.

A method which does exploit interactions is the method of Modal Control introduced by Rosenbrock (R1) more than a decade ago. He proposed that the rate of response of the natural modes (eigenvector-eigenvalue pairs of the state matrix) could be controlled by choosing

a suitable feedback gain matrix which, in effect, shifted the poles of the system. In theory, this idea can provide rapid and stable control but in practice, the ability to measure only a few of the states results in confounded estimates of modal dynamics causing the control to degenerate rapidly.

The theory of optimal control, although it held many promises, led to many disappointments when it came to applying the techniques in industry. Engineers soon realised that the word "optimal" carried no global significance, and a performance index that is optimal for one process may be totally without merit for another. Hence, the choice of an "Objective Function" to be optimised is of the utmost importance in the design of a controller. The widely used quadratic performance criterion was chosen primarily because it simplified the mathematics of the optimal control problem.

A more serious problem of this theory is that it assumes one has perfect knowledge of both the process model and its parameters, and that there is no "noise" in the system. This fact was sufficient to explain why so many computer control simulations work well, while the same control when implemented on the actual process has limited success.

There have been attempts to include noise in mathematical models and to take account of measurement errors and lack of measurement of all states through the use of Luenberger Observers and Kalman-Bucy state estimators and this will be discussed later.

Foss concludes by stating quite clearly that chemical engineers have been working on the wrong problems and only a dent has been made into the significant fundamental problems of chemical process control.

Foss enumerates some central problems to be solved:

(1) Theory for determination of a control system structure: what and how many variables should be measured, with how much accuracy; what inputs should be manipulated; how should the inputs be connected to the outputs?

(2) A practical way of formulating low order models of large multivariable systems.

(3) Parameter estimation in control models.

(4) Development of adaptive strategies to account for changing process variables.

(5) More meaningful formulation of control objective functions.

(6) The study of more complex chemical systems and a break away from the past trend to confine studies to "text book" cases borrowed from the aerospace industry.

A few other areas of endeavour may be pinpointed:

(7) Studies concerning the relation between complexity of a model and the quality of control that is derived from these models.

(8) Problems associated with applying present day multivariable control theory (which applies mainly to systems described by sets of ordinary differential equations) to systems described by partial differential equations.

This last point, the author believes, was a great shortcoming when state space control theory was "borrowed" by chemical engineers from the aerospace industries, and then applied to chemical processes, which are often only adequately (even for the purposes of control) described by partial differential equations.

(2) Weekman and Lee

Weekman and Lee (L1), in a recent publication, present some bold statements concerning advanced control practice in the chemical process industry.

Firstly their topic is refreshing, in that their emphasis is on the control of reactors and this represents a break away from the emphasis on the control of distillation, evaporation, or adsorption columns so prevalent in the literature, Fisher (F9), Shinsky (S2).

Weekman (L1) agrees readily with the views expressed by Kestenbaum et al. (K1) and Foss (F8) on the shortcomings of advanced control theory; however, he goes a lot further by giving some economic perspective to the type of problems being solved by academics versus the actual problems that confront the practitioners in the petrochemical industries.

Weekman supports his arguments using an example of a catalytic cracking plant which includes a coupled reactor-regenerator system. The conventional control of this system had been arrived at by distilled experience of many years of operation. After a theoretical study by Kurihara (K3) using simple processes models, it was demonstrated that the reactor could be well controlled by controlling the regenerator.

This novel scheme was later implemented and patented by Mobil Research.

Weekman points to the lack of good process models. He maintains though, that a complete and perfect model is not only impossible but not even necessary. He advocates the "Principle of Optimum Sloppiness" suggested by Prater: "Obtain a reasonably good model that accounts for major process variable effects and dominant dynamics". He does, however, strongly believe that the current state of the art in model building for the process industry has room for considerable improvement [Weekman (W1)]. Simplified models of complex processes are frequently inadequate and lead to erroneous process control design. This comment appears to address itself to one of the questions posed by the author while discussing Foss's (F8) critique above. Namely, does an improved process model lead to better control?

Weekman presents some rather disturbing revelations (at least for the petroleum industry) concerning the economic incentives to process control which he divides into three categories:

(1) Major benefits result from moving the steady state operation to a better operating point.

(2) Additional benefits (but significantly less than (1) above) result from improving the tightness of regulatory control about a set point.

(3) Minor benefits obtained by controllers which concentrate on fast response to set point changes with minimum excursion from some change-over profile.

Although Weekman does not use the term specifically, he implies that the petroleum industry has much more use for servo controllers than regulators. He continues to emphasise the need for better process models and this is understandable since during servo operation (start-up, shut-down or simply changing to new operating conditions) the process is operating over a wide range of conditions. This implies that any model which purports to describe the process must be valid over this same wide range.

Many complex processes are non-linear and for the application of most of modern control theory, models are usually linearised about a single operating point. Thus, their validity is restricted to within some area around this operating point. Any servo control scheme would therefore have to use the non-linear model for control design - a formidable theoretical problem for single variable control problems, let alone a multivariable servo control scheme. It is no wonder that most (if not all) start-ups and shut-downs are conducted manually in the process industry. The demands on a process model to cover such a wide range of operating conditions are for the moment very difficult to meet, nevertheless, this does point to the directions of greatest challenge.

Some of Weekman's remarks are, however, confined to the analysis of problems typical of the oil industry where specifications on product compositions may not be as critical as in other industries.

In the polymer and paper making industries, there are well documented examples (Aström (A2)) where improved quality of regulatory control has had a considerable effect on profitability. In these

processes, regulatory control is of primary importance. Other examples include any situation where operation close to a economic or safety constraint is required.

Weekman presents an interesting discussion on some difficulties of implementing a control scheme:

(1) The control scheme although designed for an isolated unit should take into account the rest of the plant as well.

(2) The control scheme should take into account the actions of a human operator and safety considerations, since it is unlikely that a control scheme will be completely automated.

(3) The control should have the ability to be gradually integrated into the existing scheme and allow a smooth change from automatic to manual operation.

Weekman points to some new directions:

(1) Closer co-operation between the control theoreticians and process operators.

(2) Integration of the process design and process control configurations: Many control problems would be eliminated if proper design was carried out.

(3) A high priority for new techniques to aid modelling for the control of chemical processes.

(4) A systematic approach to difficulties encountered in implementation of advanced control to replace an existing control scheme.

2.2 Modelling of Fixed Bed Reactors

The chemical reactor, in particular, the fixed bed chemical reactor, represents one of the more complicated processes to model in chemical engineering. Of course, uppermost in one's mind when deriving a model for a reactor (or any other process for that matter) must be the purpose for which the model is to be used. Here, the purpose is to develop a model satisfactory for use in on line regulatory control of the reactor. This necessitates large simplifications to the current reactor models that are proposed in the literature. Most of the literature on reactor modelling is based on the assumption that the model is to be used for simulation or design (most of these models are usually steady state also). As a result, the models tend to be somewhat complex and in general, unsuitable for control. Nevertheless by examining the formulation of these complex models, one gains some insight into the important effects occurring in reactors and one is led to ideas for simplifying the models for the purposes of control.

2.2.1 Steady State Models

Beek (B1) provides excellent insight into the factors surrounding a complex model of a packed bed reactor. He begins by laying out his assumptions which may be summarised as

(1) Properties of the packed bed are homogeneous and vary smoothly over the bed.

(2) Under conditions in commercial practice, axial diffusion terms in heat and mass transfer are negligible in comparison to bulk flow terms.

(3) Heat transfer at the wall may be lumped to express conditions at the wall as

$$\frac{\partial T}{\partial r} = Bi(T_w - T) \quad \text{at } r = 1$$

(4) Eddy diffusion is dominant as long as the Reynolds number is not too low.

Beek discusses some of the difficulties associated with estimation of transport properties in packed bed reactors. The essence of his observations may be summarised as:

(1) The velocity profile in the radial direction is essentially flat except for a region close to the wall, where the profile can show a maximum.

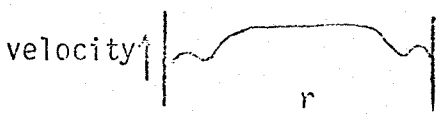

(2) The Peclet number for radial mass diffusion, $N_{Pe_{m,r}}$ is fairly constant at a value of 10, especially for Reynolds numbers greater than 80.

(3) The effective thermal conductivity (λ_{er}) is particularly difficult to estimate due to several measurement difficulties. The behaviour of the reactor is very sensitive to this parameter. Most correlations do not take into account a reaction system and apply only for reasonably large Reynolds numbers (> 40).

(4) The rate of heat transfer at the wall as characterised by the Biot number Bi, is very difficult to estimate. Correlations are hampered by the necessity of obtaining measurements

which rely on extrapolation of temperature profiles to the wall.

Finally, Beek discusses by means of an example, the numerical solution of his two-dimensional partial differential equations. It should be emphasised that Beek's treatment applies to a steady state analysis only.

Froment (F1) presents a comprehensive analysis and review of the field of fixed bed catalytic reactors. He classifies the current models in the literature into two basic types:

(a) Pseudo homogeneous models

(b) Heterogeneous models

where, in the heterogeneous models, the conditions of the solid are distinguished (and accounted for separately) from conditions in the fluid. Within each category, Froment considers steady state models of increasing complexity from a basic one-dimensional model, to a complex two-dimensional model which includes radial effects.

Froment (F2) addresses himself to the problems associated with the estimation of transport properties in fixed bed catalytic reactors. He notes that in spite of the complexity of the system, certain simplifying statements can be made for practical applications, namely: (1) the effective radial diffusivity (D_{er}) is relatively fixed by the observed fact that the radial mass Peclet number ($N_{Pe_{m,r}}$) for all practical purposes lies between 8 and 11. (2) in industrial applications, the axial heat conduction may be neglected compared to overall flow. Using an example of hydrocarbon oxidation, Froment looks at parametric sensitivity and concludes that profiles

in the reactor are insensitive to the mass transfer parameters but extremely sensitive to the heat transfer parameters; so sensitive, in fact, that the degree of precision in measurements required for current correlations is seldom achieved, and thus any predictions based on these correlations may have large errors.

In a more recent article, Froment (F3) reviews current findings in the literature and provides comments on a series of still unanswered questions in the modelling of reactors:

(1) If axial dispersion of heat and mass transfer were to significantly influence reactor profiles, extreme variations of temperature and concentration would have to occur over a few centimeters within a catalyst bed - a situation unlikely to occur in industrial situations.

(2) Because of high velocities encountered in industrial situations, differencesbetween solid and gas temperatures have been found to be small < 5°C. He does however, comment that no studies are available for transient conditions and the effect may be more important here.

(3) The existence of non-isothermal catalyst particles is unlikely.

(4) The possibility of multiple steady states have been excluded from a number of industrial reactors.

Hlavacek (H1) provides an excellent extension of Beek's (B1) work and points out some of the persisting problems associated with parameter estimates; especially for the heat transfer parameters. In particular, he comments that heat (and mass) transfer characteristics

are always obtained in the absence of chemical reaction and therefore correlations in the literature have limited validity when applied to reaction systems. Scatter in the prediction of heat transfer coefficients is still very high.

Hlavacek also considers some problems associated with the numerical integration of the reactor equations. He includes a discussion on non-linear least square estimation of kinetic and transport parameters where he talks about problems of parametric sensitivity and problems associated with temperature and concentration measurements.

A comprehensive work on the subject of parametric sensitivity in fixed bed reactors is presented by Carberry (C1). He studied the steady state behaviour of naphthalene oxidation and demonstrates the effect on predicted profiles of varying certain parameters in the reactor model. His main findings were that:

(1) The assumption of iso-thermal catalyst pellets is reasonable.

(2) Both radial and axial temperature profiles are sensitive to radial Peclet number for heat transfer ($N_{Pe_{h,r}}$) when it is varied within expected limits.

(3) Conversely, conversion and yield of product predicted by the model is insensitive to values of radial mass Peclet number ($N_{Pe_{m,r}}$).

(4) Both conversion and temperature profiles are drastically altered by relatively small variations in wall heat transfer coefficient and coolant temperature. This fact will cause considerable difficulty when trying to match model predictions to actual data.

Indeed, Carberry cautions against too much confidence in simulation studies due to problems of parameter estimation and sensitivity.

Butt and Weekman (B2) present a review of procedures for testing the relative effects of various transport phenomena occurring in heterogeneous packed bed systems. They divide these criteria into three groups, namely: Intraparticle effects, Interphase effects and Intrareactor effects.

Most (if not all) the criteria appear to apply to steady state effects and are limited to single reaction systems of a specific order. Also certain criteria require the estimation of parameters which themselves are hard to come by, thus causing them to be of limited usefulness.

2.2.2 Dynamic Models

All the above literature is concerned with steady state analysis and modelling of chemical reactors. There are a limited number of studies concerned with transient effects in packed tubular reactors. All the transient studies seen by the author neglect radial gradients. Inclusion of both axial and radial gradients for temperature and composition in a transient system would give rise to a set of three-dimensional partial differential equations which presents a very difficult computational problem.

In an interesting paper, Sinai and Foss (S1) consider an adiabatic packed bed reactor in which a non catalysed reaction occurs in the liquid phase of a solid liquid system. In their system, the

thermal and concentration wave velocities are of the same order of magnitude.

They vary the concentration and temperature inputs in a sinusoidal manner in such a way as to produce interference patterns between the concentration and thermal waves, producing constructive and destructive wave patterns which significantly influence the profiles within the reactors. This phenomena is probably limited to liquid-solid systems where the concentration and temperature wave velocities are of the same order of magnitude. In their paper the ratio of concentration to temperature wave velocity is about 0.5.

These phenomena are not expected to occur in reactors considered in the present work, where the wave velocity ratio is of the order of 1000.

Crider and Foss (C2) attempt to isolate the important factors affecting the dynamics of packed bed reactors. They conclude that the phenomena most important in transient studies are

(1) Thermal capacity of the packing which slows down the temperature wave.

(2) Resistance to heat flow between solid and fluid.

(3) Coupling of temperature and concentration effects due to reaction.

Unfortunately, all aspects of their results cannot be generalized to other systems in that they specifically studied a non catalytic liquid-solid system with small radial gradients, which they neglect in their analysis.

Crider and Foss (C3) use this same reactor under adiabatic conditions, where, by ignoring radial gradients and axial and radial diffusion, they obtain an analytical solution for a single first order reaction system.

Ferguson and Finlayson (F10) make an attempt to analyse the validity of the quasi steady state assumption often used in modelling dynamics of fixed bed reactors. By a judicious survey of models in the literature, they arrive at a set of criteria which they recommend to be used to test the validity of the quasi-steady state approximation. [The quasi-static approximation used for a gas-solid reactor system, may be described as follows: The response of the concentration profiles to say, a step input in flow, is very rapid. The temperature profiles respond much more slowly and their dynamics persist long after the rapid concentration dynamics have ended. The essential dynamics of the system thus appear to be governed by a slowly changing temperature profile coupled with concentration profiles which are always at steady state with these temperature profiles. Thus the concentration dynamics are ignored in comparison with the more enduring temperature dynamics]. An important criterion for fixed bed reactors, is the ratio of the heat to the mass wave velocities. Hansen (H2, H3) uses this ratio as a basis for neglecting the mass accumulation term.

They quote examples in the literature which show that the extra computational effort involved in solving the full dynamic equations (quasi-steady state not assumed) is anywhere between 60 to 100 times greater. This is due mainly to the fact that when the ratio of wave

velocities are very different from unity ($\sim$ 1400, in this study), the resulting differential equations are very stiff, thus requiring small time steps when being integrated.

2.2.3 Orthogonal Collocation in Chemical Reactor Theory

Since some of the original papers on orthogonal collocation applications to boundary value problems were published [Villadsen (V1)], there has been a tremendous interest in the application of collocation methods to the modelling of chemical reactors. One of the drawbacks of the complex reactor models being formulated today is the often intractable computational problems that result. The ability of collocation methods to provide workable approximate solutions to complex partial differential equations is seen as a great advantage by many workers.

Finlayson (F4) uses collocation to solve a set of partial differential equations (PDE's) describing radial temperature and concentration gradients in a reactor. He also shows how collocation may be used to express the PDE's as an approximate lumped set of ordinary differential equations. He shows how the equivalent lumped model is quite adequate for small Biot numbers (< 3.5). Larger Biot numbers imply that most of the resistance to heat transfer is in the bed itself (as opposed to being lumped at the wall) and a distributed model is required to adequately describe radial variations. This in turn, implies that higher order collocation approximations are required.

Finlayson (F5) presents a comprehensive summary of the application of collocation to chemical reaction engineering. This excellent

work first presents a summary of the general features of the method of collocation and then applies these techniques to a sulphur dioxide oxidation reactor and an ammonia reactor with counter-current cooling. Included in this paper is a detailed analysis of the importance of various transport phenomena effects in the modelling of packed bed reactors. The following is a summary of his analysis:

(1) The importance of Radial Dispersion of heat can be evaluated in terms of the Biot number for heat transfer at the wall. For large Biot number dispersion effects are marked (unless heat of reaction is very small).

(2) Axial Dispersion of heat is usually of relatively minor importance for fast flow reactors with small catalyst particles.

Finlayson uses Young and Finlayson's criterion (Y1) to determine whether axial dispersion of heat may be neglected. Mears (M1) criticises this criterion, pointing out that its derivation does not take into account radial temperature gradients.

(3) Finlayson quotes Mears' criteria (see Butt (B2)) for deciding whether the assumption of equal solid and fluid temperatures is reasonable. He criticises the criterion because it is based on reactor inlet conditions and instead suggests using an effectiveness factor obtained by solving the full set of reactor equations. The effectiveness factor, η, is defined as

$$\eta = \frac{R(\text{solid})}{R(\text{fluid})}$$

where R is the rate of reaction. η should be between $0.9 < \eta < 1.1$ to justify neglecting any temperature differences between solid and fluid. In practice, it would only be practical to compute η for simple systems.

(4) Internal resistance in catalyst pellet: If rate of diffusion is slow, significant concentration gradients can exist in the catalyst particle.

Ferguson (F6) uses collocation to reduce the computational burden for solving the transient equations that account for the diffusion of mass and energy within catalyst particles.

In his book, Finlayson (F7) devotes an entire chapter to the application of collocation to chemical reactors. Hansen (H2) uses collocation to integrate the transient equations of a packed bed gas-solid catalytic reactor. He considers a single reaction, no radial gradients and makes the quasi-steady state approximation only after the first 3 seconds. This allows him to integrate the initial concentration dynamics for the first 3 seconds using the full equations, after which time the slower temperature dynamics are integrated, using quasi-steady state equations.

A summary of the basic theory of orthogonal collocation is given in Appendix 2.

2.3 Process Reactor Control Studies

Control of present day reactors in the process industry appears to be still somewhat of an art [Lee (L1)], except perhaps for control studies on simple CSTR or batch reactors [Marroquin (M3)]. Multivariable control of plug flow reactors, however, appears to be confined to the literature as an academic excercise, [Dyring (D1), Seinfeld (S3), Chang (C4)] and the literature is extremely sparse when it comes to application of control techniques to actual processes or pilot plant reactors. An interesting paper, far ahead of its time [Tinkler (T1)(1965)] recognised this gap when it attempted to use frequency domain techniques to develop a feed-forward control algorithm for an actual fixed bed chemical reactor.

Multivariable control studies in the chemical engineering literature have concentrated almost entirely on distillation columns, adsorbers and evaporators (F9, S2). The lack of control studies on the fixed bed reactor appears to be directly attributable to modelling complexities. The processes described above (distillation, etc.) are often quite adequately described by sets of ordinary differential equations and hence are amenable to relatively direct application of state space control theory. Many fixed bed reactors, in particular, the catalytic fixed bed reactor considered in this study, require a set of partial differential equations (PDE's) to fully describe their complex dynamics. The first problem then consists of representing this set of PDE's by a set of ordinary differential equations (often linearised) so that the multivariable state space control and estimation theory

may be applied. This is not a trivial task.

A first attempt at this problem was made by Foss and his associates [Michelsen, et al. (M2)]. Foss considered an example of a fixed bed adiabatic reactor in which an exothermic non-catalytic reaction occurs in a liquid phase. He considered a single, first order reaction and neglected radial gradients in temperature and concentration, as well as axial diffusion, and intra particle resistances. He also found it necessary to account for differences between temperatures in the liquid phase and solid phase to adequately describe the dynamics (C2).

The system of hyperbolic PDE's describing Foss's system is conveniently transformed to characteristic time and the method of Orthogonal Collocation [F4, F5, F6, F7, V1] is effectively used to approximate the PDE's by a small set of ordinary differential equations.

Foss's system included an extra dynamic equation for the particle temperature. By using a single characteristic (the other characteristic direction coinciding with one of the original co-ordinate axes), he was able to rewrite all his equations in terms of characteristic time τ and true distance z. Derivatives with respect to characteristic time appeared only in the single equation describing particle temperature. This, in effect, eliminated the explicit time dependence of the remaining equations and since the size of state space model is a function only of the number of equations with explicit time derivates, the model size was considerably reduced. Problems may occur when the state space equations are written in terms of characteristic time τ (a function of

z too) instead of real time, t, when real time measurements are matched to a characteristic time model. With a single characteristic, one can circumvent this problem but it remains an inconvenience. In general though, for hyperbolic systems, one has two characteristics and then there is no simple procedure for matching either the boundary conditions or the measurements (in z and t) to characteristic time and distance in the model. Also, since characteristic distance, say x, is a function of time as well, it is unbounded and the question of using the orthogonal collocation formulae (which are based on normalised, hence bounded variables) is in doubt. In the Section 4.4, it is seen that by the "elimination" of the radial derivative terms among the partial derivatives, we obtain an equivalent set of hyperbolic equations with two characteristics and we are thus unable to take advantage of Foss's method (M2). The availability of the analytical solution for the transfer function of his system allows Foss to test out the accuracy of the approximation by examining the ability of the approximate system to correctly predict the position of the dominant zeroes of the system (those close to, and in, the positive half plane of the frequency domain). He uses six collocation points to obtain a satisfactory representation of his reactor profiles, but comments that though, in theory, an increase in the number of collocation points will increase accuracy, the resulting equations are prone to numerical ill-conditioning. He shows how the accuracy of the collocation approximation depends on the specific dynamics of the particular process. In Foss's reactor for example, if the parameter associated with heat transfer between liquid

and solid is increased, a large increase occurs in the numbers of collocation points necessary for an adequate approximation of the reactor dynamics. In this paper then, Foss develops an effective method for representing fixed bed reactor dynamics in a state space form (that is, in a set of linearised ordinary differential equations).

In a following paper, Foss and his associates [Vakil et al. (V2)] use this state space model to investigate the design of a feed forward control scheme for their fixed bed reactor. The control design is carried out through simulation of the reactor and various configurations are evaluated numerically. Due to the problems associated with concentration measurements, the system was assumed to have temperature measurements only, and concentration measurements are inferred from these through a model. The reactor simulation system is subjected to random feed disturbances in temperature and concentration and random measurement error was added. The manipulated variables consist of a concentration or temperature "injection" (using a secondary feed of different temperature) at some point α along the length of the reactor.

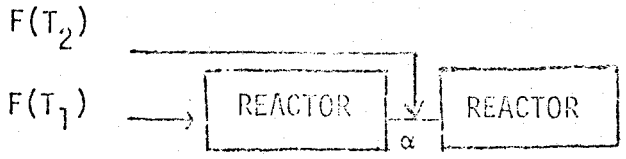

From the simulations, Foss concludes that temperature injection is the preferred manipulated variable and he compares this with the variance of the controlled variable using concentration injection as a manipulated variable. It is not clear why he does not consider the simultaneous manipulation of concentration and temperature for the

control of this multivariable system. For this study, the temperature measurements are restricted to the first section of the reactor (below injection point) and the objective is to maintain the reactor operating as close to steady state as possible. Foss makes use of a Kalman filter (to be discussed later) to estimate the states of his system. Under his measurement configuration, he found that state estimation became a severe problem and the level of his noise input (which is generated) had to be lowered considerably, before the state estimation routine could produce meaningful results. He concludes that measurements along the full length of the reactor are necessary.

An all too common finding in this paper, is that, when the sophisticated multivariable stochastic controller was compared to a first-order transfer function form of controller, the performance index of the simple controller was only 1% higher than that of the optimal stochastic controller.

Foss points to possible extensions of this work and they include investigation of:

(1) Gas solid systems where fluid residence time is small compared to thermal wave transit time.

(2) Complex reaction systems.

(3) Catalytic reactions.

(4) Non-adiabatic reactors.

(5) Use of wall heat flux and reactant flow rate as manipulated variables.

The present study attempts to investigate all of the above problems.

CHAPTER 3

A MATHEMATICAL MODEL FOR THE FIXED BED REACTOR

3.1 Introduction

We require a process control model of the reactor, suitable for on-line process control studies (see Sections 2.1 and 2.2). In Chapter 3, the mass and energy equations for the reactor are developed. This leads to a set of four coupled partial differential equations in three dimensions. These equations are far too complex to be used as a process control model, but nevertheless form the starting point for a series of simplifications (see Chapter 4) which reduces the equations to a form suitable for process control.

3.2 Process Description

The reaction considered here is the hydrogenolysis of butane. The reaction is carried out over a nickel on silica gel catalyst in a fixed bed, non-adiabatic tubular reactor. The process flow sheets are presented in Figures 1 and 2. The reactor consists of a single 2.045 cm radius tube, 28 cm long, packed with finely divided (average diameter of particle is 0.1 cm) catalyst particles. The flow rates of the two feed streams, hydrogen and butane, are controlled using a minicomputer. These feed stream flows are to be manipulated according to an algorithm, so as to maintain control of the exit concentrations. In the absence of control, these concentrations would deviate from target due

to internal or external disturbances (e.g., catalyst activity fluctuations or wall temperature fluctuations) of a stochastic or deterministic nature. The inlet gases are preheated to wall temperature by passing through a tube filled with silica gel particles, heated by an electrical resistance heater. The wall temperature of the reactor tube is controlled by flowing counter-currently, heat transfer oil (Sun Oil, No. 21) through the annulus of a cooling jacket. This heat transfer oil is continuously circulated by a Sihi (Model ZLLE 4017/155Q) centrifugal pump equipped with high temperature gland and gasket materials. Heating of the oil is provided by up to 5 electrical resistance heaters with an overall rating of about 5.8 kW. The reactor wall temperature is equal to the oil temperature and for all practical purposes, independent of length along the reactor. Oil temperature is controlled by heat exchange with air at 100 psig. Oil flows through the tube side of an American Standard (Model 200-8) single pass, heat exchanger. The control algorithm for air flow is a simple on-off type, and air flow to the shell side is computer controlled by a solenoid valve (ASCO Model 8210 D2).

Nine thermocouples (chromel-alumel) are positioned inside the reactor at equispaced points along the central axis. Several off-centre thermocouples are provided as well.

Two further thermocouples (chromel-alumel) are provided: one located in the gas preheat reactor entrance region and the other in the exit gas stream.

Temperatures of all other relevant process variables are monitored

as indicated (See Figures 1 and 2).

Exit concentration measurements are obtained using an on-line process gas chromatograph (Beckman, Model 6700). Pressure in the reactor is usually set between 1 to 2 atmospheres and pressure drop experienced by the gases flowing through the reactor is less than 0.2 atmospheres.

All data collection and process control is accomplished using a Data General 32 K Nova 2/10 minicomputer to which the reactor process has been interfaced. A Control Software Package [Tremblay (T5)] handles all the data logging and control implementation for the system. A control configuration layout is presented in Figure 3.

For details of the reactor design, control software package and process computer interfacing, the reader is referred to [Tremblay (T4)]. He designed and built the pilot plant reactor and interfaced it to the minicomputer, thus opening the possibilities of several future combined experimental and theoretical studies of which this work in conjunction with Tremblay's is the first.

3.2.1 Process Control Configuration

The necessity of setting up a sensible control configuration was elaborated on by Foss (F8) as discussed in Section 2.1. Every control configuration is specific to one's application and a good starting point is to compile a list of all possible manipulated or control variables and a list of possible response or measured variables:

Possible Manipulated Variables

(1) Hydrogen flow.

(2) Butane flow.

(3) Oil coolant or wall temperature.

(4) Inlet gas temperature.

Possible Measured Variables

(1) Temperature measurements along the central axis of the reactor.

(2) Exit concentrations of the various species.

The Objective Function

In the present study, a realistic objective is to maintain the selectivity of a product, say, propane (defined here as the change in the number of moles of the product, relative to the amount of the key reactant (butane) used up), or conversions of several of the products at some prespecified level. This level is chosen arbitrarily here, but would be based on economic considerations in an industrial situation.

In this study, the manipulated variables were selected as the butane flow and hydrogen flow. These have an advantage over the other variables in that the system responds extremely rapidly to any changes in these flows, due to the rapid concentration wave velocity. Flow control is also easy to implement and not costly. Wall temperature is often used in industry as a control variable. However, in the

present study, use of this variable for control is complicated by the fact that it has non-linear dynamics of its own, due to the configuration of the cooling system (the oil can be cooled rapidly but heating can take several minutes). The cooling does have a large effect on the reaction and at present, the wall temperature is being used as a safety variable for rapid quenching of the reaction in case of temperature runaway. The inlet gas temperature control would involve extra equipment and it has not been pursued.

Temperature measurements are more easily obtained from our process than concentration measurements and in general, this is always true. Nevertheless, a realistic objective function is expressed in terms of concentrations. Ideally then, we would prefer to measure temperatures and control concentrations. We require, however, a model which relates temperature to concentration and this is developed in Section 4.10.1.

Concentration measurements can be obtained using the process gas chromatograph (see Section 3.2). The chromatographic analysis used in this study required 361.3 seconds to produce concentration measurements of all 5 species. A fairly crude mechanical multiplexer (see Section 5.1) allowed new temperature readings to be obtained every 12 seconds (an electronic multiplexer would allow almost instantaneous temperature readings).

This study will rely primarily on temperature measurements and will use concentration measurements to check and correct for any concentration level bias found in the model.

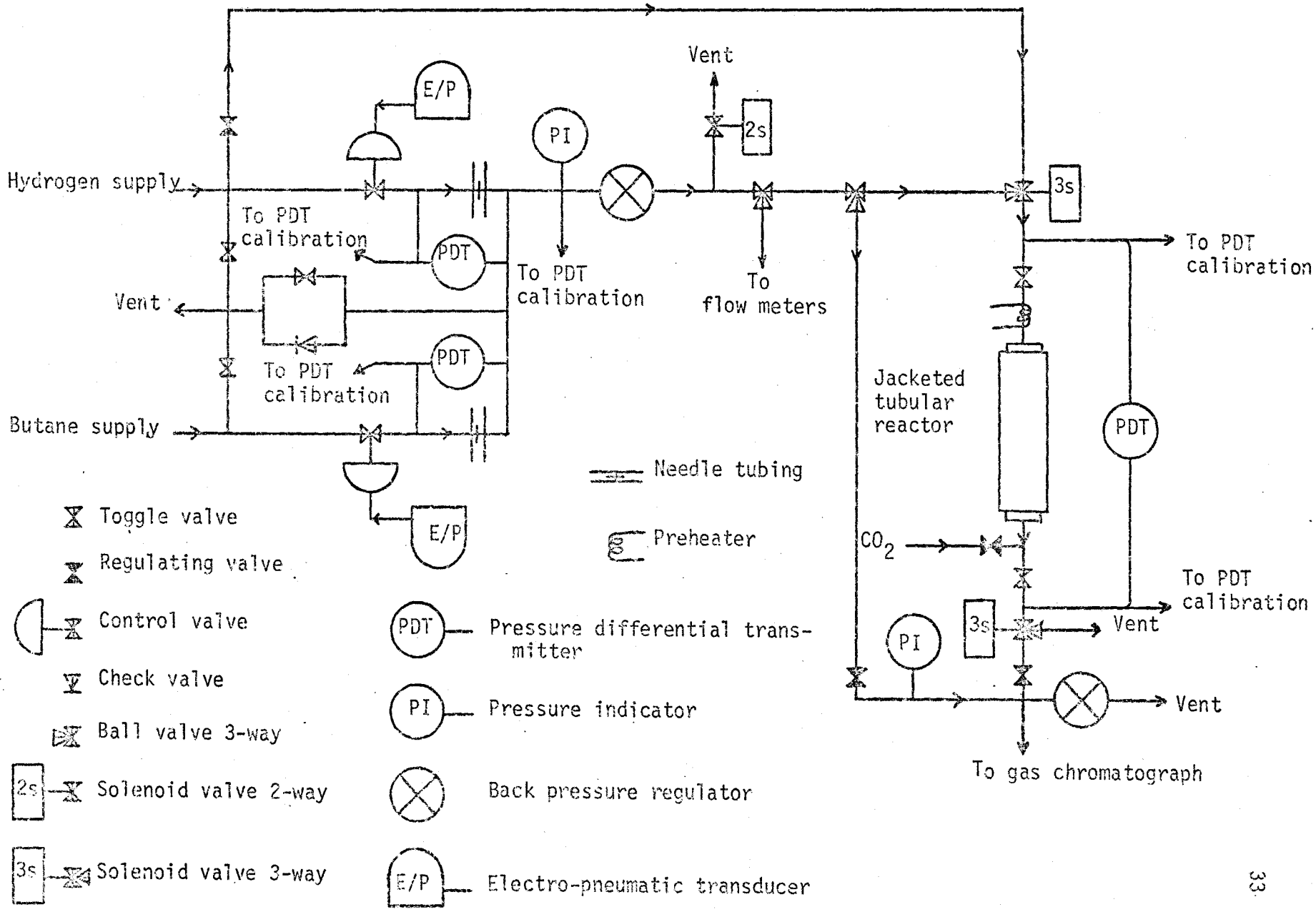

Figure 1: Process Flow Sheet for Reactor - Gas Flow System.

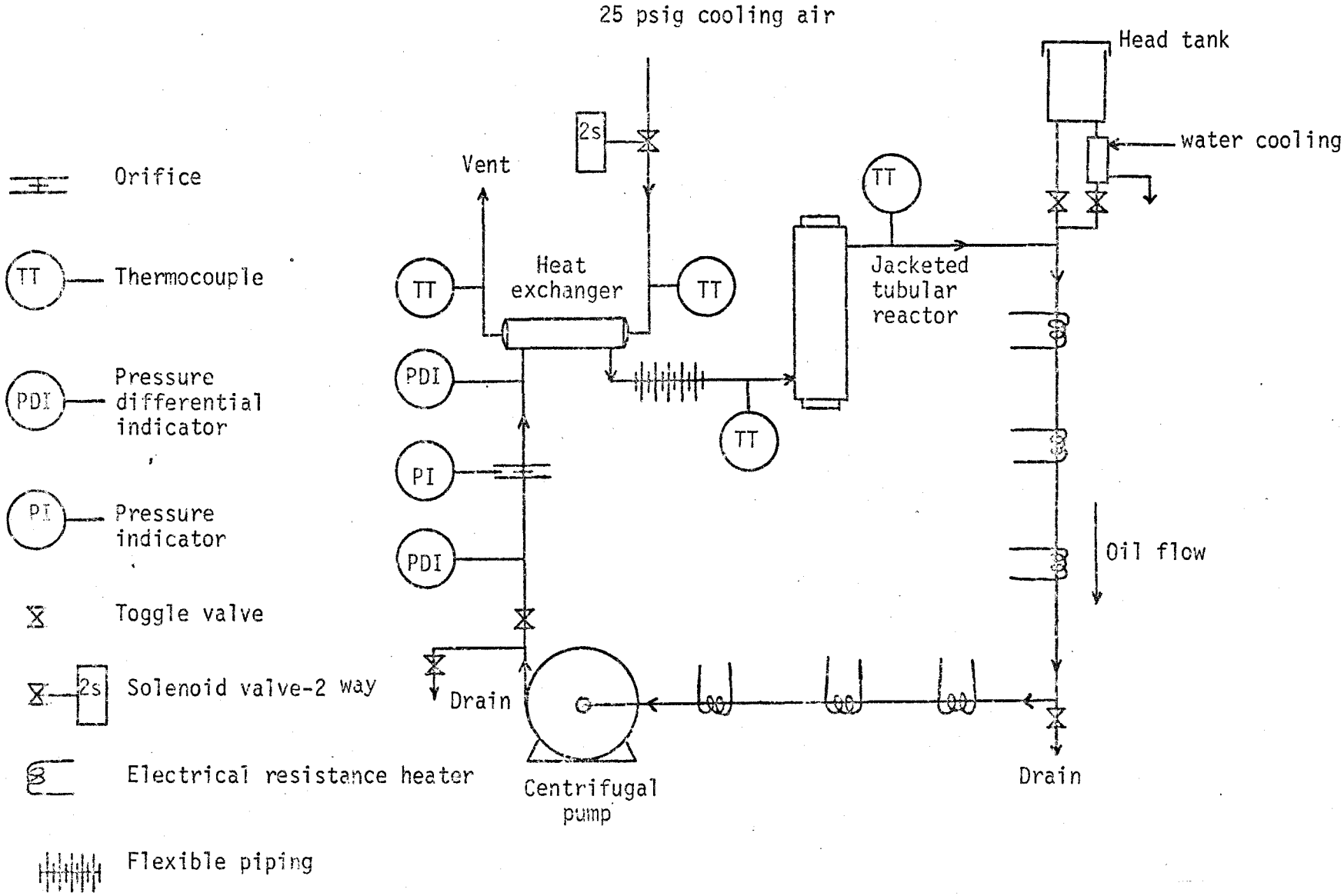

Figure 2: Process Flow Sheet for Reactor - Oil Flow System.

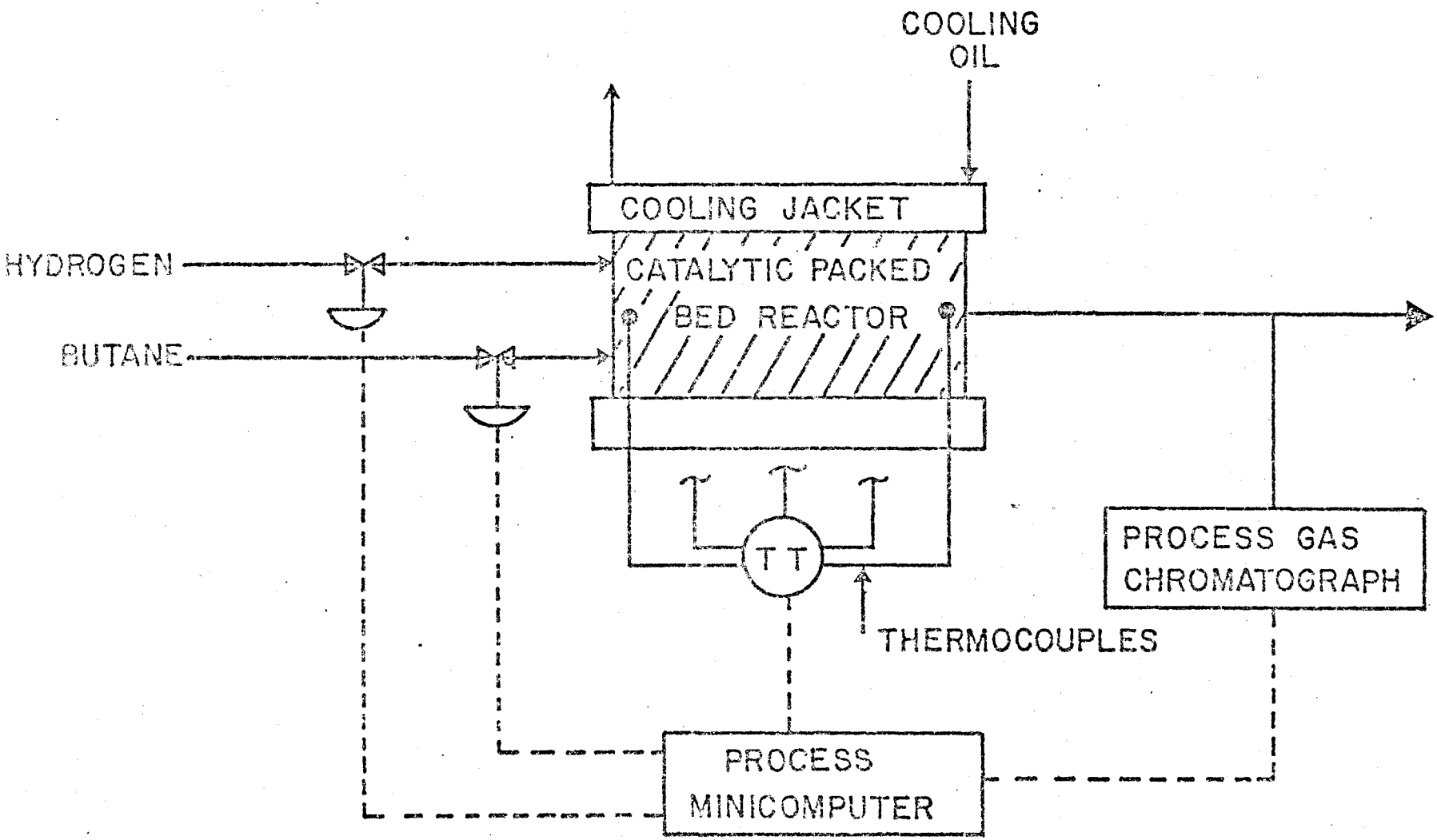

Figure 3: Reactor Control Configuration.

3.3 Reaction Kinetics

The butane hydrogenolysis reaction has been studied previously by Orlikas [O1, O2] and Shaw [S4, S5]. It is a highly exothermic series-parallel reaction that is catalysed by nickel.

A representation of the overall reaction mechanism is presented in Figure A1. The mechanism is based on the assumptions that:

(1) Butane and propane are adsorbed on the catalyst surface before a reaction takes place.

(2) The reaction products from these reactions may react further or be desorbed.

(3) Because of the low probability of breaking, two or three carbon bonds simultaneously, reactions converting butane or propane directly to methane are assumed not to occur.

The hydrogenolysis reactions may then be represented by the following four (three independent) reactions:

$$
\begin{aligned}
&(1)\quad C_4H_{10} + H_2 \rightarrow C_3H_8 + CH_4 \\
&(2)\quad C_4H_{10} + H_2 \rightarrow 2C_2H_6 \\
&(3)\quad C_3H_8 + H_2 \rightarrow C_2H_6 + CH_4 \\
&(4)\quad C_2H_6 + H_2 \rightarrow 2CH_4
\end{aligned}
\qquad (3\text{-}1)
$$

The reaction rate models associated with these reactions are given in Appendix 1.

3.4 Reactor Model Equations

An extensive analysis of the problems associated with the modelling of fixed bed reactors has been presented in Section 2.2. A discussion of the various assumptions surrounding the reactor model developed here will be presented. The reader is referred to the references enumerated and discussed in Section 2.2 to supplement this section.

In the present study, we are dealing with a non-adiabatic, fixed bed catalytic reactor. The reaction is the nickel catalysed hydrogenolysis of butane. Mass balances for the three independent species (see Section 3.3) as well as a single energy balance are required. Certain assumptions which are necessary for the development of a process control reactor model are discussed under several headings.

Catalyst Particle

In this reactor we have the rapid flow of gases over solid, porous, catalyst particles. The catalyst is prepared on silica gel porous particles [Tremblay (T2)]. The reaction is highly exothermic and occurs on and within the small, (average diameter 0.1 cm) approximately spherical catalyst particles. This reaction scheme has been studied by Orlikas (O1) and Shaw (S4). They determined that there are no interparticle or intraparticle mass transfer limitations.

They also concluded that the effect of pore diffusion on intraparticle concentration profiles is minor and hence, that concentration within the catalyst particle is uniform [Levenspiel, (L2)].

Under most conditions encountered industrially, catalyst particles

remain nearly isothermal [F1, F3, C1] even for exothermic reactions. This is especially true for the small (0.1 cm diam) catalyst particles considered here. Shaw, in his thesis (S4) provided evidence that this assumption is valid.

The presence of uniform concentration and temperature profiles within the catalyst make the probability of multiple steady states within the particle small. Industrially, this is often the case (F1, F3) and a unique steady state will be assumed here.

In situations where it is not possible to assume uniform catalyst particle profiles, the resulting complications to the model would make it unusable for control; another approach to the problem would have to be sought. We assume that the packed bed may be treated as a continuum in so far as changes occur continuously and smoothly throughout the bed. The ratio of bed diameter to catalyst diameter is about 200 and under these conditions (Hlavacek (H1)) this assumption is valid.

Gas Phase

(1) The reactor operates at low pressure and we assume the gases obey the ideal gas law.

(2) There is a minor pressure drop across the reactor (Section 3.2) and because the reaction is equimolar, we assume (provided temperature rise is not too excessive) that the gas flow may be represented as a movement of a plug down the reactor with constant average velocity, independent of radial position [(P1), see also Beek (B1)].

(3) Axial diffusion of mass and temperature has been neglected

in comparison with bulk flow or convective terms [B1, S4, O1, F3]. Shaw (S4) presents an analysis which shows that mass diffusion can certainly be neglected. There is recent evidence [M1, F3] that some error may result if temperature diffusion terms are neglected. No evidence is presented to suggest that this term would significantly alter the major dynamic effects within the reactor. Furthermore, by examining the criteria [M1, F3, see also Section 2.2.3] the effect of axial dispersion is minimal for fast flowing gases over small catalyst particles. The reactor here operates under these conditions and we neglect both heat and mass diffusion terms. From a control pcint of view, this assumption is mandatory since inclusion of these terms, apart from making the equations computationally unfeasible would force us to deal with

(a) multiple steady states in gas phase,

(b) solution of a two point boundary value problem,

both of which clearly could not be considered for a control model.

(4) For fast flowing gas-solid systems such as the one considered here, the difference between gas and solid catalyst temperatures may be considered negligible. Industrial experience appears to support this [F3, G1] and criteria in the literature for testing the validity of this assumption are not reliable (see Section 2.2.3). Hence, it appears at this stage,

to be safer to rely on reports and experience gathered from industrial situations [F3, G1]. Shaw (S4) presents an analysis to show that there is ample driving force to remove the heat generated by reaction and that essentially no temperature difference existed between catalyst pellet and gas at steady state.

From a control point of view, there is a further problem of measurement. Although theoretically, it is possible to measure separately the gas and solid temperature, in practice it is difficult. In cases where catalyst particles are sufficiently large, some workers have tried embedding the thermocouple inside the particle. To measure gas temperature only, the thermocouple may be surrounded by a meshed cage. These practices can seriously disrupt flow patterns and are not common industrial practice. There is also the question of measurement error. The difference between gas and solid temperature (< 5°K) is of the order of error associated with the thermocouple (see Section 5.1.1).

Heat Radiation Between Solid and Gas

Heat transfer by radiation from the solid catalyst to the gas can have a significant effect on the temperature dynamics in the reactor, especially at the high temperatures attainable by highly exothermic catalysed reactions. According to Hlavacek (H1), heat transfer by radiation need only be considered for operating temperature in excess of 673 °K (400°C) and since our operating temperatures should remain between 520-570°K, radiation should not be excessive. However, if radiation became significant, it would have the effect of enlarging

the convective heat transfer parameter [see Equations (3-3) and (3-4) below] and hence, this parameter should properly be considered to be an overall heat transfer coefficient. Beek (B1) also includes a radiation term in his correlation for effective radial conductivity λ_{er} - this procedure is used in Section 5.3.1 under parameter estimation.

Radial Gradients

In this reactor, extensive cooling is provided at the reactor wall to ensure that temperature runaways can be prevented. This cooling can cause steep radial gradients and temperature drops of up to 100°F have been observed across the radius (2 cm) of the reactor [Tremblay (T2), this study].

Radial gradients are almost always ignored in any unsteady state analysis of reactor systems, partly because of the resulting complications to the model. In any industrial situation where wall cooling is required for safety or control, radial gradients will exist. No-where, to our knowledge, has an attempt been made to include these gradients in any dynamic model, and the majority of dynamic studies avoid systems which exhibit appreciable radial gradients. Our reactor unavoidably, has significant radial gradients and these are accounted for in the model.

The Reactor Model

For clarity, we first distinguish between the gas temperature T_g and the solid temperature, T_s. This allows us to write two energy balances along with the mass balances for each of the three independent species. The following normalised equations result:

Mass Balance

$$\frac{-G_o}{\varepsilon L}\frac{\partial C^i}{\partial z} + \frac{D_{er}}{\varepsilon R^2 r}\frac{\partial}{\partial r}\left(r\frac{\partial C^i}{\partial r}\right) - \frac{\rho_B R^i}{\varepsilon} = \frac{\partial C^i}{\partial t} \qquad (3\text{-}2)$$

where $i = 1,2,3$ is the component number.

Energy Balance: Gas

$$\frac{-G_o C_{P_g} \rho_g}{L}\frac{\partial T_g}{\partial z} + \frac{\lambda_{er}}{R^2 r}\frac{\partial}{\partial r}\left(r\frac{\partial T_g}{\partial r}\right) + ha\rho_B(T_s - T_g) = C_{P_g}\rho_g\varepsilon\frac{\partial T_g}{\partial t} \qquad (3\text{-}3)$$

Energy Balance: Solid

$$-ha\rho_B(T_s - T_g) + \sum_{i=1}^{3}\Delta h_i R_i(T_s)\rho_B = C_{P_s}\rho_B\frac{\partial T_s}{\partial t} \qquad (3\text{-}4)$$

We may combine the two energy balances by eliminating the term between them which describes heat transfer between solid and gas, $ha\rho_B(T_s - T_g)$. If we then make the assumption of equal solid and gas temperatures and we designate the homogeneous gas/solid temperature as T, Equations (3-3) and (3-4) become

Energy Balance: Solid/Gas

$$\frac{-G_o C_{P_g} \rho_g}{L\,\bar{C}} \frac{\partial T}{\partial z} + \frac{\lambda_{er}}{R^2 \bar{C} r} \frac{\partial}{\partial r}\left(r \frac{\partial T}{\partial r}\right) + \frac{\sum_{i=1}^{3} \Delta h_i R_i \rho_B}{\bar{C}} = \frac{\partial T}{\partial t} \tag{3-5}$$

where

$$\bar{C} = [C_{P_s} \rho_B + C_{P_g} \rho_g \epsilon] \tag{3-6}$$

is a gas/solid heat capacity term and T represents a homogeneous gas/solid temperature.

Boundary Conditions

$$\begin{aligned} r = 0 \quad & \frac{\partial C^i}{\partial r} = \frac{\partial T}{\partial r} = 0 \text{ (Symmetry)} \\ r = 1 \quad & \frac{\partial C^i}{\partial r} = 0 \; ; \; \frac{\partial T}{\partial r} = B_i (T_W - T) \end{aligned} \tag{3-7}$$

$$\begin{aligned} z = 0 \quad & T = T_W \text{ for all } r \\ & C^i = C^i(\text{inlet}) \text{ for all } r,\ i = 1,2,3 \end{aligned} \tag{3-8}$$

$$\begin{aligned} t = 0 \quad & T = T(\text{initial})(r,z) \\ & C^i = C^i(\text{initial})(r,z)\ i = 1,2,3 \end{aligned} \tag{3-9}$$

The expressions for the rate equations R^i are given in Appendix 1. We can also identify [G1], the thermal (v_T) and concentration (v_C) wave velocities as

$$v_T = \frac{G_o C_{P_g} \rho_g}{L \bar{C}} \tag{3-10}$$

$$v_C = \frac{G_o}{\varepsilon L} \tag{3-11}$$

Equations (3-2) and (3-5) represent four coupled, three-dimensional, non-linear partial differential equations. In their present form, a solution (even numerically) is not feasible and we thus have to seek some approximation to these equations that will reduce them to a form suitable for use for on-line control. The method of Orthogonal Collocation (discussed in Chapter 4 and Appendix 2) is used.

CHAPTER 4

STATE SPACE REACTOR MODEL

4.1 Introduction

In Section 3.4, we developed a set of partial differential equations which describe the dynamics of the concentration and temperature profiles in our fixed bed reactor. In this section, these equations are broken down and simplified so as to fit into the framework of modern multivariable control theory which most often requires a model for the process to be expressed as a set of linear(ised) first order ordinary differential equations in the (state space) form

$$\dot{\underline{x}} = A\,\underline{x} + B\,\underline{u} \tag{4-1}$$

or using a discrete model, (t = sampling interval)

$$\underline{x}(t) = A\,\underline{x}(t-1) + B\,\underline{u}(t-1) \tag{4-2}$$

There is also an output or measurement equation associated with the dynamic equation and it is usually of the form

$$\underline{y}(t) = H\,\underline{x}(t) \tag{4-3}$$

or more generally,

$$\underline{y}(t) = H\,\underline{x}(t) + C\,\underline{u}(t-1) \tag{4-3a}$$

The set of variables contained in the $\underline{x}$ vector are known as the states. or internal variables of the system. $\underline{u}$ is a vector of control variables. $\underline{y}$ vector is a set of output or measured variables. Matrices A, B, and H are constant or time-varying matrices of the system.

Once the dynamic equations for the system have been expressed in the standard form of Equation (4-1), that is, in state space form, much of the current multivariable control theory may be used to design one or more multivariable control schemes. When dealing with real processes, it will generally not be possible to describe the system exactly in terms of the deterministic state Equations (4-1) and (4-3) and one can account for noise in the system, modelling errors and measurement errors by identifying and by adding a stochastic noise term to these equations. This will be discussed later in Chapters 5 and 6.

The first step then, is to express the set of non-linear partial differential Equations (3-2) and (3-5) in the state space form given by (4-1). Because we are going from partial differential equations (PDE's) to ordinary differential equations (ODE's) some form of discretisation of the spatial variables r and z is necessary, so as to produce an ODE in time at each grid point in the z,r domain. In general, these equations will be non-linear (since the PDE's were non-linear) and it is necessary to linearise about some operating profile in the z,r domain. This operating profile could be obtained first by solving the steady state versions of the original PDE's, or by choosing a profile from historical records. The discretisation problem appears to be relatively straightforward, but this is not so as may be illustrated

by the following example. Assume that 5 grid points are adequate for discretising the radial direction r, and 20 grid points for axial direction z. This would define a mesh of 100 grid points. At each grid point we have four ODE's in time, one for each of the three concentrations and one for the temperature. Hence, the total number of ordinary differential equations necessary to describe our system would be 400 - this is much too large a model for control.

Also, any discretisation or lumping procedure in the axial direction would probably have to take into account the position of the hot spot (and discretise more finely here). This would mean that the discretisation would have to change for different operating conditions. This is a great disadvantage. The method of Orthogonal Collocation has been very successfully applied to simplify reactor equations [F4, F5, F6, F7] and provides a powerful method for transforming PDE's to ODE's. Some of the basic aspects of this theory are discussed in Appendix 2.

4.2 Chronological Development of the State Space Model

At the onset of this work, very little experimental data was available for the reactor. An earlier version of this reactor had been built (Tremblay (T2)) and some limited steady state data were available. Initially, in order to keep the development as general as possible, in the face of limited experience with this reactor, the number of simplifying assumptions and approximations was kept to a minimum. At first, collocation approximation was used only in the radial direction, r, since the expected profiles in this direction were not severe and

low order approximations would be adequate. The reactor equations were quite general with no specific reference to the reaction environment (catalytic gas/solid here). This led to a set of 140 ordinary differential equations, i.e., a state space model of order 140. Somewhat less than an order of 400 referred to in Section 4.1, but still too large for control. A state space model reduction technique was developed to reduce the model order. We obtained an equivalent 80^{th} order model whose dynamics, it was shown, closely matched the original 140^{th} order model. Current techniques (see Section 4.6) for reducing state space model order were inadequate and no further reduction seemed possible.

Several simulation studies were performed with this 80^{th} order state model in order to develop an understanding of the dynamics of the reactor system. It was also possible, using the limited steady state data, to test out some of the collocation approximations used. This high order state model thus proved very useful as a preliminary simulation model to study the reactor system.

From further dynamic studies with this high order state model, it was soon realised, that for the time intervals of interest the quasi-steady state approximation for the concentration dynamics would be quite adequate. After making use of this assumption, our reactor model became more specific, but still described most gas/solid systems. A relatively low order collocation approximation (6^{th} order) was then introduced for the axial direction. There was not strong physical justification that a 6^{th} order approximation would adequately approximate all possible axial profiles (even though Michelsen (M2) made this

approximation). Nevertheless, a collocation approximation to the axial derivative was easy to implement and is not tied to a grid structure based on a particular temperature profile, the way a usual discretisation or lumping method may be (see Section 4.1). A further motivation for using axial collocation is that the size of the state space model is greatly reduced and is equal to the order of the collocation approximation plus one (a 7^{th} order model was obtained). Subsequent simulation studies with this 7^{th} order model and somewhat higher orders (up to 11^{th} order revealed that the dynamic features were still intact and that indeed, a low order state model for the reactor was feasible. This low order state model would be fitted to dynamic data when it became available and then used to develop an on-line control scheme for the reactor.

It is advantageous to divide up Chapter 4 into two parts: Part A, which covers material presented in Sections 4.3 to 4.7; is concerned primarily with the development of the high order state models and represents a preliminary simulation study. Part B, presented in Sections 4.8 to 4.11, is concerned with the development of a low order state model suitable for process control. The reader, if he is familiar with the ideas of collocation and interested primarily in control may wish to skip Part A and proceed directly with Part B, using Part A as a reference.

Part A: Preliminary Simulation Study and Development of a High Order State Space Model

4.3 Adaptation of Collocation Formulae to Reactor System

Although collocation has been primarily used as a numerical tool to aid the integration of non-linear differential equations, it will be used here as a method of approximating derivative terms in the partial differential equations (3-2) and (3-5). Referring to the formulae developed in Appendix 2 for derivatives, (A-20) and (A-21), it is easy to extend these formulae to partial derivatives by simply collocating with respect to a single independent variable. For example, the partial derivatives of temperature with respect to r at collocation point r_i is given by:

$$r = r_i \qquad \frac{\partial T}{\partial r}^{(n)} = \sum_{j=1}^{n+1} A_{ij}^{(n)} T_j^{(n)}(z,t) \tag{4-4}$$

$$r = r_i \qquad \frac{1}{r}\frac{\partial}{\partial r}\left(r \frac{\partial T}{\partial r}^{(n)}\right) = \sum_{j=1}^{n+1} B_{ij}^{(n)} T_j^{(n)}(z,t) \tag{4-5}$$

where $T_j(z,t)$ is written for $T(r_j,z,t)$, a function of z and t. Villadsen (V1) and Finlayson (F7) have tabulated values for the collocation weights $A_{ij}^{(n)}$ and $B_{ij}^{(n)}$.

4.4 Radial Collocation

The order of collocation approximation (n) in (4-4) and (4-5) necessary to approximate a function is not known beforehand and remains

very much a matter of judgement. Experimental measurements [Tremblay (T2)] and an examination of typical temperature and concentration radial profiles in the literature [Finlayson (F4)] indicate that often, radial gradients in temperature may be well represented by a quadratic and the corresponding radial concentration profiles by a quartic (see later).

For the symmetric radial profiles in the reactor, a suitable trial function (see (A-19)) is given by (V1)

$$T^{(n)}(r,z,t) = T(1,z,t) + (1 - r^2)\sum_{k=0}^{n-1} a_k^{(n)}(z,t)P_k(r^2) \qquad (4\text{-}6)$$

where the $a_k^{(n)}$ are unknown coefficients and P_k are Jacobi polynomials.

4.4.1 Application to Reactor Differential Equations

The technique involved here is to write the three-dimensional differential equations as an enlarged set of two-dimensional equations at the collocation points in r. We then make extensive use of the boundary conditions to derive relations between the dependent variables at the collocation points and hence eliminate some of them, reducing in turn, the number of equations.

As illustrated in Figure 3, the axial temperature profile of the reactor is measured by a set of thermocouples located along the reactor bed centre (r = o). These axial temperatures provide some indication of the overall behaviour of the reactor.

Temperature Equation

At r = o, the energy balance equation (3-5) becomes:

$$- v_T \frac{\partial T_o}{\partial z} + \frac{\lambda_{er}}{R^2 \bar{C}}\left[\frac{1}{r}\frac{\partial}{\partial r}\left(r \frac{\partial T}{\partial r}\right)\right]_o + \left.\frac{\sum_{i=1}^{3} \Delta h_i R_i \rho_B}{\bar{C}}\right|_o = \frac{\partial T_o}{\partial t} \qquad (4\text{-}7)$$

using L'Hopital's Rule

$$\left[\frac{1}{r}\frac{\partial}{\partial r}\left(r \frac{\partial T}{\partial r}\right)\right]_o = \left[2 \frac{\partial^2 T}{\partial r^2}\right]_o \qquad (4\text{-}8)$$

We now make use of orthogonal collocation to obtain an expression for Equation (4-8) in terms of T_o and the known wall temperature T_w. Using Jacobi polynomials for the approximation function and using the first collocation approximation (which results in a quadratic temperature profile), we obtain two collocation points r = 0.577, r = 1.0. The centre point is not a collocation point and in order to obtain an expression for the temperature at r = o, we write (4-6) in an alternative form (F4), T symmetric with respect to r).

$$T_j^{(n)} = \sum_{i=1}^{n+1} d_i r_j^{2i-2} \qquad j = 1, n+1 \qquad (4\text{-}9)$$

Evaluating the coefficients d_i in terms of the temperatures at the collocation points, for a first collocation approximation ((n) = 1), we obtain an extrapolation to the centre point temperature T_o. Dropping the collocation superscript (n) = 1 here, we write the extrapolation formula as

$$T_o(z,t) = \frac{3}{2} T_1(z,t) - \frac{1}{2} T_2(z,t) \tag{4-10}$$

where

$$T_j(z,t) = T(r_j,z,t)$$

The boundary condition at the wall has been characterized by Beek (B1) in terms of a Biot number B_i (see Equation (3-7)),

$$\left.\frac{\partial T}{\partial r}\right|_{r=r_2} = B_i(T_W - T) \tag{4-11}$$

Using the first collocation approximation from Equation (4-4) (omitting the collocation superscript (n) = 1, here) we have an expression for the first derivative in r, at the edge of the bed.

$$\left.\frac{\partial T}{\partial r}\right|_{r=r_2} = A_{21}T_1 + A_{22}T_2 \tag{4-12}$$

Similarly an expression for the second derivative may be derived from Equation (4-5),(4-10) and then (4-8) to give

$$\left.\frac{\partial^2 T}{\partial r^2}\right|_{r=o} = \bar{B}_{01}T_1 + \bar{B}_{02}T_2 \tag{4-13}$$

where the $\bar{B}_{0j}$'s are functions of the collocation parameters A_{ij} and B_{ij}. Equating Equations (4-11) and (4-12) and using (4-10), we may eliminate all the temperatures except T_o and T_W. By further substituting the numerical values for the collocation constants A_{ij} and $\bar{B}_{ij}$ we obtain:

$$\left.\frac{\partial^2 T}{\partial r^2}\right|_o = \frac{-2B_i}{(B_i + 2)}[T_o - T_w] \tag{4-14}$$

and

$$T_2 = T(r=1) = \left(\frac{2}{B_i + 2}\right)T_o + \left(\frac{B_i}{B_i + 2}\right)T_w \tag{4-15}$$

Equation (4-7) then becomes

$$-v_T \frac{\partial T_o}{\partial z} + \frac{\lambda_{er} 4B_i}{R^2 \bar{C}(B_i + 2)}[T_w - T_o] + \left.\frac{\sum_{i=1}^{3} \Delta h_i R_i \rho_B}{\bar{C}}\right|_o = \frac{\partial T_o}{\partial t} \tag{4-16}$$

The temperature equation has now been reduced from a three-dimensional equation in variables (r,z,t) to a two-dimensional equation in variables (z,t). This reduced equation is a function of the axial temperature T_o only but includes radial information via the wall temperature and Biot number. Radial temperature profiles can be obtained from the collocation Equation (4-9) or (4-10)(for typical steady state profiles, see Figures 6 and 7).

Concentration Equation

For the radial concentration profiles, standard boundary conditions require a zero first derivative at the reactor centre r = o, and the reactor wall, r = 1 (3-7). A suitable polynomial satisfying these requirements is a quartic and this requires a second collocation approximation and three collocation points

$$r_1 = 0.3938 \qquad r_2 = 0.8031 \qquad r_3 = 1.0$$

Again the axial point is not a collocation point. Notice also that collocation point $r_3 = 1.0$, for the second collocation approximation coincides with collocation point $r_2 = 1.0$ for the first collocation approximation used in temperature. Writing the concentration equations at points $r_o = 0$ and $r_3 = 1.0$, we obtain:

$$r = r_3 = 1.0 \quad - v_C \frac{\partial C_3^i}{\partial z} + \frac{D_{er}}{R^2 \varepsilon} \left[\frac{1}{r} \frac{\partial}{\partial r} \left(r \frac{\partial C}{\partial r}\right)\right]_{r=r_3} - \frac{R^i \rho_B}{\varepsilon} \Bigg|_{r=r_3} = \frac{\partial C_3^i}{\partial t} \tag{4-17}$$

$$r = 0 \quad - v_C \frac{\partial C_o^i}{\partial z} + \frac{D_{er}}{R^2 \varepsilon} \left[\frac{1}{r} \frac{\partial}{\partial r} \left(r \frac{\partial C^i}{\partial r}\right)\right]_{r=0} - \frac{R^i \rho_B}{\varepsilon} \Bigg|_{r=0} = \frac{\partial C_o^i}{\partial t} \tag{4-18}$$

$$i = 1,2,3$$

Proceeding in a similar manner to that followed for the temperature equation, the corresponding concentration equations (for second collocation approxmation) are:

$$C_o^i = 1.5572\, C_1^i - 0.8922\, C_2^i + 0.3350\, c_3^i \tag{4-19}$$

and from (3-7) and using the form (4-4) we obtain

$$\frac{\partial C^i}{\partial r} \Bigg|_{r=r_3} = A_{31} C_1^i + A_{32} C_2^i + A_{33} C_3^i = 0 \tag{4-20}$$

where $i = 1,2,3$ is the component number. The information that the first derivative is zero at $r = 0$ has already been included by the assumption of the quartic radial profile from which Equation (4-19) is obtained. For example, from Equation (4-9) with collocation approximation order (n) = 2,

$$C_j = d_1 + d_2 r_j^2 + d_3 r_j^4$$

which provides for symmetry in r and a zero first derivative at r = 0, as did the temperature equation. Thus for the concentration equation, we have only two Equations (4-19), (4-20) between the concentration at the four radial points, r_o, r_1, r_2, r_3, and we may express the partial derivative in r in terms of C_o at r_o and C_3 at r_3.

$$\left[\frac{1}{r}\frac{\partial}{\partial r}\left(r\frac{\partial C^i}{\partial r}\right)\right]_{r=r_3} = B_{31}C_1^i + B_{32}C_2^i + B_{33}C_3^i = \beta_{31}C_o^i + \beta_{32}C_3^i \tag{4-21}$$

$$\left[\frac{1}{r}\frac{\partial}{\partial r}\left(r\frac{\partial C^i}{\partial r}\right)\right]_{r=0} = \bar{B}_{01}C_1^i + \bar{B}_{02}C_2^i + \bar{B}_{03}C_3^i = \beta_{01}C_o^i + \beta_{02}C_3^i$$

Substituting Equations (4-21) into (4-17), (4-18), we obtain the set of differential equations

$$-v_C\frac{\partial C_3^i}{\partial z} + \frac{D_{er}}{R^2\varepsilon}\left[\beta_{31}C_o^i + \beta_{32}C_3^i\right] - \left.\frac{R^i\rho_B}{\varepsilon}\right|_{r=r_3} = \frac{\partial C_3^i}{\partial t} \tag{4-22}$$

$$-v_C\frac{\partial C_o^i}{\partial z} + \frac{D_{er}}{R^2\varepsilon}\left[\beta_{01}C_o^i + \beta_{02}C_3^i\right] - \left.\frac{R^i\rho_B}{\varepsilon}\right|_{r=0} = \frac{\partial C_o^i}{\partial t} \tag{4-23}$$

component number i = 1,2, or 3.

which together with the temperature Equations (4-15), (4-16) provide the complete collocation model

$$- v_T \frac{\partial T_o}{\partial z} + \frac{\lambda_{er} 4B_i}{R^2 \bar{C}(B_i + 2)} [T_W - T_o] + \left. \frac{\sum_{i=1}^{3} \Delta h_i R_i B}{\bar{C}} \right|_{r=0} = \frac{\partial T_o}{\partial t} \qquad (4\text{-}24)$$

$$T_3 = T(r=1) = \left(\frac{2}{B_i + 2}\right) T_o + \left(\frac{B_i}{B_i + 2}\right) T_W \qquad (4\text{-}25)$$

In the above equations, subscript o indicates conditions at the reactor centre r = 0 and subscript 3 denotes conditions at the outer radius of the bed r = 1.

We have now reduced the system to seven, two-dimensional, differential equations; six in concentration and one in temperature, including an algebraic equation for temperatures at r=1. These may now be reformulated to obtain a state space model representation (see Equation (4-1)) for the reactor).

4.5 State Space Formulation

Reducing the set of Equations (4-22), (4-23), (4-24) to the state space form given in Equation (4-1) requires linearisation about some prespecified steady or operating condition, about which regulatory control is desired. Details of the steady state solution of the above equations are provided in a later section.

In order to obtain a state space dynamic reactor model, the partial derivatives of T and C with respect to z (in Equations (4-22), (4-23) and (4-24) must be approximated in some way. There are at least two methods available: We could use Orthogonal Collocation approximation in the axial direction z using formulae similar to (4-4). However, at this stage, we were not sure of how large a collocation approximation

order (n) would be required. Other authors (Michelsen (M2)) have reported numerical ill-conditioning problems of collocation orders become too large. It thus appeared safer at this stage to search for an alternative method. Nevertheless at a later stage (see Part B), axial collocation was used with great success.

Another method of approximating the z derivative is to set up a finite difference along the z axis. Since the steady state profiles are already known and we expect only small perturbations about this steady state, the grid points may be optimally spaced, for integration accuracy, according to the slopes of the profiles in z. If we choose 20 grid points along z and linearise the 7 partial differential equations, we obtain 140 simultaneous ordinary differential equations to be solved. (cf the 400 simultaneous equations obtained if a finite difference technique were to be employed in the r direction as well; see also Section 4.1). The resulting state space formulation becomes:

$$\dot{\underline{x}} = A\underline{x} + B\underline{u} \qquad (4\text{-}26)$$

$\underline{x}$ = 140 x 1 vector of deviations from steady state in temperature, ΔT_0 and concentrations ΔC_0, ΔC_3

$\underline{u}$ = 2 x 1 vector of deviation feed flow rates (hydrogen and butane).

A = 140 x 140 matrix of constants

B = 140 x 2 matrix of constants

4.6 A State Space Model Reduction Method

It is now of interest to try to further reduce the number of simultaneous equations (140) without sacrificing the essential dynamic behaviour of the model obtained thus far. To accomplish this, an idea based on the concept of aggregation in state space dynamics (A1) is employed. Given an n-dimensional state space system:

$$\dot{\underline{x}} = A\underline{x} + B\underline{u} \tag{4-27}$$

a reduction in the dimensionality of the system to an ℓ-dimensional system

$$\dot{\underline{s}} = F\underline{s} + G\underline{u} \tag{4-28}$$

is considered using the (ℓxn) linear matrix transformation

$$\underline{s} = Z\underline{x} \tag{4-29}$$

where rank (Z) = ℓ. The statement that $\underline{s}$ satisfies (4-28) is equivalent to the condition that F and G are related to A and B by

$$F\,Z = Z\,A \tag{4-30}$$

$$G = Z\,B \tag{4-31}$$

Now Equation (4-30) is not of full rank, for $\ell < n$ and has, in general, no exact solution. In the event that A and Z satisfy the matrix equation

$$Z\,A = Z\,A\,Z'(Z\,Z')^{-1}Z \tag{4-32}$$

then (4-30) has an exact solution for F and is given by

$$F = Z A Z'(Z Z')^{-1} \qquad (4\text{-}33)$$

Nevertheless, even if (4-32) is not satisfied, (4-33) represents the best solution (in the least squares sense) to (4-30) and is often adequate for control purposes. Other methods have been suggested for reducing the system order of a state space model (Davison (D3)) using the techniques of Modal analysis, originally presented by Rosenbrock (R1). However, these methods rely on being able to calculate the eigenvalues of the A matrix. Even for our simplified system, A is of order 140 and has no special structure other than being sparse. Eigenvalue calculations on so large a scale would cause many problems.

4.6.1 Application to Averaged Concentration

In our system, strong motivation exists to transform the theoretical concentration at the centre point C_0 and at the wall C_3, into a more meaningful averaged or mixed concentration which can be measured. It is not possible to measure point concentrations and the model in its present form (4-27) cannot be used for control, where measured values of mixed concentrations at the outlet and axial temperatures are to be compared with predictions by the model.

According to Villadsen and Stewart (V1), collocation principles can be applied directly to integrals and they present a formula (see (A-22)),

$$\int_0^1 f(x)x^{a-1}dx = \sum_{i=1}^{n+1} w_i^{(n)} f(x_i) \tag{4-34}$$

where the w_i are quadrature weights, a is a geometry factor (= 2 here) The averaged or mixed concentration across a radial section is given by

$$\bar{C}^i(z,t) = 2\int_0^1 C^i(z,t,r)rdr \tag{4-35}$$

Applying (4-34) to the radial concentration and using Equations (4-19), (4-20) to eliminate C_1 and C_2 in terms of C_o and C_3 we can obtain

$$\bar{C} = w_1 C_o + w_2 C_3 \tag{4-36}$$

These integrals are highly accurate and even this low order approximation is exact if the radial concentration profiles can be represented by a polynomial of order no greater than eight.

The 140 dimensional linearised state variable Equation (4-26) contains an A matrix and $\underline{x}$ vector of the form

$$A = \begin{array}{c} \\ 60 \\ 60 \\ 20 \end{array} \begin{array}{c} \begin{array}{ccc} 60 & 60 & 20 \end{array} \\ \left[\begin{array}{c|c|c} E_o & F_o & H_o \\ \hline F_3 & E_3 & H_3 \\ \hline G' & 0 & K \end{array}\right] \end{array} \qquad \underline{x} = \left[\begin{array}{c} \Delta C_o \\ \hline \Delta C_3 \\ \hline \Delta T_o \end{array}\right] \tag{4-37}$$

where all block matrices, E, F, H, G^T, K, 0 are banded and sparse. Applying Equation (4-36) to each set of concentrations in the vector $\underline{x}$,

we obtain a relation between $\underline{s}$ and $\underline{x}$ of the form (4-29) remembering that temperatures are not transformed

$$\underline{s} = Z\underline{x} \tag{4-29}$$

where

$$Z = \begin{array}{c} \\ 60 \\ 20 \end{array} \begin{array}{c} \begin{array}{cc} 120 & 20 \end{array} \\ \left[\begin{array}{c|c} Z_1 & \\ \hline & Z_2 \end{array}\right] \end{array}$$

and

$$Z_1 = [w_1 I_{60} \mid w_2 I_{60}]$$

$$Z_2 = I_{20}$$

where I_n denotes the unit matrix of order n.

Using Equation (4-33) we obtain an expression for F by multiplying out the matrix blocks to obtain

$$F = \begin{array}{c} \\ 60 \\ 20 \end{array} \begin{array}{c} \begin{array}{cc} 60 & 60 \end{array} \\ \left[\begin{array}{c|c} F_{11} & F_{12} \\ \hline F_{21} & F_{22} \end{array}\right] \end{array}$$

where

$$\begin{aligned} F_{11} &= (w_1^2 E_o + w_1 w_2 (F_o + F_3) + w_2^2 E_3)/w^2 \\ F_{12} &= (w_1 H_0 + w_2 H_3)/w^2 \\ F_{21} &= (w_2 G')/w^2 \\ F_{22} &= K \end{aligned} \tag{4-38}$$

where $w^2 = w_1^2 + w_2^2$

The matrix G is obtained directly from Equation (4-31).

We now have a reduced set of equations

$$\dot{\underline{s}} = F\underline{s} + G\underline{u} \tag{4-39}$$

which is a system of order 80 and the state vector $\underline{s}$ consists of deviation variables of axial temperatures and averaged concentrations at each of the 20 locations in the z direction. The model is now suitable for simulation studies and comparison with experimental measurements obtained from the reactor.

It is instructive to point out at this stage, that if a reduction from the 140 equations via an aggregation matrix is intended, then the order of the resulting aggregated system (4-39) is independent of the order of the collocation approximation used in the r direction. So if, for example, one decided that it was necessary to approximate both temperature and concentration radial profiles by 10^{th} order polynomials, say, extrapolation to centre temperatures and application of quadrature for mixed concentration as above, would again reduce the system to one of order 80, for 20 grid points in the z direction. On the other hand, reduction of the number of grid points along z directly reduces the order of the system by 4 for each grid point.

A series of simulation studies was performed in order to gain insight into various aspects of the reactor dynamics and steady state characteristics. Firstly, using the available steady state data (Tremblay (T2)) we can determine how well the model Equations (3-2) and (3-5) can predict the steady state profiles measured in the reactor. Secondly,

we can perform some parametric sensitivity studies: most workers agree (H1, B1, C1) that reactor behaviour is very sensitive to heat transfer parameters but not to mass transfer parameters. Some may err in concluding that mass transfer terms may be entirely omitted; that this is not so, will be demonstrated by using radial mass diffusivity as an example.

Thirdly, using the two state space models, 140^{th} order and 80^{th} order, an evaluation of the effectiveness of the model reduction method presented in Section 4.6 can be made. Due to computational limitations, only the initial dynamics can be compared but in fact, it is this early dynamics that is the most revealing in terms of the quasi-steady state that is rapidly approached by the concentration dynamics. This happens before the slower (by a factor of $\sim$ 1400) temperature dynamics have had a chance to respond.

The details of these simulation studies are presented below.

4.7 Simulation Studies

Using a limited amount of steady state data from a previous study, Tremblay (T2), in which a reactor very similar to the one used for this study was built, and a series of simulation studies were performed. Due to the similarity between the previous reactor design and the present one, the data were considered adequate to judge the effectiveness of the collocation methods and matrix averaging techniques described above. Parameter estimates were obtained using the previous data ((T2),(T3)) and from correlations in the literature (Beek (B1)). Values of the key parameters were:

$$B_i = 43.5,\ D_{er} = 0.316\ cm^2/s,\ \lambda_{er} = 0.0018\ cal/(cm°K\ s)$$

Other pertinent reactor data is presented in Table 1a.

4.7.1 Steady State Behaviour

One of the modifications to the original reactor was to enlarge the gas feed stream preheat section. Previously (T2) the inlet gas entering the catalyst bed was below the wall temperature. In the new design, the assumption that the inlet gas is at wall temperature should be valid. Apart from this difference, we expect similar profiles in the two reactors. A Feed preheat section was also added later.

In order to compare the steady state temperature profile data with profiles from the collocation model, the steady state versions of Equations (4-22), (4-23) and (4-24) were solved. Because the highly exothermic nature of the reactions resulted in steep temperature gradients around the hot spot temperature along the z axis, a variable step size integration procedure, Hamming's Modified Predictor-Corrector, was used. Computation time on a CDC 6400 was about 20 CPU seconds. Typical profiles are shown in Figure 4. By comparison, a 4^{th} order Runge-Kutta method required about 45 CPU seconds for comparable accuracy.

Figure 5 compares the axial temperature profile predicted by the model equations with that obtained experimentally for the previous reactor. Apart from the difference in entering gas temperatures, these profiles are in good agreement ($D_{er} = 0.316$). No point concentration measurements are available. Nevertheless, the overall predicted conversion of butane (77%)

TABLE 1a

Reactor Parameters for Simulation Studies

(Kinetic Parameters are given separately in Appendix 1)

T_w	= 520°K
B_i	= 43.5
$G_o(H_2)$	= 60 cm^3/s at STP
$G_o(C_4H_{10})$	= 5 cm^3/s at STP
R	= 2.045 cm
Reactor Pressure	= 1.0 Atm
Catalyst Activity	= 2.35
L	= 28.0 cm
ε	= 0.4
D_{er}	= 0.316 cm^2/s
C_{p_s}	= 0.22 cal/(g°k)
ρ_B	= 0.72 g/cm^3
d_p	= 0.1 cm
λ_{er}	= 0.0018 cal/(cm°K s)
Inlet Concentrations	= pure Butane and Hydrogen
Inlet Temperature	= T_w (520°K)

Heats of Reaction (linear approximation) for 4 reactions given in Section 3.3 (Units: cal/g mole)

Δh_1	= - 12,560 - 5.0(T - 298)
Δh_2	= - 10,322 - 6.3(T - 298)

TABLE 1a (continued)

Reactor Parameters for Simulation Studies

Δh_3 = - 13,305 - 3.28(T - 298) OMITTED IN PROGRAM

Δh_4 = - 15,542 - 2.52(T - 298)

Radial Collocation Points

r_1 = 0.577 r_2 = 1.0 Ref. Villadsen (V1)

Axial Collocation Points (Section 4.9) ((n) = 6)

z_0 = 0.0

z_1 = 0.03377

z_2 = 0.16940 Ref. Kopal (K2)

z_3 = 0.38069

z_4 = 0.61931

z_5 = 0.83060

z_6 = 0.96623

z_7 = 1.0

agrees well with the actual value obtained experimentally (76%). In addition, the model is able to predict variations in hot spot locations and butane conversions observed experimentally (Trembaly (T2)). Although these tests are by no means exhaustive, they do provide some confidence in the collocation methods used here.

Typical axial concentration profiles, radially averaged for the four hydrocarbon species are shown in Figure 8. These correspond to temperature profile (2) in Figure 4, where a 49% conversion of butane (C_4) and a 52% selectivity to propane (C_3) is achieved. The existence of appreciable radial gradients in temperature (confirming experimental measurements) and concentration profiles are illustrated in Figures 6 and 7.

4.7.2 Parametric Sensitivity

Parametric sensitivity has been studied in some detail in the literature for the steady state fixed bed reactor (Froment, F(1), F(2), F(3), Carberry (C1), for details, see Section 2.2.1 above). This section is concerned in particular, with the influence of D_{er}. Radial variations in temperature and concentrations have been characterized by the Peclet numbers for effective radial heat $N_{Pe_{h,r}}$ and mass $N_{Pe_{m,r}}$ transfer. Equivalently, the effective radial thermal conductivity, λ_{er}, and effective radial mass diffusivity, D_{er}, may be used. For all practical purposes $N_{Pe_{m,r}}$ takes on values between 8 and 11 for most reactor systems (F2). A general result emerging from these studies shows that simulation

profiles are insensitive to the actual value assumed for $N_{Pe_{m,r}}$ within this range. A precise estimate of it is therefore not required. In contrast, the profiles are highly sensitive to the corresponding Peclet number for effective radial heat transfer. It is important not to interpret "insensitive" as implying "unimportant", since the latter interpretation would imply that the term $\frac{D_{er}}{\varepsilon R^2 r} \frac{\partial}{\partial r} (\frac{\partial C}{\partial r})$ in Equation (3-2) may be neglected altogether. The result of forcing D_{er} to a small value ($D_{er} = 0.05$, $N_{Pe_{m,r}} \doteq 60$) in our simulation is shown in Figure 5. The result is a 20% drop in the conversion as predicted by the model as well as an alteration of both the hotspot temperature and its location. For parametric sensitivity to λ_{er}, see Figure 5a and Section 5.5.1.

4.7.3 Dynamic Behaviour

The dynamic characteristics of the reactor are best viewed in terms of the concentration and temperature wave velocities, v_C and v_T respectively. Since v_C is of the order of 1400 x v_T in this sytem, two distinct phases of the response are observable. The rapid response as the concentration wave passes through the reactor occurs under the influence of an almost constant temperature profile. The concentration profiles rapidly reach a pseudo steady state which then gradually change as the slower temperature wave passes through the reactor. These dynamics are typical of Quasi-Steady State Systems.

Unsteady state solutions for the reactor for step and pulse changes in hydrogen flow rate were obtained by integrating both the reduced 80 x 80 system (Equation (4-39)) and the 140 x 140 system (Equation (4-26)).

Because of the very large ratio of wave velocities, a variable step size integration method was used (Hamming's modified predictor corrector). Integration times on a CDC 6400 were about 4 seconds and 2 seconds CPU time per second of reaction time for the full and reduced models, respectively. It should be remarked at this stage, that dynamic equations of this type, with a very large ratio of wave velocities, are stiff differential equations. This in turn implies that one requires a small time step to properly integrate the system and hence the computational burden is greatly increased. In particular, the rapid initial concentration dynamics required especially small integration time steps, which may be gradually increased as concentrations reached their quasi-steady state. Hence, a variable step size integration was well suited to this problem.

Recall that the concentration variables in the reduced 80 x 80 model are radially averaged. After integration of the full 140 x 140 model, radial point concentrations are available which can then be averaged for comparison with the results of the reduced system. The comparison should indicate any loss of information caused by the matrix aggregation technique. As mentioned above, the concentration dynamics respond rapidly. Table 1 compares the dynamic profiles obtained from the two systems for a 10% step decrease in the flow of hydrogen. Responses are summarized for one feed (H_2) and one intermediate (C_3). Note that the agreement between the two profiles is good to at least three significant figures. A quasi-steady state is reached within 3 seconds and profiles at 6 seconds show little change. The quasi-steady state nature of the concentration dynamics is illustrated in Figure 9. Temperature

profiles respond only marginally in this short time period. The agreement between the profiles of the 140 x 140 and 80 x 80 models, indicates that the aggregation technique applied here is able to reduce the model order while retaining the dynamic behaviour of the system.

In order to examine the slower dynamics of the temperature profile, a much larger step change was made in hydrogen flow. From an examination of the reaction kinetics (Section 3.3) and the corresponding rates (see Appendix 1), it can be determined that a decrease in the hydrogen flow tends to increase the reaction rate and raise the temperature. Previous studies (Tremblay (T2)) and Tremblay and Wright (T3) have shown that the temperature transients may persist from 3 to more than 20 minutes for perturbations in inlet flow rates. The simulation model is consistent with these observations. Figure 10 illustrates the dynamic behaviour of the temperature profiles resulting from a 40% downward stepped pulse in hydrogen flow site lasting for 40 seconds. The entire profile rises initially (curve (2)) and continues to rise for some time after the input has been restored to its initial value. Only after about five minutes does it begin to return to the initial steady state (see the initial section of curve 3).

The hotspot location moves from about z = .59 to z = 0.61 during this change. The temperature transient at the hotspot is potentially the most sensitive measurement which can readily be used for control purposes. The dynamic response of the hot spot temperature is shown in Figure 11.

Axial Distance z	Concentrations									
	t = 0⁻ (steady state)		t = 3 seconds				t = 6 seconds			
	140 x 140 & 80 x 80		140 x 140		80 x 80		140 x 140		80 x 80	
	H_2	C_3	H_2	C_3	H_2	C_3	H_2	C_3	H_2	C_3
0	.2163	0	.2145	0	.2145	0	.2145	0	.2145	0
.1	.2152	.4830	.2133	.5072	.2133	.5070	.2133	.5072	.2133	.5071
.2	.2138	1.001	.2119	1.028	.2119	1.028	.2119	1.028	.2119	1.028
.3	.2122	1.541	.2103	1.569	.2103	1.569	.2103	1.570	.2103	1.569
.4	.2104	2.090	.2085	2.119	.2085	2.119	.2085	2.119	.2085	2.119
.5	.2086	2.630	.2066	2.661	.2066	2.661	.2066	2.661	.2066	2.661
.6	.2067	3.142	.2047	3.171	.2047	3.171	.2047	3.171	.2047	3.172
.7	.2049	3.600	.2029	3.628	.2030	3.628	.2030	3.628	.2030	3.628
.8	.2033	3.994	.2013	4.019	.2014	4.019	.2014	4.019	.2014	4.019
.9	.2020	4.329	.2000	4.351	.2001	4.352	.2001	4.351	.2001	4.352
1.0	.2008	4.619	.1989	4.638	.1989	4.639	.1989	4.638	.1989	4.639

TABLE 1

Dynamic Response of 80x80 and 140x140 systems to a 10% step decrease in Hydrogen. Radially averaged concentrations of Hydrogen $H_2 \times 10^{-4}$ moles/cc and Propane $C_3 \times 10^{-7}$ moles/cc. z = normalized axial distance.

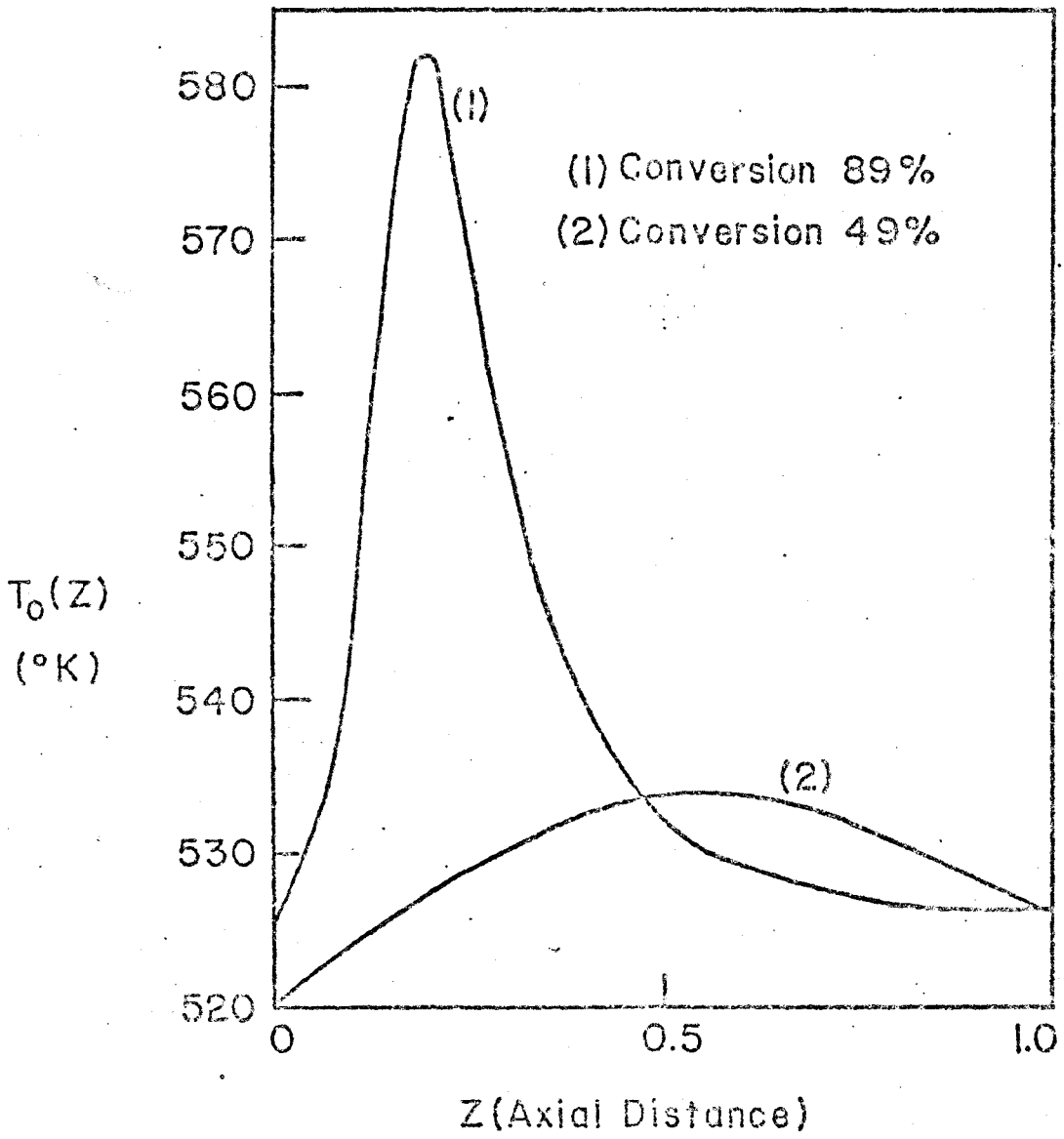

Figure 4: Typical Steady-State Central Axis Temperature Profiles in the Reactor (simulation).

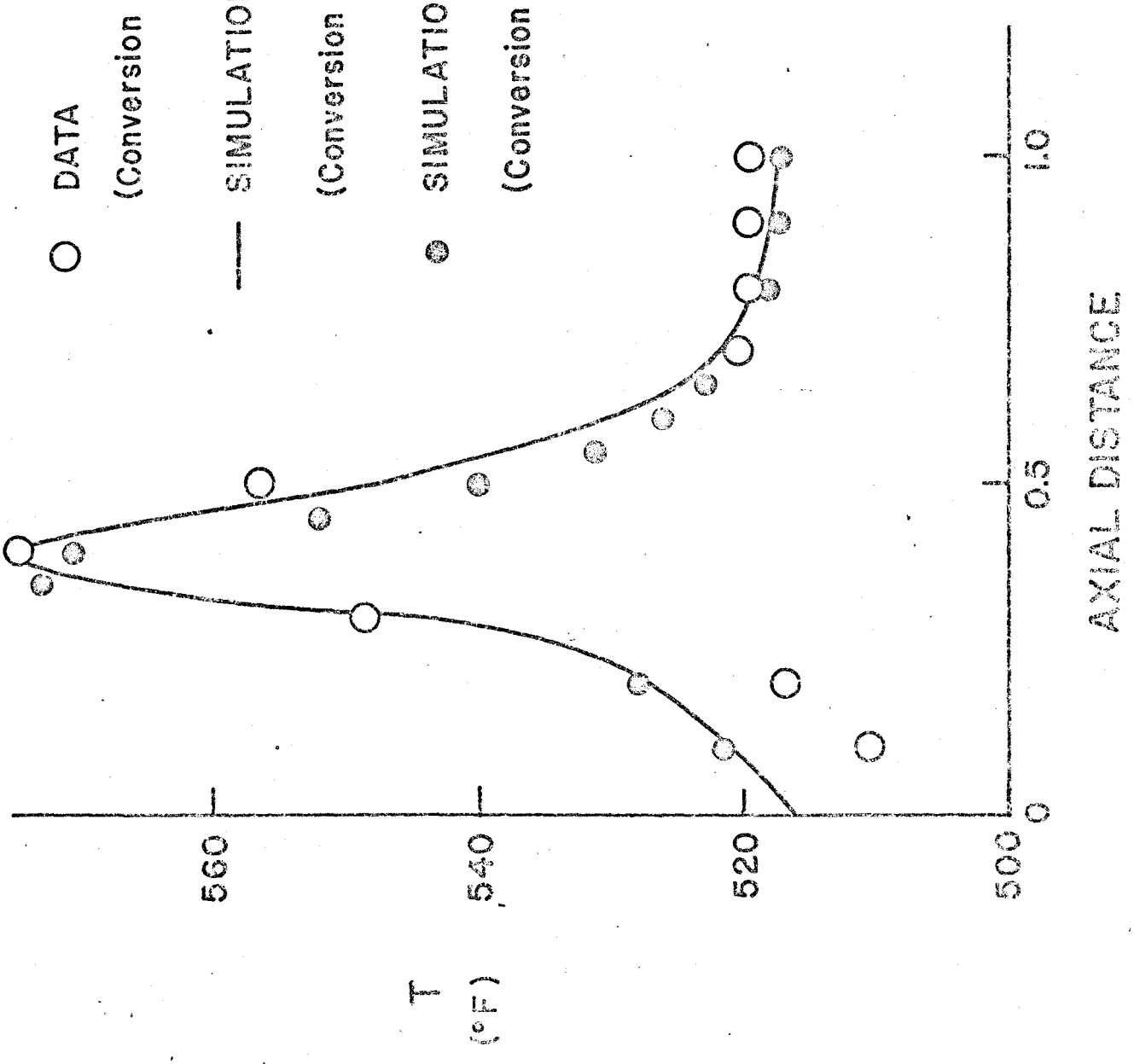

Figure 5: Comparison of Steady-State Temperature Data with Simulation Profiles. Influence of D_{er}.

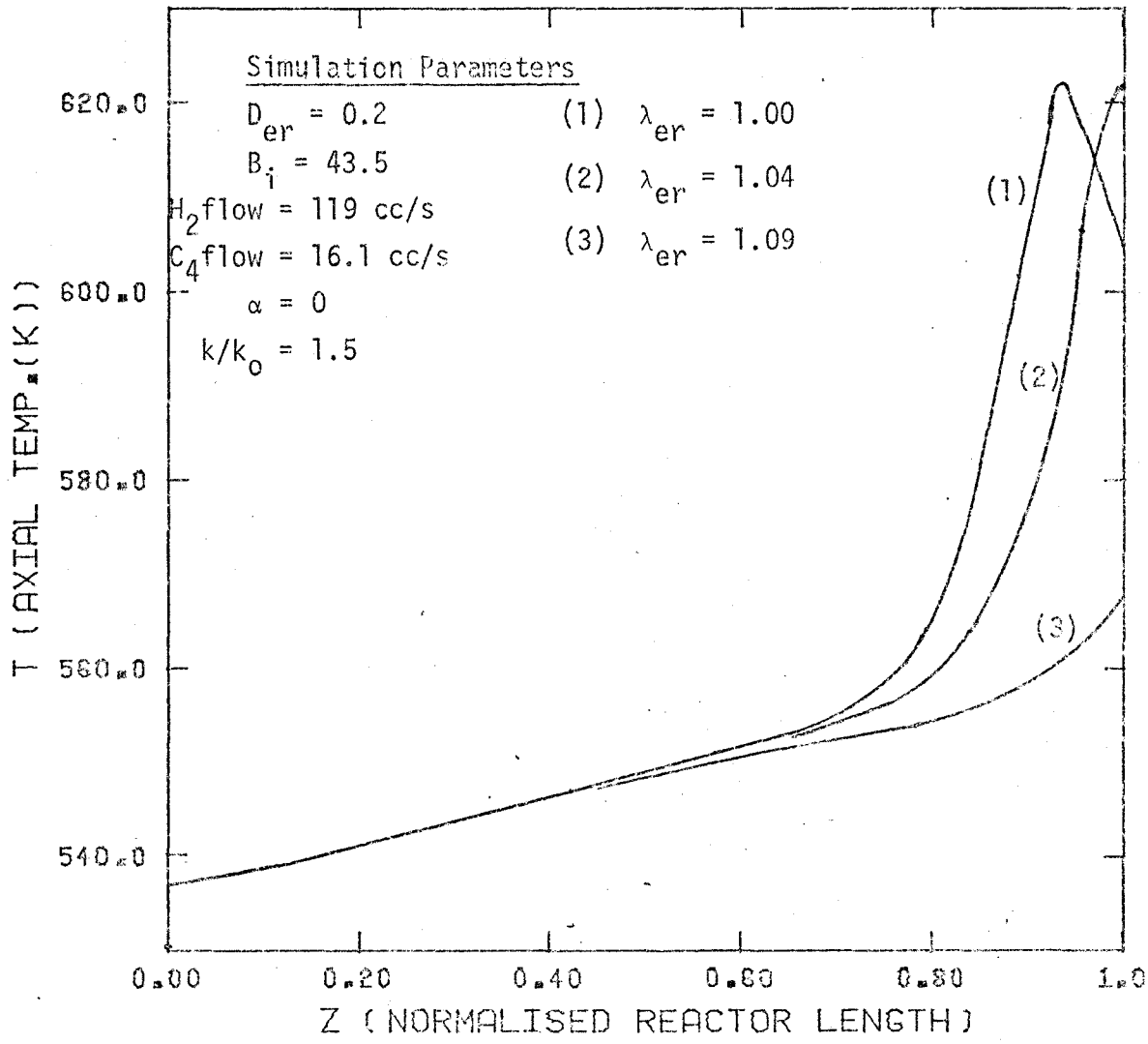

Figure 5a: Parametric Sensitivity to Thermal Conductivity, λ_{er}.

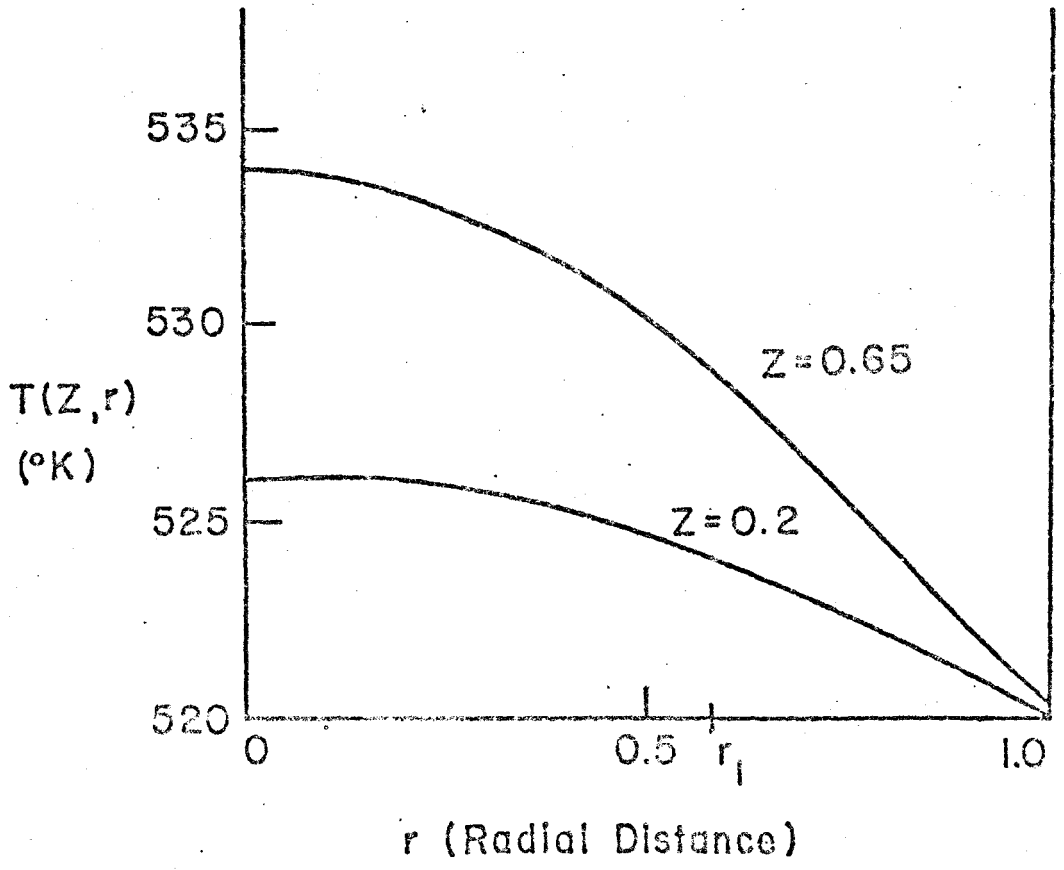

Figure 6: Radial Reactor Temperature Profiles (Steady State Simulation).

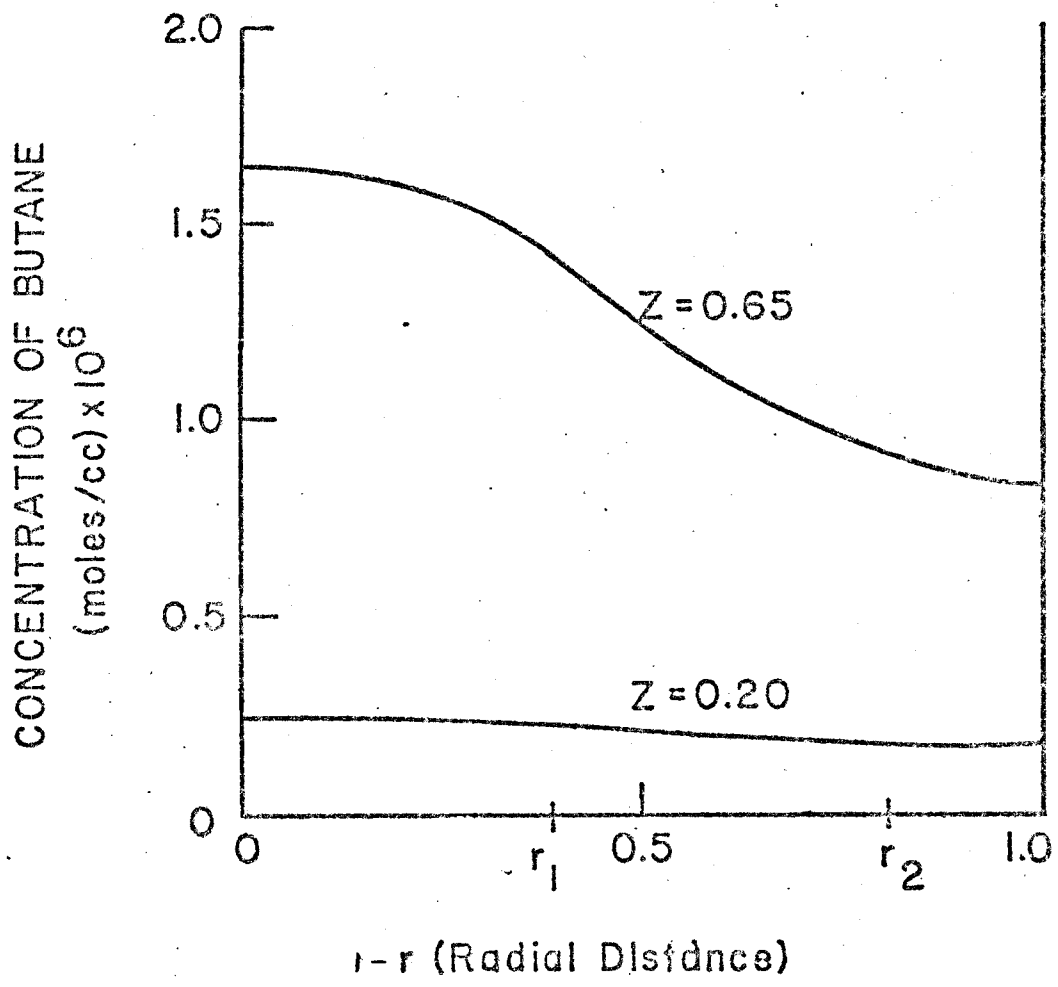

Figure 7: Radial Reactor Concentration Profile for Butane (Steady State Simulation).

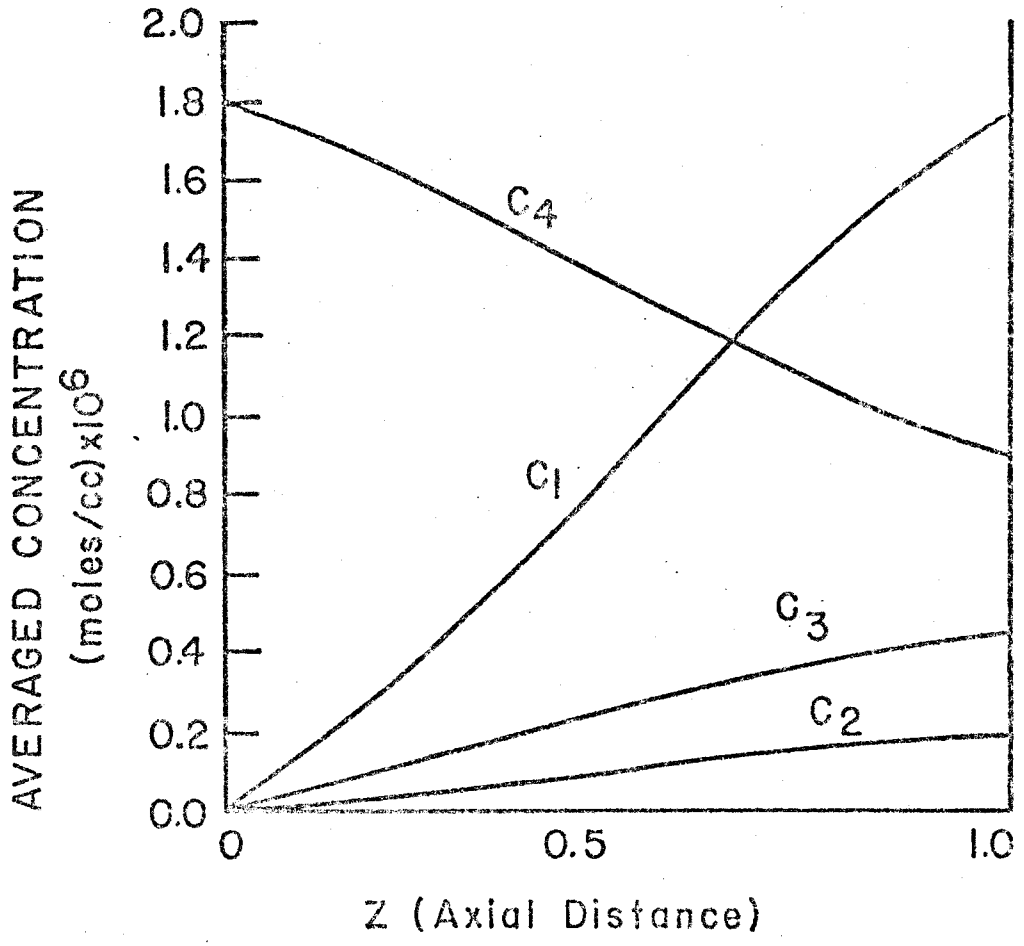

Figure 8: Steady State (averaged) Concentration Profiles Along the Reactor (Butane Conversion 49%) (Simulation).

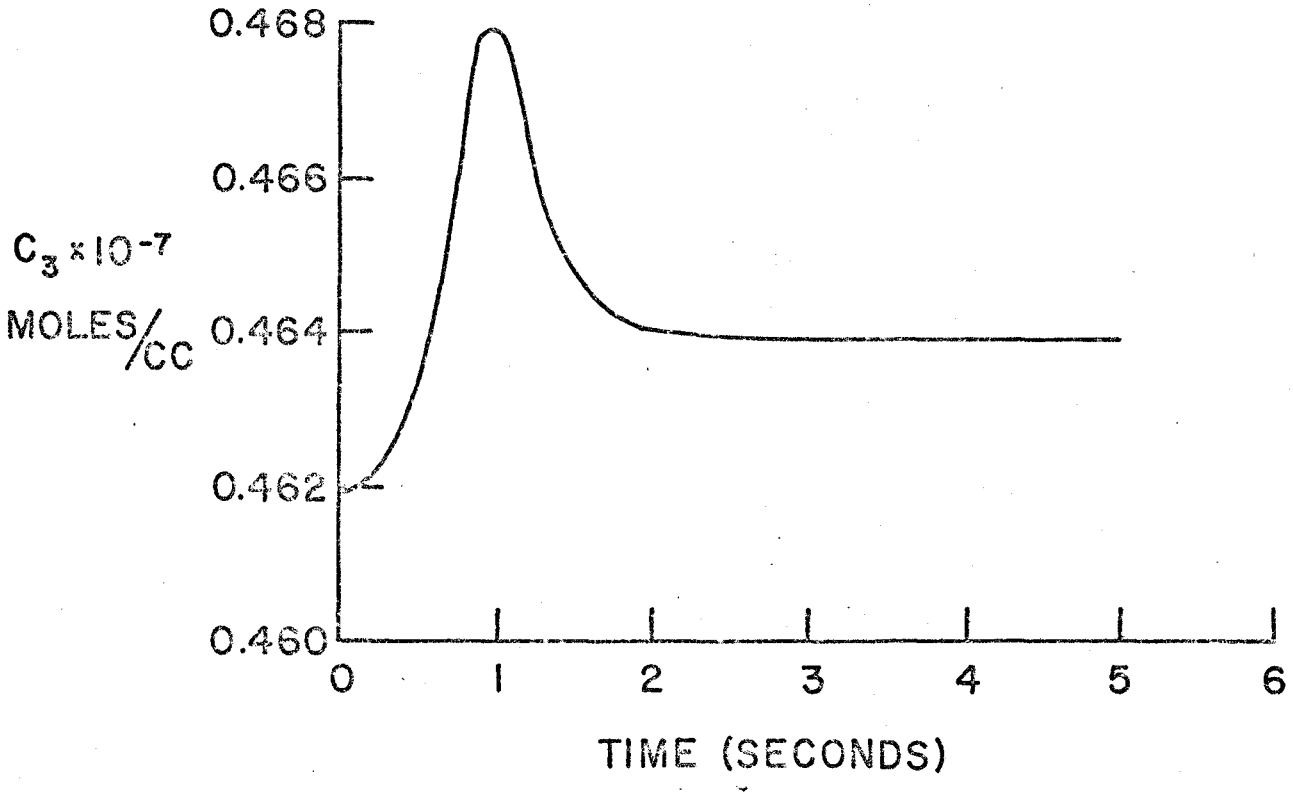

Figure 9: Exit (averaged) Concentration of Propane in Response to a 10% Step Down in H_2 Flow (80^{th} Order Simulation).

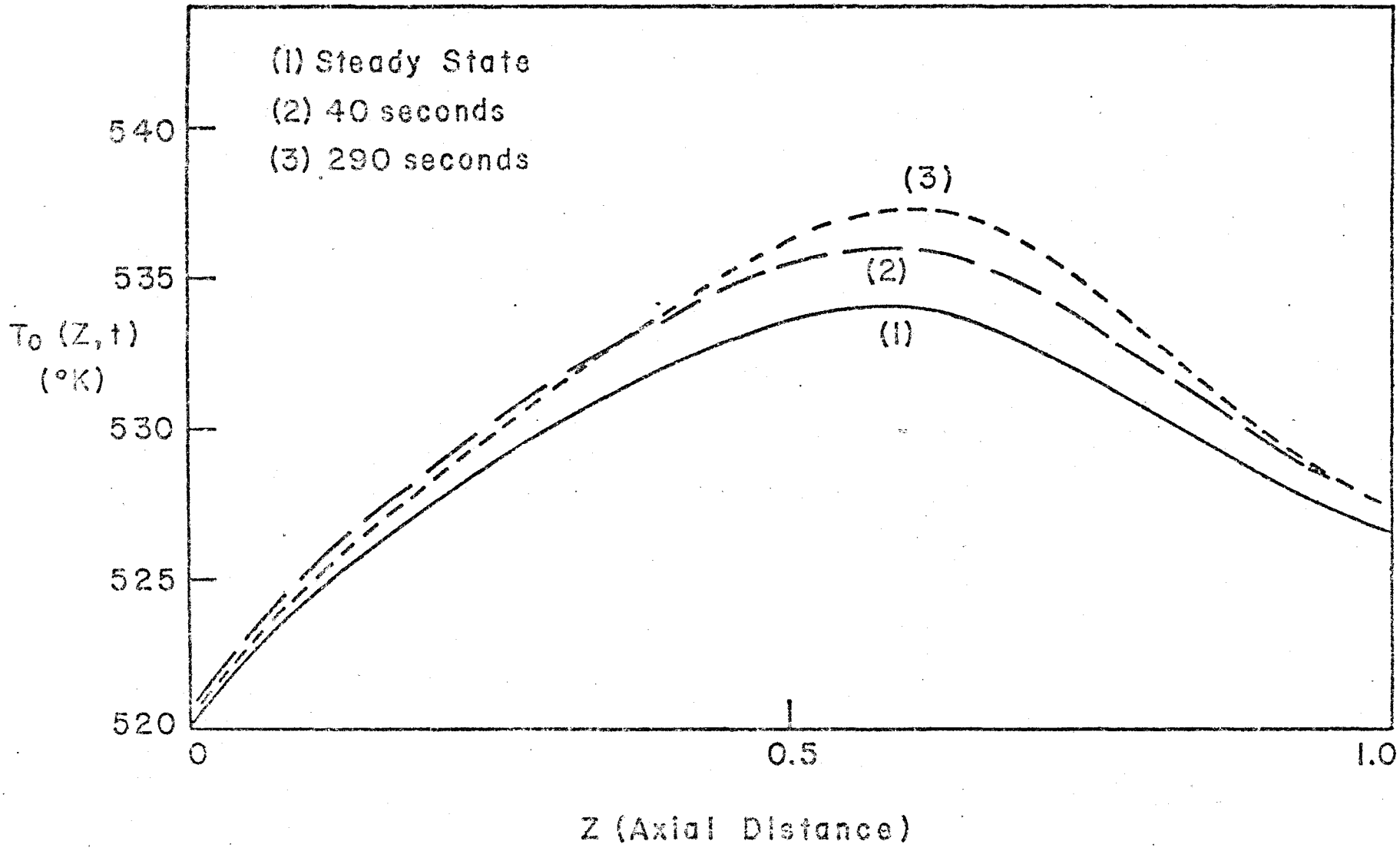

Figure 10: Dynamic Response of the Central Axis Temperature Profile to a Down Pulse in the H_2 Flow. (80^{th} Order Simulation).

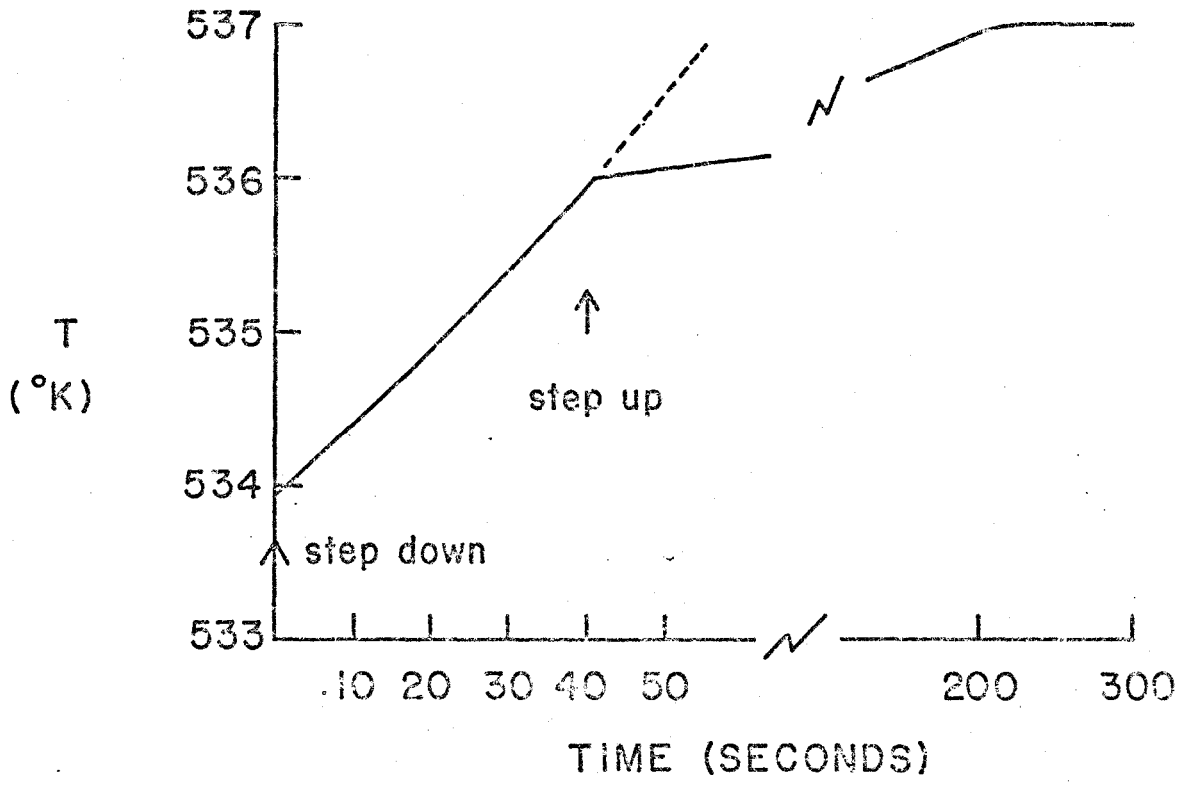

Figure 11: Hot Spot Temperature Dynamics in Response to a 40% Pulse in H_2 Flow. (80^{th} Order Simulation).

Part B: Development of a Low Order State Space Model for Process Control

4.8 Quasi-Steady State Approximation

Up until this point, the development has been perfectly general in the sense that no specific reaction scheme or reactant properties has been assumed in the development of the mathematical model in Chapter 3. However in the present reactor, as with most solid catalysed gas reactions, the ratio of the concentration wave velocity v_C to the thermal wave velocity v_T (see Equations (3-10) and (3-11)) is very large ($\sim$ 1400, here). This in effect, implies that the concentration profiles reach a quasi-steady state rapidly in response to some shock to the system (see Section 4.7.3, Figure 9) and this quasi-steady state then follows the slowly changing temperature profile. This quasi-steady state dynamic character of the reactor was discussed in Sections 2.2.2 and 4.2, where it is mentioned that, although the quasi-steady state approximation is often used, it is seldom verified for a specific system. In this respect, the 80^{th} order and 140^{th} order models were helpful and indicated that within about 3 seconds, the concentration dynamics had steadied out (Section 4.7.3, Figure 9). Since we are interested in sampling intervals of the order of 60 seconds (so that we can follow the temperature dynamics), the quasi-steady state approximation is quite adequate for our system (and indeed, for most gas/solid fixed bed reactor systems (see Section 2.2.2)).

The quasi-steady state approximation allows us to set the concentration time derivatives approximately to zero: in Equations (4-22) and (4-23) we can thus write

$$\frac{\partial C^i}{\partial t} \simeq 0 \tag{4-40}$$

Note that (4-40) does not imply that concentrations are not a function of time, since concentrations are coupled to temperatures via (4-41) (previously (4-24))

$$- v_T \frac{\partial T_o}{\partial z} + \frac{\lambda_{er} 4B_i}{R^2 \bar{C}(B_i + 2)} [T_w - T_o] + \left. \frac{\sum_{i=1}^{3} \Delta h_i R_i \rho_B}{\bar{C}} \right|_{r=0} = \frac{\partial T_o}{\partial t} \tag{4-41}$$

where reaction rates R_i are a function of concentrations, and temperatures obviously change with time according to (4-41). Incorporating the quasi-steady state assumption, the concentration Equations (4-22) and (4-23) become:

$$\frac{\partial C_o^i}{\partial z} = \frac{D_{er}}{\varepsilon R^2 v_C} [\beta_{31} C_o^i + \beta_{32} C_3^i] - \left. \frac{R^i \rho_B}{\varepsilon v_C} \right|_{r=r_3} \tag{4-42}$$

$$\frac{\partial C_3^i}{\partial z} = \frac{D_{er}}{\varepsilon R^2 v_C} [\beta_{01} C_o^i + \beta_{02} C_3^i] - \left. \frac{R^i \rho_B}{\varepsilon v_C} \right|_{r=0} \tag{4-43}$$

4.9 Axial Collocation

Typical concentration profiles along the length of the reactor, obtained from steady state simulations (Figure 8) indicate that these profiles can be approximated by relatively low order polynomials. However, certain temperature profiles (curve 1, Figure 4) may need a much higher

order. Michelsen (M2) used axial collocation for his reactor and was able to adequately represent the dynamic behaviour of his reactor using 6 collocation points. Although more collocation points can reduce approximation error, numerical ill-conditioning induced by the collocation weights begins to swamp the error.

One of the problems of fitting high order polynomials to process curves is that the polynomials, if of sufficiently high order, may begin to ripple along the curve and since we are using these collocation formulae to approximate derivatives, the dangers are apparent. The order of the collocation approximation must be chosen with these facts in mind. It is seen in the next section that the order (n') of the state space model becomes equal to the order of the collocation approximation (n), plus 1 (see also discussion in Section 4.1 and 4.2). A 6^{th} order collocation approximation was tentatively assumed ((n) = 6) (this implies 7 collocation points, excluding $z_0 = 0$, where we have constant inlet conditions over a sample period). The corresponding 7^{th} order model together with other models of different size was simulated and compared. A non-symmetric function is required and Finlayson (F7) suggested one of the form

$$T^{(n)} = T(z = 0) + z \sum_{i=1}^{n+1} a_i^{(n)} P_{i-1}(z) \qquad (4\text{-}44)$$

where $a_i^{(n)}$ are coefficients to be determined and P_i are Legendre polynomials, (n) is the order of approximation and $T^{(n)}$ is a polynomial of order n+1. An analagous expression for the first derivative (see 4-4) is obtained for collocation point z_i at $z = z_i$:

$$z = z_i \quad \frac{\partial T}{\partial z}^{(n)} = \sum_{i=1}^{n+1} D_{ij}^{(n)} T_j^{(n)}(z,t) \tag{4-45}$$

A corresponding expression for the concentration derivative may be written. The $D_{ij}^{(n)}$ weight may be calculated according to Finlayson (F7), Chapter 5.

4.9.1 Application to Reactor Equations

Rewriting Equations (4-41), (4-42), (4-43)) using (4-45) to approximate the axial z derivative, one obtains a set of (n+1) ODE's from the temperature Equation (4-41), at n+1 (= 7 here) different axial collocation points z_i. Two sets of algebraic equations are obtained from the concentration Equations (4-42) and (4-43). The temperature differential equations are obtained as

$$z = z_i \quad \frac{dT_o(i)}{dt} = - v_T \frac{\partial T_o}{\partial z}\bigg|_{z_i} + \frac{\lambda_{er} 4B_i}{R^2 \bar{C}(B_i + 2)} [T_W - T_o(i)] + \frac{\sum_{i=1}^{3} \Delta h_i R_i \rho_B}{\bar{C}}\bigg|_{\substack{r=0 \\ z=z_i}} \tag{4-46}$$

$i = 1,2,\ldots n'$ where $n' = n+1$

When we subsitute Equation (4-45) for the axial derivatives where they appear, we obtain two sets of algebraic equations from Equations (4-42), (4-43) and a set of n+1 ordinary differential equations from Equation (4-46).

All equations at this stage are non-linear and to obtain the standard state space equation (see Equation (4-39) we must linearise the algebraic and differential equations about some operating profile. An operating profile can be calculated from the non-linear steady state versions of Equations (4-41), (4-42), (4-43) with (4-25)), by simply setting all time derivatives to zero and integrating the resulting set of non-linear ordinary differential equations in z. If we express the radial temperature at the edge of the bed, T_3, in terms of the temperature along the central axis, T_0, using Equation (4-25) we can linearise the two sets of algebraic equations and the set of ordinary differential equations in terms of the deviation variables $\Delta\underline{C}_o$, $\Delta\underline{C}_3$, $\Delta\underline{T}_o$, together with two controls $\Delta u_1, \Delta u_2$ representing the flow rates of the two reactants. The following equations are obtained:

$$A_1\Delta\underline{C}_o = A_2\Delta\underline{T}_o + A_3\Delta\underline{C}_1 + A_4\Delta\underline{u} \tag{4-47}$$

$$B_1\Delta\underline{C}_1 = B_2\Delta\underline{T}_o + B_3\Delta\underline{C}_o + B_4\Delta\underline{u} \tag{4-48}$$

$$\frac{d\Delta\underline{T}_o}{dt} = E_1\Delta\underline{T}_o + E_2\Delta\underline{C}_o + E_3\Delta\underline{u} \tag{4-49}$$

calling the state space model order $n' = n+1$, we then have:

$$\underset{3n'x1}{\Delta\underline{C}_o} = [\Delta C_o^1(z_1)\Delta C_o^1(z_2)\ldots\Delta C_o^1(z_{n'}),\ldots,\Delta C_o^3(z_1)\ldots\Delta C_o^3(z_{n'})]'$$

$$\underset{n'x1}{\Delta\underline{T}_o} = [\Delta T_o(z_1)\Delta T_o(z_2)\ldots\Delta T_o(z_{n'})]'$$

$$\underset{2x1}{\Delta u} = [\Delta u_1 \Delta u_2]'$$

and A_j, B_j, E_j, j = 1,2,3,(4) are matrices of constants representing the partial derivatives of the various terms in Equations (4-41), (4-42), and (4-43) evaluated at a given operating profile.

It is possible using Equations (4-47) to (4-49) to eliminate concentration to obtain a self consistent set of ordinary differential equations in temperature alone.

From (4-47) and (4-48)

$$\Delta \underset{-}{C}_o = X_1 \Delta \underset{-}{T}_o + X_2 \Delta \underset{-}{u} \tag{4-50}$$

substituting into (4-49) gives

$$\underset{n' x 1}{\frac{d\Delta \underset{-}{T}_o}{dt}} = \underset{n' x n'}{\overline{A}} \; \Delta \underset{-}{T}_o + \underset{n' x 2}{\overline{B}} \; \Delta \underset{-}{u} \tag{4-51}$$

where

$$X_1 = (A_1 - A_3 B_1^{-1} B_3)^{-1} (A_2 + A_3 B_1^{-1} B_2)$$

$$X_2 = (A_1 - A_3 B_1^{-1} B_3)^{-1} (A_4 + A_3 B_1^{-1} B_4) \tag{4-52}$$

$$\overline{A} = E_1 + E_2 X_1$$

$$\overline{B} = E_3 + E_2 X_2$$

Equation (4-51) is a self consistent set of n' linear state

equations in temperature where $n' = n+1$ and n is the order of the collocation approximation in (4-45). In our case, a value of $n'=7$ was tentatively assumed to be adequate after simulation with higher orders (up to n=11) resulted in essentially identical profiles. Lower values of n' (< 5) began showing differences in the profiles.

4.10 Discrete State Space Model

The state space model (4-51) is now in the standard form of Equation (4-53) and can be used to formulate optimal control schemes.

$$\dot{\underline{x}} = A\underline{x} + B\underline{u} \tag{4-53}$$

$$\underline{y} = H\underline{x} \tag{4-53a}$$

However, since the reactor is to be controlled directly by a digital computer, it will be more convenient to have it in the corresponding discrete form.

The formal discrete solution to Equation (4-53) is well known and may be expressed as (Noton (N1)):

$$\underline{x}(t+1) = \exp[At]\underline{x}(t) + \int_0^t \exp[A(t-s)]B\underline{u}(s)ds \tag{4-54}$$

where t is the sampling interval and exp[ ] represents the exponential matrix.

Assuming that control is implemented in a step-wise manner at the sampling instants and the control variables held constant over the interval, s, that is

$$u(s) = u(t) \qquad (4\text{-}55)$$

$$t \leq s < t + 1$$

Noton (N1) provides a simple and effective method for expressing Equation (4-54) in the form

$$\underline{x}(t + 1) = F\underline{x}(t) + G\underline{u}(t) \qquad (4\text{-}56)$$

This indirect method for evaluating the exponential matrix involves integrating the continuous form (4-53), up until time t with the initial conditions given by

$$\underline{x}(o) = [1\ 0\ 0\ --\ 0]',\ \underline{u}(o) = [0\ 0]'.$$

The solution at $\underline{x}(t)$ is seen from (4-54) to be the first column of exp[At]. By proceeding in this manner until each element of $\underline{x}(o)$ and $\underline{u}(o)$ has in turn been set to unity (the others remaining at zero), we can obtain all the columns of the discrete form matrices F and G in Equation (4-56).

In the state Equation (4-51), the 7 state variables ($n' = 7$) are the deviation temperatures (about the operating profile) at the n' collocation points along the central axis of the reactor. In the actual reactor, temperature measurements will be available at 9 equally spaced points along the central axis. These 9 axial temperatures will have to be expressed in terms of the 7 states, $\underline{x}_i$, in order to obtain a measurement equation of the form (see (4-3))

$$\underline{y}(t) = H\underline{x}(t) \tag{4-57}$$

This problem will be discussed in Section 5.1.1. The concentrations may also be expressed as a function of the 7 states, $\underline{x}_i$; this is discussed in the next section.

4.10.1 Concentration as a Function of Temperature

The measurement equation given in (4-3a) is general enough to accommodate the form suggested by Equation (4-50) for concentration as a function of temperature. Since we are more interested in mixed (radially averaged) concentrations at the reactor exit, Equation (4-50) has to be modified for averaged concentrations.

Following Villadsen (V1), the radially averaged concentrations throughout the reactor may be obtained using the collocation integration formulae (see Equation (4-3)) and Section 4.6.1).

$$\bar{C}^i(z,t) = 2\int_0^1 C^i(z,t,r)rdr = \sum_{j=1}^{n+1} w_j^{(n)} C^i(z,t,r_j) \tag{4-58}$$

where $w_j^{(n)}$ are n^{th} order collocation integration weights. Assuming a quartic radial profile for concentration, we obtain (see Section 4.6.1)

$$\bar{C}^i = w_1 C_o^{\ i} + w_2 C_3^{\ i}, \qquad i = 1,2,3 \tag{4-59}$$

and in terms of deviation variables

$$\Delta\bar{C}^i = w_1 \Delta C_o^{\ i} + w_2 \Delta C_3^{\ i}, \quad i = 1,2,3 \tag{4-60}$$

The expression for ΔC_o^i in Equation (4-50) together with an analogous one for ΔC_3^i may be substituted into (4-60) to obtain an expression for the vector of radially averaged (deviation) concentrations $\Delta\bar{\underline{C}}$ as a function of (deviation) temperatures and (deviation) manipulated variables at the previous time interval in the form

$$\Delta\bar{\underline{C}}(t) = X_3\Delta\underline{T}_o(t) + X_4\Delta u(t-1) \qquad (4\text{-}61)$$

The mixed exit concentration vector $\Delta\bar{\underline{C}}_{ex}$ (at z = 1.0) can be obtained by selecting that row of matrices X_3 and X_4 which correspond to exit conditions for each of the three species. Thus the three element vector of radially averaged exit concentrations can be expressed in terms of the temperatures and flows as

$$\underset{3x1}{\Delta\bar{\underline{C}}_{ex}(t)} = \underset{3x7}{M}\Delta\underline{T}_o(t) + \underset{3x2}{N}\,\underline{u}(t-1) \qquad (4\text{-}62)$$

4.11 Simulation Studies

4.11.1 Steady State Behaviour

The steady states of the quasi-steady state model Equations (4-41) to (4-43) and the full dynamic Equations (4-22) to (4-25) are identical and have been studied in Section 4.7.1.

4.11.2 Dynamic Behaviour

In the absence of sufficient dynamic data at this stage, no detailed comparison of the dynamic behaviour of the 7^{th} order state space model could be made. Nevertheless, general trends and approximate values of time constants available from the previous experimental study (Tremblay (T2) indicated realistic dynamic behaviour of the model.

In Figure 12 some results of a dynamic simulation using this model (Equation (4-51)), are shown. Starting at the initial steady state curve (1) a 3% increase in the hydrogen flow was made. Curve (2) represents the dynamic response after 10 minutes and curve (3) represents the final steady state as predicted from the linearised state space model. Computations were performed using a Bulirsch-Stoer (B10) integration method and required 1 second of CDC 6400 computation time for 250 seconds of reactor time. A considerable improvement on the previous model (Section 4.7.3).

To investigate the effects of axial collocation and of linearising the model about its original steady state (1), the new steady-state profile (at a 3% increase in hydrogen flow) was also computed using Equations (4-41),to (4-43) which contain none of the above approximations. This profile is shown as curve (4). The combined effect of non-linearities and axial collocation are obviously quite strong and presumably the success of a control scheme based on the linearised state space model (4-51) will depend on the magnitude of the disturbances present and upon the severity and stability of the operating profile about which control is to be attempted.

The response of the linearised model (4-51) to a pulse (+ 10%) in hydrogen flow rate lasting for 120 seconds is shown in Figure 13. The most noteworthy observations are that the hotspot location shifts significantly during the transient. The final steady state profile agrees with the initial one after about 50 minutes. These responses will have to be evaluated in light of the actual reactor data but in the meantime give some indication of the reactor model performance.

In the next section, the model is fitted to experimental dynamic data. This places us in a much better position to evaluate the model performance.

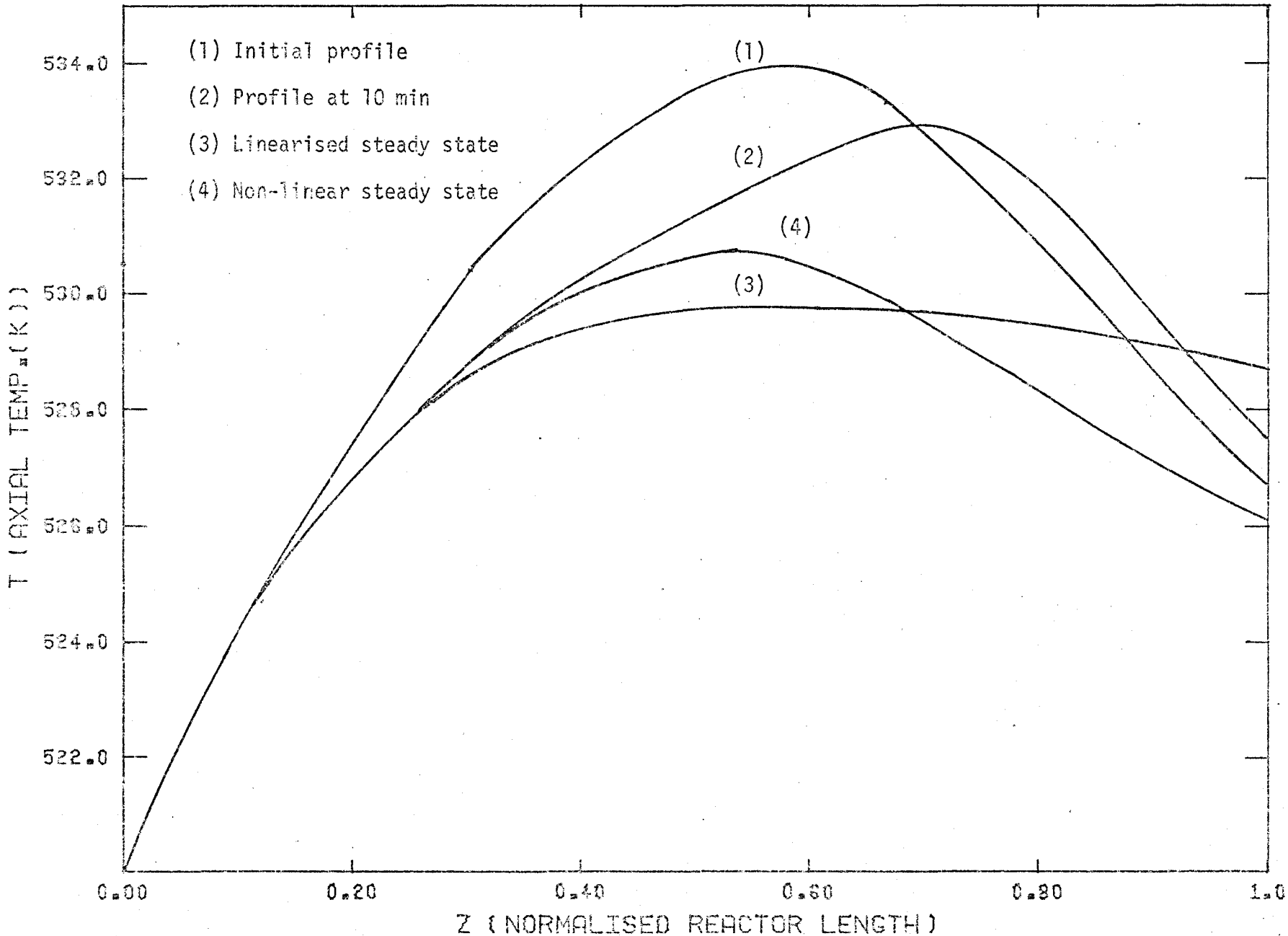

Figure 12: Typical Dynamic Temperature Profiles in Response to a + 3% Step in H_2 Flow (7^{th} Order Simulation).

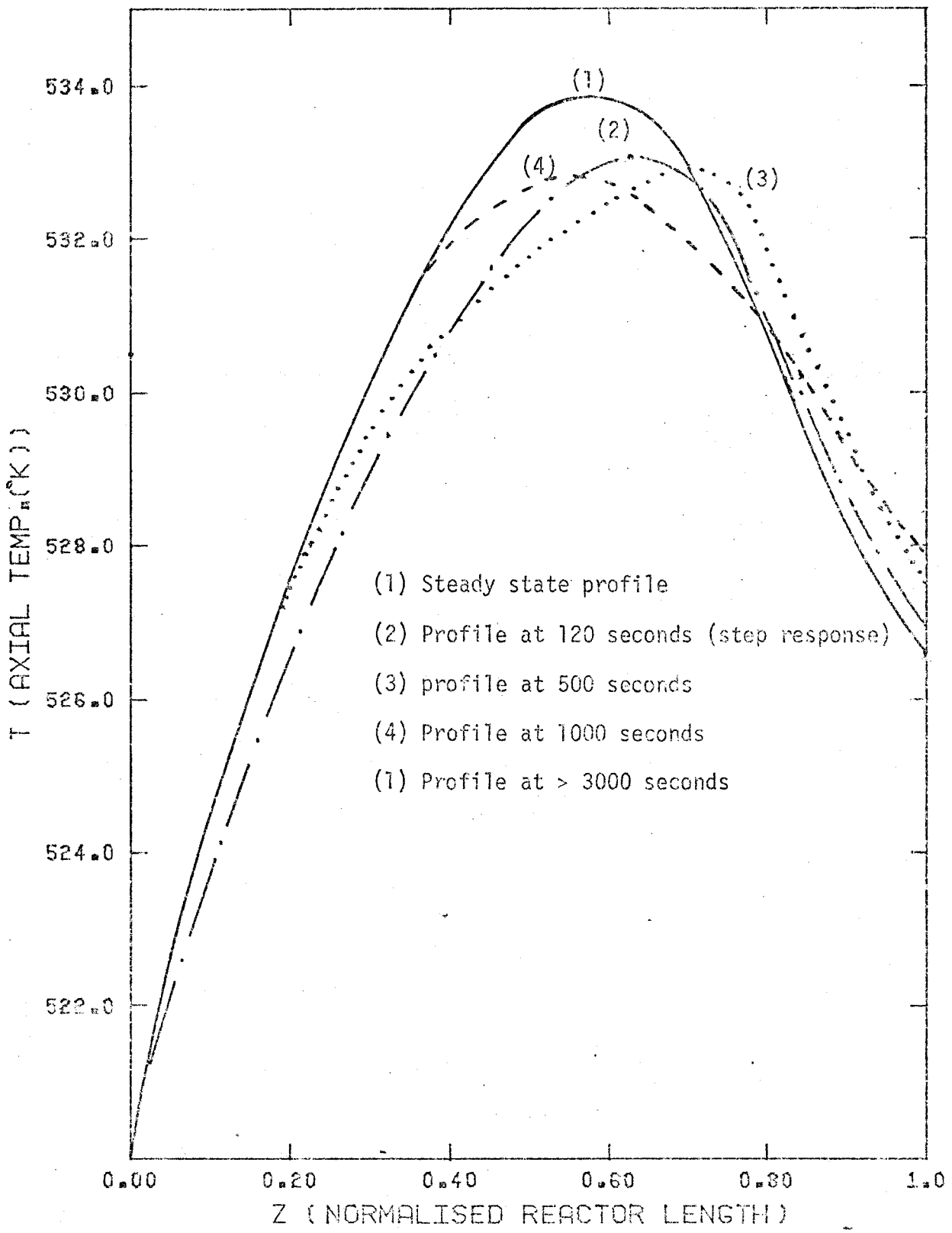

Figure 13: Typical Dynamic Temperature Profiles in Response to a + 10% Pulse in H_2 Flow, Length of pulse 120 sec (7^{th} Order Simulation).

CHAPTER 5

FITTING THE REACTOR MODEL TO EXPERIMENTAL DATA

5.1 Introduction

A process description has been given in Section 3.2. In this section, we describe how the reactor was configured for the purpose of data collection. These data were used in estimating the parameters in the state space model prior to its use for on-line control of the reactor. We describe here what measurements were taken, how the data were collected and the techniques used, first, to fit the dynamic model, and then the dynamic-stochastic state space model.

5.1.1 Measurements

In Section 3.2.1, the advantage of measuring temperatures instead of concentrations for a reactor system was presented. In Section 4.10.1, an expression was derived relating the exit concentrations to the axial temperatures and inlet flows (controls). Initially, we rely on temperature measurements and any concentration information is obtained from Equation (4-62).

Temperatures in the reactor are obtained sequentially using a mechanical multiplexer activated once a second by a relay in the minicomputer. The multiplexer connects each thermocouple in turn to an amplifier/transmitter which transmits the signal to the computer. Each thermocouple is read once every 12 seconds. A completely digital

multiplex system, together with individual amplification for each thermocouple signal, would have permitted more rapid scanning of the temperatures, and measurement noise levels would have been reduced. Noise level on the thermocouples was estimated by setting the reactor temperature to some constant value and then taking temperature readings for several minutes. The data indicated two things:

(i) $\pm 2\sigma$ limits for temperature measurements were of the order of $\pm 4°C$.

(ii) a level bias was detected for certain thermocouples. In particular, the second thermocouple from the entrance had a bias of - 4.5°C. Other thermocouples (usually only one or two) developed smaller biases, and furthermore, these biases were not constant for each experimental run. The exact reason for these biases could not be determined, but was probably due to contact resistances in the thermocouple welds. See Figure 16.

It was mentioned in Section 3.2 and 4.10 that axial temperature measurements are available at nine positions along the length of the reactor. However, the 7^{th} order state model for control is given in terms of (deviation) temperatures at the 7 collocation points in z (see Section 4.9.1). The normalised distances at which 9 temperature measurements were available are compared with the 7 collocation points.

Measurements	Collocation Points
0.0	0.0
.034	.034
.158	.169
.282	.381
.407	.619
.531	.831
.655	.966
.779	1.0
.904	
1.0	

The 9 measured temperatures were "converted" to 7 temperatures at the collocation points by:

(1) selecting the measurement temperature closest to a collocation point;

(2) choosing the two measurement temperatures on either side of this centre temperature;

(3) using quadratic interpolation. An alternative method would have been to express the 9 measured temperatures as a function of the 7 collocation point temperatures through a polynomial model but this was considered less reliable.

With the 7 interpolated collocation temperatures, the measurement equation (see 4-53a) becomes

$$\underline{y}(t) = I_7 \underline{x}(t)$$

where I_7 is the 7^{th} order unit matrix

Input flow measurements of the two reactants, Hydrogen and Butane, were obtained by measuring pressure drop across lengths (162 and 19 cm, respectively) of stainless steel needle tubing (I.D.'s 0.137 and 0.0838 cm respectively). This pressure drop is converted to a voltage by a differential pressure (DP) transmitter which transmits the voltage signal to the minicomputer.

From the reaction scheme (Section 3.3), the stoichiometric ratio of Hydrogen to Butane is 3.0. If the feed ratio becomes less than this, carbon is deposited on the catalyst causing it to deactivate, thus leading to a shutdown of the reactor. The minimum hydrogen flow rate was set at 3.5 times the butane flow rate for process operation.

Flow rates of the reactants were maintained at their set points through single loop PI flow controllers. The flow controller for the hydrogen flow had a fairly damped,smooth response. The butane flow control was more erratic and tended to oscillate somewhat in response to a step change in set point. This was due to the fact that the lower flows of butane caused a smaller pressure drop signal to be sent to the DP transmitter (which has a noise level of its own). Thus the feedback signals for the butane flow control loop had a lower signal to noise ratio than those for the hydrogen flow control. The time constants for both flow control loops were nevertheless no more than 1-2 seconds, and since the intended sampling interval for the system was 60 seconds, the dynamics of these loops could be neglected, relative to the sampling interval.

Although the length of the reactor is given as 28.0 cm, only 25.6 cm was used; the last few cm were filled with inactive catalyst. The catalyst bed is supported by a sintered stainless steel disk (Type H, pore size: 5 microns). This disk (due to the mechanical configuration) is at the reactor wall temperature, and caused the downstream end of temperature profile to be dragged down to the wall temperature. This in effect would require an extra boundary condition on the reactor energy equation. The inactive catalyst minimised the effect of the sintered disk.

5.1.2 Catalyst Activity

One of the most important parameters as far as reactor performance is concerned, is the catalyst activity. This parameter cannot be directly measured and must be estimated, a posteriori, in conjuction with several other parameters.

From the reactor model equations (Section 3.4) and the reaction rate equations (Appendix 1), one can see that no provision is made for a time varying catalyst activity. Certainly, from experience gained with this catalyst in previous years (O1, S4), no significant loss of activity was expected during the period of an experimental run ($\sim$ 10 hours). This fact was confirmed in our own experimental work. However, after a run, the reactor is shut down and the catalyst is stored inside the reactor under a blanket of hydrogen or carbon dioxide. Some loss of activity was evident after a period of several days (especially under hydrogen blanket storage). This is detected by the fact that a

higher wall temperature is necessary to achieve the same hot spot temperatures that were obtained previously with a lower wall temperature. The loss of activity may of course, be due to either the shutdown or startup procedure since no catalyst deactiviation was observed during an experimental run.

Nevertheless, this presented a problem for parameter estimation. The parameter estimation was done off-line and usually took several days. For this period, the reactor was shut down. The parameter estimates obtained, would then no longer be valid for the next run. This problem is somewhat due to the laboratory nature of the experiments. An industrial process reactor is not often shut down (unless there is a failure or production considerations demand it) and if catalyst activity is constant during operation, the off-line parameter estimates would be valid and could be implemented several days later in an on-line switch-over to the updated control model.

An alternative solution is to simply start up the reactor with fresh catalyst every time. However, preparation of two batches of catalyst to an exact specification was very difficult (see Tremblay (T4)).

Another alternative that was used successfully in a previous study on an isothermal packed-bed reactor (O1, S4), was to recondition the catalyst in the reactor at temperatures 150°K or more above operating conditions prior to a run. This was tried by Tremblay in his earlier reactor (T2) but led to severe leakages of hot smoking oil. For the reactor used in this study, catalyst was conditioned externally

and transferred under blanket CO_2 to the reactor. Even so, prior to a run in this study, the hot spot was permitted to rise well above operating conditions for several minutes before cooling and commencement of a run. For a rapidly changing catalyst activity, one would have to specifically take account of the activity change by modelling it, or using an adaptive strategy for updating the control model on-line (see Tremblay (T4)).

5.2 Data Collection Under Closed Loop

In classical linear system identification techniques (frequency response and pulse testing methods), data are collected under open loop as required by the theory. However, in this situation, we have a non-linear model of the reactor which is linearised about some operating profile and thus is valid only in this region. Response data must thus be collected within a restricted region around the operating profile. Therefore, some type of feedback control, implemented either by an operator or computer, is necessary while the data are being collected. Care must be exercised in analysing this closed loop data [(B3), (B4) and (S8)]. Box and MacGregor show (B3) that if standard statistical model identification techniques (using cross and auto-correlation analysis) are applied to closed loop data from a linear process, under a linear feedback control law, the controller transfer function, rather than the system transfer function, will be identified. They show how the addition of a deliberately added random component, i.e., a "dither" signal, to the feedback loop (while causing some loss in the quality

of control) allows one to properly identify the process transfer function.

Parameter estimation with closed loop data is discussed by Box and MacGregor (B4). They show that it may not be possible to estimate all parameters of a given linear dynamic-stochastic model separately, and that under certain conditions, the covariance matrix of the model parameters becomes singular. They derive the necessary and sufficient conditions for a singular estimation problem. The addition of a dither signal to the feedback loop while collecting data, breaks the estimation singularity and dramatically improves the estimation problem. Thus, just to ensure identifiability, "dither" signals were added to the reactor control signals during data collection. A white noise signal was added to the hydrogen flow control loop and an autoregressive signal to the butane flow which was left under open loop. The system is shown schematically in Figure 14.

The proportional-integral (PI) controller for the hydrogen flow rate used a function of the temperatures measured along the central axis of the reactor as an effective controlled variable. This function of temperatures was chosen to include information about both the height of the hot spot temperature and its axial position along the bed. Various linear and non-linear functions of the temperatures were tried, none of which appeared significantly superior to the rest. A controlled variable of the form (5-1) appeared to be the most adaptable:

$$T_{eff} = \sum_{i=1}^{n} \alpha_i T_i \qquad (5\text{-}1)$$

where the α_i are position weights and were selected to suit a particular temperature profile about which data was collected. For many profiles, this type of function gave adequate control and variations of the temperature profiles about a given operating profile were suitably restricted. Unfortunately, the expression in (5-1) was not adequate for all operating temperature profiles, particularly for profiles where the hot spot was well centered but not too high. In fact, this central position was difficult to control and experimentally appeared very much to behave as though it was an unstable steady state. Any slight change in the flow controls would cause the hot spot to soar upwards by 100 to 200°C. An opposite change in flows could just as easily cause a sudden quenching of the reaction. The severity of the control problem was thus very dependent on the chosen operating temperature profile about which control was desired. Data were collected about a suitable profile over several hours with a discrete sampling interval of 60 seconds. Usually about 100 data points were selected for the parameter estimation stage.

Dynamic data for the experimental runs is given in Appendix 3.

5.3 Parameter Estimation and Model Fitting

The reactor partial differential equations contain several parameters which must be estimated from multiresponse data. In this section we discuss briefly, multiresponse estimation theory and show

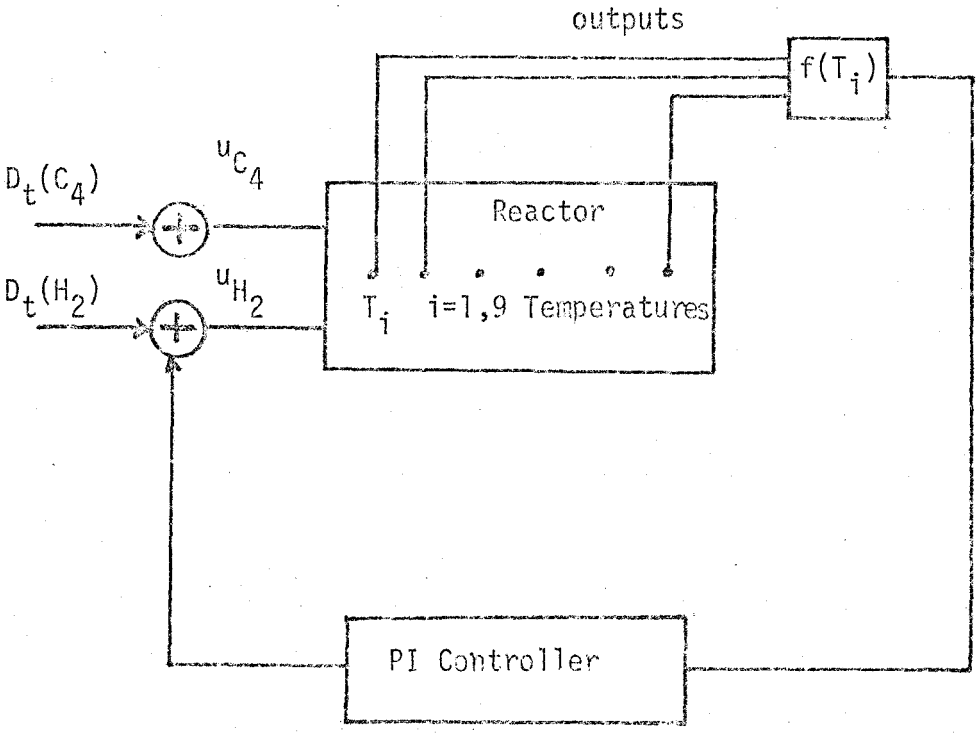

$D_t(C_4)$ dither signal for butane (Autoregressive(1) $\phi = 0.6$)

$D_t(H_2)$ dither signal for hydrogen (White noise)

u_{C_4} Butane flow

u_{H_2} Hydrogen flow

Figure 14: Closed Loop Data Collection Configuration (Temperature Measurements only).

how it is applied when fitting the state space model to the reactor data.

5.3.1 Multiresponse Estimation

Least squares parameter estimation in systems where a single response is measured is a well known procedure. Justification for this method relies on the assumption that the measurement errors are independent normally distributed random variables, with zero mean and constant variance. The least squares criterion for single response systems can be derived using a Bayesian approach. Box and Draper (B5) have used a Bayesian approach to obtain a multivariate criterion to be minimised, when estimating common parameters in multiresponse systems. Using a multivariate Bayesian posterior density function, they first obtain the marginal distribution of the parameters and then show how one can maximise this by minimising the determinant, J:

$$J = \left| \sum_{i=1}^{N} \underline{\varepsilon}_i(\underline{\beta})\underline{\varepsilon}_i'(\underline{\beta}) \right| \qquad (5\text{-}2)$$

where $\underline{\beta}$ vector of the unknown parameters.

$\underline{\varepsilon}_i$ vector of residuals for the i^{th} data set

The $\underline{\varepsilon}_i$ are the residuals obtained when the model predictions are subtracted from the measured responses. Equation (5-2) represents the multivariate generalisation of the single response least squares criteria.

The determinant J may be minimised by several of the available optimisation techniques (gradient, direct search, simplex, etc. (see Himmelblau (H4)).

An iterative approach to obtaining the parameter estimates is given by Wilson (W2), who first obtains a conditional estimate of the dispersion matrix, D:

$$\hat{D}(\hat{\underline{\beta}}) = \frac{1}{N - m - 1} \sum_{i=1}^{N} \underline{\varepsilon}_i(\underline{\beta})\underline{\varepsilon}'_i(\underline{\beta}) \qquad (5\text{-}3)$$

where ^ indicates "estimate", and m is the number of responses. He then obtains a conditional estimate of the parameter vector $\underline{\beta}$, conditional on D, and by iterating between these two conditional estimates, he shows how the unconditional estimate of the parameters is obtained. A summary of his method and an algorithm is given by Jutan (J1).

5.3.2 A Method for Parameter Estimation in a State Space Model

In Section 4.10.1, we derived a 7^{th} order discrete state space model. If all temperatures along the length of the reactor are measured, the output vector will be 7x1 and the measurement matrix, 7x7:

$$\underset{7x1}{\underline{y}} = \underset{7x7}{H}\,\underset{7x1}{\underline{x}} \qquad (5\text{-}4)$$

For our state model we have (see (4-56))

$$\underset{7x1}{\underline{x}(t+1)} = \underset{7x7}{A}\underline{x}(t) + \underset{7x2}{B}\underline{u}(t) \qquad (5\text{-}5)$$

One common method for fitting a state space model is to simply guess the order of the state model, consider the elements of matrices, A, B, H to be parameters, and fit these parameters to the data by a least squares method. However, the number of parameters (126 if A, B and H are full) would be prohibitive even if a sparse canonical representation were used. Clearly a different approach is required.

An examination of the differential equations for the reactor (Section 3.4) shows that there are only a few parameters or groups of parameters which require estimation. One can identify four such parameters:

(1) D_{er} (effective radial diffusivity)

(2) (k/k_o) (catalyst activity, see Appendix 1)

(3) B_i (Biot number)

(4) λ_{er} (effective radial thermal conductivity)

There are of course, a whole series of parameters associated with the kinetics of the reaction system. For the present, these parameters are considered "known" and a further discussion is given in Section 5.3.3.

In Section 4.7.2, the reactor temperature profiles were shown to be insensitive to D_{er} and a precise estimate was not required. In Section 2.2, estimation of the Biot number B_i is discussed. Large

values of B_i imply that most of the resistance to heat transfer is in the bed itself rather than being lumped at the wall (Section 2.2.3). However, once B_i is larger than about 20, the precise value of B_i becomes less important as seen by Equation (4-16) where B_i occurs in a term of the form

$$\frac{\lambda_{er}^4}{R^2\bar{C}} \cdot \frac{B_i}{(B_i + 2)}$$

The Biot number for our reactor was estimated from the literature (B1) to be 43.5, and simulation studies showed quite clearly that any value of this order of magnitude produced essentially identical profiles.

Therefore, the primary estimation problem was reduced to two important parameters (k/k_o) and λ_{er}. In Chapter 4, it was shown that beginning with the partial differential equations, one could obtain a state model by the following stages:

(1) Apply collocation in radial direction,

(2) Solve steady state equations to obtain an operating profile,

(3) Apply collocation in axial direction,

(4) Linearise the collocated equations about an operating profile,

(5) Eliminate the concentration variables to obtain a continuous state model in the temperatures,

(6) Integrate the continuous model to obtain a discrete state space model of the form

$$\underline{x}(t+1) = A\underline{x}(t) + B\underline{u}(t)$$

The equation relating concentrations to temperatures (4-62) follows stage (6), and is written in the form

$$\underline{C}(t) = H\underline{x}(t) + G\underline{u}(t-1) \ .$$

The overall algorithm may thus be viewed as a "mapping" of a few physical parameters into the state matrices, A, B, H and G.

In stage (2) above, one of two approaches could be taken. The operating temperature profile was in fact the steady state profile obtained by solving the steady state versions of all 7 PDE's: 6 concentration and 1 temperature (4-22) to (4-24). Alternatively, the operating temperature profile was obtained by averaging the temperature data in time to obtain an average operating temperature profile. The concentration profiles corresponding to this, were obtained by solving the steady states of the remaining 6 concentration Equations (4-22) to (4-23).

Once the state model is in the discrete form, the residuals may be obtained by iteratively solving for the states $\underline{x}(t)$ at t = 0,1,2,... etc., and then using the measurement equation to obtain the predicted output temperatures from $\underline{y}(t) = H\underline{x}(t)$, where (from Section 5.1.1) $H = I_7$, the 7^{th} order unit matrix. The residuals N(t) are calculated as

$$\underline{N}(t) = \underline{y}(t)_{observed} - \underline{y}(t) \qquad (5\text{-}6)$$

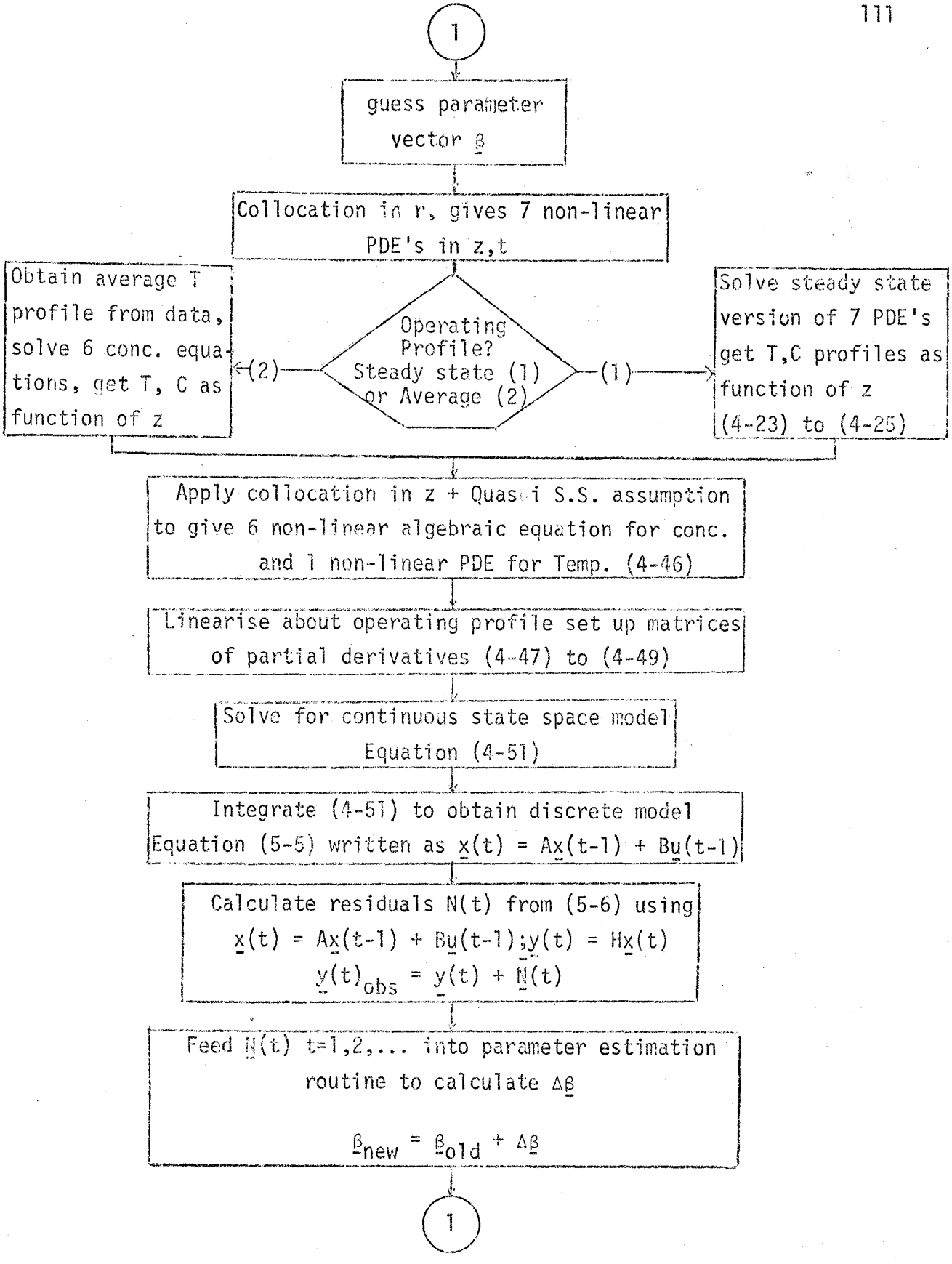

Figure 15: Flow Chart for Parameter Estimation Algorithm.

The residuals are fed to a multivariate parameter estimation routine which updates the initial parameter guesses in accordance with minimisation of the determinant J in (5-2). A flow sheet of the estimation algorithm is presented in Figure 15.

5.3.3 Application to Reactor Data

Several difficulties were encountered when the estimation algorithm in Figure 15 was applied to the reactor data.

(1) The estimation surface was very rough and many of the mimimisation routines simply converged on any one of the many local minima that were encountered.

(2) Extreme parametric sensitivity existed for the two important parameters, k/k_o and λ_{er}. Examination of the energy differential equation showed that these parameters featured prominently in the subtraction of two large, almost equal numbers. This can be demonstrated by writing the steady state energy balance equation as (see (4-24)),

$$\frac{dT}{dz} = \frac{\lambda_{er}(\text{heat removal}) - (k/k_o)(\text{heat generation})}{v_T} \qquad (5\text{-}7)$$

The small temperature wave velocity v_T ($= \sim 10^{-4}$) (prevalent in gas solid systems) magnifies the sensitivity of the derivative to the parameters λ_{er} and k/k_o. Often changes in the 3rd or 4th significant figure could cause dramatic changes in the reactor profiles. This situation was aggravated by the highly exothermic nature of the heat generation terms. The parametric sensitivity of the steady state temperature profile

to small changes in λ_{er} is illustrated in Figure 5a.

In order to obtain a sturdier control of the sensitivity of these two parameters, a third parameter was introduced by expanding the thermal conductivity parameter into effectively two parameters

$$\lambda_{er} = \lambda_o + \alpha(T^4 - T_w^4) \tag{5-8}$$

The extra parameter α allowed for fine tuning of λ_{er}. This particular form was chosen to i dentify the α parameter with a radiation effect, that would cause additional heat removal at high temperatures. See Section 3.4.

(3) High positive correlation existed among the parameters especially between λ_o and (k/k_o). This is again due to the form of Equation (5-7) where these parameters govern almost equal but opposite effects. Correlations of up to 0.998 were quite common and caused severe convergence difficulties. See Appendix 3.

(4) A large computational effort was involved in fitting these state models. It is evident from Figure 15, that a once through calculation to obtain the residuals involves a great deal of numerical computation(16-25 secs CPU time on a CDC 6400). It was thus important to use a highly efficient minimisation routine that required a minimum number of function evaluations to obtain an acceptable model fit. Marquardt's method (M4) proved to be superior to other methods used (Simplex, Powell, steepest descent, see (H1)).

(5) There existed, in effect, a discontinuity in the estimation

surface. This occurred when a particular set of parameter estimates gave rise to a dynamic A matrix for which the discrete state model had one or more eigenvalues outside the unit circle. The model is then dynamically unstable and the states increase in time without bound. The residuals become infinite and the response surface exhibits a discontinuity. These discontinuities were scattered across the response surface and appeared suddenly, for what seemed to be quite reasonable sets of parameters.

(6) All elements of the multivariate residual (noise) vector $\underline{N}(t)$ as previously indicated, represent the noise content of axial temperatures measured in the reactor. It is almost certain that, since we are dealing with noise content of related temperatures along a reactor profile, some of the elements of the noise vector $\underline{N}(t)$ are linearly dependent. It is reasonable to expect that any underlying noise or disturbance, affects the profile in such a way that certain temperatures would always tend to move in the same direction and manner as others. This implies that there are only a few fundamental disturbances which make up the 7 noise sequences in $\underline{N}(t)$ and that in fact, the $\underline{N}(t)$ vector is not fully 7-dimensional. This problem is dealt with in Section 5.4. Nevertheless, this linear dependence amongst elements of $\underline{N}(t)$, implies that the determinant criterion J in (5-2) will be nearly singular irrespective of how close we are to a minimum. This led to numerical instability and caused many of the minimisation routines to fail. A more stable objective function was simply the sum of the sum of squares of the residuals which does however, imply, for statistical justification, that there is no correlation between the elements of $\underline{N}(t)$

and that all the variances are equal (B5). This, in fact, was not true, but the procedure can be justified simply as a minimisation of a closeness of fit criterion to obtain reasonable estimates for the dynamic parameters. When a proper characterisation of the noise was added (see Section 5.4) more statistical justification was possible.

Further Observations on Estimation Difficulties

In Section 5.3.2, four important parameters were identified. This assumed that all the kinetic parameters (except catalyst activity) are known (from a previous study (O1, S4), see Appendix 1). It is common practice to perform kinetic studies on one reactor (for experimental convenience) and then use the kinetic estimates obtained on this reactor when dealing with the same reaction in what may be a completely different reactor (size, type). However, it is true to say that the kinetic parameters estimated by studies on one reactor may not be valid for a new reactor. In fact, the parameters obtained should be treated as prior information and re-estimated along with the new parameters (H5). In our problem unfortunately, the introduction of 10 or 12 more kinetic parameters would make our estimation problem computationally unfeasible.

It may however be possible to update these kinetic parameters in a conditional fashion as described by Wilson (W2) (see Section 5.3.1). From the fitted models (see later), it appeared that the kinetic parameters obtained from the previous study (O1, S4) were adequate, and did not require re-estimation.

Procedure Adopted for Fitting a Model

(A) Time average the dynamic data from the reactor. This provided an average operating profile. It also showed up any thermocouple biases that existed (see Section 5.1.1 and also Figure 16) and these were corrected for by providing a counter bias so that the data point lay on a smooth curve passing through the remaining temperatures.

(B) Use the steady state version of the partial differential Equations ((4-22) to (4-24)), to set up a steady state grid search with the objective as the sum of squares of deviations from the given operating profile from step (A). This provided a feasible initial estimate for the parameter vector.

(C) Using a non-linear least squares routine based on Marquardt's method (M4), fit the steady state version of the reactor equations (see step (B)) to the operating profile. This provided reasonable initial estimates for the final dynamic data fit.

(D) Proceed with the dynamic model fit using estimates from step (C). Several iterations (B)to (D) were usually required.

Results

It was mentioned previously (Section 5.3.2) that for the dynamic fit, two alternative procedures were adopted: linearisation about the steady state temperature profile of the model, or linearisation about an average operating profile obtained from reactor data records. Usually,

these two profiles were similar, but in general, the average profile (see step (A)), was better centred in the data. In fact, there is no special motivation for linearising about a steady state in the vicinity of the operating profile and,as mentioned previously (Section 5.2), the experiments showed that the steady state in the vicinity of the operating profile appeared to be unstable, and any slight change in the flow controls caused large changes in the reactor temperature profile. It was thus not possible to obtain the steady state experimentally under open loop.

Results of the fitting process are illustrated in Figures 16, 17, 18 and 19 for a particular run 26 May, 1976 and the state space model obtained is given in Appendix 3. Figure 16 shows the operating profile obtained by averaging the dynamic data in time. Biases on thermocouples 2 and 7 are clearly shown and counter biases are added to make all data points lie on a smooth curve.

Figure 17 shows the operating profile as well as how well the dynamic model (which is linearised about this operating profile) predicts the dynamic data. In this figure, the profiles at t = 4 and t = 11 minutes are shown as well as the 2 σ limits for the thermocouple measurement error,calculated by taking the average variance of the $\underline{N}(t)$ vector. The predicted profiles are well within these 2 σ limits indicating a good fit. An overall measure of the fit for all time is given by the sum of the variances of $\underline{N}(t)$; for Figure 17, this value is 48.5 indicating a good fit. Total sum of squares of residuals was 2867. The dynamic data, the estimation program used and the state space model obtained are

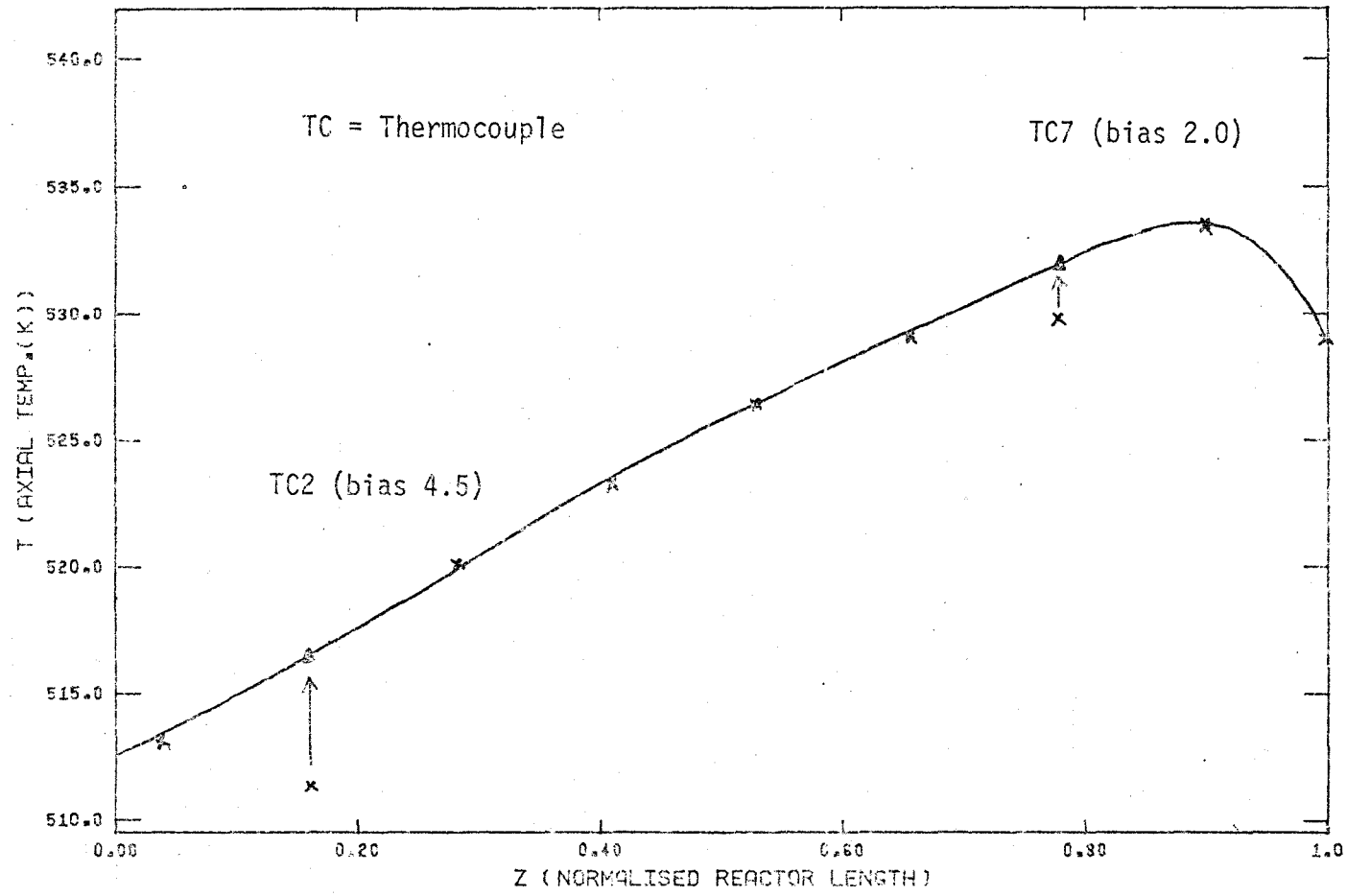

Figure 16: Time Average Operating Profile (26 May Data).

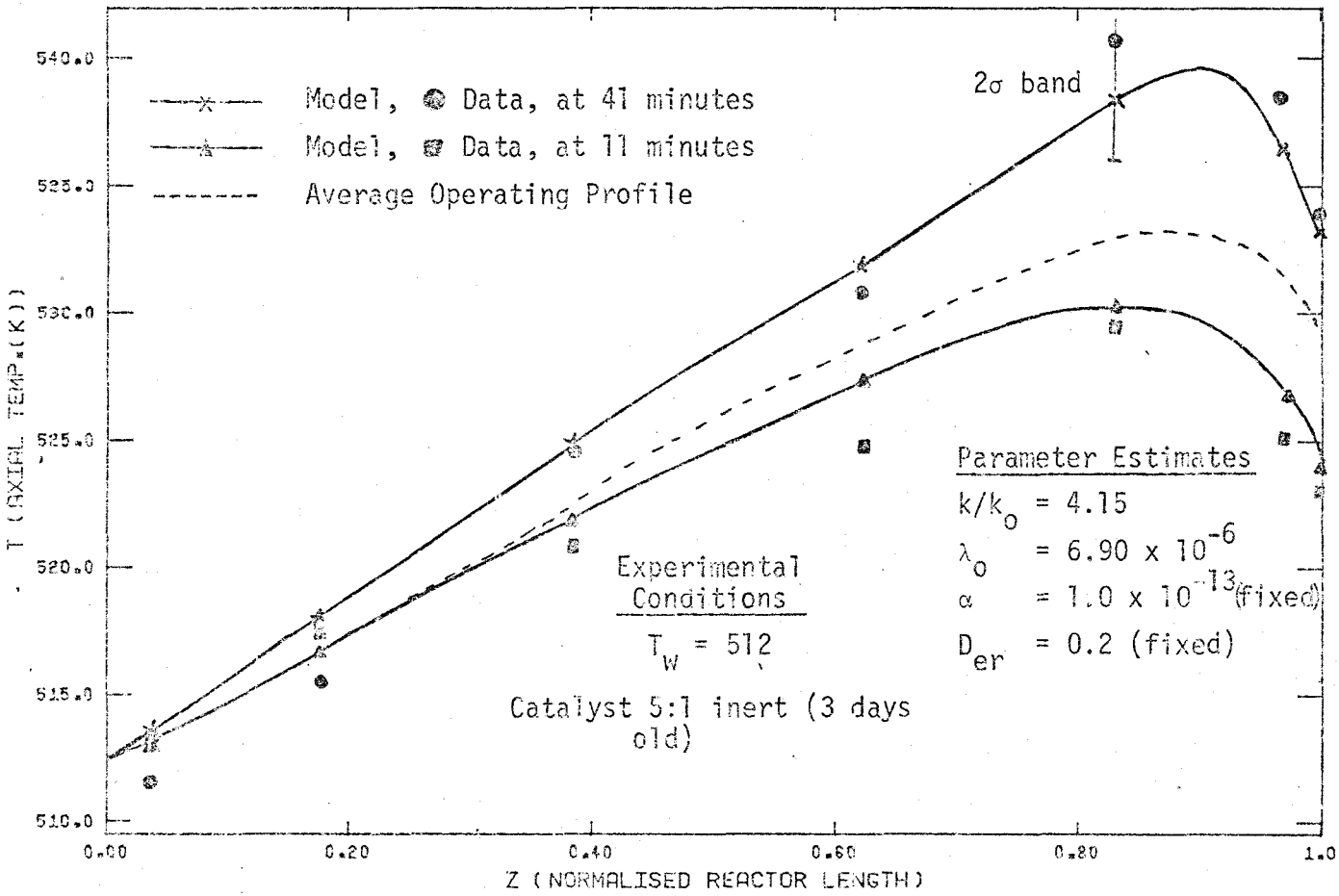

Figure 17: Axial Temperature Profiles, Model vs. Data (Linearisation about Average Profile in Figure 16) (26 May Data).

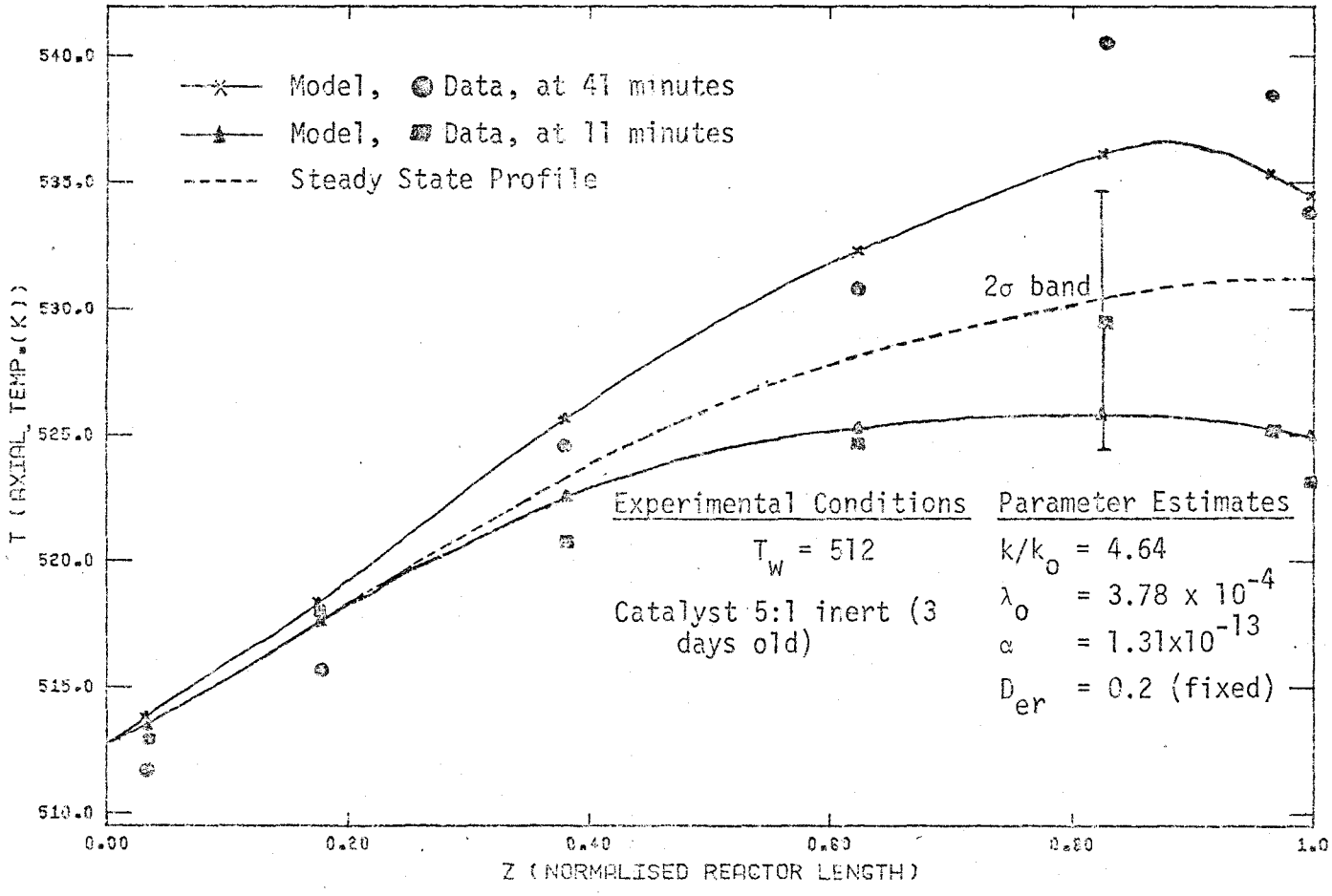

Figure 18: Axial Temperature Profiles, Model vs. Data (Linearisation about Steady State Profile) (26 May Data).

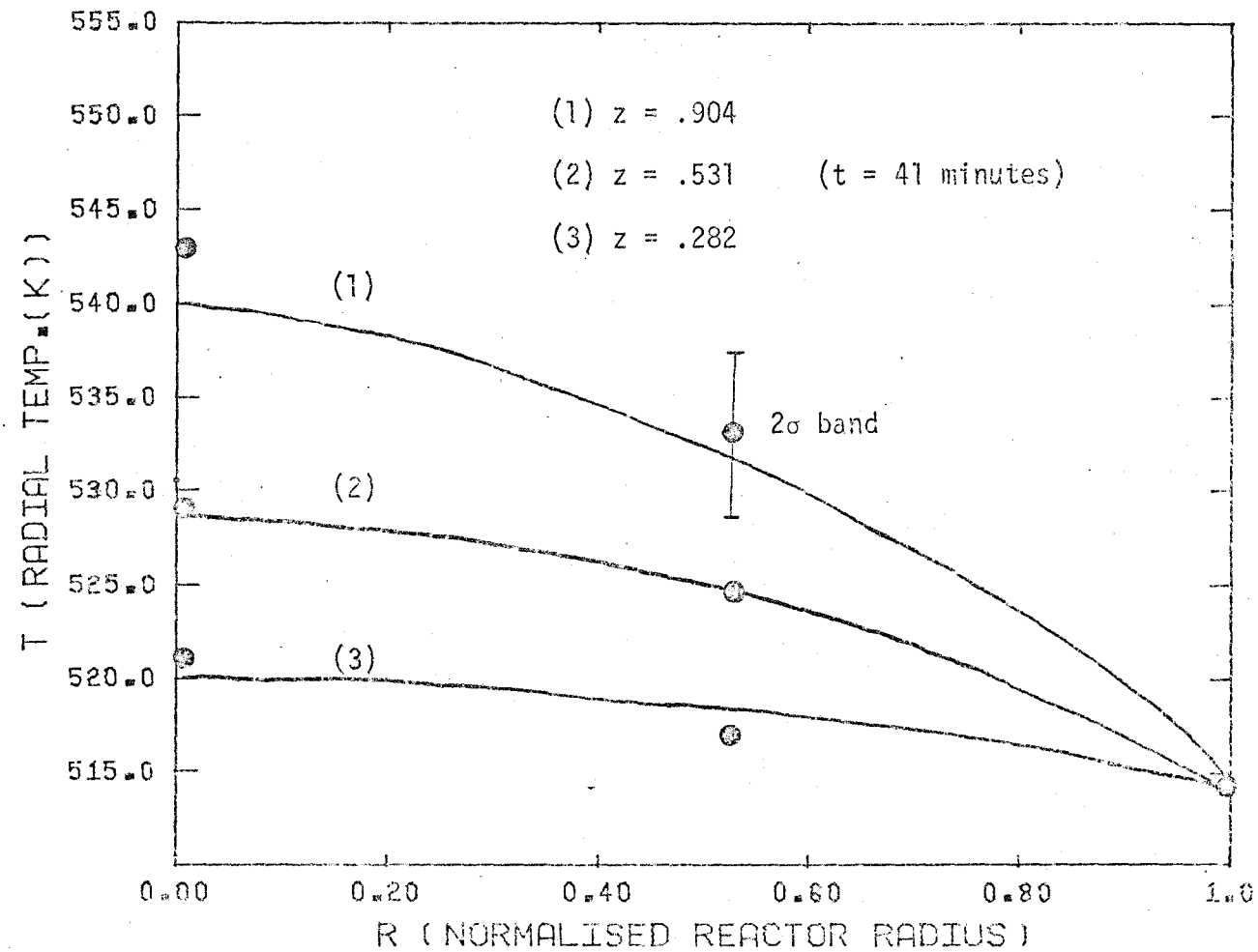

Figure 19: Radial Temperature Profile at t = 41 minutes (for Different Axial Positions, z) Model vs. Data (26 May Data, Figure 17).

given in Appendix 3.

In Figure 18, the dynamic model was fitted by linearising about a steady state (close to the operating profile) obtained from the model (see Section 5.3.2). The model predictions are again compared with the data at t = 41 minutes and t = 11 minutes. The 2 σ limits for the data point (near the hot spot) is shown. All the model predictions lie within these 2 σ limits but the overall fit for all time is not quite as good as that shown in Figure 17 as verified by an increase in sum of variance value to 55.6. Total sum of squares was 3282.

Thermocouples were placed at the radial collocation points r = 0.577 (see Section 4.4.1), at three different axial positions. In Figure 19, the three radial profiles predicted by the model at t = 41 minutes are compared with the data. The good fit obtained implies that the model assumption of quadratic radial temperature profiles (Section 4.4) was quite adequate and that radial gradients were significant.

Concentration Data

All the above model fitting used only temperature data. Towards the end of this study, the gas chromatograph (see Section 3.2) was successfully interfaced by Tremblay (T4) making concentration data available. The chromatograph required 361.3 seconds to complete an analysis of all five mole fractions on the product (H_2, C_4, C_3, C_2, C_1). At the end of an analysis, the computer is signalled to collect the relevant data. The chromatograph thus controls the times at which concentration data are available and it was not possible to properly

synchronise the temperature data (which is controlled by the computer) with the concentration data.

Nevertheless, a major value of the concentration data was to eliminate any level biases in the model predictions that were evident in the mole fractions and in the overall conversion. For the purposes of a model fit, using both temperature and concentration data (mole fractions (MF)), the mole fractions were approximately matched up to correspond to every sixth 1 minute sampling interval for the temperatures.

A simple sum of squares criteria was used to fit the concentration and temperature simultaneously

$$J = \sum_{t=o}^{N} \sum_{j=1}^{7} [T_{jt}(\text{data}) - T_{jt}(\text{model})]^2$$

$$+ \lambda \sum_{t=o}^{N/6} \sum_{j=1}^{4} w_j [MF_{jt}(\text{data}) - MF_{jt}(\text{model})]^2$$

where λ, w_j are weighting factors. The fitted state space matrices are given in Appendix 3, 23 September data.

Results

Initially, the same set of parameters λ_o, α and k/k_o (see (5-8) and Section 5.3.2) were used to fit the model to both the concentration and temperature data. In order to improve the concentration fit, an extra parameter D_{er} was introduced. A change in D_{er} did not affect the

temperature profile much, but significantly improved the concentration fit. In order to keep the total number of parameters to a minimum, parameter α was fixed at a previously estimated value. It was mentioned previously that λ_o and k/k_o were highly correlated, when fitting the temperature data alone. The sum of squares estimation surface would be a long cigar shape. Typical correlation matrices for 26 May and 23 September data are given in Appendix 3. A pair of values for λ_o and k/k_o lying anywhere along this ridge

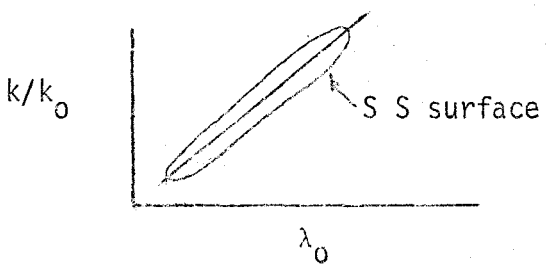

gave similar sums of squares of residuals, for the temperatures. The inclusion of the concentration data effectively positioned the pair $(\lambda_o, k/k_o)$ along this ridge so as to match up the concentration data, while maintaining a good temperature fit.

The temperature profile fit is compared with data in Figure 20. The axial temperature profile are shown at two times (t = 36, t = 82 minutes). The 2 σ thermocouple error band on the data points is given, showing that the model predictions are well within this band, and that the temperature dynamics have been well matched. The sum of the variances for the 7 temperatures, $\sum \sigma_{N_i}^2$, was 39.8 indicating that the overall temperature dynamics too, were well matched.

The mole fraction data was approximately synchronised to the model predictions at every sixth one minute sampling interval. Taking this into account, the model mole fraction predictions were compared and the data is presented in Figure 21. This figure indicates that both the level and the dynamic trends in mole fractions of the various species have been well matched by the model. The conversion of butane is also plotted. The mole fraction of the fourth component C_2 was too small to be detected by the gas chromatograph and the data showed zero for this value, (the model predicted an average of .006).

In spite of this relatively crude synchronisation of temperature and concentration data, the model appears to predict the overall mole fraction trends and levels well, while at the same time, maintaining a good fit on the temperatures. We have thus been able to obtain adequate fits of the state model to both temperature and concentration dynamic data using the algorithm described in Section 5.3.2.

We can compare this with the method of fitting an empirically chosen model (canonical state variable or transfer function form) directly to the data by estimating the large number of parameters occurring in these forms. In this latter case, a minimum of prior information about the physical reactor is used. The starting point for the method used here is the PDE's describing the dynamics of the reactor and in a sense, maximum prior information is used. Some of the advantages and disadvantages of the method used here are given below.

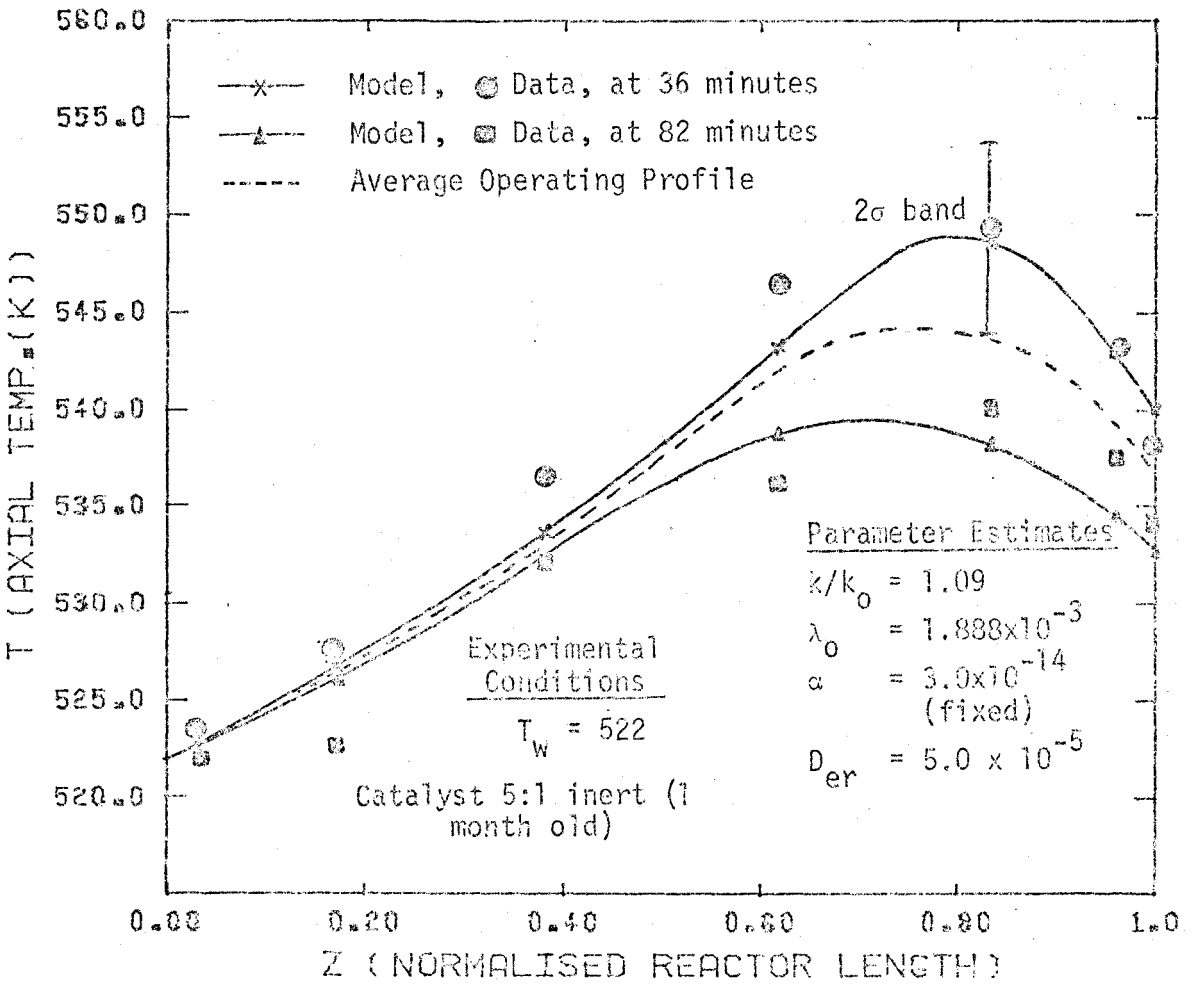

Figure 20: Axial Temperature Profiles, Model vs. Data (Linearisation about Average Profile) (23 September Data).

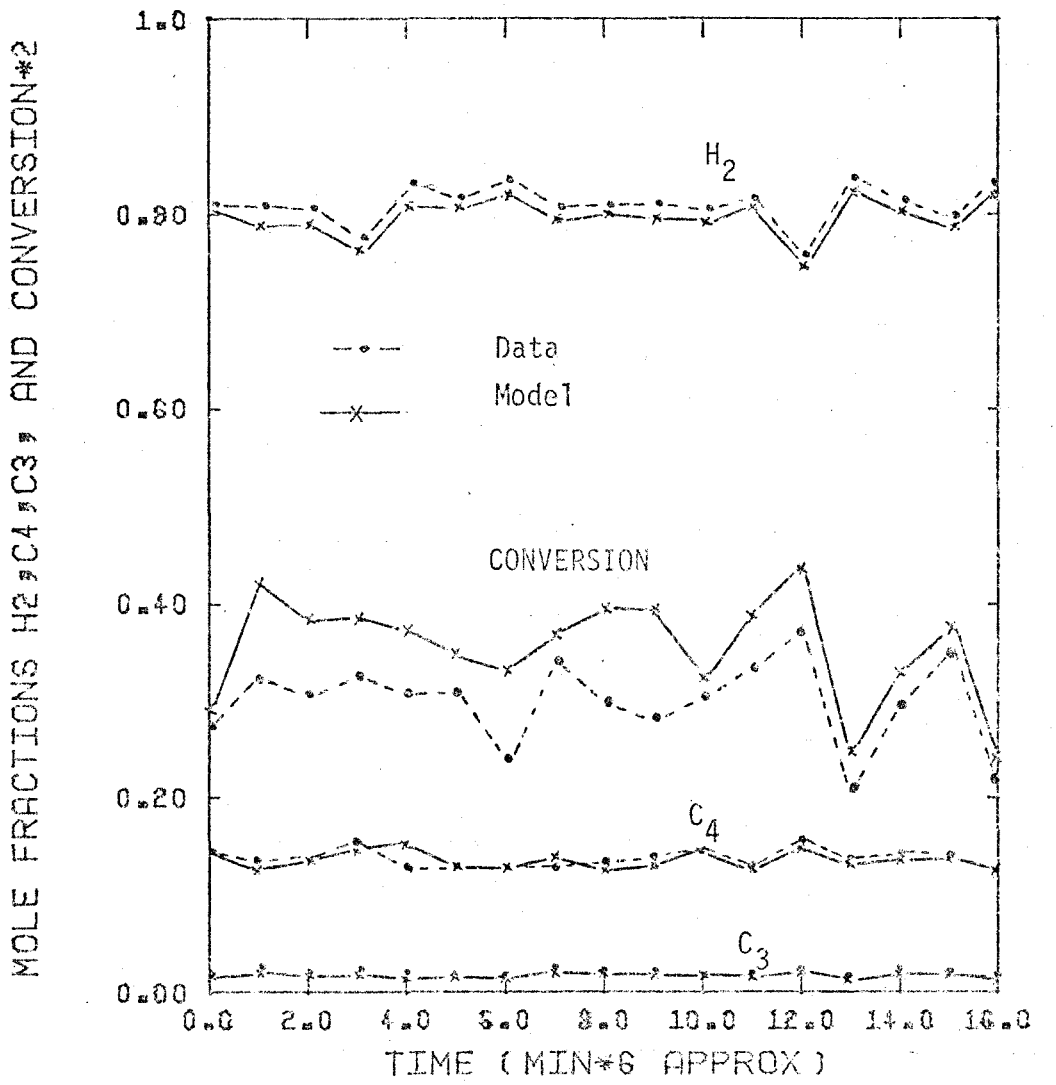

Figure 21: Reactor Exit Mole Fractions, Model vs. Data (23 September).

Advantages

(i) A small number of parameters can be used to fit the data; all have physical meaning and can often be estimated from the literature.

(ii) The number of parameters to be estimated does not increase with the order of the state model. So, if in fact we required a 10^{th} order state model to adequately describe the dynamics, we would still have only two or three parameters and these would be "mapped" into a 10^{th} order model using the algorithm in 5.3.2 with relatively minor increase in computation time.

(iii) Extensive information is provided through the model: axial concentration profiles may be calculated from the states of the model; radial profiles of both concentration and temperature are obtained as a function of the states of the model.

Disadvantages

(i) The partial differential equations of the reactor model are difficult to work with and many simplification stages are required.

(ii) Computational time may be excessive.

(iii) Ill-conditioning may be induced into the estimation surface by all the numerical steps required in the estimation procedure.

(iv) A large effort must be expended to obtain a usable model for this system - a point which may curtail the interest of industry. Nevertheless, the model fitted here does provide an adequate description of all the complex temperature-concentration dynamics in both the radial and axial direction as well as extremely useful relations which allow prediction of concentrations from temperature.

So far, we have dealt with a description and modelling, only of the deterministic dynamics of the reactor. In order to fully describe the true dynamic-stochastic nature of the system, the stochastic noise characteristics of the system must be modelled.

5.4 Building a Noise Model

The representation of the deterministic dynamics of a system in the state space form has been discussed. From (4-2) the state equation is

$$\underline{x}(t+1) = A\underline{x}(t) + B\underline{u}(t) \tag{5-9}$$

with a measurement equation

$$\underline{y}(t) = H\underline{x}(t) \tag{5-10}$$

This model provides a description for only that part of the output ($\underline{y}(t)$) variations caused by changes made in the manipulated variables $\underline{u}(t)$. Equation (5-9) does not account for deterministic load disturbances.

These could be accounted for by adding an additional term. The model is deterministic in that it allows for no model error, no measurement error nor any random process disturbances. Obviously these effects are important or else there would be no regulatory control problem. This noise or disturbance part of the system that cannot be explained by the deterministic model (5-9) and (5-10) must be accounted for by a stochastic model.

There are basically two approaches to modelling these stochastic components. The first makes the assumption that all the disturbances can be represented by introducing additive white noise vectors to the state equation and the measurement equation. The combined dynamic stochastic model then takes the form

$$\underline{x}(t+1) = A\underline{x}(t) + B\underline{u}(t) + \underline{w}(t) \tag{5-11}$$

$$\underline{y}(t) = H\underline{x}(t) + \underline{v}(t) \tag{5-12}$$

where $\underline{w}(t)$ and $\underline{v}(t)$ are independent white noise vectors with covariance matrices

$$\begin{aligned} &E[\underline{w}(t)\underline{w}'(t+k)] = Rw \\ &E[\underline{w}(t)\underline{v}'(t+k)] = 0 \quad \text{for all } k \\ &E(\underline{v}(t)\underline{v}'(t+k)] = Rv \end{aligned} \tag{5-13}$$

$\underline{w}(t)$ is usually thought of as representing the process noise or disturbances and modelling error, and $\underline{v}(t)$ represents the measurement noise.

It is in general, not possible to uniquely identify these two noise sources from input-output data, nor is it necessary from a control standpoint (M5). The stochastic parameters to be estimated in the model (5-11), (5-12) are the elements of the covariance matrices Rw and Rv. Since unique estimation of full Rw and Rv matrices is not in general possible from input-output data, some simplification in their structure (i.e., restriction to diagonal form) is often made (H6), and the reduced number of parameters adjusted in some manner to best fit the data or give the best control when the stochastic control algorithm, derived from (5-11) and (5-12), is implemented.

One problem with such a crude representation of the stochastic part of the model is that all the noise is assumed to enter into the process like an input and pass through the process. The time dependence of the noise is thus governed solely by the dynamic characteristics of the deterministic model. In practice, since many types of disturbances or noise do enter the process in this manner, this may be a reasonable assumption. However, in other cases, where the major disturbances are generated elsewhere in the system (e.g., internally in the catalyst particles) this structure for the noise may be poor.

The alternative is to independently identify and fit a state space model for the actual stochastic disturbances in the system from input-output data. The combined dynamic stochastic system can be represented as an augmented state space model.

5.4.1 A Dynamic-Stochastic State Space Model

To identify and fit a noise model for a state space model from input-output data, one must treat the residual vector $\underline{N}(t)$(see (5-6)) as the stochastic noise sequence and write the dynamic-stochastic model as

$$\underline{x}(t+1) = A\underline{x}(t) + B\underline{u}(t) \tag{5-14}$$

$$\underline{y}(t) = H\underline{x}(t) + \underline{N}(t) \tag{5-15}$$

In general, $\underline{N}(t)$ can be modelled by a multivariable linear autoregressive integrated-moving average (ARIMA) time series model (B6, W2) of the form

$$\phi(B)\nabla^{d}\underline{N}(t) = \theta(B)\underline{a}(t) \tag{5-16}$$

where

$\phi(B)$ is a matrix autoregressive polynomial of back shift operators B

∇^{d} is a d^{th} difference operator

$\theta(B)$ is a matrix moving average polynomial in B

B is a back shift operator such that $B\underline{N}(t) = \underline{N}(t-1)$

$\underline{a}(t)$ is a white noise vector sequence with covariance matrix $\sum$

The identification and estimation of the single variable noise models is discussed by Box, et al. (B6) and for multivariable noise models by Wilson (W2). It can be shown that under certain conditions (B6), any

purely moving average (MA) process of finite order may be represented by a purely autoregressive process (AR) of infinite order. Many common stochastic disturbances are well approximated by an auto-regressive process of finite order, say p^{th} order.

$$\phi_p^*(B)\nabla^d \underline{N}(t) = \underline{a}(t) \tag{5-17}$$

The AR parameters appear linearly in the models (5-16) and (5-17) and may be estimated by linear least squares methods. Estimation of the moving average parameters is a non-linear problem. If the noise model is stationary (mean level of the disturbances is constant) then we may represent the multivariable noise model as say a p^{th} order AR model

$$\phi_p(B)\underline{N}(t) = \underline{a}(t) \tag{5-18}$$

If for simplicity, we begin with a first order AR model AR(1) then (5-18) becomes

$$(1 - \phi B)\underline{N}(t) = \underline{a}(t)$$

or

$$\underline{N}(t) = \phi\underline{N}(t - 1) + \underline{a}(t) \tag{5-19}$$

where ϕ is a full matrix of parameters of order m (see (5-20)).

For n states, m measurements, and p control variables, then in (5-14), (5-15) and (5-19), the orders of the matrices are

$$\begin{aligned} &A(nxn) && \underline{x}(nx1) \\ &B(nxp) && \underline{y}(mx1) \\ &H(mxn) && \underline{u}(px1) \\ &\phi(mxm) && \underline{N}(mx1) \end{aligned} \tag{5-20}$$

After fitting the dynamic-stochastic state model in the form (5-14), (5-15) with an identified noise model (5-19), one can obtain the standard dynamic stochastic model form (5-11) and (5-12) as follows.

Define m new states $\underline{s}(t)$ such that

$$\underline{N}(t) = \underline{s}(t) \tag{5-21}$$

then adding (5-19) to (5-14) and (5-15) we have

$$\begin{matrix} n \\ m \end{matrix}\begin{bmatrix} \underline{x}(t+1) \\ \hline \underline{s}(t+1) \end{bmatrix} = \begin{matrix} n \\ m \end{matrix}\begin{bmatrix} \overset{n}{A} & \overset{m}{0} \\ \hline 0 & \phi \end{bmatrix}\begin{bmatrix} \underline{x}(t) \\ \hline \underline{s}(t) \end{bmatrix} + \begin{matrix} n \\ m \end{matrix}\begin{bmatrix} B \\ \hline 0 \end{bmatrix}\underline{u}(t) + \begin{bmatrix} 0 \\ \hline I_m \end{bmatrix}\underline{a}(t) \tag{5-22}$$

$$y(t) = H\underline{x}(t) + \underline{s}(t)$$

or

$$y(t) = [H \mid I_m]\begin{bmatrix} \underline{x}(t) \\ \hline \underline{s}(t) \end{bmatrix} \tag{5-23}$$

if we define

$$A^* = \begin{bmatrix} A & 0 \\ \hline 0 & \phi \end{bmatrix} \qquad (m+n) \times (m+n)$$

$$B^* = \begin{bmatrix} B \\ \hline 0 \end{bmatrix} \qquad (m+n) \times p$$

$$\underline{w}^*(t) = \begin{bmatrix} 0 \\ \hline I_m \end{bmatrix} \underline{a}(t) \quad (m+n) \times 1 \tag{5-24}$$

$$\underline{v}^*(t) = 0$$

$$H^* = [H \mid I_m] \qquad m \times (m+n)$$

$$\underline{x}^*(t) = \begin{bmatrix} \underline{x}(t) \\ \hline \underline{s}(t) \end{bmatrix} \qquad (m+n) \times 1$$

Then the augmented dynamic stochastic model can also be represented in the form (5-11) and (5-12).

$$\underline{x}^*(t+1) = A^*\underline{x}^*(t) + B^*\underline{u}(t) + \underline{w}^*(t) \tag{5-25}$$

$$\underline{y}(t) = H^*\underline{x}^*(t) + \underline{v}^*(t) \tag{5-26}$$

where

$$Rw^* = \begin{matrix} \\ n \end{matrix} \begin{bmatrix} 0 & 0 \\ \hline 0 & \sum \end{bmatrix} \quad \text{and} \quad \sum = E[\underline{a}(t)\underline{a}'(t)]$$

and

$$Rv^* = 0 \tag{5-27}$$

For an AR(2) model one would have to define 2m new states $\underline{s}(t)$

and the state model would be of order (n+2m).

5.4.2 Parameter Estimation

Least squares estimation of the ϕ matrix of parameters in the AR(1) model in (5-19) is a linear problem. Define the autocovariance matrix at lag k as

$$\Gamma(k) = E[\underline{N}(t)\underline{N}'(t + k)]$$

and

$$\Gamma'(k) = \Gamma(-k) \tag{5-28}$$

then for AR(1) and model (5-19)

$$\Gamma'(k) = \phi\, \Gamma'(k - 1) \qquad k \geq 1$$

For k = 1

$$\Gamma'(1) = \phi\, \Gamma'(0)$$

and therefore

$$\phi = \Gamma'(1)\Gamma(0)^{-1} \tag{5-29}$$

For k = 0

$$\Gamma(0) = \phi\, \Gamma(1) + \sum \tag{5-30}$$

where

$$\sum = E[\underline{a}(t)\underline{a}'(t)] \quad \text{(see (5-27))} \tag{5-31}$$

substituting for ϕ we get

$$\Gamma(0) = \Gamma'(1)\Gamma(0)^{-1}\Gamma(1) + \sum \qquad (5\text{-}32)$$

Once the residuals have been obtained, ϕ is easily estimated from (5-29). The estimation algorithm was detailed in Section 5.3.2 and in Figure 15, and may be extended to include estimation of the stochastic parameters ϕ in a conditional manner (W2).

Algorithm

1. Guess dynamic parameters λ_{er}, (k/k_o), etc.
2. Obtain residuals $\underline{N}(t)$.
3. Estimate ϕ from (5-29) conditional on dynamic parameters.
4. Calculate $\underline{a}(t)$'s recursively from (5-19).
5. Feed $\underline{a}(t)$'s to a minimisation routine to minimise the determinant criterion (5-2).
6. Obtain updates for the dynamic parameters conditional on ϕ and return to step 2.

Results

The residuals in the dynamic stochastic models are the $\underline{a}(t)$'s, the variance-covariance or dispersion matrix (see (5-3)) of the $\underline{a}(t)$'s $\sum$, can be used as a measure of the goodness of fit of the model. The lower limit for the variances of $\underline{a}(t)$ is the variance of the measurement error and from Section 5.1.1, this is known to be of the order of

$$\sigma^2_{meas} \simeq 4.0$$

The variance-covariance matrix for the dynamic, $D_{\underline{N}(t)}$, and the dynamic-stochastic model, $D_{\underline{a}(t)}$, is given in Table 2. These matrices are for the same data illustrated in Figures 16 to 19 and discussed in Section 5.3.3 (i.e., 26 May, 1976 run).

From Table 2, it is seen that the sum of variances $\sum_{i=1}^{7} \sigma^2_{a_i}$ has been reduced to 27.4, from 48.5 for $\sum_{i=1}^{7} \sigma_{a_i}^2$ (see also Figure 17) by the incorporation of the stochastic model.

Recalling that D is the covariance matrix for the 7 axial temperatures in the bed in the order T_1 to T_7, Table 2 shows that the covariance between temperatures has been reduced, especially between temperatures early in the bed. All the variances $\sigma_{a_i}^2$ have been reduced close to the measurement error, suggesting that the noise sequence $\underline{N}(t)$ has been adequately accounted for by the assumption of an AR(1) noise model. The dynamic stochastic parameters were first estimated by minimising the sum of the sum of squares of the temperature residuals J^*

$$J^* = \sum_{\text{all } t} \underline{a}'(t)\underline{a}(t) \qquad (5\text{-}33)$$

The estimates from this minimisation routine were then fed to a routine that minimised the determinant J (5-2) but little change occurred.

Towards the end of this study, a multivariate identification and checking program became available (W3). This program calculated multivariable auto-correlation and quasi-partial correlation matrices for a

TABLE 2: Variance-Covariance Matrices for Dynamic and Dynamic Stochastic Models for Data Taken 26 May, 1976

$D_{\underline{N}(t)} =$

6.65	.93	1.65	2.13	- .44	- .04	.18
	4.66	.139	.88	.20	-1.56	- .89
		3.77	2.41	1.01	2.84	2.75
			6.36	1.81	3.28	2.46
	symmetric			7.60	7.40	6.30
					12.17	10.54
						10.35

Variance-Covariance matrix for $\underline{N}(t)$'s

$$\sum_{i=1}^{7} \sigma_{a_i}^2 = 48.5$$

Total sum of squares = 2867

$D_{\underline{e}(t)} =$

3.83	.59	1.34	1.95	- .25	.55	.34
	4.23	.39	1.26	.97	- .39	.065
		3.23	1.84	.20	1.64	1.71
			5.09	.28	1.24	.91
	symmetric			3.19	1.34	1.26
					3.62	3.36
						4.17

Variance-Covariance matrix for $\underline{a}(t)$'s

$$\sum_{i=1}^{7} \sigma_{a_i}^2 = 27.4$$

Total sum of squares = 1615

multivariable time series. The $\underline{a}(t)$ series calculated from (5-19) was tested and showed no evidence of auto-correlation in time: the 95% confidence band around zero was 0.263; the largest element in the auto-correlation matrix at lag 1 was 0.232 and the average of the absolute values of all the elements in the matrix was $\sim$ 0.06. This confirmed that the $\underline{a}(t)$ was a white noise sequence and that the AR(1) model in (5-19) was adequate.

The stochastic part of the model was thus properly identified; a noise model was developed and jointly fitted with the dynamic model. A large improvement in the model fit was obtained, as indicated by the reduction of the dispersion matrix ($D_{\underline{N}(t)}$ to $D_{\underline{a}(t)}$) down close to measurement error (4.0's along the diagonal). In the next section, the possibility of reducing the dimensionality of the noise model is examined.

5.5 Dimensionality Reduction for the Noise Model

In Section 5.3.3 (step (6)) it was pointed out that the 7 states in the model are related temperatures along the reactor profile. It is thus quite possible that a few (2 or 3) underlying disturbances in the system affect groups of these temperatures in a similar manner. It is then these few fundamental disturbances expressed as a linear combination of the 7 temperatures that determine the actual dimensionality of the noise vector $\underline{N}(t)$, which may in fact be much less than 7. The order of the augmented dynamic stochastic model (Section 5.4.1, (5-24) is directly proportional to the dimensionality of the noise model $\underline{N}(t)$.

It is thus possible to reduce the order of the dynamic-stochastic model. Furthermore, an analysis which shows up the fundamental disturbances in the system as seen through the temperature measurements, may provide a deeper insight into and better understanding of, the process. Of prime interest here is the development of a dynamic-stochastic process model for the purpose of control. If one can determine the fundamental disturbances in the system, then the control scheme need take only these few into account. In the next section, a canonical analysis of the noise model is used to select out the fundamental disturbances in the system.

5.5.1 Canonical Analysis of the Noise Model

MacGregor (M6) has applied a canonical analysis to multivariate noise models. For simplicity he considered a first order autoregressive model (see (5-19))

$$\underline{N}(t) = \phi\underline{N}(t-1) + \underline{a}(t) \tag{5-34}$$

It was shown in Section 5.4.2 that for this system, the auto-covariance at lag k given by

$$\Gamma(k) = E[\underline{N}(t)\underline{N}'(t+k)]$$

may be used to obtain the following relationships

$$\phi = \Gamma'(1)\Gamma(0)^{-1} \tag{5-35}$$

$$\Gamma(0) = \Gamma'(1)\Gamma(0)^{-1}\Gamma(1) + \sum \tag{5-36}$$

Suppose that there exists some canonical form for $\underline{N}(t)$ such that most of its "activity" could be represented by a few linear combinations of the N(t)'s say $\dot{N}_1(t) = \underset{1xm}{\underline{\ell}_1'}\underline{N}(t), \dot{N}_2(t) = \underline{\ell}_2'\underline{N}(t)$, etc. Box and Tiao (B7) have developed a scale free measure of the "activity" by using the idea of the most forecastable variation. Using this idea, the first principal component

$$\dot{N}_1(t) = \underline{\ell}_1'\underline{N}(t) = \underline{\ell}_1'\phi\underline{N}(t-1) + \underline{\ell}_1'\underline{a}(t) = \hat{\dot{N}}_1(t-1,1) + \dot{a}_1(t)$$

is obtained by finding that linear combination $\underline{\ell}_1$ which maximises the ratio of the variance of the one step ahead forecast $\hat{\dot{N}}_1(t,1)$ to the variance of the forecast error $\dot{a}_1(t)$.

MacGregor presents several alternative objective functions that could be maximised (see (5-39) to (5-41)). The most convenient one being

$$\underset{\underline{\ell}_1}{\text{Max}} \quad \frac{V[\hat{\dot{N}}_1(t,1)]}{V[\dot{a}_1(t)]} = \frac{\underline{\ell}_1'\phi\Gamma(0)\phi'\underline{\ell}_1}{\underline{\ell}_1'\sum\underline{\ell}_1}$$

$$\text{From (5-35) and (5-36)} = \frac{\underline{\ell}_1'\Gamma'(1)\Gamma(0)^{-1}\Gamma(1)\underline{\ell}_1}{\underline{\ell}_1'[\Gamma(0) - \Gamma'(1)\Gamma(0)^{-1}\Gamma(1)]\underline{\ell}_1} \tag{5-37}$$

where V[x] is the variance of x. Equation (5-37) is known as a "Rayleigh Quotient" (N2) and the solution of (5-37) is obtained by solving

the generalised eigenvalue problem

$$[\Gamma'(1)\Gamma(0)^{-1}\Gamma(1) - \lambda \Sigma]\underline{\ell}_1 = 0 \qquad (5\text{-}38)$$

The maximum value of (5-37) is equal to λ_1, the largest generalised eigenvalue of (5-38) and the corresponding generalised eigenvector $\underline{\ell}_1$ gives that linear combination of the N(t)'s which maximises (5-37). If alternatively, we had maximised the ratio

$$\frac{V[\hat{N}_1(t,1)]}{V[\dot{N}_1(t)]}$$

and obtained the corresponding largest eigenvalue $\mu_1 (0 < \mu_1 < 1)$ from

$$[\Gamma'(1)\Gamma(0)^{-1}\Gamma(1) - \mu\,\Gamma(0)]\underline{\ell}_1 = 0 \qquad (5\text{-}38a)$$

we can see from (5-36) that if

$$\underset{\ell_1}{\text{Max}} \quad \frac{V[\hat{N}_1(t,1)]}{V[\dot{N}_1(t)]} = \mu_1 \qquad (0 < \mu_1 < 1) \qquad (5\text{-}39)$$

then

$$\underset{\ell_1}{\text{Max}} \quad \frac{V[\hat{N}_1(t,1)]}{V[\dot{a}_1(t)]} = \lambda_1 = \frac{\mu_1}{1 - \mu_1} \qquad (5\text{-}40)$$

also

$$\underset{\ell_1}{\text{Max}} \quad \frac{V[\dot{a}_1(t)]}{V[\dot{N}_1(t)]} = 1 - \mu_1 \qquad (5\text{-}41)$$

All the covariance matrices are symmetric positive definite (others can be positive semi-definite) and at most there can be m real positive roots $\mu_1 > \mu_2 > \mu_m$ and all $\mu_i < 1$. The generalised mxm modal

matrix L, formed by letting each ℓ_i' be a row, simultaneously diagonalises (N2) $\Gamma'(1)\Gamma(0)^{-1}\Gamma(1)$ and $\sum$ in (5-38); we can also choose the normalisation of the eigenvectors such that

$$(V[\underline{\dot{a}}(t)] =) \; L \sum L' = I_m = \dot{\sum} \tag{5-42}$$

A non-singular transformation of the AR(1) model (5-34) gives

$$\begin{aligned} \underline{\dot{N}}(t) = L\underline{N}(t) &= L\phi\underline{N}(t-1) + L\underline{a}(t) \\ &= (L\phi L^{-1})L\underline{N}(t-1) + L\underline{a}(t) \\ &= \dot{\phi}\underline{\dot{N}}(t-1) + \underline{\dot{a}}(t) \end{aligned} \tag{5-43}$$

Furthermore from (5-42) and (5-36) because L simultaneously diagonalises $\sum$ and $\phi\Gamma(1)$, both the $\dot{a}(t)$'s and the $\dot{N}(t)$'s will be uncorrelated with each other. From (5-42), the $\dot{a}(t)$'s will have equal variances and from (5-41), each $V[\dot{N}_j(t)] = \frac{1}{1-\mu_j}$. The new canonical noise variables, $\dot{N}_1(t)$, $\dot{N}_2(t)\ldots\dot{N}_m(t)$ account for the most activity, the next most activity and so on. Say we have determined that, of the m eigenvalues λ_i found, the last r were not significantly different from zero. This would imply, using (5-37), (5-40) and (5-42) that

$$\underline{\ell}_j'\phi\Gamma(0)\phi'\underline{\ell}_j = \frac{\mu_j}{1-\mu_j} = 0 \qquad j=m-4+1,..m$$

$$\text{this implies } \phi'\underline{\ell}_i = 0 \qquad\qquad j=m-r+1,...m \tag{5-44}$$

or that r eigenvalues of ϕ are zero and that the noise model (5-34) is not fully m dimensional but may be represented as a (m-r) dimensional model. This also implies that the corresponding linear combination of the N(t)'s for measured temperatures, y(t)'s, are white noise sequences.

$$\ell_j' \underline{N}(t) = \dot{N}_j(t) = \dot{a}_j(t) \qquad j=m-r+1,\ldots m \tag{5-45}$$

These last r elements of $\underline{\dot{N}}(t)$ therefore contain no information (not forecastable) and may be eliminated from the noise model. Making use of (5-44) we can write the canonical noise model from (5-43) as

$$\begin{bmatrix} \dot{N}_1(t) \\ \vdots \\ \dot{N}(t)_{m-r} \\ \hline \dot{N}(t)_{m-r+1} \\ \vdots \\ \dot{N}_m(t) \end{bmatrix} = \left[\begin{array}{c:c} \dot{\phi}_{m-r} & \dot{\phi}_r \\ \hline 0 & 0 \end{array}\right] \cdot \begin{bmatrix} \dot{N}_1(t-1) \\ \vdots \\ \dot{N}_{m-r}(t-1) \\ \hline \dot{N}(t-1)_{m-r+1} \\ \vdots \\ \dot{N}_m(t-1) \end{bmatrix} + \begin{bmatrix} \dot{a}_1(t) \\ \vdots \\ \dot{a}(t)_{m-r} \\ \hline \dot{a}(t)_{m-r+1} \\ \vdots \\ \dot{a}_m(t) \end{bmatrix} \tag{5-46}$$

where $\dot{\phi}_{m-r}$ is obtained as the upper left partition of $\dot{\phi}_m = L\phi L^{-1}$. The forecastable part of the noise model is then

$$\underset{m-r}{\underline{\dot{N}}(t)} = \underset{(m-r)x(m-r)}{\dot{\phi}_{m-r}} \underset{m-r}{\underline{\dot{N}}(t-1)} + \underset{(m-r)x1}{\underset{m-r}{\underline{a}(t)}} + \dot{\phi}_r \underset{r}{\underline{a}(t-1)} \tag{5-47a}$$

The last term in (5-47a) can be added to $\underset{m-r}{\underline{\dot{a}}(t)}$ to give a new correlated white noise sequence $\underline{\dot{\alpha}}(t)$, say, where $\underline{\dot{\alpha}}(t) = \underline{\dot{a}}_{m-r}(t) + \dot{\phi}_r \underline{a}_r(t-1)$. However, numerically, the elements of $\dot{\phi}_r$ were of the same order of magnitude as

the lower portion of $L\phi L^{-1}$ which is zero by hypothesis. So as a good approximation, $\phi_r \underline{a}_r(t-1)$ was neglected in comparison with the remaining terms, and (5-47a) is written as

$$\underset{m-r}{\dot{\underline{N}}}(t) = \dot{\phi}_{m-r} \underset{m-r}{\dot{\underline{N}}}(t-1) + \underset{m-r}{\dot{\underline{a}}}(t) \tag{5-47}$$

(5-47) is the reduced dimension noise model and in order to write the augmented dynamic-stochastic state model (Section 5.4.1) we would need to define only (m-r) new states (see Equation (5-21)) and the augmented state model would be of order (n+m-r) for an AR(1) noise model.

It is advantageous to be able to test for the significance of the remaining r eigenvalues, once the first m-r eigenvalues, assumed to be non zero, have been removed. Following MacGregor (M6) we first develop an overall test for the hypothesis H_o that $\phi = 0$. This test can be based on the ratio of the generalised variances given by

$$\Lambda = \frac{|\Sigma|}{|\Gamma(0)|} = \frac{|\Gamma(0) - \Gamma'(1)\Gamma(0)^{-1}\Gamma(1)|}{|\Gamma(0)|} \tag{5-48}$$

Assuming normality for $\underline{a}(t)$, Bartlett (B8, B9) proposed an approximate test based on the fact that under the hypothesis H_o: $\phi = 0$,

$$-[(N - m)' - \tfrac{1}{2}(2m + 1)]\ln\Lambda = \chi^2_{2m} \tag{5-49}$$

N = number of data points, m = dimension of $\underline{N}(t)$

Hence (5-48) is asymtotically distributed as a Chi-squared distribution with 2m degrees of freedom.

Now (5-48) can be written as (using (5-38a)

$$\Lambda = \frac{|I_m - r'(1)r(0)^{-1}r(1)r(0)^{-1}|}{|I_m|} = \frac{|I_m - \mu|}{|I_m|} = \prod_{j=1}^{m}(1 - \mu_j) \qquad (5\text{-}50)$$

and thus Λ provides an overall test of the hypothesis that all the canonical eigenvalues μ_j are equal to zero. However, we are more interested in testing the hypothesis that given the eigenvalues $\mu_1, \mu_2 \cdots \mu_{m-r}$ are non zero, what is the probability that the remaining r eigenvalues $\mu_{m-r+1} \cdots \mu_m$ are zero. Bartlett showed that if we calculate

$$\Lambda = \Lambda'\Lambda'' = \prod_{i=1}^{m-r}(1 - \mu_i) \prod_{j=m-r+1}^{m}(1 - \mu_j) \qquad (5\text{-}51)$$

the χ^2 test approximation for Λ may be extended to Λ'' giving

$$-\left[(N - m) - \frac{1}{2}(2m + 1)\right]\ln\Lambda'' = \chi^2_{2r} \qquad (5\text{-}52)$$

as being asymtotically distributed as Chi-square with 2r degrees of freedom. (5-52) may thus be used to test the hypothesis that the remaining r eigenvalues are zero.

5.5.2 Application to Reactor Data

The canonical analysis described in the section above was applied to the residual sequence for the data illustrated in Figures 17 to 19 and dispersion matrix $D_{\underline{N}(t)}$ given in Table 2.

The matrices $r(0) = D_{\underline{N}(t)}$, $r(1)$ and ϕ, calculated from (5-35), are given in Table 3. The eigenvalues of ϕ were calculated to be

Real	λ_ϕ	Imaginary
0.8208		0.1487 ± i 0.1397
0.7207		
0.4230		0.0869 ± i 0.0868

indicating that the largest root .8208 was not too close to unity and that stationary behaviour for the AR(1) noise model could be expected. The $\sum$ matrix was calculated from (5-36) and the generalised eigenvalue problem (5-38) was solved using EISPACK (E1) and provided the following solution (eigenvectors normalised such that $L\sum L' = I$).

Generalised Eigenvalues λ, μ

(see (5-38)) λ	$\mu = \frac{\lambda}{1+\lambda}$ (see (5-38a)
3.361	0.7707
1.040	0.5098
0.2706	0.2130
0.1130	0.1051
0.0318	0.0308
0.0156	0.0154
0.0057	0.0057

TABLE 3: Autocovariance Matrices and ϕ matrix for Reactor Data

$\Gamma(0) = D_{\underline{N}}(t)$ (Table 2)

$$\Gamma(1) = \begin{bmatrix} 4.23 & .43 & .37 & .067 & -.45 & -1.25 & -.64 \\ .97 & .81 & .042 & .23 & -.54 & -.77 & -.71 \\ 1.50 & -.23 & .72 & 1.44 & .82 & 1.09 & .90 \\ 1.18 & -.49 & 1.13 & 2.32 & .25 & 2.82 & 1.86 \\ .004 & -1.23 & 1.38 & 1.81 & 4.71 & 7.04 & 6.13 \\ .32 & -1.27 & 1.31 & 2.55 & 6.99 & 9.68 & 8.22 \\ .82 & -.80 & 1.32 & 2.26 & 5.96 & 8.24 & 7.21 \end{bmatrix}$$

$$\phi = \begin{bmatrix} .61 & .073 & .15 & -.081 & .032 & -.21 & .25 \\ .058 & .21 & -.067 & -.078 & -.23 & -.011 & .13 \\ .002 & -.11 & .10 & .16 & .27 & -.34 & .24 \\ -.13 & -.007 & .20 & .30 & .14 & -.11 & .12 \\ -.054 & .038 & -.36 & .23 & .06 & .49 & .085 \\ -.15 & .041 & -.36 & .21 & .27 & .60 & .070 \\ -.024 & .002 & -.29 & .057 & .31 & .37 & .20 \end{bmatrix}$$

Modal Matrix L of Generalised Eigenvectors

$$L = \begin{bmatrix} .09965 & .03533 & .1647 & -.0635 & -.1940 & .5982 & .1494 \\ -.5721 & .0683 & .1260 & .1409 & -.1807 & .2650 & -.3134 \\ .00069 & .3305 & -.3280 & -.3220 & -.2457 & .2444 & .1183 \\ .0934 & .2710 & -.2191 & .0613 & .0669 & .5869 & -.6961 \\ -.0545 & .3401 & .0594 & .1625 & -.3020 & .0255 & .2231 \\ .0710 & -.1631 & -.4968 & .2656 & -.3343 & .1084 & .1361 \\ -.0922 & -.07142 & -.2506 & .2720 & .3479 & -.8219 & .6268. \end{bmatrix}$$

where $L = \begin{bmatrix} \ell'_1 \\ \ell'_2 \\ \vdots \\ \ell'_7 \end{bmatrix}$ and the elements in ℓ' refer to the temperature measurements y_1 to y_7, from left to right.

From the values of μ above, we suspect that only the first $(m-r) = 2$ or 3 eigenvalues will be of significance and we can test this using (5-52) where $N = 60$, $m = 7$

TABLE 4: Significance Test for Generalised Eigenvalues

H_0: last r μ's = 0	Λ''	$-[(N-m) - \frac{1}{2}(2m+1)]\ln\Lambda''$	$\chi^2_{2r}(.05)$
r=4	0.8525	7.25	15.5
r=5	0.6709	18.16	18.3

The χ^2 values at the 95% significance level indicate that certainly the last 4 μ's are zero and possibly the last 5. If we use the result that the last 4 μ's are zero, this implies that the canonical noise model

(5-47) will be of third order. Hence there are only three linear combinations of the N(t)'s that have a significant amount of activity or information and only these three canonical noise variates $\dot{N}_1(t)$, $\dot{N}_2(t)$ and $\dot{N}_3(t)$ need be included in the noise model. The reduced dimension $\dot{\phi}_3$ is calculated as (see 5-47)

$\dot{\phi}_3$ = top left 3x3 partition of $(L\phi L^{-1})$ is given by

$$\begin{bmatrix} \dot{N}_1(t) \\ \dot{N}_2(t) \\ \dot{N}_3(t) \end{bmatrix} = \begin{bmatrix} ..862 & -.127 & -.061 \\ -.045 & .681 & .027 \\ -.008 & -.018 & .432 \end{bmatrix} \cdot \begin{bmatrix} \dot{N}_1(t-1) \\ \dot{N}_2(t-1) \\ \dot{N}_3(t-1) \end{bmatrix} + \begin{bmatrix} \dot{a}_1(t) \\ \dot{a}_2(t) \\ \dot{a}_3(t) \end{bmatrix} \qquad (5\text{-}53)$$

$$\underline{\dot{N}}_3(t) = \dot{\phi}_3 \cdot \underline{\dot{N}}_3(t-1) + \underline{\dot{a}}_3(t)$$

What physical interpretation can be put on the first three rows of L, selected by the canonical analysis, to be the linear combinations of the output which contain the most information? The linear combination for the most information (ℓ_1', the first row of L) places the largest weight (-.5982) on the second last measurement $y_6(t)$. From Figure 17, we see that this corresponds to the average position in time of hot spot temperature. This confirms an intuitive feeling that the hot spot is the single most important measurement in the reactor bed. The second linear combination places a large weight (-.5721) on the temperature

$y_1(t)$ closest to the bed inlet. The inlet temperature is governed closely by (see Section 3.2) the wall temperature and the feed preheater. The wall temperature control configuration (because of its on-off nature) would induce slow cycling dynamics to an otherwise constant inlet temperature. Furthermore,when dynamic data was collected, the total flowrate of gas tended to cycle due to the AR(1) dither signal that was added to the butane flow (see Figure 14). The gas preheater was set at a constant heating value irrespective of the gas flow through it, and therefore induced inlet temperature swings whenever the total flow changed.

The knowledge that the cooling loop and gas preheater was causing a disturbance in the system would probably lead to a re-design of these elements in an industrial reactor to eliminate these effects. Here, this is not possible and instead these disturbances are incorporated into the noise model.

The third linear combination in L appears to place less weight on the previous two temperatures but instead weights all the remaining temperatures nearly equally, indicating that the average level of the temperature profile exhibited the third largest variation.

The canonical analysis thus provides a method for reducing the dimensionality of the dynamic stochastic model. Further, it provides useful, intuitive, information about the underlying disturbances present in the process, which might, with proper interpretation of the underlying physical causes enable one to eliminate them.

CHAPTER 6

CONTROL STUDIES

6.1 Introduction

In Chapter 4, Part B, a linear state space model for reactor control was developed. In this chapter, the state model is used to develop a linear multivariable, quadratic feedback control algorithm, for regulatory control of the reactor (see Section 6.3.1). Kalman Filter theory (Section 6.3.2) is used to obtain state estimates for the system. Two approaches are adopted in designing the controller and the Kalman Filter from the reactor model. In Section 6.4, the white noise terms in the stochastic state space model ($w(t)$ and $v(t)$, see Equations (5-11) and (5-12)) are not identified and modelled independently, but instead are approximated by adding a $\underline{w}(t)$ and $\underline{v}(t)$ (with estimated diagonal covariance matrices) directly to the dynamic model. The parameters in these covariance matrices are chosen such that the corresponding state estimates approach their measured values in the least squares sense. In Section 6.5, the reduced dimensional noise model obtained in Section 5.5. is used directly to derive an augmented state model from which the characteristics of the noise terms $\underline{w}(t)$ and $\underline{v}(t)$ are obtained.

In Section 6.6, the control algorithms developed from the two approaches (in Sections 6.4 and 6.5) are implemented on the reactor in a series of DDC control studies. The two controllers are compared with

each other (using predicted concentrations) as well as with a single loop PI controller with feedback on the hot spot temperature. A final control run which uses the best of the two multivariable algorithms was implemented and the outputs from this controller were compared to concentration data from the gas chromatograph. This section is intended primarily as an initial control study on the reactor. Several future control studies are planned (see Chapter 7) as well as a present parallel study based on an adaptive control scheme (Tremblay (T4)). Numerical values of all control matrices used in this section are presented in Appendix 3.

6.2 Direct Digital Control (DDC) Configuration

A description of the experimental setup as well as the process control configuration has been given in Section 3.2. An equation relating temperature measurements to concentrations was given in Section 4.10.1. This enables one to develop a control scheme based on an objective function expressed in terms of concentrations. Actual concentration measurements from the process gas chromatograph (Section 3.2) were not used as part of the control algorithms developed here.

Some control simulations were performed with arbitrary noise characteristics to obtain some experience with the multivariable control algorithms and to determine what levels of constrained control would be reasonable for the reactor system (J2). Real Time Control Software was developed using a Data General Nova 2/10 minicomputer operating under a Real Time Disk Operating System (RDOS). Data General's Real Time Fortran language was used to write a multivariable, linear

quadratic control "task" as a module program which formed part of a general data aquisition and control package [Tremblay (T5)].

A Flowsheet of the control algorithm is given below:

Control Algorithm

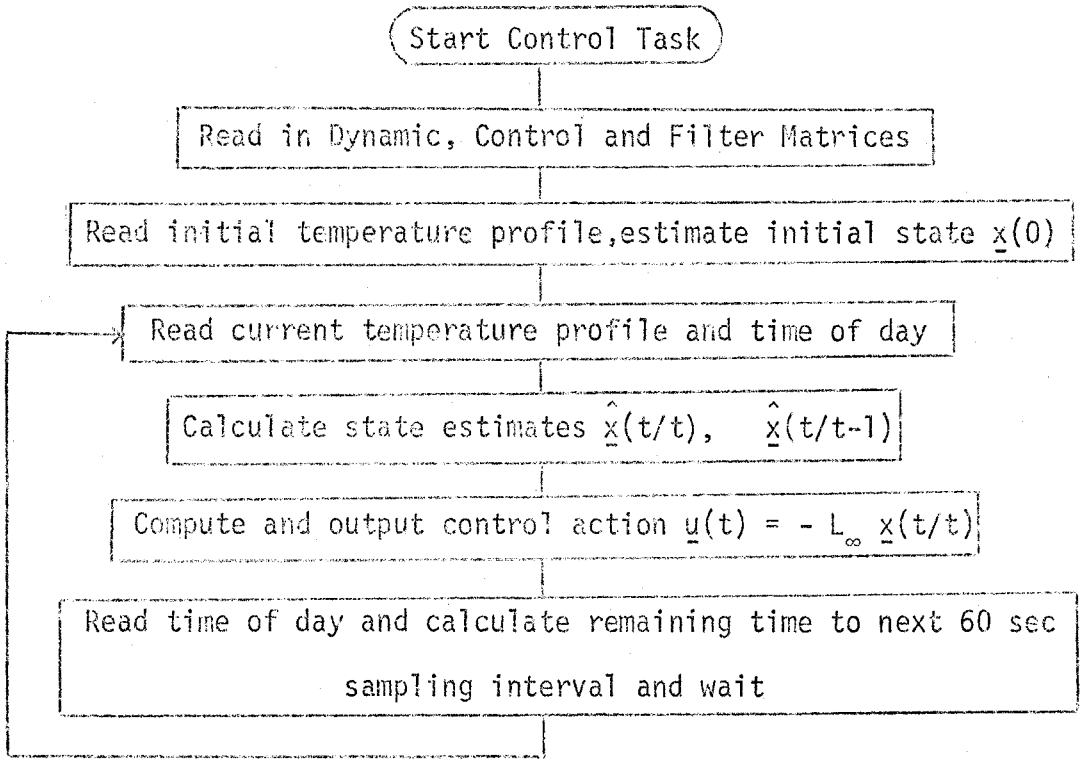

6.3 Optimal Stochastic Control Theory

6.3.1 Linear-Quadratic, Stochastic Feedback Control

The design of constrained feedback controllers for linear, discrete, state space systems is well known [(N1), (A3), (S7)]. Analytical solutions to the general problem are available for systems which can be formulated with a quadratic performance criterion or objective function.

Consider the linear discrete state space Equations

$$\underline{x}(t+1) = A\underline{x}(t) + B\underline{u}(t) + \underline{w}(t) \tag{6-1}$$

$$\underline{y}(t) = H\underline{x}(t) + \underline{v}(t) \tag{6-2}$$

where (6-1) and (6-2) are defined as in (5-11) and (5-12) and for convenience, all variables are in deviation form.

Suppose it is desired to find the sequence of discrete control policies $\underline{u}(t)$, $\underline{u}(t+1)$,...$u(N)$ which will optimise the quadratic performance criterion

$$\underset{\substack{u(t) \\ 0 \leq t < N}}{\text{Min}} \quad E\left[\sum_{t=0}^{N-1} \{\underline{x}'(t)Q_1\underline{x}(t) + \underline{u}'(t)Q_2\underline{u}(t) + \underline{u}'(t)V\underline{x}(t) + \underline{x}'(t)V'\underline{u}(t)\}\right] \tag{6-3}$$

where E[x] is the expectation of x.

Q_1 and Q_2 are symmetric positive semi-definite matrices. This quadratic performance criterion is quite general and includes the case of minimum mean square error control, subject to a constraint Q, on the variance of the manipulated variables, that is

$$\underset{u(t)}{\text{Min}} \quad E\left[\sum_{t=0}^{N-1} \{\underline{C}'(t)\underline{C}(t) + \underline{u}'(t)Q\underline{u}(t)\}\right] \tag{6-4}$$

Remembering that the exit (deviation) concentrations $\underline{C}(t)$, (or $\Delta\underline{C}_{ex}$) may be expressed as a linear combination of the states $\underline{x}(t)$ and (deviation) controls $\underline{u}(t)$ (or $\Delta\underline{u}$) (see Section 4.10.1); in the present notation we

can write

$$\underline{C}(t) = Q_3\underline{x}(t) + Q_4\underline{u}(t-1) \tag{6-5}$$

A reasonable performance criterion would be to minimise the sum of the variances of the exit deviation concentrations $\underline{C}$ (or $\Delta\underline{C}_{ex}$), subject to a constraint Q on the variances of the input flowrates $\underline{u}$. This is obtained by comparing (6-5) and (6-4) to (6-3) and choosing

$$\begin{aligned} Q_1 &= Q_3' Q_3 \\ Q_2 &= Q + Q_4' Q_4 \\ V &= Q_4' Q_3 \end{aligned} \tag{6-6}$$

Q is usually chosen as a diagonal matrix of the form

$$Q = \begin{bmatrix} \lambda_1 & 0 \\ 0 & \lambda_2 \end{bmatrix} \tag{6-7}$$

where λ_i are Lagrange multipliers or simply cost parameters to be adjusted to obtain a desired level of constraint on the inputs $\underline{u}(t)$.

The steady state solution (as final time $N \to \infty$) to the optimal control problem is given by

$$\underline{u}(t) = -L_\infty \hat{\underline{x}}(t/\tau) \tag{6-8}$$

where $\underline{u}(t)$ is the optimal control setting to be applied at time t and $\hat{\underline{x}}(t/\tau)$ is the conditional expectation of the state vector $E[\underline{x}(t)|\underline{Y}(\tau)]$.

where $Y'(\tau) = (\underline{y}(\tau), \underline{y}(\tau-1)....)$ represents the data available (up to time τ) for computing the control action at time t. This conditional state expectation is obtained from the Kalman Filter (see Section 6.3.2). L_∞ is a constant feedback gain matrix obtained as the steady state solution to the matrix Riccatii equations

$$L(t) = [Q_2 + B'S(t+1)B]^{-1}[V + B'S(t+1)A]$$
$$S(t) = A'S(t+1)[A - BL(t)] - V'L(t) + Q_1 \qquad (6\text{-}9)$$

with initial concentration $S(t) = Q_1$.

6.3.2 The Kalman Filter

The discrete Kalman Filter has been derived in several ways (S6, J3) and only the final equations will be given here.

Consider the general dynamic-stochastic model in Section 6.3.1.

$$\underline{x}(t+1) = A\underline{x}(t) + B\underline{u}(t) + \underline{w}(t) \qquad (6\text{-}10)$$

$$\underline{y}(t) = H\underline{x}(t) + \underline{v}(t) \qquad (6\text{-}11)$$

where as before, $\underline{x}(t)$ is an nx1 state vector, $\underline{y}(t)$ is an mx1 vector of observed outputs and u(t) is an px1 vector of input variables. $\underline{w}(t)$ and $\underline{v}(t)$ are white Gaussian noise vectors with zero mean and covariances,

$$E[\underline{w}(t)\underline{w}(t)'] = Rw$$
$$E[\underline{w}(t)\underline{v}'(t+k)] = 0 \qquad \text{all } k$$
$$E[\underline{v}(t)\underline{v}'(t)] = Rv$$

The conditional simultaneous and delayed state estimates are given by

$$\hat{\underline{x}}(t/t) = \hat{\underline{x}}(t/t-1) + K(t)[\underline{y}(t) - H\hat{\underline{x}}(t/t-1)] \tag{6-12}$$

$$\hat{\underline{x}}(t/t-1) = A\hat{\underline{x}}(t-1/t-1) + B\underline{u}(t-1) \tag{6-13}$$

K(t) is the Kalman gain and in general, one is interested in the steady state gain K_∞ which is obtained as the steady state solution to the following matrix Riccat i equations

$$K(t) = P(t+1/t)H'[HP(t+1/t)H' + Rv]^{-1} \tag{6-14}$$

$$P(t/t) = P(t/t-1) - K(t)HP(t/t-1) \tag{6-15}$$

$$P(t+1/t) = AP(t/t)A' + Rw \tag{6-16}$$

where $P(\cdot)$ is the conditional covariance matrix for the state estimate $\hat{x}(\cdot)$ in (6-12) and (6-13) and $P_\infty(\cdot)$, the corresponding steady state value.

In the reactor system, there is no appreciable time lag or transport delay and a change in the input $\underline{u}$ is registered at the output before the next sampling interval 60 seconds later. We thus require the simultaneous state estimate $\hat{\underline{x}}(t/t)$ in (6-12) and the optimal control algorithm (6-8) becomes

$$\underline{u}(t) = - L_\infty \hat{\underline{x}}(t/t) \tag{6-17}$$

Variance Formulae

Variance formulae for the closed loop system (6-10), (6-11) and (6-17) are easily derived (M5). These formulae are useful for calculating, a priori, the covariance matrices of the inputs $\underline{u}$ and outputs $\underline{y}$ for a given constrained feedback control matrix L_∞ derived from a constraint matrix Q;see (6-7). The constraint, Q is varied until the variances of the inputs and the outputs are jointly acceptable. It would be unacceptable for the input flow control valves to bang open and closed frequently and some level of constraint on u (introduced through Q) usually makes for smoother control action without appreciably increasing the variances of the output ((M5) , see also below).

The covariance matrices of $\underline{u}$ and $\underline{y}$ are calculated from (M5)

$$E[\underline{y}(t)\underline{y}'(t)] = H\,\Gamma_X(0)H' + Rv \tag{6-18}$$

$$E[\underline{u}(t)\underline{u}'(t)] = L_\infty[\Gamma_X(0) - P_\infty(t/t)]L_\infty' \tag{6-19}$$

where $\Gamma_X(0)$ is the covariance matrix of the state vector $\underline{x}(t)$, and can be obtained by solving the matrix Riccatti equation

$$\Gamma_X(0) = E[\underline{x}(t)\underline{x}'(t)] = D\Gamma_X(0)D' + DP_\infty(t/t)L_\infty'B' + BL_\infty P_\infty(t/t)D' + BL_\infty P_\infty(t/t)L_\infty'B' + Rw \tag{6-20}$$

where $D = (A - BL_\infty)$. These matrix Riccatti equations are most conveniently solved numerically using an iterative approach (W3).

6.4 Control Synthesis Using a Model with Approximate Noise Characteristics

In Section 5.1.1, we discussed how 9 measured temperatures were interpolated to provide measurements of the 7 states. This ensured that the measurement matrix H in (6-11) was the unit matrix I_7. The measurement error $\underline{v}(t)$ in (6-11) can be approximated by estimating the pure error in the temperature measurements ($\sigma_i^2 \simeq 4.0$ °C, Section 5.1.1) and choosing the covariance matrix Rv to be

$$Rv = \text{diagonal } \langle 4.0 \rangle \tag{6-21}$$

6.4.1 Determination of the Covariance Matrix Rw

In order to determine K_∞ from (6-14) to (6-16) we require both Rv and Rw. $\underline{w}(t)$ is often referred to as the "generation" noise and is difficult to interpret physically in the way $\underline{v}(t)$ can (see Section 5.4). For simplicity then, we assume that $\underline{w}(t)$ can be approximated by specifying a covariance matrix Rw as

$$Rw = \text{diagonal } \langle \beta \rangle \tag{6-22}$$

where β is a single parameter to be chosen. A similar idea was proposed by Hamilton et al. (H6) where the ratio between the diagonals of Rv and Rw was used to weight the state estimate. A large ratio of Rv to Rw caused the model's contribution to be emphasised in the state estimate while a small ratio caused the data to be emphasised.

In this study, β and the corresponding $K_\infty(\beta)$ were chosen by minimising the following objective function

$$J_{K_\infty} = \sum_{t=o}^{N} [\underset{\sim}{y}(t)_{data} - \underset{\sim}{\hat{x}}(t/t-1)]' [\underset{\sim}{y}(t)_{data} - \underset{\sim}{\hat{x}}(t/t-1)] \qquad (6\text{-}23)$$

(6-23) is minimised off-line based on a set of collected data ($\underset{\sim}{y}(t)_{data}$), and $\underset{\sim}{\hat{x}}(t/t-1)$ is calculated from (6-12) and (6-13). The following algorithm was used.

Algorithm to Calculate K_∞

(1) Given a fixed Rv

(2) Choose β, hence Rw

(3) Calculate K_∞ using (6-14) to (6-16)

(4) Calculate $\underset{\sim}{\hat{x}}(t/t-1)$ using (6-12) and (6-13)

(5) Calculate Objective (6-23)

(6) Return to (2) iterating until a minimum in (6-23) is obtained.

Application to Reactor Data

The sum of squares surface was not very sensitive to the value of β as indicated below

Rw diagonal $<\beta>$	J_{K_∞}
β = 1.0	2765
β = 2.5	2752
β = 4.0	2770

A value for β = 2.5 was selected as being satisfactory. For comparison, the sum of squares of residuals for the same set of data (26 May) (sum of variances 48.5, Table 2) was 2867. This sum of squares was obtained by

accounting for all noise in the model by a noise term $\underline{N}(t)$ at the output (Section 5.4.1). The more realistic representation of the noise entering both the dynamic model and the measurement equation through $\underline{w}(t)$ and $\underline{v}(t)$ respectively, accounts partly for the reduced sum of squares value for J_{K_∞} (=2752).

6.4.2 Determination of Input Constraint Q

A satisfactory constraint Q may be chosen by calculating the variances of the outputs $\underline{y}$ and inputs $\underline{u}$ from the variance formulae (6-18) and (6-19). These variances should be jointly acceptable for a given Q. For simplicity, Q was chosen to be

$$Q = \lambda I_2 \tag{6-24}$$

and the single parameter λ was varied until a satisfactory combination of input-output variances was obtained.

Application to Reactor Data

From the table below, a value of $\lambda = 10^{-4}$ was selected as giving satisfactory variances for both input flow rates, u_{C_4} and u_{H_2} as well as for the average variance of the outputs $\underline{y}$. The individual variances for each of the outputs was also adequate. When applied to the 26 May data, the following results were obtained.

λ	Var u_{C_4}	Var u_{H_2}	$\sum V[y_i]$	$V[y_{av}]$
10^{-2}	.510	.048	68.92	9.85
10^{-3}	.639	.049	68.34	9.76
10^{-4}	.973	1.372	66.90	9.56
10^{-5}	4.034	26.02	65.58	9.37

One can see that little is to be gained in terms of reducing the output variance if we reduce the constraint λ below 10^{-4}. However, the large increase in the variance of the two flows would be undesirable.

6.5 Control Synthesis Using a Model with Identified Noise Characteristics

In Section 5.4.1, the technique for augmenting the state equation to take account of a noise model was demonstrated. In Section 5.5.1, a reduced order noise model was developed. In this section, an augmented state equation is derived as well as an augmented objective function.

6.5.1 Augmented State Equation

In Section 5.5.1, a transformation matrix L was obtained that separated the 7^{th} order residual vector $\underline{N}(t)$ into three canonical variates $\underline{N}_3(t)$ (see (5-53)), the remaining four being indistinguishable from white noise (see (5-45)).

We can thus write (see (5-43), (5-45) and (5-46))

$$L\underline{N}(t) = \begin{bmatrix} \dot{N}_1(t) \\ \dot{N}_2(t) \\ \dot{N}_3(t) \\ \dot{a}_4(t) \\ \dot{a}_5(t) \\ \dot{a}_6(t) \\ \dot{a}_7(t) \end{bmatrix} = \begin{bmatrix} \dot{N}_1(t) \\ \dot{N}_2(t) \\ \dot{N}_3(t) \\ \hline \\ 0_4 \\ \\ \\ \end{bmatrix} + \begin{bmatrix} \\ 0_3 \\ \\ \hline \\ \dot{a}_4(t) \\ \dot{a}_5(t) \\ \dot{a}_6(t) \\ \dot{a}_7(t) \end{bmatrix} \qquad (6\text{-}25)$$

The measurement Equation (5-15) is transformed to canonical variates

$$L\,\underline{y}(t) = LH\underline{x}(t) + L\underline{N}(t)$$

or

$$\dot{\underline{y}}(t) = \dot{H}\underline{x}(t) + \begin{bmatrix} \dot{\underline{N}}_3(t) \\ \hline 0_4 \end{bmatrix} + \begin{bmatrix} 0_3 \\ \hline \dot{\underline{a}}_4(t) \end{bmatrix} \qquad (6\text{-}26)$$

where $\dot{}$ represents canonical transforms and $\dot{\underline{N}}_3$ and $\dot{\underline{a}}_4$ are two parts (three and four-dimensional, respectively) of the canonical noise vector $\dot{\underline{N}}(t)$. Following Section 5.4.1, the state vector $\underline{x}$ is augmented and defined as

$$\underline{x}^*(t) = \begin{bmatrix} \underline{x}(t) \\ \hline \dot{\underline{N}}_3(t) \end{bmatrix} \begin{matrix} 7 \\ 3 \end{matrix} \qquad (6\text{-}27)$$

Making use of (6-27) in (6-26) we obtain

$$\dot{\underline{y}}(t) = H^*\underline{x}^*(t) + \underline{y}^*(t) \qquad (6\text{-}28)$$

where $H^* = \begin{bmatrix} H & \vdots & I_3 \\ \cdots & \cdots & \cdots \\ & \vdots & 0 \end{bmatrix}$

and

$$\underline{v}^*(t) = \begin{bmatrix} 0_3 \\ \hline \underline{a}_r(t) \end{bmatrix} \tag{6-29}$$

The noise model (5-53)

$$\underline{N}_3(t) = \phi_3 \underline{N}_3(t-1) + \underline{a}_3(t) \tag{5-53}$$

is incorporated into the dynamic state model (see Section 5.4.1) as

$$\underline{x}^*(t) = \begin{bmatrix} \underline{x}(t) \\ \hline \underline{N}_3(t) \end{bmatrix} = \begin{bmatrix} A & \vdots & 0 \\ \cdots & \cdots & \cdots \\ 0 & \vdots & \phi \end{bmatrix} \underline{x}^*(t-1) + \begin{bmatrix} B \\ \hline 0 \end{bmatrix} \underline{u}(t-1) + \begin{bmatrix} 0 \\ \hline \underline{a}_3(t) \end{bmatrix}$$

or

$$\underline{x}^*(t) = A^* \underline{x}^*(t-1) + B^* \underline{u}(t-1) + \underline{w}^*(t) \tag{6-30}$$

Hence, from (6-29) and (6-30), $v^*(t)$ and $w^*(t)$ are obtained directly and because of the normalisation (5-42), the covariance matrices are

$$Rv^* = 7 \begin{bmatrix} 0_3 & \vdots & 0 \\ \cdots & \cdots & \cdots \\ 0 & \vdots & I_4 \end{bmatrix}^{7}$$

$$Rw^* = 10 \begin{bmatrix} 0_7 & \vdots & 0 \\ \cdots & \cdots & \cdots \\ 0 & \vdots & I_3 \end{bmatrix}^{10} \tag{6-31}$$

6.5.2 Augmented Objective Function

An augmented objective function must be expressed as a quadratic function of the augmented tenth order state vector $\underset{\sim}{x}^*(t)$. The theoretical values of the concentrations can be obtained from the seventh order state model in the form (see (6-5))

$$\underset{\sim}{C}(t) = \underset{7x1}{Z}\ \underset{\sim}{x}(t) + \underset{2x1}{P}\ \underset{\sim}{u}(t-1) \tag{6-32}$$

The observed concentrations, if they were available at each time t, would be modelled as

$$\underset{\sim}{C}_{obs}(t) = Z\underset{\sim}{x}(t) + P\underset{\sim}{u}(t-1) + \underset{\sim}{M}(t) \tag{6-36}$$

where $\underset{\sim}{M}(t)$ is a multivariable noise model for the concentrations analagous to the $\underset{\sim}{N}(t)$ for temperatures. However, since $\underset{\sim}{C}_{obs}(t)$ is unavailable at every sampling interval, hence $\underset{\sim}{M}(t)$, the best approximation at this time is to assume that the augmented state model is perfect and write $\underset{\sim}{C}(t)$ as a direct function of $\underset{\sim}{y}(t)$, calling it $\underset{\sim}{C}^*(t)$,

$$\begin{aligned}\underset{\sim}{C}^*(t) &= Z\underset{\sim}{y}(t) + P\underset{\sim}{u}(t-1)\\ &= Z(H\underset{\sim}{x}(t) + \underset{\sim}{N}(t)) + P\underset{\sim}{u}(t-1)\\ \text{if } H = I_7 \quad &= Z\underset{\sim}{x}(t) + P\underset{\sim}{u}(t-1) + Z\underset{\sim}{N}(t)\end{aligned} \tag{6-34}$$

So in effect, the assumption is that $\underset{\sim}{M}(t) = Z\underset{\sim}{N}(t)$, i.e., all the disturbances that appear in the temperatures are propagated through to the concentrations in this manner. This is, of course, not necessarily true, but is the best approximation, in the absence of concentration

data for control. (6-34) can be written in terms of the augmented state $\underset{\sim}{x}^*(t)$

$$\underset{3x1}{\underset{\sim}{C}^*} = \underset{3x7}{Z}\,\underset{\sim}{x}(t) + P\underset{\sim}{u}(t-1) + ZL^{-1}(L\underset{\sim}{N}(t))$$

$$= Z\underset{\sim}{x}(t) + P\underset{\sim}{u}(t-1) + ZL^{-1}\begin{bmatrix}\dot{\underset{\sim}{N}}_3(t)\\ \hline 0\end{bmatrix} + ZL^{-1}\begin{bmatrix}0_3\\ \hline \dot{\underset{\sim}{a}}_4(t)\end{bmatrix}$$

Let $ZL^{-1} = 3[(ZL^{-1})_A \vdots (ZL^{-1})_B]$

then

$$\underset{\sim}{C}^*(t) = 3[\overset{7}{Z} \vdots (ZL^{-1})_A]\begin{bmatrix}\underset{\sim}{x}(t)\\ \hline \dot{\underset{\sim}{N}}_3(t)\end{bmatrix} + P\underset{\sim}{u}(t-1) + (ZL^{-1})_B\dot{\underset{\sim}{a}}_4(t)$$

$$\underset{3x1}{\underset{\sim}{C}^*(t)} = Z^*\underset{\sim}{x}^*(t) + P\underset{\sim}{u}(t-1) + \dot{\underset{\sim}{\varepsilon}}_3(t) \qquad (6\text{-}35)$$

where

$$\underset{3x10}{Z^*} = [Z \vdots (ZL^{-1})_A]$$

and

$$\dot{\underset{\sim}{\varepsilon}}_3(t) = (ZL^{-1})_B\dot{\underset{\sim}{\varepsilon}}_4(t)$$

a white noise vector.

In (6-35), the concentrations $\underset{\sim}{C}^*(t)$ are expressed as a function of the ten states in $\underset{\sim}{x}^*$ and the augmented objective function is calculated from (6-4) as

$$\min_{\underset{\sim}{u}(t)} \; E\Big[\sum_{t=0}^{N-1}\{\underset{\sim}{C}^{*'}(t)\underset{\sim}{C}^*(t) + \underset{\sim}{u}'(t)Q\underset{\sim}{u}(t)\}\Big] \qquad (6\text{-}36)$$

Application to Reactor Data

The $\underset{2x10}{L_\infty}$ and $\underset{10x7}{K_\infty}$ may be calculated as before in Section 6.3. For this state space model structure, the control matrix L_∞ for the 10x10 system and the corresponding 7x7 system are related according to

$$\underset{2x10}{L_\infty} = [\underset{2x7}{L_\infty} \vdots L_\infty^*]$$

where L^* are the additional elements required for the three additional states in $\underline{x}^*(t)$, the first elements being identical to the seventh order system. The K_∞, due to the simple structure of $\underline{w}^*(t)$ and $\underline{v}^*(t)$ (and thus Rv^* and Rw^*) in (6-31), turns out to be structured as

$$K_\infty = \begin{array}{c} \\ 7 \\ 3 \end{array} \begin{array}{c} \overset{7}{\left[\begin{array}{c} 0_7 \\ \hline I_3 \vdots 0 \end{array}\right]} \end{array}$$

6.6 DDC Control of the Reactor

As mentioned previously the control algorithms are based solely on temperature measurements, although the objective function is expressed as a function of the concentrations. The two control algorithms developed in Sections 6.4 and 6.5 were implemented on the reactor. A single loop control scheme based on control of the hot spot temperature by regulating the hydrogen flow was also tested to provide a comparison. Without the availability of concentration data, the basis used for comparison was the ability of the control algorithms to hold the mole fractions of the various species (as predicted by the model) steady, at their target values, in the presence of stochastic process disturbances. The ability of the algorithms to control the reactor (i.e., to prevent reactor runaway) for step disturbances in the major load variable (the wall temperature) was also tested.

When concentration data became available at a later stage (23 September), the state model was refitted using both concentration and temperature data (see Appendix 3, 23 September data and end of Chapter 5). The 7^{th} order (see (6.4)) control algorithm derived from this model, was implemented and the controller evaluated, in terms of the variations in the measured concentrations in the exit gases. A comparison could also be made between the measured concentrations and those predicted by the model.

6.6.1 Catalyst Deactivation

The problems associated with catalyst deactivation were discussed in Section 5.1.2. From the control standpoint, this problem presented a severe test for the robustness of the control algorithms developed. These algorithms were obtained directly from the state models which were fitted (off-line) to the reactor data obtained several days or months earlier. The reactor could not be left running over this period and when the control algorithms were eventually implemented, a noticeable decline in the catalyst activity was observed. A lower temperature profile was obtained for the same wall temperature and gas flow rates previously used. In order to approximate the previous conditions (under which the model was fitted), the wall temperature was raised by a few degrees to offset the decline in catalyst activity. This, of course, was not entirely satisfactory since an increase in wall temperature cannot compensate exactly for a loss in catalyst activity. As a result, some redistribution of products could be expected to occur. Nevertheless, under these conditions, a similar temperature profile was obtained for the same flow conditions previously used. The robustness of the controllers is a measure of their ability to control the reactor under these somewhat different conditions.

6.6.2 Control Using the 7^{th} Order State Model

A control run, using a 7^{th} order algorithm (derived according to Section 6.4) was implemented on the reactor a few days after fresh catalyst had been installed.

In Figure 22, a plot of the objective function (6-4) with constraint Q = 0, versus the flow controls of hydrogen and butane, is presented, together with the mole fractions of the various species and the conversion of butane. The objective in Figure 22 is minimised if the mole fractions of all species are held as closely as possible about their respective operating levels, in spite of the presence of disturbances. For the first 30 minutes, during which time the reactor is subject to only the inherent stochastic disturbances, the controller is able to hold (with fairly smooth control action) all the mole fractions as well as the conversion reasonably constant. The objective function J, rises by less than 0.1, over this period. Previous attempts at steady state open loop runs indicated that removal of the control during this period would cause the conversion to drop to zero (reaction quenched) or soar to 100% (reactor runaway), i.e., the reactor was open loop unstable. The stochastic control algorithms developed here, are designed specifically to compensate for the stochastic noise disturbances present in the process. Nevertheless, a good test of the robustness of the algorithm is to examine its response to a deterministic load disturbance. The most severe load disturbance in this system would be to step up the wall coolant temperature by even a few degrees. Without control, the highly exothermic nature of the reactions would cause a reactor temperature runaway, giving rise to near 100% conversion and hot spot temperature in excess of 400°C.

After approximately 30 minutes under control, a 5°c step in the wall coolant temperature was made. The controller promptly responded (see Figure 22) by reducing the butane flow rate, thus cutting

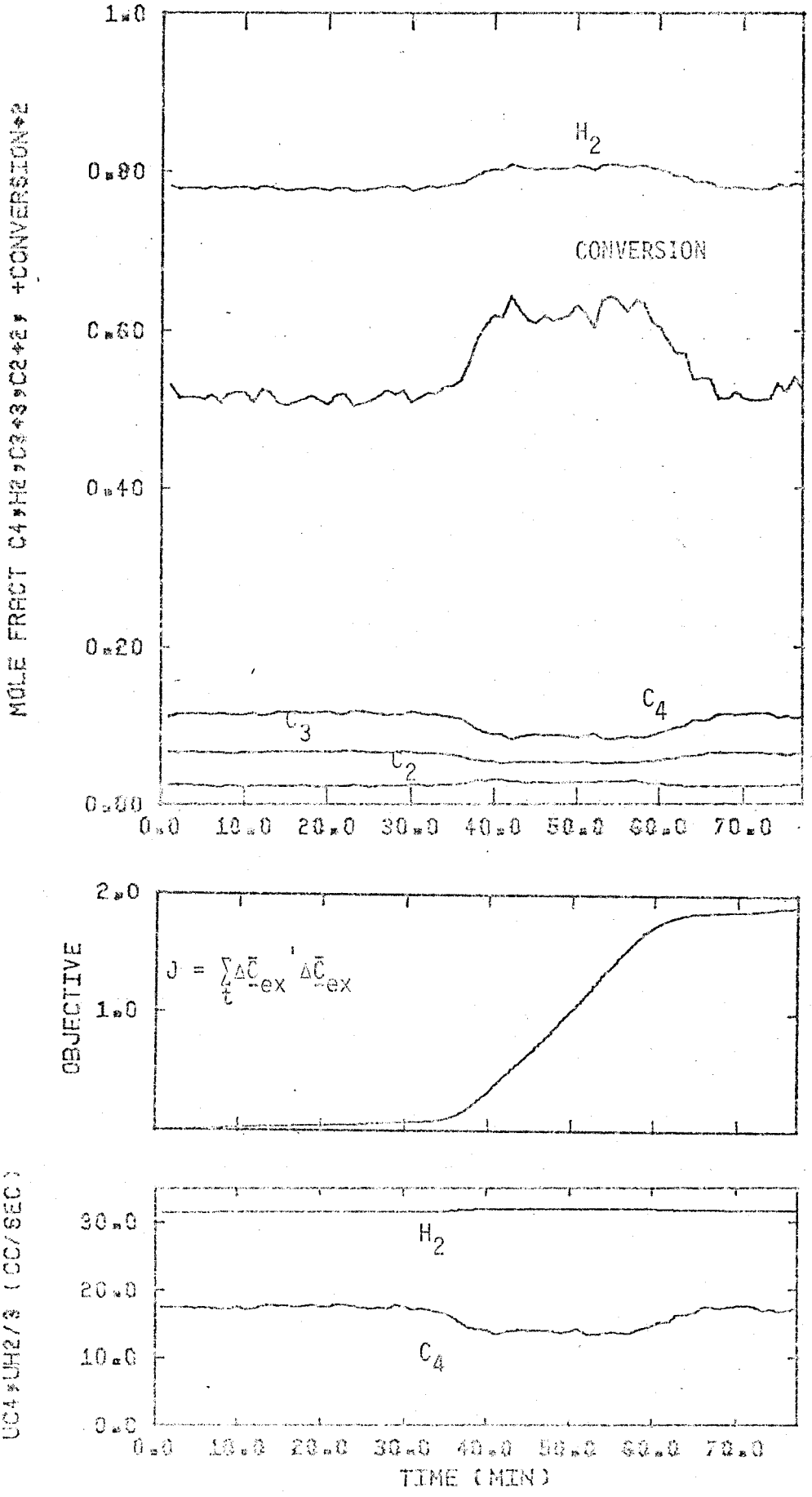

Figure 22: Reactor Control Run Using 7th Order Control Algorithm.

off the potential supply of heat (through the exothermic reaction) and preventing reactor runaway. The flow rate of hydrogen is increased slightly (which tends to decrease the reaction rate (see Appendix 1)), but the controller obviously sees the butane flow as the more important manipulated variable. Some offset in the concentrations is apparent under this severe load disturbance. This is because the stochastic controller is of a proportional state feed back form and contains no integral action; although, if this type of disturbance were common, integral action could be incorporated through the use of additional states. After the process had stabilised at its new level, the wall temperature was stepped back down by 5°C and the flow controls returned to their original levels. The rate of increase of the (cumulative) objective function is reduced accordingly, rising to just under 2.6 for the total 77 minute control run.

6.6.3 Control using the Augmented (10^{th} Order) State Model

The control run using the 10^{th} order algorithm, developed in Section 6.5, was performed within a few hours after the control run using the 7^{th} order algorithm, to reduce the possibility of a change in catalyst activity. The same procedure was followed as for the previous run. The results of this control run are presented in Figure 23. The 10^{th} order controller holds the mole fractions of the various species fairly constant over the first 30 minutes. The quality of the control is not quite as good as the 7^{th} order control. This is evident in the control action (especially of butane) and the mole fraction responses which are not as smooth as those shown in Figure 22. The

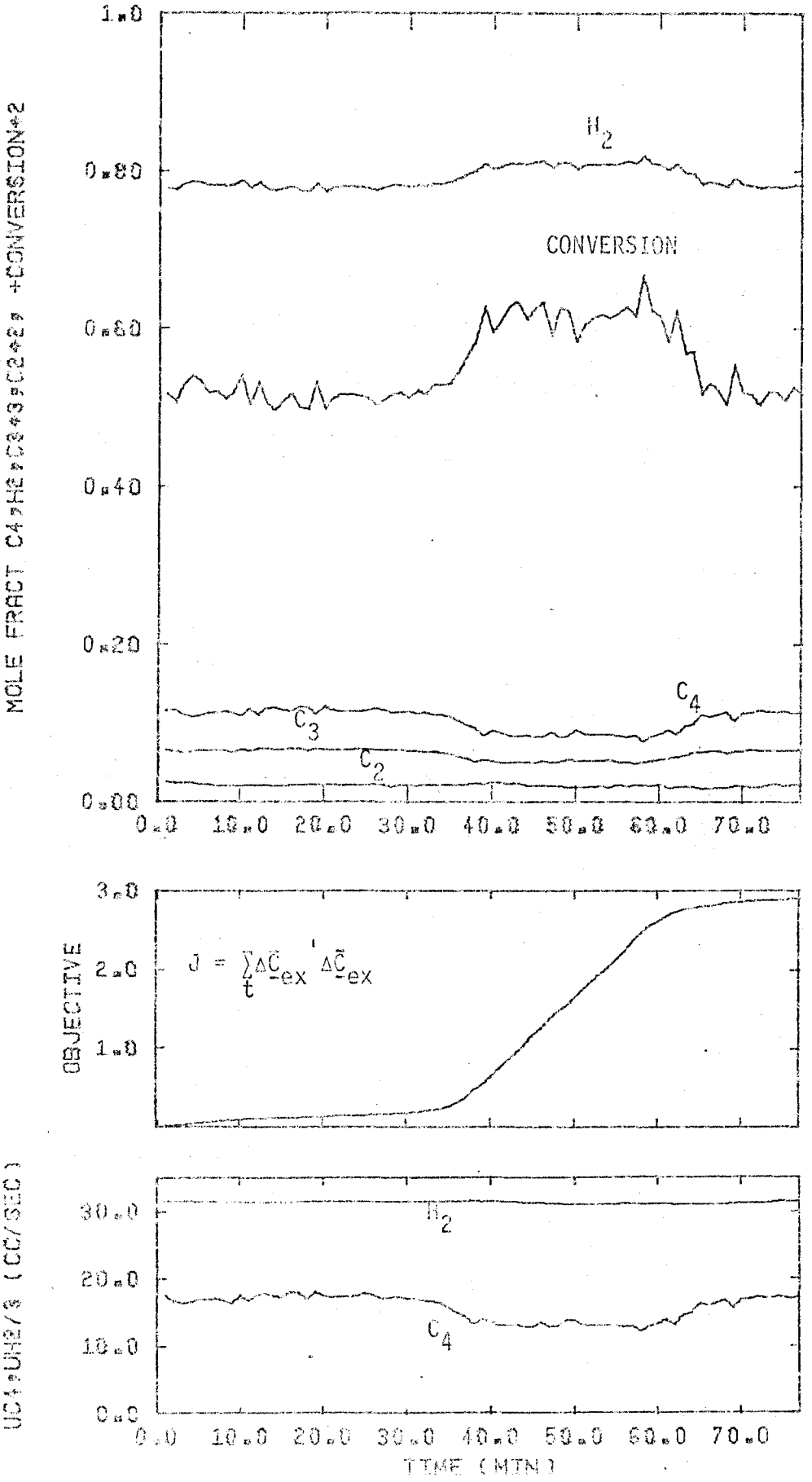

Figure 23: Reactor Control Run using 10th Order Control Algorithm.

objective in Figure 23 rises to about 0.2 over the first 30 minute period, compared to 0.1 for Figure 22. The butane conversion too, shows more variation than that in Figure 22. A step up of 5°C in the wall temperature was introduced after 30 minutes and this controller responded similarly to the previous one by immediately reducing the butane to prevent reactor runaway. The offsets for the two controllers are approximately equal as seen by comparing the change in levels for the conversion and various mole fractions in Figures 22 and 23. The (cumulative) objective function rises to just under 3.0 for the same period (77 minutes) as the previous control run (where a value under 2.0 was obtained). The wall temperature was again stepped down 5°C and the process returns to its previous level. Some reasons for the relative performance of the two controllers are discussed in the following section.

6.6.4 Robustness of the Controllers

A preliminary control run was carried out in which the performances of both the 7^{th} and 10^{th} order algorithms were evaluated. In this run, the catalyst was very weak and conditions were quite different from those under which data was taken for fitting the state model.

A marked characteristic of the control algorithm derived from the 7^{th} order dynamic-stochastic state model in 6.4 was its robustness. In this preliminary control run, the seventh order control algorithm was still able to control the reactor well. The robustness of this 7^{th} order control can be attributed to the fact that diagonal matrices with

equal elements were used for the noise covariance matrices Rv and Rw. This in effect, spreads the disturbances equally across all the temperature states. Should the hot spot temperature change its position due to a change in catalyst activity, the hot spot at the new position is accorded equal weight by the Kalman filter, in obtaining the state estimates. This was not the case for the augmented 10^{th} order state model, which models the actual disturbance characteristics and locations present in the process, at the time of data collection.

In the preliminary control run, the 10^{th} order control algorithm controlled the process poorly and much cycling and wandering of the reactor profiles was observed.

The poor performance of the 10^{th} order algorithm was attributed to its lack of robustness. It was not able to accommodate the change in the process disturbance characteristics caused by a change in catalyst activity between the time the data was collected and the control was implemented. When the model was fitted, the data showed the hot spot positioned towards the exit end of the reactor ($z = .831$, see Figure 16). In deriving and fitting the reduced order noise model, most of the "activity" and disturbances were associated specifically with the hot spot temperature in this position. The linear combinations of temperatures containing the most "activity" or information were obtained and introduced into the augmented state model, (see Sections 5.5 and 6.5). At a later stage when the control run was performed, the hot spot had moved (due to a drop in catalyst activity) towards the centre of the reactor. The previous linear combinations of temperature which contained the most activity, no longer contained most of the

disturbance information. This led to a degradation of control.

For the final control run presented in Figure 23, the catalyst was fairly fresh and the profiles were closer to those under which the model was fitted. The controller performance thus improved considerably but was still not as good as that of the 7^{th} order model (Figure 22).

6.6.5 Single Loop Control

It was mentioned that historically, the reactor was controlled by fixing the butane flow and implementing a single loop PI controller on the hydrogen flow. It was evident, from an examination of the data from a control run, that if a controller could regulate both the position and height of the hot spot, the product distribution too, would be well controlled (given that the catalyst activity was constant). An attempt was therefore made to regulate the hot spot temperature (see Section 5.2) about that value from the operating profile about which the reactor was to be regulated. This corresponded to a zero objective function in (6-4). This PI controller was usually tuned on-line. The bases for tuning were stability of the reactor and speed of response to step disturbances in wall temperature and flows (see also Tremblay (T2)). The proportional gain was obtained by trial and error (in the absence of integral action) and then sufficient integral action was introduced to remove any observed offset. The controller gains usually took several hours to obtain and depended on many factors including wall temperature, catalyst activity, and upper and lower constraints imposed upon the flow rates. This control run was performed one day

before the multivariable control runs in Sections 6.6.2 and 6.6.3. The catalyst was thus probably slightly more active. The results of this run are presented in Figure 24. The flow rate of butane, u_{C_4}, is shown as a constant next to the hydrogen flow control which exhibits a wandering cyclic behaviour. This occurs even over the first 30 minutes, where the PI controller is attempting to regulate the hot spot in presence of stochastic disturbances. The cumulative objective function rises up to 20.0 over this period (about 10 times that for the multivariable schemes). The mole fractions and conversion (as predicted by the state model) are seen to oscillate considerably about their mean values. A 5°C step in the wall temperature introduced after 30 minutes, causes the hydrogen to increase to its upper limit. An upper and lower constraint of 120 and 80 cc/sec (1 atm, 25°C) was imposed by means of the control software to stabilise the control action. The rapid drop to almost zero conversion (due to increased hydrogen flow) predicted by the model is almost certainly not accurate and is the result of the fact that, with hydrogen at its upper limit of 120 cc/s , the linearised state model predictions will have a large error. In spite of the presence of integral action, the mole fractions still have some offset over the period 35 to 45 minutes, after which the wall temperature was stepped back down again by 5°C. The (cumulative) objective rises to about 65, over a 60 minute control run - a considerable increase over the multivariable schemes in Sections 6.6.2 and 6.6.3.

The multivariable control schemes (which followed this run) indicated that butane was the preferred manipulated variable, in contrast to hydrogen flow which historically was used for control.

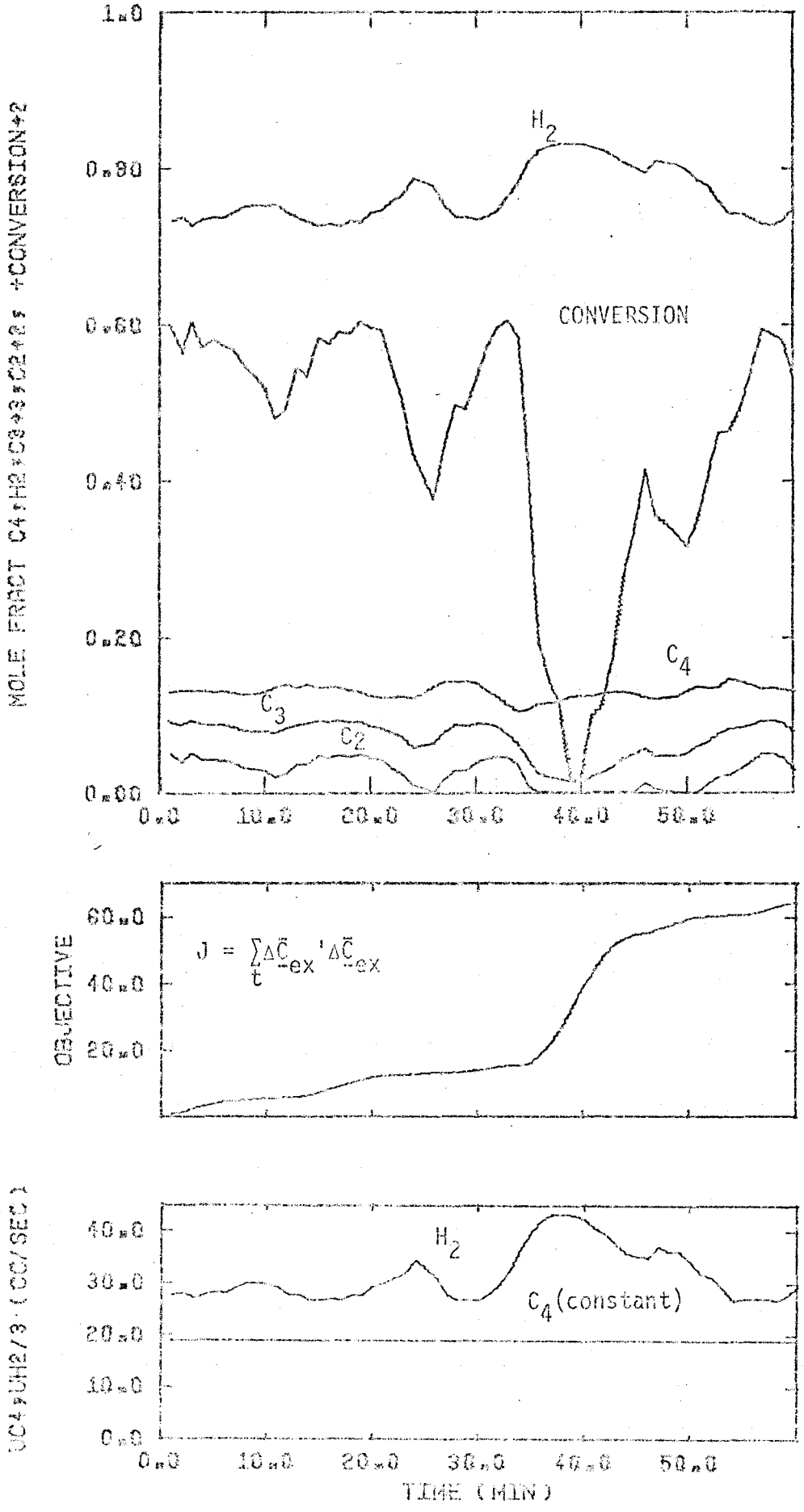

Figure 24: Single Loop PI Control Run.

On this basis, a single loop butane PI controller was later implemented by Tremblay (T4). He found that using butane flow as the controller for a data collection run, allowed him to obtain higher hot spot temperatures (up to 300°C) with less danger of reactor temperature runaway.

However, large manipulations in the butane flow were often required on Tremblay's run and this would have the effect of upsetting the production rates of the various products. This controller may thus be of limited usefulness in an industrial environment.

6.6.6 A Control Run With Concentration Data

The concentrations predicted by the model in the previous runs, used only temperature measurements. At the very end of this study, the gas chromatograph was successfully interfaced and concentration data could be obtained. The multivariable controller's ability to regulate the actual concentrations (measured by the gas chromatograph) could therefore be evaluated. An exact comparison between predicted mole fractions and the data was not possible due to a lack of proper synchronisation between temperature and concentration data (see end of Chapter 5). Nevertheless, the comparisons (shown in Figure 25) generated a lot of confidence in the model and the control algorithm. The state model was fitted to both concentration and temperature data (see Chapter 5 with Figures 20 and 21) and used to derive a 7^{th} order control algorithm (the 7^{th} order algorithm was shown in previous sections to be superior and more robust than the 10^{th} order algorithm). The noise structure for Rw and Rv used in the 26 May run was used again (see Appendix 3). The data for fitting this state model was collected 10

days before the control run and some loss of catalyst activity was observed when the control run was performed. To offset this, the wall temperature was raised by 3°C and thus some bias in the product distribution and levels was expected. In spite of this, the model predicted the mole fractions and conversion remarkably well as shown in Figure 25. The controller is seen to hold the mole fractions fairly constant and close to the values measured by the chromatograph, over the initial period of control, 60 minutes, where only stochastic disturbances were present. Over this period, the cumulative objective rose to 0.07, as compared to 0.1 over a 30 minute period in Figure 22.

Again a 5°C step in the wall temperature was introduced (at 60 minutes) and as before, the controller prevented reactor runaway by dropping the butane flow significantly and raising the hydrogen flow slightly. The offset in the levels is again due to the absence of integral action in the control algorithm. Even at the new level, the model is able to predict the mole fractions well. After approximately 35 minutes at the offset levels, the wall temperature was stepped back down by 5°C and the mole fractions and conversion returned to their previous levels. The total rise in the objective function over the 130 minute control run was 0.68.

A state space model has been fitted, using both concentration and temperature data. This model adequately predicts the concentration dynamics and levels in the reactor. The control algorithm derived from this model is able to regulate the reactor in the face of stochastic and deterministic load disturbances.

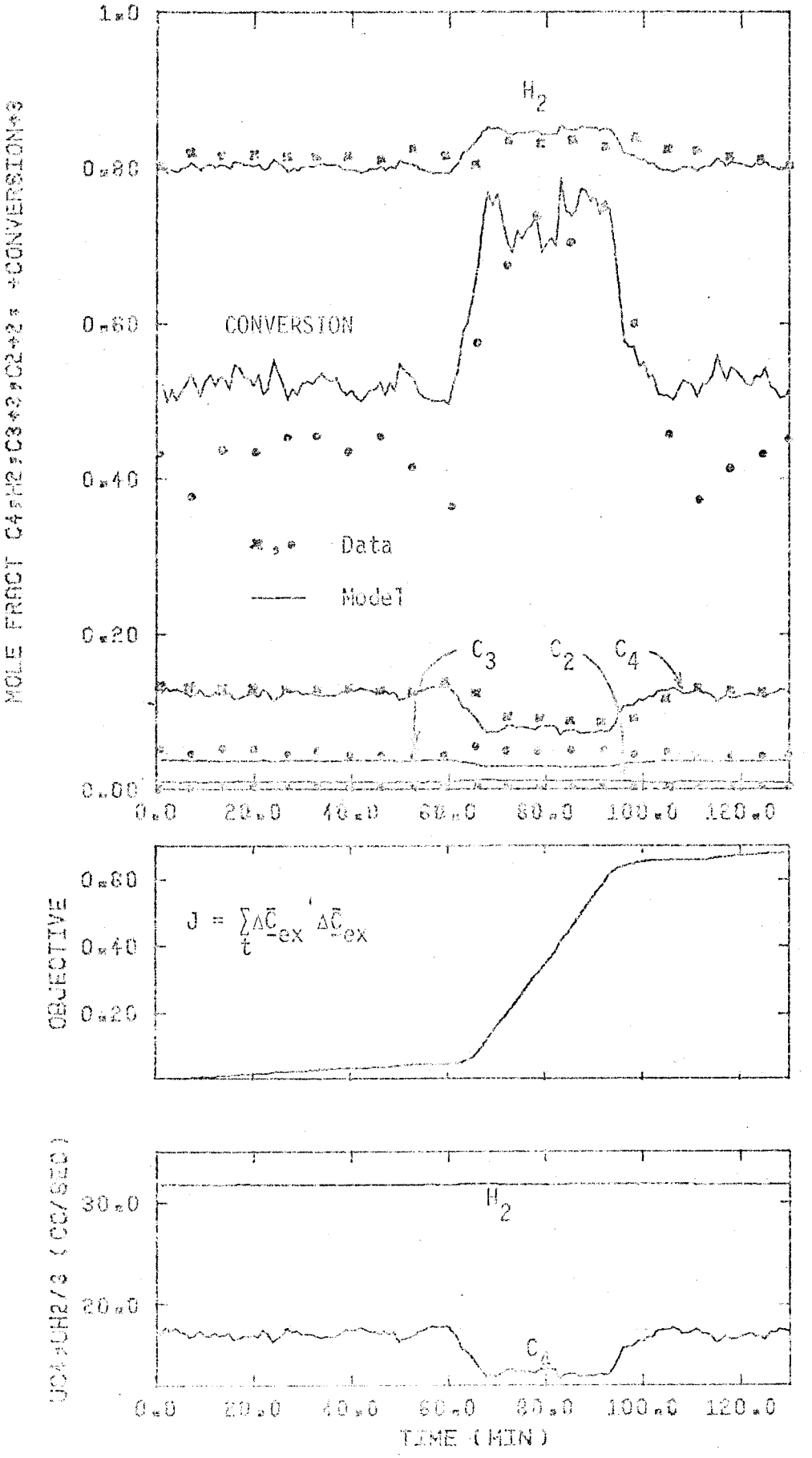

Figure 25: Reactor Exit Mole Fractions Under Control, Model vs. Data.

The multivariable control studies discussed in this section were the first to be implemented on this reactor. They have demonstrated that this reactor can be well regulated by means of a multivariable linear quadratic stochastic feedback controller. The emphasis has been on applied control studies in the hope that the implications of these studies may be extended to include industrial process control problems.

CHAPTER 7

CONCLUSIONS AND FUTURE WORK

An attempt has been made to apply the concepts of multivariable stochastic modelling and control theory to a complex chemical process. The non-adiabatic fixed bed catalytic reactor represents a challenge from the modelling, the parameter estimation, and the control points of view. This study is the first apparent published work in the application of multivariable stochastic modelling and control theory to an actual fixed bed reactor. As such, it attempts to close a large existing gap between the theory and application of modern stochastic control theory. Motivation for this study is amply expounded upon by the authors whose work is discussed in Section 2.1, and an attempt was made to bear their philosphy in mind throughout the period of this work.

In particular, this thesis has examined the problems of formulating a comprehensive process model for the reactor. This model consisted of a set of four simultaneous, non-linear partial differential equations.

The method of orthogonal collocation was used successfully to simplify the process model in two stages. Initially, a high order state space model, suitable for simulation studies, was developed and finally, a low order state space reactor model suitable for on-line DDC studies resulted.

A method of obtaining the parameter matrices in the state model by estimating a few parameters (which have physical meaning) in the partial

differential equations was developed. This method was successfully used to fit the state model to first, dynamic temperature data and then, to dynamic temperature and concentration data from the reactor.

The stochastic noise disturbances present in the reactor system were characterised and two procedures for modelling these disturbances were applied. This resulted in two dynamic-stochastic state space models for the reactor; a seventh order model and a tenth order model.

Optimal stochastic feedback control algorithms (to regulate reactor exit concentrations) were derived from these two models and successfully implemented on the reactor in a series of DDC control studies. The two control algorithms showed considerable improvement over a single loop PI controller which was implemented as a base case for comparison.

In a final multivariable control run, the model demonstrated its ability to predict the actual exit reactor concentrations (as measured by the process gas chromatograph) and the control algorithm was able to regulate these concentrations well.

A large effort was necessary to obtain a low order state model for this reactor. This model however, provides extensive information about the system, allowing one to relate concentrations to temperatures and to predict dynamic temperature and concentration profiles in the radial and axial directions. In an industrial environment, the value of the information provided by this extensive model and the quality of the control schemes developed from it, would have to be weighed against the cost in man-hours of developing the model. This thesis seeks to demonstrate that extensive process models can be obtained and successfully

used to derive and implement multivariable control schemes, which did show considerable improvement over single loop schemes here. This thesis thus argues in favour of opening industrial process control problems to modern control theory.

Future Work

A direct extension of this work would be the development of a combined concentration and temperature noise model and the inclusion of both temperature and concentration measurements in a state estimator. The fact that these measurements are available at different time intervals poses an interesting problem.

The Extended Kalman Filter, which uses a linear filter equation coupled with a non-linear state model would provide an interesting application to the reactor. The development of a non-linear state model would increase its range of application and could lead to the development of a servo control scheme which may be used for startup, shutdown and optimal changeover control schemes.

Some technique which specifically accounts for the changing catalyst activity on the reactor would be of great interest. Either the rate of change of catalyst activity could be modelled or some on-line adaptive scheme could be developed to track the changes in catalyst activity.

There are, at present, several on-going or planned studies on the reactor. Tremblay (T4) has developed a control scheme based on a

multivariable model reference adaptive control technique which uses concentration and temperature measurements. The adaptive ability of the control scheme should be able to track any changes in catalyst activity. Some of the non-linearities in the process should be accounted for and this would allow one to operate at a variety of conditions.

Wong (W3) is studying the identification and estimation of a multivariable transfer-function noise model from the input-output data of the reactor. This empirical or black-box model will be used to derive and implement a multivariable stochastic controller which will provide a direct comparison with this study.

Harris (H7) is examining the application of a univariate self-tuning regulator to the reactor.

The reactor is sufficiently varied and complex a system to provide an interesting application for a variety of modelling and control studies and it is hoped that this study will provide some ground work for these studies.

REFERENCES

(A1) Aoki, M. "Control of Large Scale Dynamic Systems by Aggregation", IEEE Trans. Aut. Contr. AC-13 (3), 246 (1968).

(A2) Aström, K.J., "Computer Control of a Paper Machine - an Application of Linear Stochastic Control Theory", IBM J. Res. Dev. 11, 389 (1967).

(A3) Aström, K.J., Introduction to Stochastic Control Theory, Acad. Press , N.Y. (1970).

(B1) Beek, J., "Design of Packed Catalytic Reactors", Adv. Chemical Eng., Vol. 3, 203 (1962).

(B2) Butt, J.B. and Weekman, V.W., "Characterisation of the Activity, Selectivity and Aging Properties of Heterogeneous Catalysts", AIChE Symp. Series, No. 143, 70, 27 (1974).

(B3) Box, G.E.P. and MacGregor, J.E., "The Analysis of Closed-Loop Dynamic Stochastic Systems", Technometrics No. 3, 16, 391 (1974).

(B4) Box, G.E.P. and MacGregor, J.F., "Parameter Estimation with Closed-Loop Operating Data", S.O.C. Report #99, Faculty of Engineering, McMaster University, Hamilton, Ontario, July (1975).

(B5) Box, G.E.P. and Draper, N.R., "The Bayesian Estimation of Common Parameters from Several Responses", Biometrika 52, 355 (1965).

(B6) Box, G.E.P. and Jenkins, G.M., Time Series Analysis Forecasting and Control, Holden Day, San Francisco (1970).

(B7) Box, G.E.P. and Tiao, Personal Communication to J.F. MacGregor (1971).

(B8) Bartlett, M.S., "Further Aspects on the Theory of Multiple Regression", Proc. Camb. Phil. Soc. 34, 33 (1938).

(B9) Bartlett, M.S., "Multivariate Analysis". J.R.S.S.(B) 9, 176 (1947).

(B10) Burlisch, R. and Stoer, J., "Numerical Treatment of Ordinary Differential Equations by Extrapolation Methods", Numerishe Mathematik 8, No. 1, 1-13 (1966).

(C1) Carberry, J.J. and White, D., "On the Role of Transport Phenomena in Catalytic Reactor Behaviour", Ind. Eng. Chem. 61 (7), 27 (1969).

(C2) Crider, J.E. and Foss, A.S., "Computational Studies of Transients in Packed Tubular Chemical Reactors", AIChE 12 (3), 514 (1966).

(C3) Crider, J.E. and Foss, A.S., "An Analytical Solution for the Dynamics of a Packed Adiabatic Chemical Reactor", AIChE 14 (1), 77 (1968).

(C4) Chang, K.S., C.E.S. 25 (9), 1405 (1971).

(D1) Dyring, J., Kummel, M., "Analogue Simulation and Control of a Tubular Reactor", Chem. Eng. J. 5 (1), 93 (1973).

(D2) Dewash, L., Froment, G.F., C.E.S. 26 (5), 631 (1971).

(D3) Davison, E.J., "A Method of Simplifying Linear Dynamic Systems", IEEE Trans. Aut. Cont. AC-11 (1), 93 (1966).

(E1) EISPACK An Eigenvalue Eigenvector Subroutine Package Available Through McMaster University Fortran Library, Hamilton, Ontario.

(F1) Froment, G.F., Adv. Chem. Ser. 109, "Chemical Reaction Engineering", American Chemical Soc., p. 1-34 (1972).

(F2) Froment, G.F., "Fixed Bed Catalytic Reactors", Ind. Eng. Chem. 59 (2), 18 (1967).

(F3) Froment, G.F., Chem. Eng. Techn. 46 (9), 381 (1974).

(F4) Finlayson, B.A., "Packed Bed Reactor Analysis by Orthogonal Collocation", C.E.S. 26, 1081 (1971).

(F5) Finlayson, B.A., "Orthogonal Collocation in Chemical Reaction Engineering", Cat. Rev.-Sci. Eng. 10 (1), 69-138 (1974).

(F6) Ferguson, N.B. and Finlayson, B.A., "Transient Chemical Reaction Analysis by Orthogonal Collocation", Chem. Eng. Journal 1, 372 (1970).

(F7) Finlayson, B.A., Method of Weighted Residuals and Variational Principles, Acad. Press, N.Y. (1972).

(F8) Foss, A.S., "Critique of Chemical Process Control Theory", AIChE 19 (2), 209 (1973).

(F9) Fisher, D.G. and Seborg, D.E., "Advanced Computer Control Improves Process Performance", Instrumentation Technology 20, 71 (1973).

(F10) Ferguson, N.B. and Finlayson, B.A., "Transient Modelling of a Catalytic Converter to Reduce Nitric Oxide in Automobile Exhaust", AIChE 20 (3), 539 (1974).

(F11) Friedly, D., Dynamic Behaviour of Processes, Prentice Hall (1972).

(F12) Finlayson, B.A., "Applications of the Method of Weighted Residuals and Variational Methods: 1", B.C.E. 14 (1), 53 (1969).

(G1) Gould, L.A., Chemical Process Control: Theory and Applications, Addison Wesley, Mass. (1969).

(H1) Hlavacek, V., "Aspects in Design of Packed Catalytic Reactors", Ind. Eng. Chem. 62 (7), 8 (1970).

(H2) Hansen, K. Waede, "Simulation of the Transient Behaviour of a Pilot Plant Fixed Bed Reactor", C.E.S. 28, 723 (1973).

(H3) Hansen, K. Waede, "Analysis of Transient Models for Tubular Reactors by Orthogonal Collocation", C.E.S. 26, 1555 (1971).

(H4) Himmelblau, D.M., Process Analysis by Statistical Methods, John Wiley (1970).

(H5) Hoffman, T.W. and Reilly, P.M., "Transferring Information from One Experiment to Another", To be published (1977).

(H6) Hamilton, J.C., Seborg, D.E. and Fischer, D.G., "An Experimental Evaluation of Kalman Filtering", AIChE 19, No. 5, 901 (1973).

(H7) Harris, T., M.Eng. Thesis, McMaster University, Hamilton, Ontario, To be published (1977).

(J1) Jutan, A., "A Parameter Estimation Program for Multiresponse Data using a Bayesian Approach", SOC Report #117, Faculty of Engineering, McMaster University, Hamilton, Ontario, February (1976).

(J2) Jutan, A., et al., "State Space Modelling for the Control of a Non-Adiabatic Packed Bed Catalytic Reactor", SOC Report #114, Faculty of Engineering, McMaster University, Hamilton, Ontario, January (1976).

(J3) Jazwinski, A.H., Stochastic Processes and Filtering Theory, Acad. Press, N.Y. (1970).

(K1) Kestenbaum, A. et al. "Design Concepts for Process Control", Ind. Eng. Chem. Proc. Des. Dev. 15 (1), (1976).

(K2) Kopal, Z., Numerical Analysis, (1955).

(K3) Kurihara, H., "Optimal Control of a Fluid Catalytic Cracking Process", Ph.D. Thesis, M.I.T., Cambridge, Mass. (1967).

(L1) Lee, W. and Weekman, V.W., "Advanced Control Practice in the Chemical Process Industry: A View from Industry", AIChE 22 (1), 27 (1976).

(L2) Levenspiel, O., Chemical Reaction Engineering, John Wiley (1967).

(M1) Mears, D.E., Ind. Eng. Chem. Fund. 15 (1), 20 (1976).

(M2) Michelsen, M.L., Vakil, H.B. and Foss, A.S., "State Space Formulation of Fixed Bed Reactor Dynamics", Ind. Eng. Chem. Fund. 12 (3), 323 (1973).

(M3) Marroquin, G., et al., "Practical Control of Batch Reactors", C.E.S. 28 (4). 993 (1973).

(M4) Marquardt, D.W., "An Algorithm for Least Squares Estimation of Non-Linear Parameters", J. Soc. Ind. Appl. Math. 2, No. 2, (1963).

(M5) MacGregor, J.F., "Optimal Discrete Stochastic Control Theory for Process Application", CJChE 51, 468 (1973).

(M6) MacGregor, J.F., "Topics in the Control of Linear Processes Subject to Stochastic Disturbances", Ph.D. Thesis, University of Wisconsin at Madison, Wisconsin, U.S.A. (1971).

(N1) Noton, A.R.M., Introduction to Variational Methods in Control Engineering, Pergamon Press (1965).

(N2) Nobel, Ben., Applied Linear Algebra, Prentice Hall (1969).

(O1) Orlikas, A., "Kinetic Study of the Hydrogenolysis of n-Butane on Nickel Catalyst", M.Eng. Thesis, McMaster University, Hamilton, Ontario (1970).

(O2) Orlikas, A., Hoffman, T.W., Shaw, I.D.and Reilly, P.M., Can. J. Chem. Eng. 50, 628-636 (1972).

(P1) Paris, J.R. and Stevens, W.F., "Mathematical Models for a Packed Bed Chemical Reactor", Can. J. Chem. Eng. 48, 100 (1970).

(R1) Rosenbrock, H.H., "Distinctive Problems of Process Control", Chem Eng. Prog. 58 (9), 43 (1962).

(S1) Sinai, J. and Foss, A.S., "Experimental and Computational Studies of the Dynamics of a Fixed Bed Chemical Reactor", AIChE 16 (4), 638 (1970).

(S2) Shinsky, F.G., "Stable Distillation Control Through Proper Pairing of Variables", ISA Trans. 10 (4), (1971).

(S3) Seinfeld, J.H., Ind. Eng. Chem. Fund. 9 (4), 651 (1971).

(S4) Shaw, I.D., "Modelling and Discrimination Studies in a Catalytic Fluidised Bed Reactor, Ph.D. Thesis, McMaster University, Hamilton, Ontario (1974).

(S5) Shaw, I.D., Hoffman, T.W., Orlikas, A. and Reilly, P.M., Can. J. Chem. Eng. 50, 637-643 (1972).

(S6) Sage, A.P. and Melsa, J.L., Estimation Theory with Applications to Communications and Control, McGraw-Hill (1971).

(S7) Sage, A.P., Optimum Systems Control, Prentice-Hall (1968).

(S8) Soderström, T., Gustavsson, I. and Ljung, L., "Indentifiability Conditions for Linear Systems Operating in Closed Loop", Int. J. Cont. 21, No. 2, 243-255 (1975).

(T1) Tinkler, L. and Lamb, T., "Dynamics of a Fixed Bed Chemical Reactor - Design of a Feed Forward Control Scheme", Chem. Eng. Prog. Symp. Ser. No. 56, Vol. 61, p. 155 (1965).

(T2) Tremblay, J.P., "Computer Control of a Butane Hydrogenolysis Reactor", M.Eng. Thesis, McMaster University, Hamilton, Ontario, (1973).

(T3) Tremblay, J.P. and Wright, J.D., "Computer Control of Butane Hydrogenolysis Reactor", Can. J. Chem. Eng. 52, 845 (1974).

(T4) Tremblay, J.P., Ph.D. Thesis, McMaster University, Hamilton, Ontario, (to be published).

(T5) Tremblay, J.P., "GOSEX - A Generalised Operating Software Executive Program", SOC-NOVA Report #3.01, McMaster University, Hamilton, Ontario (1975).

(V1) Villadsen, J.V. and Stewart, W.E., "Solution of Boundary Value Problems by Orthogonal Collocation", C.E.S. 22, 1483-1501 (1967).

(V2) Vakil, H.B., Michelsen, M.L. and Foss, A.S., "Fixed Bed Reactor Control with State Estimation", Ind. Eng. Chem. Fund. 12 (3) (1973).

(W1) Weekman, V.W., Jr., "Industrial Process Models - State of the Art", to be published in Chemical Reaction Engineering - I, Adv. in Chem. Ser., Washington, D.C.

(W2) Wilson, G.T., "Modelling Linear Systems for Multivariable Control", Ph.D. Thesis, University of Lancester (1970).

(W3) Wong, L.K., M.Eng. Thesis, McMaster University, Hamilton, Ontario, to be published (1977).

(Y1) Young, L.C. and Finlayson, B.A., Ind. Eng. Chem. Fund. 12, 412-422 (1973).

APPENDIX 1

BUTANE HYDROGENOLYSIS KINETICS

The kinetics of the n-butane hydrogenolysis reaction on a nickel on silica catalyst have been modelled by Orlikas (O1) and Shaw (S4). The fundamental work done by Orlikas was improved by Shaw. They have postulated a mechanism for the reaction and it is represented by Figure A-1. This mechanism is based on the following assumptions:

- butane and propane are absorbed on the catalyst surface and reaction takes place entirely as a surface-catalyzed reaction.
- the reaction products from these reactions may react further or be desorbed.
- because of low probability of breaking two or three carbon bonds simultaneously, reactions converting butane and propane to methane are assumed not to occur.

The formal mechanistic model based on these assumptions has been established and is presented below. From a number of treatments with actual experimental data, the parameters have been estimated to yield the best fit.

Figure A-1

OVERALL REACTION SCHEME FOR THE HYDROGENOLYSIS OF BUTANE

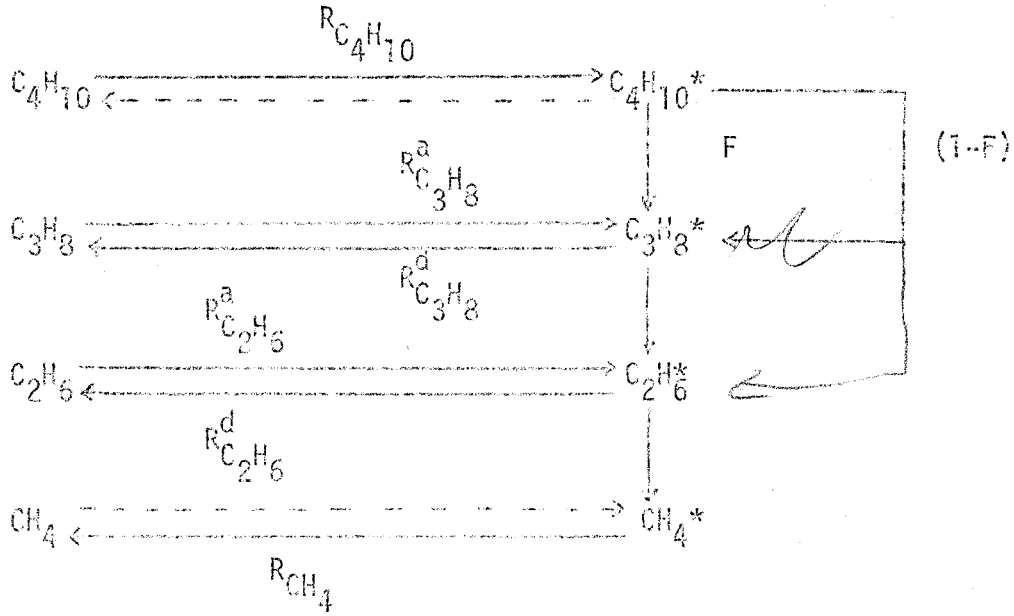

$R_{C_4H_{10}}$ = rate of cracking of butane

$R^a_{C_3H_8}$ = rate of adsorption of propane

$R^d_{C_3H_8}$ = rate of desorption of propane

$R^a_{C_2H_6}$ = rate of adsorption of ethane

$R^d_{C_2H_6}$ = rate of desorption of ethane

R_{CH_4} = rate of production of methane

F = fraction of $C_4H_{10}^*$ that cracks to $C_3H_8^*$

——————→ Reaction Paths Considered

- - - - - - - - - - - - → Assumed = 0

Reaction Rates of the Reaction Species

Net rate of disappearance of butane

$$R_{C_4H_{10}} = k/k_o \cdot A \cdot P^{m'}_{C_4H_{10}} \cdot P^{n'}_{H_2}$$

where $A = k_B \cdot \exp\{-\Delta E_B/RT\}$

Net rate of appearance of propane

$$R_{C_3H_8} = \frac{F \cdot R_{C_4H_{10}} - k/k_o \cdot B \cdot P^{m''}_{C_3H_8} \cdot P^{n''}_{H_2}}{1 + C}$$

where $B = k_{P1} \cdot \exp\{-\Delta E_{P1}/RT\}$

$$C = k_{P2} \cdot \exp\{-\Delta E_{P2}/RT\}$$

Net rate of appearance of ethane

$$R_{C_2H_6} = \frac{(2-F) \cdot R_{C_4H_{10}} - R_{C_3H_8} - k/k_o \cdot D \cdot P^{m'''}_{C_2H_6} \cdot P^{n'''}_{H_2}}{1 + G}$$

where $D = k_{E1} \cdot \exp\{-\Delta E_{E1}/RT\}$

$$G = k_{E2} \cdot \exp\{-\Delta E_{E2}/RT\}$$

Net rate of appearance of methane

$$R_{CH_4} = 4 \cdot R_{C_4H_{10}} - 3 \cdot R_{C_3H_8} - 2 \cdot R_{C_2H_6}$$

Net rate of disappearance of hydrogen

$$R_{H_2} = 3 \cdot R_{C_4H_{10}} - 2 \cdot R_{C_3H_8} - R_{C_2H_6}$$

where

F = fraction of butane which reacts to propane

k/k_o = catalyst activity (dimensionless)

k_B = frequency factor for butane (moles-sec^{-1}-gm catalyst^{-1}-atm$^{(m'+n')}$)

ΔE_B = activation energy for rate of butane cracking (cal-gm mole^{-1})

m' = exponent on butane partial pressure

n' = exponent on hydrogen partial pressure in the butane rate expression

$P_{C_4H_{10}}$ = partial pressure of butane (atm)

P_{H_2} = partial pressure of hydrogen (atm)

k_{P1} = pre-exponential factor in propane rate expression (moles-sec^{-1}-gm catalyst^{-1}-atm$^{-(m''+n'')}$)

k_{P2} = pre-exponential factor in propane rate expression (dimensionless)

$\Delta E_{P1}, \Delta E_{P2}$ = activation energies in propane rate expression (cal-gm mole^{-1})

m'' = exponent on propane partial pressure

n'' = exponent on hydrogen partial pressure in the propane rate expression

$P_{C_3H_8}$ = partial pressure of propane (atm)

k_{E1} = pre-exponential factor in ethane rate expression (moles-sec^{-1}-gm catalyst^{-1}-atm$^{-(m'''+n''')}$)

k_{E2} = pre-exponential factor in ethane rate expression (dimensionless)

$\Delta E_{E1}, \Delta E_{E2}$ = activation energies in ethane rate expression (cal-gm mole^{-1})

m'' = exponent on ethane partial pressure

n'' = exponent on hydrogen partial pressure in the ethane rate expression

$P_{C_2H_6}$ = partial pressure of ethane (atm)

R_i = rate of disappearance or appearance of component i (gm moles-sec^{-1}-gm catalyst^{-1})

T = reacting temperature (°K)

R = universal gas law constant (atm-cm^{+3}-gm mole^{-1}-°K^{-1})

Values of Kinetic Parameters Ref. Shaw (S4)

(a) Butane rate

$k_B = 10^{15.6}$ $\quad m' = 1$

$\Delta E_B = 5.1 \times 10^4$ $\quad n' = -2.34$ (or -2.15)

(b) Propane rate expression

$k_{P1} = 10^{10.6}$ $\quad \Delta E_{P2} = 3.0 \times 10^4$

$k_{P2} = 10^{12.2}$ $\quad m'' = 1.0$

$\Delta E_{P1} = 4.0 \times 10^4$ $\quad n'' = -2.15$ (or -2.08)

(c) Ethane rate expression

$k_{E1} = 10^{4.52}$ $\quad\quad$ $\Delta E_{E2} = 1.6 \times 10^{4}$

$k_{E2} = 10^{6.81}$ $\quad\quad$ $m''' = 1.0$

$\Delta E_{E1} = 2.6 \times 10^{4}$ $\quad\quad$ $n''' = -2.21$

APPENDIX 2

A SUMMARY OF ORTHOGONAL COLLOCATION THEORY

Since the initial paper by Villadsen and Stewart (V1), Orthogonal Collocation has become a popular technique for approximating the solution to differential equations. The method of Orthogonal Collocation is simply one of the many methods of the more familiar group of approximation methods known under the general heading of the Methods of Weighted Residuals (MWR) (F12). However, Collocation methods are generally easier to use than other methods, hence their popularity. The basic idea of collocation and its relation to MWR may be illustrated as follows:

Consider as an example, a boundary value problem of the form

$$\nabla^2 T = 0 \qquad \text{(A-1)}$$

where ∇^2 is the Laplacian operator in x,y,z space. The boundary conditions are specifed as

$$T = T_0 \quad \text{on boundary} \qquad \text{(A-2)}$$

To obtain an approximate solution to (A-1) by MWR, we first choose a trial function of the form

$$T^{(n)} = T_0 + \sum_{i=1}^{N} c_i u_i \qquad \text{(A-3)}$$

where u_i are chosen approximating functions which allow the boundary condition (A-2) to be satisfied and also allow for any symmetry exhibited by the problem. c_i are unknown constants to be determined and (n) is the order of approximation. Notice how the trial function (A-3) incorporates the boundary condition into its structure. We substitute this trial function into the differential Equation (A-1) and since the trial function is unlikely to be an exact solution, we obtain a residual function, R defined as

$$R(c_i,x,y,z) = \nabla^2 T_o + \sum_{i=1}^{n} c_i \nabla^2 u_i \qquad (A-4)$$

Since the boundary condition T_o and chosen the functions u_i are known, the residual R, is a known function of position x,y,z for any given set of constants c_i. In MWR, we choose the constants c_i in such a way that the residual is minimised in some weighted average sense. The weighted (w_j) integrals of the residual are set equal to zero

$$\langle w_j, R\rangle = 0 \qquad j=1,2,\ldots n \qquad (A-5)$$

where

$$\langle w_j, R\rangle = \int_v w_j R dx dy dz$$

and v is the domain of integration.

Combining Equations (A-4) and (A-5) gives

$$\sum_{i=1}^{n} c_i \langle w_j, \nabla^2 u_i\rangle = -\langle w_j, \nabla^2 T_o\rangle \qquad (A-6)$$

or simply

$$\sum_{i=1}^{n} B_{ji} c_i = d_j \qquad j=1,2,\ldots n \tag{A-7}$$

where

$$B_{ji} = \langle w_j, \nabla^2 u_i \rangle \quad \text{and} \quad d_j = - \langle w_j, \nabla^2 T_o \rangle \tag{A-8}$$

The unknown constants are then simply obtained from (A-7) as

$$c_j = \sum_{i=1}^{n} B_{ij}^{-1} d_j \tag{A-9}$$

These constants when substituted into (A-3) given the approximate solution to (A-1).

The relation between the various MWR and the Collocation method can be stated simply in terms of the weights w_j, used in (A-5).

(1) Subdomain method $\quad w_j = \begin{cases} 1 & -x,y,z \text{ in } v_j \\ 0 & -x,y,z \text{ not in } v_j \end{cases}$

(2) Method of Moments $\quad w_j = x^j$

(3) Method of Galerkin $\quad w_j = u_j$

(4) Collocation method $\quad w_j = \delta(x-x_j,\ y-y_j,\ z-z_j)$

where δ refers to the dirac delta function. The use of this function makes evaluation of the integrals in (A-8) particularly simple and hence the unknown coefficients c_i are easily obtained.

Dealing with Orthogonal Collocation in particular now, we see that first a trial function $T^{(n)}$ is chosen with n undetermined coefficients

c_i. These coefficients are then chosen so that the residual function R is exactly zero at each of the n selected points in domain V. This can be verified, since using the definition of the dirac delta function Equation (A-5) becomes

$$R_j = 0 \qquad j=1,2,\ldots n \tag{A-10}$$

Because the residual vanishes at these points, the approximate solution will be exact at these so-called collocation points. Notice also, that the boundary condition is satisfied exactly by choosing the trial function $T^{(n)}$ appropriately. This particular type of collocation is called Interior Collocation (V1).

Two questions remain to be resolved:

(1) Location of the collocation points in domain V.

(2) Choice of the approximating function type u_i

The collocation points j, at which the residuals R_j are set to zero are not chosen randomly, but according to a method which minimises the average error over the whole domain. The choice of collocation points can best be illustrated by means of a quadrature example:

Say we wish to obtain an approximation to the integral I of a symmetric function F(x) over a normalised domain V

$$I = \int_0^1 F dx \tag{A-11}$$

Choose an n^{th} order trial function $F^{(n)}$ of the form, say

$$F^{(n)} = F(1) + (1 - x^2)[C_0^{(n)} + C_1^{(n)}x^2 + \ldots + C_{n-1}^{(n)}x^{2n-2}] \quad (A\text{-}12)$$

The superscript (n) on the coefficients $C_i^{(n)}$, is to emphasise that the coefficients change as the order of approximation changes. Say the optimal collocation points to be determined are written as $x_1, x_2, \ldots x_n$. Because F(x) is symmetric (given), the residual function R_i must vanish at $\pm x_1, \pm x_2, \ldots \pm x_n$, the collocation points. If F is the exact function, then the residual function R may be represented as

$$F - F^{(n)} = R^{(n)} \quad (A\text{-}13)$$

This residual itself can be expanded about the collocation points as follows

$$R^{(n)} = (1 - x^2)[(x_1^2 - x^2)(x_2^2 - x^2)\ldots(x_n^2 - x^2)](b_0^{(n)} + b_1^{(n)}x^2 + b_2^{(n)}x^4 + \ldots) \quad (A\text{-}14)$$

Integration of (A-13) gives

$$\int_0^1 F dx = \int_0^1 F^{(n)} dx + \int_0^1 R^{(n)} dx \quad (A\text{-}15)$$

The last term in (A-15) represents the quadrature error which, from (A-14), depends on the collocation points x_i. To minimise this error, we select the n collocation points so that the first n coefficients $b_0, b_1 \ldots b_{n-1}$ make no contribution to the error integral. This defines the following set of orthogonality conditions:

$$\int_0^1 (1 - x^2)(x_1^2 - x^2)..(x_n^2 - x^2)x^{2k}dx = 0 \quad k=0,1,...n-1 \qquad (A-16)$$

Equations (A-16) uniquely determine the collocation points x_i. With the points thus selected, the integral will be exact if the actual degree of F does not exceed 4n (since all the coefficients $b_i^{(n)}$ are zero beyond $b_{n-1}^{(n)}$ for any function F of degree 4n or less). The calculation of the collocation points can be simplified by rewriting (A-16) in the form

$$\int_0^1 (1 - x^2)P_n(x^2)x^{2k}dx = 0 \quad k=0,1,...n-1 \qquad (A-17)$$

and finding the zeroes of the polynomials $P_n(x^2)$. Furthermore, successive application of (A-17) for n-1,2, etc., generates a family of polynomials, $P_i(x^2)$ which satisfy the orthogonality relations.

$$\int_0^1 (1 - x^2)P_i(x^2)P_j(x^2)dx = \begin{cases} 0 & \text{if } i \neq k \\ d_i & \text{if } i = k \end{cases} \qquad (A-18)$$

The polynomials P_i are in fact, Jacobi polynomials, roots of which are well known. So the collocation points are chosen to be the roots of Jacobi polynomials.

These same polynomials may be used as approximating functions since they form a complete set and provide good approximation properties (Y1).

A typical symmetric trial function is given by

$$T^{(n)} = T(1) + (1 - x^2)\sum_{i=0}^{n-1} c_i^{(n)}P_i(x^2) \qquad (A-19)$$

Derivative and Quadrature Formulae

Once these trial functions are available, they may be used to generate quadrature formulae (V1). One can also develop an expression for the first derivative and Laplacian of $T^{(n)}$ by simply taking derivatives in (A-19). This provides expressions for the derivatives in terms of the unknown coefficients $c_i^{(n)}$; these in turn, may be expressed, using linear algebra (V1), in terms of the temperatures themselves at the collocation points. Based on this, Villadsen (V1) and Finlayson (F7) provide a set of formulae for quadrature and derivatives

$$\text{at } x = x_i \qquad \frac{dT}{dx}^{(n)} = \sum_{j=1}^{n+1} A_{ij}^{(n)} T^{(n)}(x_j) \tag{A-20}$$

$$\text{at } x = x_i \qquad x^{1-a} \frac{d}{dx}\left(x^{-(1-a)} \frac{dT}{dx}^{(n)}\right) = \sum_{j=1}^{n+1} B_{ij}^{(n)} T^{(n)}(x_j) \tag{A-21}$$

$$\int_0^1 f(x) x^{a-1} dx = \sum_{i=1}^{n+1} w_i^{(n)} f(x_i) \tag{A-22}$$

Where a is a geometry factor,

a = 1 flat geometry

a = 2 cylindrical geometry

a = 3 spherical geometry

The first two equations are exact provided the true function order does not exceed 2n. The quadrature is exact for functions up to 4n (V1).

The quadrature formulae are of a familiar form but the derivative formulae are new and they may be viewed as extended finite difference formulae: instead of expressing the derivative at a particular

point in terms of function values on either side of that point, the derivative at point x_i is given in terms of function values across the whole function.

APPENDIX 3

ESTIMATION ROUTINE, DATA AND STATE SPACE MATRICES

(1) State Space Parameter estimation routine using Dynamic Temperature data.

This routine linearises about a given average temperature profile described by a spline function:

NPAR = number of parameters (dynamic)

TIN = sampling interval (60 sec)

PRESS = reactor pressure (1.65 atm)

RI(NPAR) = vector of parameters

RI(1) = k/k_o

RI(2) = λ_o $\quad (\lambda_{er} = \lambda_o + \alpha(T^4 - T_w^4))$

ALP = α (fixed here)

BI = Biot number (43.5)

TW = T_w wall temp (512°K)

COND = constant 1.0 (ignore)

SUBROUTINE UWHAUS Parameter estimation routine using Marquardt's Method (Ref. J.F. MacGregor, Department of Chemical Engineering, McMaster University, Hamilton, Ontario).

(2) Dynamic Temperature data for 26 May run (included as data behind collocation and spline constants for routine in (1)).

(3) Fitted State Space and Control Matrices (26 May).

(4) Dynamic Temperature and mole fraction data (23 September) approximately synchronised (see Chapter 5) as 1,1;2,7;3,13....17,97.

(5) Fitted State Space and Control Matrices (23 September)

(6) Typical parameter correlations matrices for 26 May, 23 September fits.

NOTES

Fitted Control Matrices are identified as

A - discrete A matrix in $\underline{x}(t+1) = A\underline{x}(t) + B\underline{u}(t)$

B - discrete B matrix

L - L_∞ feedback gain matrix in $\underline{u}(t) = -L_\infty \hat{\underline{x}}(t/t)$

Constraint: $Q = \lambda I$, $\lambda = 10^{-4}$ 26 May, $\lambda = 5 \times 10^{-5}$ 23 September.

K - K_∞ Kalman Gain

HI - Measurement matrix $\overset{3x3}{H_i}$, (see Equation (4-62)) in $\Delta\underset{ex}{\tilde{C}}(t) = H_i\underline{x}(t) + C_i\Delta u(t-1)$

CI - Measurement matrix $\overset{3x2}{N}$ (see Equation (4-62))

Operating Flow Rates (cm^3/s)	STP Flows		Reactor Inlet Conditions	
	H_2	C_4	T_w	Pressure
26 May	86.3	16.9	512°K	1.65 (atm)
23 September	87.4	16.1	522°K	1.65 (atm)

Convert STP flows to reactor inlet conditions when calculating controls $\underline{u}$.

```
ATTACH(UWHAUS,ID=HPPJ,CY=4)
ATTACH,IMSLIB.
ATTACH,SSPLIB.
REL,57000.
FTN.
REDUCE.
LDSET(LIB=IMSLIB)
LDSET(LIB=SSPLIB)
LOAD(UWHAUS)
LGO.

      PROGRAM TEST (INPUT,OUTPUT,PUNCH,TAPE5=INPUT,TAPE6=OUTPUT,
     1    TAPE7=PUNCH)
C     ******************************************************************
C   MAIN PROGRAM FOR DYNAMIC ESTIMATION OF REACTOR PARAMETERS
C   LINEARISATION ABOUT GIVEN OPERATING TEMPERATURE PROFILE (FIT USING
C   SPLINE FUNCTION)
C   DYNAMIC TEMP PROFILE IS FIT TO 7*7 STATE MODEL USING TEMP AND INPUT
C   FLOW DATA FROM REACTOR EXPERIMENT
C     ******************************************************************
      EXTERNAL OBJECT
      COMMON Y,U
      COMMON /KNOT/ CI(3,3),YXI(3),XKI(3),NXK
      COMMON/PARM/ BI ,EG
      COMMON/F1/NPAR,NO,NDATA,TIN
      COMMON /AAA/AA  ,N
      COMMON /X7/ COND,ALP
      COMMON /X1/ DER,E,XL,R,XK,TW,RHOB,AX
      COMMON /MOD/ GSH,GSC,CD,SS
      DIMENSION W(4)
      DIMENSION YI(700),R1(4),DIFF(3),SIGNS(3),SCRAT(2900)
      DIMENSION   Y(7,101),U(2,100),U1(2,100)
      DIMENSION AA(8,8)
      DIMENSION X(3,4)
      EQUIVALENCE (U1,YI)
C       $$$*****PARAMETER ALP IS MULTIPLIED BY 1.0E-10 INTERNALLY
C     BETA(2)=RADIAL HEAT CONDUCTIVITY AND IS MOLTIPLIED BY 10**-3 INTERNALLY
      NAMELIST/INFO1/DER   ,BI
      NAMELIST/INFO2/TW,GSH,GSC
      NAMELIST/INFO3/         COND,CD   ,SS
C    ER=DERIVATIVE FACTOR
      ER=1.0E-06
C     TO+Y =D+ILY TEMP IN DEG CELCIUS
      TDAY=25.
      NDATA=60
C       NXK=NUMBER OF KNOT POINTS
      NXK=3
      NXK1=NXK-1
      NO=7
      NI=2
```

```
      NPAR=2
      EPS=1.0E-09
      TIN=60.
100   FORMAT(8F10.4)
C  READ IN REACTOR PARAMETERS(GSC.GSH  NOT NEEDED (RECLLCULATED))
      READ(5,INFO1)
      READ(5,INFO2)
      READ(5,INFO3)
      WRITE(6,INFO1)
      WRITE(6,INFO2)
      WRITE(6,INFO3)
       NN=NO+1
C  READ IN COLLOCATION MATRICES
      DO 600 I=1,NN
       READ(5,100)(AA(I,J),J=1,NN)
600   WRITE(6,100)(AA(I,J),J=1,NN)
C*********     READ KNOT  DATA FOR SPLINE FIT TO OPERATING TEMP PROFILE
      DO 171 I=1,NXK1
        READ(5,1171)(CI(I,J),J=1,3)
171    WRITE(6,1171)(CI(I,J),J=1,3)
      READ(5,1171)(YXI(I),I=1,NXK1)
      WRITE(6,1171)(YXI(I),I=1,NXK1)
1171   FORMAT(3F12.4)
      XKI(1)=0.
      XKI(2)=0.82
       XKI(3)=1.0
      DO 10 I=1,NDATA
      READ(5,1001)(Y(J,I),J=1,NO),(U1(J,I),J=1,NI),II
1001   FORMAT(1H ,9F8.2,I8)
1002   FORMAT(1H0,9F8.2,I8)
10    WRITE(6,1002)(Y(J,I),J=1,NO),(U1(J,I),J=1,NI),II
C     CALC OF STEADY STATE (AVERAGE) INPUT FLOWS
       GSC=0.
       GSH=0.
       CT=273./(TDAY+273.)
       DO 20 K=1,NDATA
       GSH=GSH+U1(1,K)*CT
       GSC=GSC+U1(2,K)*CT
20     CONTINUE
       GSH=GSH/NDATA
       GSC=GSC/NDATA
       WRITE(6,1003) GSH,GSC
1003   FORMAT(*    GSH=*,G12.3,/,*    GSC=*,G12.3)
C      CONVERSION OF U(1)=UC4,U(2)=UH2 DATA TO STP CONDITIONS -STEADY STATE
       DO 11 I=1,NDATA
       U(1,I)=U1(2,I)      *273./(TDAY+273.)     -GSC
       U(2,I)=U1(1,I)      *273./(TDAY+273.)     -GSH
11     CONTINUE
C   CONVERT TO REACTOR INLET CONDITIONS TW,PRESS
       PRESS=1.65
```

```
      COREC=TW/(273.*PRESS)
      DO 12 I=1,NDATA
      DO 12 J=1,2
12    U(J,I)=U(J,I)*COREC
C      DATA SHIFTED IN TIME USE ONE LESS IN ESTIMATION PROG
C  PARAMETERS ACTIVITY R1(1),AND  2 THERMAL CONDUCTIVITY PARAM R1(2),ALP(SET)
      R1(1)=4.0184
      R1(2)=.017734
       ALP=1.48E-13
      NDATA=NDATA-1
C  PARAMETERS FOR ESTIMATION PROGRAM UWHAUS (MARQUARDT,S METHOD)
      MIT=1
      FNU=10.
      FLAM=0.015
      EPS1=1.0E-06
      EPS2=1.0E-04
      DIFF(1)=DIFF(2)=1.0E-03
      SIGNS(1)=1.0
      SIGNS(2)=1.
      NOB=(NDATA*NO)
      DO 500 I=1,NOB
500    YI(I)=0.
      CALL UWHAUS(1,OBJECT,NOB,YI,NPAR,R1,DIFF,SIGNS,EPS1,EPS2,MIT,
     1  FLAM,FNU,SCRAT)
      STOP
      END

      FUNCTION TNOT(Z)
C  SPLINE FUNCTION FOR GIVEN OPERATING PROFILE
      COMMON /KNOT/C(3,3),Y(3),XK(3),NXK
      NXK1=NXK-1
      J=0
       DO 10 I=1,NXK1
      IF(Z.GE.XK(I).AND.Z.LT.XK(I+1))J=I
10    CONTINUE
      IF(Z.GE.XK(NXK))J=NXK1
      D=Z-XK(J)
       IF(D.LT.0.)STOP11
      TNOT=((C(J,3)*D+C(J,2))*D    +C(J,1))*D    +Y(J)
      RETURN
      END

       SUBROUTINE OBJECT(NPROB,X,FF,NOB,NP)
C     ************************************************************************
CC  CALCULATION OF OBJECTIVE FOR USE WITH ESTIMATION ROUTINE
CC  WITH COMMENT CARDS IN PLACE AS IS, SUB OBJECT CALCULATES RESIDUALS
CC  FOR USE WITH SUB UWHAUS
CC  REMOVE C FROM CARDS SET D1=0. ,THEN SUB OBJECT(X,F) CALCULATES DETERMINANT
CC  WHICH IS M.V. GENERALISATION OF  OF LEAST SQUARES,NOW USE ANY OTHER
C   OPTIMASATION ROUTINE E.G. SIMPLEX
```

```
C     ************************************************************************
C       SUBROUTINE OBJECT(X,F)
      COMMON/F1/NPAR,NO,NDATA,TIN
      DIMENSION Y(4)
      DIMENSION P(7,7)
C       DIMENSION WK(50) ,WK1(7)
      DIMENSION FF(700)
      DIMENSION AT(7,100)
      DIMENSION X(4)
      CALL MODEL(X,NPAR,NO,NDATA,TIN,AT,1)
      N=NO
       NTF=NDATA
C        CALCULATION OF   OBJECTIVE FUNCTION
      DO 60 K=1,N
      DO 60 M=K,N
      P(K,M)=0.
      DO 62 L=1,NTF
      IF(P(K,M).GE.1.0E+50)GO TO 62
      P(K,M)=P(K,M)+AT(K,L)*AT(M,L)
62     CONTINUE
      P(K,M)=P(K,M)/FLOAT(NTF)
60     CONTINUE
      DO 61 I=1,N
      DO 61 J=1,N
61    P(J,I)=P(I,J)
      WRITE(6,104)
      SUM=0.
      DO 500  I=1,N
500   SUM=SUM+P(I,I)
104   FORMAT(1H ,//,* CONDITIONAL D MATRIX*//)
      DO 20 I=1,NO
20     WRITE(6,102)(P(I,J),J=1,NO)
102   FORMAT(7E15.4)
      D1=1.
       IF(D1.EQ.1.) GO TO 1000
C     CALL LINV3F(P,WK1,4,N,N,D1,D2,WK,IERS)
      WRITE(6,63)IERS
63     FORMAT(*    IER=*,I5)
      IF(IERS.EQ.130)GO TO 64
      GO TO 65
64    WRITE(6,69)
69    FORMAT(* MATRIX NUMERICALLY SINGULAR E+50 ASSUM+D*)
      DET=1.0E+50
      GO TO 68
65    IF(D1.LE.0.)GO TO 64
      ZD=ALOG10(D1)+D2*ALOG10(2.)
      IF(ZD.GT.100.)GO TO 66
      GO TO 67
66    DET=1.0E+100
      GO TO 68
```

```
      DET=D1*2.**D2
      CONTINUE
C       SUM OF SQUARES OBJECTIVW
        F=DET
      WRITE(6,100)(Y(I),I=1,NPAR)
      WRITE(6,101) DET
100   FORMAT(*    CURRENT PARAMETERS*,/,(E12.5))
101    FORMAT(*   CURRENT OBJECTIVE=*,E15.5)
      GO TO 1001
1000   CONTINUE
      WRITE(6,302) SUM
302    FORMAT(*     NORMALISED SUM OF SQUARES =*,G12.5)
C  PLACE ALL AT(S ON TOP TO FORM ONE LONG COLUMN GIVES SUM OF SUM OF SQUARES
        DO 501 I=1,NO
        DO 501 J=1,NDATA
501     FF((I-1)*NDATA *J)=AT(I,J)
1001   CONTINUE
      RETURN
      END

      SUBROUTINE MODEL(      THETA,NP,NM,NTF,TIN,AI,NSWTCH)
      ************************************************************************
C   SUB TO CALCULATE RESIDUALS OF STATA SPACE MODEL, GIVEN PARAMETERS
C   IN ORIGINAL P.D.E.,S  OF THE REACTOR MODEL
      ************************************************************************
C
C         DATA FORMAT
C
C     READ IN  U STEADY STATE  (USS)  AT STP CONDITIONS
C     THROUGH INFO 2  (NAMELIST)  ,GSH,GSC
C      READ IN DELTA U=    U(TW,PRESSURE)-USS(TW,PRESSURE)
C       AND TEMPERATURE PROFILE  T(TIME)
       COMMON YD,UD,WK1,WK2,WK3,WK4,    WK6,WK,A1,B1,A2,B2
       COMMON /PRES/PRESS
C    YD  IS A VECTOR OF PROCESS OUTPUTS
C     UD  IS A VECTOR OF  PROCESS INPUTS
C     THETA IS A VECTOR OF PARAMETERS
C       NP =NUM  OF PARAMETERS
C     NM  IS DIMENSION OF MODEL AS  SET IN DIMENSIONS STATEMENTS
C     NTF =TOTAL TIME /SAMPLING INTERVAL TIN
C      TIN  = SAMPLING INTERVAL IN SECS
C         AT  IS VECTOR  OF RISIDUALS SAME DIMENSION AS YD
C     DIMENSION OF YD((NM,NTF),AT(NM,NTF),UD(2,NTF)THETA((NP)
       EXTERNAL DERIV1
       EXTERNAL DERIV
       DIMENSION YSS(7)
       DIMENSION Y1(11),RE(11),WK(333)
       DIMENSION   X1(7),X0(7)
       DIMENSION THETA(4),AT(7,100),YD(7,101),UD(2,100)
C     IF NSWTCH=0  MINIMUM OTPUT,SET=1 FOR LAST RUN ONLY
```

```
C       IF    SS EQUALS 1.0  ONLY STEADY STATE WILL BE CALCULATED
CC    IF  CD=0. NO CARDS WILL BE PUNCHED
C       XKE=  BETA +ALP*(T**4-TW**4)
        DIMENSION LW1(21),LW2(21)
        DIMENSION X(8),Y(8),P(7,7)  ,YZ(8)
        DIMENSION AA(8,8),AL(2,7,7),BT(2,7,7),GM(2,7,7),DL(7,7)
C FOR DIFFERENT ORDER MODELS CHANGE DIMENSIONS IN REDUCE AND SUB SIGHPP
        DIMENSION  E1(7,8)
        COMMON /MOD/ GSH,GSC,CD,SS
        DIMENSION A1(21,21),A11(441),B1(21,21),B11(441)
        DIMENSION A2(21,7),A21(147),B2(21,7),B21(147),A3(21),B3(21)
        DIMENSION A4(21,2), A41(42),B4(21,2),B41(42)
        DIMENSION A(7,7),B(7,21),G(7,2),AZ(49),BZ(147),GZ(14)
        DIMENSION WK1(441),WK2(441),WK3(441),WK4(441),WK5(441)
        DIMENSION VECR(7,7),VECI(7,7),EVR(7),EVI(7)
        DIMENSION WK6(441)     ,WK7(14)
        EQUIVALENCE (A1,A11,WK5),(B1,B11)     ,(A2,A21),(B2,B21)
        EQUIVALENCE (A4,A41),(B4,B41),(A,AZ),(B,BZ),(G,GZ )
        EQUIVALENCE (WK1,GM),(WK2,AL),(WK3,BT)
        EQUIVALENCE (VECR,A21),(VECI,B21)
        COMMON /X1/ DER,E,XL,R,XK,TW,RHOB,AX
        COMMON /X2/ AL1,AL2,AL3
        COMMON /X3/ XK0
        COMMON /X4/ CPS,BETA,DERM
        COMMON /X6/ GH,GC
        COMMON/PARM/ BI ,EP
        COMMON /X7/ COND,ALP
        COMMON /AAA/AA  ,N
        COMMON /REAC/ XKE1,XKE2,DEE1,DEE2,  XKP1,XKP2,DEP1,DEP2,XKB,DEB
        COMMON /Z1/ A,B
        COMMON /Z2/ UC,UH
        WRITE(6,1300)
1300    FORMAT(1H1)
        CALL SECOND(TIME)
        WRITE(6,998)TIME
C         IPRINT=NUMBER OF PRINTS FOR DYNAMIC PROFILES AT EACH FIT
        IPRINT=1
C       TRANSFORMED VARIABLES
        XK0=THETA(1)
        BETA=THETA(2)*1.0E-03
        WRITE(6,6000)THETA
6000    FORMAT(E12.4)
        WRITE(6,6612)XK0,BETA
6612    FORMAT(*    XK0=*,G12.5,/,*    BETA=*,G12.5)
100     FORMAT(8F10.5)
2000    FORMAT(7E11.4)
        E=0.4
        XL=25.6
        DERM=500.
        PRESS=1.65
```

```
      DP=0.1
       R=2.045
      AX=13.1
      RHOB=0.72
      CPS=0.22
      GC=GSC*TW/273.     /PRESS
      GH=GSH*TW/273.   /PRESS
      G0=GH+GC
      XK=22.4E-3*TW/273.
      XK=XK/PRESS
      G0K=G0*XK
      AL1=DER*E*XL/R/R*8.
      AL2=2./(BI+2.)
      AL3=BI/(BI+2.)
      ZH=GH/G0K
      ZC=GC/G0K
      N=NM
      X(1)=0.
      X(2)=0.03377
      X(3)=0.16940
      X(4)=0.38069
      X(5)=0.61931
      X(6)=0.83060
      X(7)=0.96623
      X(8)=1.0
      W1=2./3.
      W0=1./3.
C     CONSTANTS FOR REACTION RATES
      DEB=5.1E+4/1.99
      XKB=10**15.6
      XKP1=10**10.6
      XKP2=10**12.2
      DEP1=4.0E+4/1.99
      DEP2=3.0E+4/1.99
      XKE1=10**4.52
      XKE2=10**6.81
      DEE1=2.6E+4/1.99
      DEE2=1.6E+4/1.99
      NN=N+1
C   INITIAL CONDITIONS
      DO 50 I=1,6
      Y(I)=1.0E-15
50    P(I,1)=1.0E-15
      Y(7)=TW
C     P(X,1)  LATER REFERS TO THE SECOND POINT AT X(2)
      P(7,1)=Y(7)
      WRITE(6,101)
101   FORMAT(1H1)
      XX=0.
      C11=0.
```

```
      C10=0.
      C21=0.
      C20=0.
      C41=ZC
      CH1=ZH
      C31=0.
       C40=ZC
      CH0=ZH
      C30=0.
      T0=TW
      T1=TW
       C4AV=W1*C41 +W0*C40
      C3AV=W1*C31+W0*C30
      CHAV=W1*CH1+W0*CH0
      WRITE(6,102)XX,C41,CH1,C31,C21,C11,C40,CH0,    C30,C20,C10,T1,
     1   T0,C4AV,CHAV,C3AV
  102 FORMAT(//F13.5,7E13.5,/,8E13.5)
      EPS=1.0E-03
      DO 51 J=1,N
      DO 120 II=1,7
  120 EVI(II)=Y(II)
      H=X(J+1)-X(J)
      H=H/10.
      ZT=X(J)
  701 CALL DREBS(DERIV,Y,ZT,6,3,2,0,H,1.0E-6,EPS,YZ,EVI,WK1,IER)
      Y(7)=TNOT(ZT)
      WRITE(6,250)ZT,Y
  250 FORMAT(F10.3,7E12.4)
      IF(ZT.GT.X(J+1))STOP10
      IF(ZT.EQ.X(J+1))GO  TO 700
      IF((ZT+H)-X(J+1))701,701,702
  702 H=X(J+1)-ZT
      GO TO 701
  700 CONTINUE
      IF(IER.EQ.129)WRITE(6,103)
  103 FORMAT(* HREDUCED BY 100 , CONVERGENCE NOT OBTAINED*)
      DO 52 K=1,6
   52 IF(Y(K).LE.0.  )Y(K)=1.0E-15
      IF(Y(7).LT.TW)Y(7)=TW
      IF(Y(4).GT.ZC)Y(4)=ZC-1.0E-15
      IF(Y(1).GT.ZC)Y(1)=ZC-1.0E-15
      IF(Y(5).GT.ZH)Y(5)=ZH-1.0E-15
      IF(Y(2).GT.ZH)Y(2)=ZH-1.0E-15
      DO 53  K=1,7
   53 P(K,J)=Y(K)
      C41=ZC-Y(4)
      CH1=ZH-Y(5)
      C31=Y(6)
      C21=3.*Y(4)  -2.*Y(6)  -Y(5)
      C11=2.*Y(5)  +Y(6)  -2.*Y(4)
```

```
      C40 =ZC-Y(1)
      CH0=ZH-Y(2)
      C30=Y(3)
      C20=3.*Y(1) -2.*Y(3) -Y(2)
      C10=2.*Y(2) +Y(3) -2.*Y(1)
      T0=Y(7)
       C4AV=W1*C41 +W0*C40
      C3AV=W1*C31+W0*C30
      CHAV=W1*CH1+W0*CH0
      WRITE(6,102)ZT     ,C41,CH1,C31,C21,C11,C40,CH0,    C30,C20,C10,T1,
     1    T0,C4AV,CHAV,C3AV
      T1=AL2*T0+AL3*TW
51    CONTINUE
      CALL SECOND(TIME)
      WRITE(6,998)TIME
      IF(SS.EQ.1.) RETURN

C
C        STORE STEADY STATE TEMPERATURE PROFILES IN YSS TO BE USED IN RESIDUALS
      DO 420 I=1,NM
420    YSS(I)=P(7,I)
C
C  CALCULATION OF DERIVATIVES
      DO 180 I=1,2
      NS=I-1
      DO 180 J=1,N
      F41=P(4,J)
      FH1=P(5,J)
      F31=P(6,J)
      F40=P(1,J)
      FH0=P(2,J)
      F30=P(3,J)
      T=P(7,J)
      T1=AL2*T +AL3*TW
      S4=T*ER
      C1=F40*(1.+ER)
      AL(I,J,1)=(RC4P(GH,GC,C1 ,FH0,F30,F41,FH1,F31,T,NS)
     1          -RC4P(GH,GC,F40 ,FH0,F30,F41,FH1,F31,T,NS)   )/(F40*ER)
      C2=F41*(1.+ER)
      Q=1.+ER
      AL(I,J,2)=(RC4P(GH,GC,F40,FH0,F30,C2 ,FH1,F31,T,NS)
     1          -RC4P(GH,GC,F40,FH0,F30,F41,FH1,F31,T,NS))/(F41*ER)
      C5=T*Q
      TL=T
      AL(I,J,3)=(RC4P(GH,GC,F40,FH0,F30,F41,FH1,F31,C5  ,NS)
     1          -RC4P(GH,GC,F40,FH0,F30,F41,FH1,F31,TL  ,NS))/S4
      BT(I,J,3)=(RH2P(GH,GC,F40,FH0,F30,F41,FH1,F31,C5 ,NS)
     1          -RH2P(GH,GC,F40,FH0,F30,F41,FH1,F31,TL  ,NS))/S4
      GM(I,J,3)=(RC3P(GH,GC,F40,FH0,F30,F41,FH1,F31,C5  ,NS)
     1          -RC3P(GH,GC,F40,FH0,F30,F41,FH1,F31,TL  ,NS))/S4
```

```
      C6=GC*Q
      AL(I,J,4)=(RC4P(GH,C6,F40,FH0,F30,F41,FH1,F31,T,NS)
     1          - RC4P(GH,GC,F40,FH0,F30,F41,FH1,F31,T,NS) )/(GC*ER)
      BT(I,J,4)=(RH2P(GH,C6,F40,FH0,F30,F41,FH1,F31,T,NS)
     1          - RH2P(GH,GC,F40,FH0,F30,F41,FH1,F31,T,NS) )/(GC*ER)
      GM(I,J,4)=(RC3P(GH,C6,F40,FH0,F30,F41,FH1,F31,T,NS)
     1          - RC3P(GH,GC,F40,FH0,F30,F41,FH1,F31,T,NS) )/(GC*ER)
      C7= GH*Q
      AL(I,J,5)=(RC4P(C7,GC,F40,FH0,F30,F41,FH1,F31,T,NS)
     1          - RC4P(GH,GC,F40,FH0,F30,F41,FH1,F31,T,NS) )/(GH*ER)
      BT(I,J,5)=(RH2P(C7,GC,F40,FH0,F30,F41,FH1,F31,T,NS)
     1          - RH2P(GH,GC,F40,FH0,F30,F41,FH1,F31,T,NS) )/(GH*ER)
      GM(I,J,5)=(RC3P(C7,GC,F40,FH0,F30,F41,FH1,F31,T,NS)
     1          - RC3P(GH,GC,F40,FH0,F30,F41,FH1,F31,T,NS) )/(GH*ER)
      C8=FH1*(1.+ER*NS)
      S2=(FH0*(1 -NS)+FH1*NS)*ER
      C9=FH0*(1.+ER*(1 -NS))
      AL(I,J,6)=(RC4P(GH,GC,F40,C9 ,F30,F41,C8 ,F31,T,NS)
     1          -RC4P(GH,GC,F40,FH0,F30,F41,FH1,F31,T,NS) )/S2
C     XXXXXXXXXXXXXXXXXXXXXXXXXXXXX
      C1=FH0*Q
      BT(I,J,1)=(RH2P(GH,GC,F40,C1 ,F30,F41,FH1,F31,T,NS)
     1          - RH2P(GH,GC,F40,FH0,F30,F41,FH1,F31,T,NS) )/(FH0*ER)
      C2=FH1*Q
      BT(I,J,2)=(RH2P(GH,GC,F40,FH0,F30,F41,C2 ,F31,T,NS)
     1          - RH2P(GH,GC,F40,FH0,F30,F41,FH1,F31,T,NS) )/(FH1*ER)
      C9=F40*(1.+ER*(1 -NS))
      C8=F41*(1.+ER*NS )
      C10=F31*(1.+ER*NS)
      C11=F30*(1.+ER*(1 -NS))
      S1=(F40*(1-NS)+F41*NS)*ER
      BT(I,J,6)=(RH2P(GH,GC,C9 ,FH0,F30,C8 ,FH1,F31,T,NS)
     1          -  RH2P(GH,GC,F40,FH0,F30,F41,FH1,F31,T,NS) )/S1
      S5=(F30*(1-NS)+F31*NS)*ER
      BT(I,J,7)=(RH2P(GH,GC,F40,FH0,C11,F41,FH1,C10,T,NS)
     1          -  RH2P(GH,GC,F40,FH0,F30,F41,FH1,F31,T,NS) )/(S5)
CXXXXXXXXXXXXXXXXXXXXXXXXXXXXXXX
      C1=F30*Q
      GM(I,J,1)=(RC3P(GH,GC,F40,FH0,C1 ,F41,FH1,F31,T,NS)
     1          -  RC3P(GH,GC,F40,FH0,F30,F41,FH1,F31,T,NS) )/(F30*ER)
      C2=F31*Q
      GM(I,J,2)=(RC3P(GH,GC,F40,FH0,F30,F41,FH1,C2 ,T,NS)
     1          -RC3P(GH,GC,F40,FH0,F30,F41,FH1,F31,T,NS) )/(F31*ER)
      C8=F41*(1.+ER*NS)
      C10=FH1*(1.+ER*NS)
      C9=F40*(1.+ER*(1-NS))
      C11=FH0*(1.+ER*(1-NS))
      GM(I,J,6)=(RC3P(GH,GC,C9 ,FH0,F30,C8 ,FH1,F31,T,NS)
     1          -  RC3P(GH,GC,F40,FH0,F30,F41,FH1,F31,T,NS) )/S1
      GM(I,J,7)=(RC3P(GH,GC,F40,C11,F30,F41,C10,F31,T,NS)
```

```
     1          - RC3P(GH,GC,F40,FH0,F30,F41,FH1,F31,T,NS)   )/S2
180   CONTINUE
C     CALCULATION OF HEAT DERIVATIVS
C     FEED IN ALL VALUES OF TEMP FROM X(0) TO X(N)
      DO 183 KK=1,N
183   Y(KK+1)=P(7,KK)
      Y(1)=TW
      DO 181 J=1,N
      F40=P(1,J)
      FH0=P(2,J)
       F30=P(3,J)
C  ORIG NOTATION FOR AA SAME ,BEGIN WITH AA(2,1)
      C1=F40*Q
      K=J+1
      DL(J,1)=( SIGHP(GH,GC,C1  ,FH0,F30,Y(K))
     1        -   SIGHP(GH,GC,F40,FH0,F30,Y(K)))/(F40*ER)
      C2=GC*Q
      DL(J,4)=(SIGHPP(GH,C2,F40,FH0,F30,Y     ,K)
     1        - SIGHPP(GH,GC,F40,FH0,F30,Y     ,K) )/(GC*ER)
      C3=GH*Q
      DL(J,5)=(SIGHPP(C3,GC,F40,FH0,F30,Y     ,K)
     1        -   SIGHPP(GH,GC,F40,FH0,F30,Y     ,K) )/(GH*ER)
      C4=FH0*Q
      DL(J,6)=(SIGHP (GH,GC,F40,C4  ,F30,Y(K))
     1        -   SIGHP (GH,GC,F40,FH0,F30,Y(K)))/(FH0*ER)
      C5=F30*Q
      DL(J,7)=( SIGHP(GH,GC,F40,FH0,C5  ,Y(K))
     1        -   SIGHP(GH,GC,F40,FH0,F30,Y(K)))/(F30*ER)
      YZ(1)=TW
      DO 181 L=1,N
      DO 182  I=1,N
 182  YZ(I+1) =P(7,I)
      K1=L+1
      YZ(K1)=Y(K1)*Q
      E1(J,K1)=(SIGHPP(GH,GC,F40,FH0,F30,YZ  ,K)
     1        -   SIGHPP(GH,GC,F40,FH0,F30,Y     ,K))/( Y(K1)*ER)
181   CONTINUE
C   SET UP MATRICES
C       ZERO MATRICES
      N3=N*3
      DO 500  I=1,N3
      DO 500  J=1,N3
      A1(I,J)=0.
500   B1(I,J)=0.
      DO 507   J=1,N3
      DO 508  I=1,N
      B(I,J)=0.
      A2(J,I)=0.
508   B2(J,I)=0.
      A3(J)=0.
```

```
      B3(J)=0.
      DO 507 K=1,2
      A4(J,K)=0.
507   B4(J,K)=0.
      DO 509 I=1,N
      DO 509 J=1,N
509   A(I,J)=0.
      DO 510 I=1,2
      DO 510 J=1,N
510   G(J,I)=0.

C     A1    AND   B1  MATRIX
      DO 501 I=1,N
      DO 502 J=1,N
      K=I+N
      L=J+N
      K1=I+2*N
      L1=J+2*N
      A1(I,J)=-AA(I+1,J+1)
      B1(I,J)=-AA(I+1,J+1)
      A1(K,L)=-AA(I+1,J+1)
      B1(K,L)=-AA(I+1,J+1)
      A1(K1,L1)= +AA(I+1,J+1)
      B1(K1,L1)= +AA(I+1,J+1)
502   CONTINUE
      A1(I,1)=A1(I,1) -AL(1,I,1)
      B1(I,1)=B1(I,1) -AL(2,I,2)
      A1(K,1+N)=A1(K,1+N) -BT(1,I,1)
      B1(K,1+N)=B1(K,1+N) -BT(2,I,2)
      A1(K1,1+2*N)=A1(K1,1+2*N) -GM(1,I,1)
      B1(K1,1+2*N)=B1(K1,1+2*N) -GM(2,I,2)
      B1(K,I)=-BT(2,I,6)
      A1(K,I)=-BT(1,I,6)
      A1(K1,I)=-GM(1,I,6)
      B1(K1,I)=-GM(2,I,6)
      A1(I,K)=-AL(1,I,6)
      B1(I,K)=-AL(2,I,6)
      A1(K,K1)=-BT(1,I,7)
      B1(K,K1)=-BT(2,I,7)
      A1(K1,K)=-GM(1,I,7)
      B1(K1,K)=-GM(2,I,7)
501   CONTINUE
C   A2    AND   B2  MATRICES
      DO 503 I=1,N
      K1=I+2*N
      K=I+N
      A2(I,I)=AL(1,I,3)
      B2(I,I)=AL(2,I,3)
      A2(K,I)=BT(1,I,3)
      B2(K,I)=BT(2,I,3)
```

```
      A2(K1,I)=GM(1,I,3)
      B2(K1,I)=GM(2,I,3)
C       MATRICES A3   AND B3
      A3(I)=AL(1,I,2)
      B3(I)=AL(2,I,1)
      A3(K)=BT(1,I,2)
      B3(K)=BT(2,I,1)
      A3(K1)=GM(1,I,2)
      B3(K1)=GM(2,I,1)
C    MATRICES A4   AND B4
503   CONTINUE
      DO 504 J=1,2
      JJ=J+3
      DO 504 I=1,N
      K=I+N
      K1=I+2*N
      A4(I,J)=AL(1,I,JJ)
      B4(I,J)=AL(2,I,JJ)
      A4(K,J)=BT(1,I,JJ)
      B4(K,J)=BT(2,I,JJ)
      A4(K1,J)=GM(1,I,JJ)
      B4(K1,J)=GM(2,I,JJ)
504     CONTINUE
C     A   MATRIX
      DO 505   I=1,N
      DO 505   J=1,N
      K=J+1
505   A(I,J)=E1(I,K)
C    B   AND G   MATRIX
      DO 506 I=1,N
      K=I+N
      K1=I+2*N
      B(I,I)=DL(I,1)
      B(I,K)=DL(I,6)
      B(I,K1)=DL(I,7)
      DO 506 J=1,2
      JJ=J+3
      G(I,J)=DL(I,JJ)
506   CONTINUE

C  CALC OF REDUCED N*N SYSTEM, ABAR AND BBAR
      CALL MINV(B11,N3,D,LW1,LW2)
      DX=ABS(D)
      IF(DX.LT.1.0E-06) WRITE(6,1000)  D
1000  FORMAT(* SINGULAR MATRIX, D=*,E10.4)
      CALL MPRD(A3,B11,WK1,N3,N3,2,0,N3)
      CALL MPRD(WK1,B3,WK2,N3,N3,0,2,N3)
      CALL GMSUB(A11,WK2,WK3,N3,N3)
      CALL GMPRD(WK1,B21,WK2,N3,N3,N)
      CALL GMADD(WK2,A21,WK4,N3,N)
```

```
      CALL GMPRD(WK1,B41,WK2,N3,N3,2)
      CALL GMADD(WK2,A41,WK1,N3,2)
      CALL MINV(WK3,N3,D,LW1,LW2)
      DX=ABS(D)
      IF(DX.LT.1.0E-06) WRITE(6,1002)
1002  FORMAT(*   SINGULAR MATRIX 2*)
      CALL GMPRD(WK3,WK4,A21,N3,N3,N)
      CALL GMPRD(WK3,WK1,WK6,N3,N3,2)
      CALL GMPRD(BZ,A21,WK2,N,N3,N)
      CALL GMADD(WK2,AZ,WK4,N,N)
      CALL GMPRD(BZ,WK6,WK2,N,N3,2)
      CALL GMADD(WK2,GZ,WK3,N,2)
      ISI=2*N
      DO 2505  I=1,ISI
2505   WK7(I)=WK3(I)
      CALL GMTRA(WK4,WK1,N,N)
      CALL GMTRA(WK3,WK2,N,2)
      WRITE(6,2503)
2503   FORMAT( //,*          CONTINUOUS MATRIX A*,//)
      DO 512 I=1,N
      J1=(I-1)*N +1
      J2=J1+N-1
      WRITE(6,2000)   (WK1(J),J=J1,J2)
      IF(CD.NE.0.)WRITE(7,2000)(WK1(J),J=J1,J2)
512    CONTINUE
      WRITE(6,2504)
2504  FORMAT(//,*           CONTINUOUS MATRIX  B*//)
      DO  513 I=1,N
      J1=(I-1)*2 +1
      J2=J1+1
      WRITE(6,2000)  (WK2(J),J=J1,J2)
      IF(CD.NE.0.)WRITE(7,2000)(WK2(J),J=J1,J2)
513   CONTINUE
      IF(CD.NE.0.)WRITE(7,2000)(P(7,I),I=1,N)
      IF(NSWTCH.EQ.0) GO TO 2501
C     C    CALCULATION OF OUTPUT MATRICES ZT  AND ZU
      CALL MPRD(B3,A21,WK1,N3,N3,2,0,N)
      CALL GMADD(WK1,B21,WK2,N3,N)
      CALL GMPRD(B11,WK2,WK1,N3,N3,N)
      CALL MPRD(B3,WK6,WK2,N3,N3,2,0,2)
      CALL GMADD(WK2,B41,WK3,N3,2)
      CALL GMPRD(B11,WK3,WK2,N3,N3,2)
C*****************************************
      CALL SMPY(WK1,W1,WK3,N3,N,0)
      CALL SMPY(A21,W0,WK1,N3,N,0)
      CALL GMADD(WK1,WK3,WK5,N3,N)
      CALL SMPY(WK2,W1,WK3,N3,2,0)
      CALL SMPY(WK6,W0,WK1,N3,2,0)
      CALL GMADD(WK1,WK3,WK6,N3,2)
      CALL GMTRA(WK5,WK1,N3,N)
```

```
      CALL GMTRA(WK6,WK2,N3,2)
      WRITE(6,1500)
1500   FORMAT(* MATRICES ZT  AND ZW IN FAV=ZT.DT0  +ZW.DU*          )
      DO 520 I=1,N3
      J1=(I-1)*N+1
      J2=J1+N-1
520   WRITE(6,2000)(WK1(J),J=J1,J2)
      DO 521 I=1,N3
      J1=(I-1)*2+1
      J2=J1+1
521   WRITE(6,2000)(WK2(J),J=J1,J2)
C   CALCULATION OF HTH MATRIX   ********************************************
211    FORMAT(*  MATRIX H *)
      WRITE(6,211)
      K4=0
      K5=1
      K6=N
      DO 201 I=N,N3,N
      DO 200 J=1,N
      CALL LOCV(I,J,IR,N3,N,0)
      K3=J+K4
200   WK1(K3)=WK5(IR)
      WRITE(6,2000)(WK1(II),II=K5,K6)
      IF(CD.NE.0.)WRITE(7,2000)(WK1(M),M=K5,K6)
      K6=K6+N
      K5=K5+N
201    K4=K4+N
205   FORMAT(* HTH  MATRIX *)
      WRITE(6,205)
      CALL GMTRA(WK1,WK2, N,3)
      CALL GMPRD(WK1,WK2,WK3,N,3,N)
      CALL GMTRA(WK3,WK2,N,N)
      DO 203 I=1,N
      J1=(I-1)*N+1
      J2=J1+N-1
      WRITE(6,2000)(WK2(M),M=J1,J2)
      IF(CD.NE.0.)WRITE(7,2000)(WK2(J),J=J1,J2)
203   CONTINUE
C   CALCULTATE EIGENVALUES   OF DYMAMIC MATRIX A
      DO 514 I=1,N
      DO 514 J=1,N
      CALL LOCV(I,J,IR,N,N,0)
514   A(I,J)=WK4(IR)
      CALL EIGENP(N,N,A,48.,EVR,EVI,VECR,VECI,IND)
      IF(IND.EQ.2)WRITE(6,2001)
2001  FORMAT(* EIGEN CALCULATION SUCCESSFUL* )
      WRITE(6,2002)
2002  FORMAT(//,* EIGENVALUES*)
      DO 515 I=1,N
515   WRITE(6,2003)EVR(I),EVI(I)
```

```
2003  FORMAT(2E20.6)
2501   CONTINUE
      CALL SECOND(TIME)
      WRITE(6,998)TIME
998    FORMAT(*         CPU TIME=*,F10.2)

C     CALCULATION OF  DISCREET SYSTEM
10     FORMAT(7E11.4)
      NM2=NM+2
      H=TIN
      WRITE(6,30)
30     FORMAT( *        DISCRETE MATRICES A,B  COLUMNS*)
      N=NM
      DO 20 I=1,N
      DO 20 J=1,N
      CALL LOCV(I,J,IR,N,N,0)
20    A(I,J)=WK4(IR)
      DO 21 I=1,N
      DO 21 J=1,2
      CALL LOCV(I,J,IR,N,2,0)
21     B(I,J)=WK7(IR)
      DO 41 K=1,NM2
      DO 23 I=1,NM2
23    Y(I)=0.
      Y(K)=1.
      UC=Y(NM+1)
      UH=Y(NM+2)
      ZT=0.
      DO 22 I=1,N
22    Y1(I)=Y(I)
      EPSU=1.E-04
      HH=H/10.
      XX=H
401    CALL DREBS(DERIV1,Y,ZT,N,4,2,0,HH,1.0E-6,EPSU,RR,Y1,WK,IER)
      IF(ZT.GT.XX)STOP12
      IF(ZT.EQ.XX)GO TO 400
      IF((ZT+HH)-XX)401,401,402
402   HH=XX-ZT
      GO TO 401
400   CONTINUE
      IF(IER.EQ.129)STOP13
      WRITE(6,10) (Y(I),I=1,N)
      IF(K.GT.N) GO TO 32
      DO 33 J=1,N
33    P(J,K)=Y(J)
      GO TO 42
32     CONTINUE
      DO 34 J=1,N
34    DL(J,K-N)=Y(J)
42     IF(CD.EQ.0.)GO TO 41
```

```
      IF(NSWTCH.EQ.0) GO TO 41
      WRITE(7,10)(Y(I),I=1,N)
41     CONTINUE
      CALL SECOND(TIME)
      WRITE(6,998)TIME
C       GENERATION OF RESIDUALS AT
C     CALCULATION OF INITIAL STATES
      DO 40 IK=1,N
40    X0(IK)=YD(IK,1)-YSS(IK)
      CNT=0
      WRITE(6,6131)X0
6131   FORMAT(7G12.3)
6133  FORMAT(I10,7G12.3)
      DO 38  IT=1,NTF
      DO 39 IK=1,N
39    X1(IK)=0.
      DO 35 I=1,N
      DO 35 J=1,N
35    X1(I)=P(I,J)*X0(J)+X1(I)
      DO 36 I=1,N
      DO 36 J=1,2
36    X1(I)=X1(I)+DL(I,J)*UD(J,IT)
      DO 37 I=1,N
C         AT,S   FOR    Y=H*X
C   DATA MATCHED AS Y(T), U(T)
C   DATA IN THE FORM TEMP(TIME) VS. DELTA U(TIME)
      AT(I,IT)=YD(I,IT+1)-YSS(I)-X1(I)
37     X0(I)=X1(I)
      CNT=CNT+1
      IF(CNT.EQ.IPRINT)GO TO 6132
      GO TO 6134
6132   WRITE(6,6131)X1
       WRITE(6,6133)IT,(AT(I,IT),I=1,N)
C      PUNCH RESIDUALS FOR OFF-LINE ANALYSIS
      IF(CD.NE.0.)WRITE(7,7003) IT,(AT(I,IT),I=1,N)
7003  FORMAT(I3,7E11.4)
      CNT=0
6134   CONTINUE
38    CONTINUE
          CALL NOISE(AT,N,NTF)
      IF(CD.EQ.0.) GO TO 7000
      DO 7001 IT=1,NTF
      WRITE(6,7003)IT,(AT(I,IT),I=1,N)
7001  WRITE(7,7003)IT,(AT(I,IT),I=1,N)
7000  CONTINUE
      CALL SECOND(TIME)
      WRITE(6,998)TIME
      RETURN
      END
```

```
      SUBROUTINE DERIV1(Y,Z,N,DY)
      COMMON /Z2/ UC,UH
      COMMON /Z1/ A,B
      DIMENSION A(7,7),B(7,21)
      DIMENSION Y(1),DY(1)
      DO 10 I=1,N
      DY(I)=0.
      DO 10 J=1,N
10    DY(I)=DY(I) +A(I,J)*Y(J)
      DO 11 I=1,N
11    DY(I)=DY(I)+B(I,1)*UC+B(I,2)*UH
      RETURN
       END

      SUBROUTINE DERIV(Y,Z,N,DY)
      COMMON /X1/ DER,E,XL,R,XK,TW,RHOB,AX
      COMMON /X4/ CPS,BETA,DERM
      COMMON /X5/ GD,  CBAR,RHOG,CPG
      COMMON /X6/ GH,GC
      DIMENSION  Y(7),DY(7)
      F41=Y(4)
      FH1=Y(5)
      F31=Y(6)
      F40=Y(1)
      F30=Y(3)
      FH0=Y(2)
      T=TNOT(Z)
      DO 10 J=1,2
      LL=J-1
      L=3*LL
      DY(1+L)=-RC4P(GH,GC,F40,FH0,F30,F41,FH1,F31,T,LL)
      DY(2+L)=-RH2P(GH,GC,F40,FH0,F30,F41,FH1,F31,T,LL)
10    DY(3+L)= RC3P(GH,GC,F40,FH0,F30,F41,FH1,F31,T,LL)
      DUM7=SIGHP(GH,GC,F40,FH0,F30,T)
C     SETS CORRECT VALUES FOR RHOG,CPG,ETC.
      D1=GD*RHOG*CPG/(AX*XL*CBAR)
      DY(7)=DUM7/D1
      AD7=ABS(DY(7))
C     IF(AD7.GT.DERM)DY(7)=)Y(7)/AD7*DERM
      RETURN
       END
      FUNCTION RC4P(GH,GC,F40,FH0,F30,F41,FH1,F31,T,NS)
      COMMON /X1/ DER,E,XL,R,XK,TW,RHOB,AX
      COMMON /X2/  AL1,AL2,AL3
      COMMON /X3/ XKD
      COMMON /X4/ CPS,BETA,DERM
      GD=GH +GC
      D1=AL1*AX/GD*(F41-F40)
      Z=1.0E+6
      D2=RHOB*Z*XL*AX/GD
```

```
      IF(NS.EQ.0)GO TO 10
      GO TO 11
10    D1=-D1
      GO TO 13
11    CONTINUE
      T1=AL2*T+AL3*TW
      RC4P=D1-D2*RC4(GH,GC,F41,FH1,T1)
      GO TO 14
13    RC4P=D1-D2*RC4(GH,GC,F40,FH0,T)
14    CONTINUE
      RETURN
      END
      FUNCTION RC4(GH,GC,F4,FH,T)
      COMMON /REAC/ XKE1,XKE2,DEE1,DEE2,  XKP1,XKP2,DEP1,DEP2,XKB,DEB
      COMMON /X1/ DER,E,XL,R,XK,TW,RHOB,AX
      COMMON /X3/ XK0
      G0=GH+GC
      G0K=G0*XK
      ZC=GC/G0K
      ZH=GH/G0K
      IF(F4.GT.ZC)F4=ZC-1.0E-15
      IF(FH.GT.ZH)FH=ZH-1.0E-15
      IF(T.LT.TW)T=TW
      S=1.0E-06
      ZCF=(ZC-F4)*S
      ZHF=(ZH-FH)*S
      XA=XKB*EXP(-DEB/T)
      D1=XK0*XA
      D2=(82.057*T)**(-1.15)*ZCF*ZHF**(-2.15)
      RC4=D1*D2
      RETURN
      END
      FUNCTION RC3(GH,GC,F4,FH,F3,T)
      COMMON /REAC/ XKE1,XKE2,DEE1,DEE2,  XKP1,XKP2,DEP1,DEP2,XKB,DEB
      COMMON /X1/ DER,E,XL,R,XK,TW,RHOB,AX
      COMMON /X3/ XK0
      G0=GC+GH
      G0K=G0*XK
      ZH=GH/G0K
      IF(FH.GT.ZH)FH=ZH-1.0E-15
      IF(T.LT.TW)T=TW
      F=0.9
      S=1.0E-06
      ZHF=(ZH-FH)*S
      FX=F3*S
      XB=XKP1*EXP(-DEP1/T)
      D2=1.+XKP2*EXP(-DEP2/T)
      D1=XB*(82.057*T)**(-1.07)*FX*ZHF**(-2.07)
      RC3=(F*RC4(GH,GC,F4,FH,T)-XK0*D1)/D2
      RETURN
```

```
      END
      FUNCTION RC2(GH,GC,F4,FH,F3,T)
      COMMON /PEAC/ XKE1,XKE2,DEE1,DEE2,  XKP1,XKP2,DEP1,DEP2,XKB,DEB
      COMMON /X1/ DER,E,XL,R,XK,TW,RHOB,AX
      COMMON /X3/ XK0
      F=0.9
      G0=GH+GC
      G0K=GC*XK
      S=1.0E-06
      D4=3.*F4-2.*F3  -FH
      IF(D4.LT.0.)D4=1.0E-15
      IF(FH.GT.(GH/G0K))FH=GH/G0K -1.0E-15
      IF(T.LT.TW)T=TW
      ZHF=(GH/G0K-FH) *S
      XD=XKE1*EXP(-DEE1/T)
      D1=XKE2*EXP(-DEE2/T) +1.
      D2=D4*S*ZHF**(-2.21)
      D3=D2*XK0*XD*(82.057*T)**(-1.21)
      RC2=((2.-F)*RC4(GH,GC,F4,FH,T)-RC3(GH,GC,F4,FH,F3,T)-D3)/D1
      RETURN
      END
      FUNCTION  RH2(GH,GC,F4,FH,F3,T)
      D1=3.*RC4(GH,GC,F4,FH,T)-2.*RC3(GH,GC,F4,FH,F3,T)
      RH2=D1-   RC2(GH,GC,F4,FH,F3,T)
      RETURN
      END
      FUNCTION SIGDH(GH,GC,F4,FH,F3,T)
      COMMON /X1/ DER,E,XL,R,XK,TW,RHOB,AX
      F=0.9
      IF(T.LT.TW)T=TW
      DH1=-12560.-5.0*(T-298.)
      DH2=-10322. -6.30*(T-298.)
      DH4=-15542. -2.52*(T-298.)
      D4=RC4(GH,GC,F4,FH,T)
      D3=RC3(GH,GC,F4,FH,F3,T)
      D2=RC2(GH,GC,F4,FH,F3,T)
      SIGDH=-(DH1*F*D4+DH2*(1.-F)*D4 +DH4*(-D2+(2.-F)*D4-D3))
      RETURN
      END
      FUNCTION RH2P(GH,GC,F40,FH0,F30,F41,FH1,F31,T,NS)
      COMMON /X1/ DER,E,XL,R,XK,TW,RHOB,AX
      COMMON /X2/  AL1,AL2,AL3
      COMMON /X3/ XK0
      G0=GH +GC
      D1=AL1*AX/GC*(FH1-FH0)
      Z=1.0E+06
      D2=RHOB*Z*XL*AX/G0
      IF(NS.EQ.0)GO TO 10
      GO TO 11
10     D1=-D1
```

```
      GO TO 13
11    CONTINUE
      T1=AL2*T +AL3*TW
      RH2P=D1-D2*RH2(GH,GC,F41,FH1,F31,T1)
      GO TO 14
13    RH2P =D1-D2*RH2(GH,GC,F40,FH0,F30,T)
14    RETURN
      END
      FUNCTION  RC3P(GH,GC,F40,FH0,F30,F41,FH1,F31,T,NS)
      COMMON /X1/ DER,E,XL,R,XK,TW,RHOB,AX
      COMMON /X2/  AL1,AL2,AL3
      COMMON /X3/ XK0
      G0=GH +GC
      D1=-AL1*AX/G0*(F31-F30)
      Z=1.0E+06
      D2=RHOB*Z*XL*AX/G0
      IF(NS.EQ.0)GO TO 10
      GO TO 11
10    D1=-D1
      GO TO 13
11    CONTINUE
      T1=AL2*T+AL3*TW
      RC3P=D1+D2*RC3(GH,GC,F41,FH1,F31,T1)
      GO TO 14
13    RC3P=D1+D2*RC3(GH,GC,F40,FH0,F30,T)
14    RETURN
      END
      FUNCTION SIGHP(GH,GC,F40,FH0,F30,T)
      COMMON /PRES/PRESS
      COMMON /X1/ DER,E,XL,R,XK,TW,RHOB,AX
      COMMON /X2/  AL1,AL2,AL3
      COMMON /X4/ CPS,BETA,DERM
      COMMON /X5/ GD,  CBAR,RHOG,CPG
      COMMON /X7/ COND,ALP
      G0=GH +GC
      GD=G0
      XKE=  BETA +ALP*(T**4-TW**4)
      RHOG=(GH*0.09  +GC*2.6)*0.273/(TW*G0) *COND*PRESS
      CPG=(GH*0.306  +GC*1.95)/(GH*0.09  +GC*2.6)
      CBAR= CPS*RHOB +CPG*RHOG*E
      IF (T.LT.TW)T=TW
      D1=XKE*4.*AL3*(TW-T)/(CBAR*R*R)
      SIGHP=D1+SIGDH(GH,GC,F40,FH0,F30,T) *RHOB/CBAR
      RETURN
      END
      FUNCTION SIGHPP(GH,GC,F40,FH0,F30,TT,IZ)
      COMMON /PRES/PRESS
      COMMON /X1/ DER,E,XL,R,XK,TW,RHOB,AX
      COMMON /X2/ AL1,AL2,AL3
      COMMON /X4/ CPS,BETA,DERM
```

```
      COMMON /X7/ COND,ALP
      COMMON /AAA/AA   ,N
      DIMENSION AA(8,8)
      DIMENSION TT(1)
      G0=GH+GC
      RHOG=(GH*0.09 +GC*2.6)*0.273/(TW*G0) *COND*PRESS
      CPG=(GH*0.306 +GC*1.95)/(GH*0.09  +GC*2.6)
      CBAR= CPS*RHOB +CPG*RHOG*E
      FACT=-G0*RHOG*CPG/(CBAR*XL*AX)
C  NOTATION FOR  AA DOES NOT CHANGE,BEGIN WITH AA(2,1) TO AA(2,8)
      TEMP=TT(IZ)
      NN=N+1
      SUM=0.
C  CALC  Z DERIVATIVE USING ALL VALUES OF T FROM Z=0 TO Z=1.0
      DO 10 I=1,NN
10       SUM=AA(IZ,I)  *TT(I) +SUM
      SIGHPP=FACT*SUM+SIGHP(GH,GC,F40,FH0,F30,TEMP)
      RETURN
      END
       SUBROUTINE NOISE(XNT,N,NTF)
C     ***************************************************************
CC  CONVERT XNT (N(T)) TO WHITE NOISE SEQUENCE A(T) AND ESTIMATE PHI
CC  IN N(T)=PHI* N(T-1) +A(T)
C     ***************************************************************
      EQUIVALENCE (GM0,GM00),(GM1,GM11),(PSI,PSI1)
      DIMENSION PSI(7,7),XNT(7,100),XAT(7,100)
      DIMENSION  GM0(7,7),GM1(7,7),GM00(49),GM11(49),PSI1(49),LW1(20)
      DIMENSION LW2(20)     ,GM11T(49)
C
CC       CALCULATE GM0
      DO 10 I=1,N
      DO 10 J=I,N
      GM0(I,J)=0.
      DO 11 IT=1,NTF
11    GM0(I,J)=GM0(I,J)  + XNT(I,IT)*XNT(J,IT)
10    GM0(I,J)=GM0(I,J)/FLOAT(NTF)
CC
CC       CALCULATE GM1
      NTF1=NTF-1
      DO 13 I=1,N
      DO 13 J=1,N
      GM1(I,J)=0.
      DO 14 IT=1,NTF1
14    GM1(I,J)=GM1(I,J)+   XNT(I,IT)*XNT(J,IT+1)
13    GM1(I,J)=GM1(I,J)/FLOAT(NTF1)
C     SYMMETRIC MATRIX
      DO 12 I=1,N
      DO 12 J=1,N
12    GM0(J,I)=GM0(I,J)
      WRITE(6,36)
```

```
36      FORMAT(*          MATRIX    GM0*)
        DO 25 I=1,N
        WRITE(7,26)(GM0(I,J),J=1,N)
25      WRITE(6,24)(GM0(I,J),J=1,N)
        WRITE(6,27)
27      FORMAT(*          MATRIX  GM1*)
        DO 28 I=1,N
        WRITE(7,26)(GM1(I,J),J=1,N)
28      WRITE(6,24)(GM1(I,J),J=1,N)
C       CALCULATE INVERSE OF GM0
        CALL MINV(GM00,N,D,LW1,LW2)
        IF((ABS(D)).LT.1.0E-20)WRITE(6,20) D
20      FORMAT(*          VARIANCE OF NT SINGULAR,   DETERNINT=*,E15.5)
        CALL GMTRA(GM11,GM11T,N,N)
        CALL GMPRD(GM11T,GM00,PSI1,N,N,N)
C         CALCULATE ACTUAL AT,S
        DO 18 IT=2,NTF
        DO 18 I=1,N
        GM11(I)=0.
        DO 17 J=1,N
17      GM11(I)=GM11(I) +PSI(I,J)*XNT(J,IT-1)
18      XAT(I,IT)=XNT(I,IT)-GM11(I)
C       ZERO INITIAL AT
        DO 21 I=1,N
21      XAT(I,1)=0.
        WRITE(6,22)
22      FORMAT(//,*                     MATRIX   PSI FOR AR(1)*//)
        DO 23 I=1,N
        WRITE(7,26)(PSI(I,J),J=1,N)
23      WRITE(6,24)(PSI(I,J),J=1,N)
26      FORMAT(7E11.4)
24      FORMAT(1H ,/, 7E12.4)
C*********STORE NEW AT,S
        DO  29 I=1,N
        DO  29 J=1,NTF
29      XNT(I,J)=XAT(I,J)
        RETURN
        END
```

```
$INFO1  DER=  .20,BI=43.5  $
$INFO2  TW=512.  ,GSH=94.0,GSC=18.0   $
$INFO3   COND=1.0,CO=0.0,SS=0.  $
-42.99568   47.98619   -6.68527    2.61727   -1.60883    1.36345   -1.67713    1.00000
-18.27349   14.28639    5.15263   -1.77232    1.05006    -.87704    1.07243    -.63866
  5.21260  -10.55017    2.34937    4.16398   -1.95552    1.51240   -1.79576    1.06310
 -2.63639    4.68812   -5.37940     .50619    4.19076   -2.52631    2.77761   -1.62059
  1.62059   -2.77761    2.52631   -4.19076    -.50619    5.37940   -4.68812    2.63639
 -1.06310    1.79576   -1.51240    1.95552   -4.16398   -2.34937   10.55017   -5.21260
   .63866   -1.07243     .87704   -1.05006    1.77232   -5.15263  -14.28639   18.27349
 -1.00000    1.67713   -1.36345    1.60883   -2.61727    6.68527  -47.98619   42.99568
```

31.1011	-5.8801	-.7527	
19.9393	-7.7318	-1182.3189	
511.5271	532.6612		

513.0	516.9	523.9	528.6	532.1	529.0	527.0	90.0	15.0	10
513.0	517.8	522.0	529.3	530.6	526.0	523.0	90.0	15.0	10
513.0	519.9	526.1	526.6	529.9	528.2	525.0	90.0	15.0	10
517.0	518.7	526.1	530.3	529.4	529.2	527.0	90.0	15.0	10
518.0	514.7	522.1	528.5	530.8	528.8	525.0	90.0	15.0	10
517.0	512.7	523.0	527.9	528.8	527.5	527.0	90.0	15.0	10
516.0	514.8	524.0	525.6	528.1	527.8	525.0	90.0	15.0	10
513.0	516.9	521.4	525.7	530.0	529.6	528.0	90.0	15.0	10
514.0	513.8	520.4	524.6	531.0	528.1	525.0	90.0	18.0	10
517.0	518.6	524.1	527.0	530.7	529.1	527.0	90.0	18.0	10
513.0	517.8	520.4	524.5	529.8	524.9	523.0	90.0	18.0	10
516.0	519.7	524.2	527.1	530.1	530.2	528.0	90.0	18.0	10
518.0	520.6	523.3	530.7	529.4	528.3	525.0	90.0	18.0	10
513.0	516.8	521.1	525.3	532.2	528.4	527.0	90.0	18.0	10
516.0	516.7	523.9	530.3	533.3	530.1	527.0	90.0	18.0	10
515.0	514.7	520.2	523.4	531.9	529.0	527.0	90.0	18.0	10
516.0	513.7	521.8	526.0	528.6	529.9	527.0	90.0	18.0	10
512.0	515.9	521.1	525.5	530.3	527.5	526.0	90.0	18.0	10
512.0	520.9	522.3	528.1	533.6	528.3	527.0	90.0	18.0	10
512.0	516.9	523.6	525.6	533.9	532.0	531.0	90.0	18.0	10
515.0	519.8	521.0	529.8	532.6	531.1	529.0	90.0	18.0	10
515.0	520.7	523.0	530.9	534.4	531.1	528.0	90.0	18.0	10
514.0	517.7	520.1	527.0	532.3	528.5	526.0	90.0	18.0	10
512.0	515.8	521.8	526.3	534.4	532.7	530.0	90.0	18.0	10
511.0	515.9	520.1	526.1	531.9	529.6	527.0	90.0	18.0	10
512.0	517.8	519.2	525.7	533.6	529.0	526.0	90.0	18.0	10
509.0	517.8	518.1	525.8	530.5	529.0	528.0	90.0	18.0	10
511.0	516.8	520.9	527.9	533.9	531.6	529.0	90.0	18.0	10
511.0	521.0	523.3	528.1	536.4	532.4	531.0	90.0	18.0	10
511.0	514.0	524.8	529.8	533.5	533.8	531.0	90.0	18.0	10
509.0	514.9	523.5	526.7	532.7	533.3	531.0	90.0	18.0	10
511.0	515.9	524.0	524.3	532.5	534.9	533.0	90.0	18.0	10
510.0	520.9	523.0	529.8	536.2	531.9	530.0	90.0	18.0	10
512.0	517.9	526.9	531.9	534.3	535.3	533.0	90.0	18.0	10
515.0	517.7	522.2	529.3	531.2	530.0	529.0	90.0	18.0	10
511.0	516.9	525.5	528.5	535.2	531.9	531.0	90.0	18.0	10
511.0	515.9	522.7	531.2	532.4	533.9	531.0	90.0	20.0	10
513.0	516.8	522.8	529.9	536.5	532.9	527.0	90.0	20.0	10
509.0	516.0	525.8	529.8	534.6	535.3	533.0	90.0	20.0	10
512.0	519.9	524.2	530.9	538.0	535.6	533.0	90.0	20.0	10
511.0	515.0	524.5	530.8	540.3	538.9	534.0	90.0	20.0	10
511.0	517.9	525.5	533.0	539.8	541.6	537.0	94.0	19.0	10
512.0	517.8	525.5	532.7	542.1	542.6	537.0	96.0	20.0	10
510.0	514.0	520.7	532.1	540.0	542.9	536.0	104.0	19.0	10
512.0	515.9	524.4	529.0	540.6	543.6	540.0	116.0	20.0	10
509.0	516.9	519.0	527.0	539.9	539.0	538.0	121.0	21.0	10
510.0	515.9	521.2	528.1	536.0	539.5	537.0	128.0	20.0	10

510.0	512.0	520.1	525.5	531.5	534.9	533.0	130.0	20.0	10
512.0	510.8	520.1	525.8	528.9	532.4	531.0	125.0	21.0	10
511.0	514.8	518.6	525.6	526.6	527.6	527.0	114.0	19.0	10
509.0	512.8	515.5	517.8	525.4	525.6	525.0	96.0	21.0	10
506.0	516.0	516.4	516.6	528.3	524.5	522.0	94.0	21.0	10
512.0	512.9	519.2	523.8	526.9	527.6	527.0	90.0	20.0	10
511.0	512.9	521.1	525.6	530.8	529.6	528.0	90.0	20.0	10
512.0	512.9	523.8	530.1	527.8	529.3	527.0	90.0	19.0	10
512.0	515.8	518.9	528.3	534.1	529.4	527.0	90.0	19.0	10
512.0	519.7	522.2	529.1	533.2	530.5	529.0	90.0	20.0	10
512.0	513.8	523.7	525.1	531.8	530.8	527.0	99.0	22.0	10
513.0	516.7	522.4	527.7	537.0	530.3	528.0	94.0	21.0	10
512.0	516.9	522.9	532.7	535.6	533.6	531.0	99.0	22.0	10

MAY 26 FITTED CONTROL MATRICES

MATRIX A (COLUMNS)

.3646E+00	.4625E+00	-.1205E+00	.5922E-01	-.5655E-01	-.2166E-02	.1112E-01
-.1809E+00	.7302E+00	.3588E+00	-.1521E+00	.4187E-01	-.9262E-01	-.7875E-01
.8638E-01	-.1718E+00	.7648E+00	.2810E+00	-.1899E+00	-.3523E-01	-.4388E-01
-.5718E-01	.9669E-01	-.1757E+00	.8042E+00	.2705E+00	-.2328E+00	-.1820E+00
.5385E-01	-.8556E-01	.1295E+00	-.2370E+00	.9243E+00	.4826E+00	.1665E+00
-.6371E-01	.9857E-01	-.1402E+00	.2166E+00	-.4316E+00	.7604E+00	.9833E+00
.3709E-01	-.5709E-01	.8020E-01	-.1207E+00	.2229E+00	-.3010E+00	-.2947E+00

MATRIX B(COLUMNS)

.4176E-01	.1065E+00	.2327E+00	.4552E+00	.7327E+00	.6927E+00	.6344E+00
-.1654E-01	-.4196E-01	-.6212E-01	-.9716E-01	-.1288E+00	-.7073E-01	-.4220E-01

MATRIX L (ROWS)

-.1411E-01	.2809E-01	.1054E+00	.3113E+00	.3687E+00	.3966E-01	.1865E-01
-.1208E+00	-.2059E+00	-.2430E+00	.1618E-01	.2013E+00	-.2425E+00	.6733E-01

MATRIX K (COLUMNS)

.4135E+00	-.3398E-02	-.1642E-02	-.4106E-03	.2754E-02	.2583E-02	-.2639E-02
-.3398E-02	.5008E+00	.5390E-02	-.2524E-02	-.6342E-02	-.8380E-02	.1310E-02
-.1642E-02	.5390E-02	.5069E+00	-.7135E-02	-.9835E-03	-.3171E-02	-.1489E-01
-.4106E-03	-.2524E-02	-.7135E-02	.5126E+00	-.1815E-01	-.2082E-01	.1567E-03
.2754E-02	-.6342E-02	-.9835E-03	-.1815E-01	.5458E+00	.1798E-01	-.3152E-01
.2583E-02	-.8380E-02	-.3171E-02	-.2082E-01	.1798E-01	.4998E+00	.1083E+00
-.2639E-02	.1310E-02	-.1489E-01	.1567E-03	-.3152E-01	.1083E+00	.5081E+00

OPERATING TEMP PROFILE

.5126E+03	.5166E+03	.5225E+03	.5284E+03	.5329E+03	.5317E+03	.5291E+03

MATRIX HI (ROWS)

.3991E-02	.1680E-01	.2795E-01	.4120E-01	.2946E-01	.1575E-01	-.2230E-02
.4783E-02	.1341E-01	.2868E-01	.4712E-01	.5410E-01	.2227E-01	-.3458E-05
.1860E-02	.5760E-02	.8573E-02	.1053E-01	.8599E-02	.3941E-02	-.1474E-03

MATRIX CI (COL 1 +COL 2)

.1291	.1495	.06125	-0.04707	-.05548	-.02210

DYNAMIC DATA SEP 23 (TEMPERATURES +CONCENTRATIONS)

AXIAL TEMPS T1 - T7 , UH2 , UC4 (CC/SEC)

523.0	524.4	532.6	538.6	539.0	536.6	534.0	97.0	18.0	1
524.0	525.3	530.8	540.0	540.0	536.7	533.0	90.0	18.0	2
524.0	528.4	533.1	544.0	541.2	537.0	534.0	92.0	18.0	3
523.0	526.4	531.9	542.5	543.8	536.8	534.0	90.0	18.0	4
525.0	525.4	535.8	546.1	544.9	541.2	537.0	95.0	18.0	5
523.0	526.4	533.5	543.5	546.3	538.0	533.0	90.0	18.0	6
523.0	525.4	533.4	544.4	546.1	538.0	533.0	96.0	18.0	7
524.0	528.4	535.5	547.2	548.9	539.9	535.0	100.0	18.0	8
522.0	527.4	534.7	541.8	547.6	538.9	534.0	98.0	18.0	9
525.0	526.2	533.6	545.2	547.5	539.5	534.0	98.0	18.0	10
525.0	526.4	535.4	545.5	549.1	543.1	538.0	101.0	18.0	11
521.0	527.4	533.8	542.9	545.6	541.3	536.0	96.0	18.0	12
523.0	527.3	531.9	544.2	546.2	541.2	536.0	95.0	18.0	13
520.0	529.5	532.9	542.4	547.0	542.5	540.0	96.0	18.0	14
523.0	527.4	532.8	542.4	547.0	541.0	537.0	92.0	18.0	15
521.0	525.4	530.8	542.3	545.0	539.1	534.0	90.0	16.0	16
519.0	525.6	532.9	542.7	545.0	540.1	536.0	91.0	16.0	17
524.0	526.3	531.9	539.6	546.2	539.0	534.0	90.0	17.0	18
522.0	526.4	531.8	541.6	544.3	540.2	536.0	91.0	20.0	19
521.0	526.4	531.9	542.5	545.3	540.2	535.0	90.0	18.0	20
523.0	527.4	532.8	542.4	546.1	538.8	536.0	94.0	18.0	21
522.0	526.4	534.7	543.9	545.4	539.5	536.0	91.0	16.0	22
524.0	525.3	531.7	543.2	546.0	540.6	536.0	90.0	16.0	23
526.0	529.2	534.8	545.3	546.9	538.4	534.0	92.0	16.0	24
525.0	528.4	531.9	541.4	546.3	539.6	534.0	91.0	15.0	25
524.0	529.3	532.1	543.4	544.9	539.1	534.0	89.0	15.0	26
524.0	527.4	532.0	543.3	545.7	539.6	535.0	89.0	17.0	27
524.0	524.4	532.8	542.8	543.9	539.6	536.0	90.0	16.0	28
525.0	527.3	532.0	541.6	544.5	538.0	534.0	89.0	16.0	29
525.0	528.3	532.0	543.5	543.5	537.6	533.0	89.0	16.0	30
522.0	527.4	534.0	540.4	543.3	539.2	535.0	89.0	16.0	31
524.0	526.3	531.9	540.9	543.0	538.1	534.0	91.0	20.0	32
522.0	527.4	533.7	544.8	543.3	539.0	536.0	93.0	22.0	33
521.0	525.5	536.4	545.2	544.4	539.1	535.0	96.0	19.0	34
525.0	527.3	534.4	548.0	548.5	541.1	535.0	106.0	19.0	35
523.0	527.3	536.4	546.6	549.0	543.1	538.0	103.0	18.0	36
520.0	524.4	532.5	544.8	549.8	541.5	536.0	108.0	18.0	37
525.0	526.2	532.8	544.1	549.0	542.1	537.0	111.0	18.0	38
522.0	525.3	530.0	539.3	546.5	540.1	535.0	102.0	16.0	39
525.0	527.1	531.0	540.5	545.3	539.6	535.0	95.0	17.0	40
523.0	526.3	530.3	539.6	544.2	539.6	536.0	89.0	17.0	41
524.0	528.4	533.4	540.4	543.1	541.8	538.0	86.0	16.0	42
522.0	526.5	535.0	542.5	542.8	540.9	536.0	84.0	16.0	43
523.0	525.3	530.8	540.5	543.8	538.0	534.0	85.0	16.0	44
523.0	528.4	535.0	543.1	544.6	539.0	535.0	84.0	16.0	45
523.0	526.4	532.7	541.8	543.1	536.9	534.0	84.0	16.0	46

520.0	524.6	534.6	542.4	542.5	539.3	534.0	85.0	17.0	47
525.0	526.4	534.6	546.6	545.0	538.5	534.0	92.0	17.0	48
523.0	526.5	535.6	546.9	544.2	539.6	536.0	96.0	17.0	49
522.0	526.4	534.4	546.4	546.2	539.0	534.0	96.0	18.0	50
522.0	526.3	532.8	546.3	544.8	538.0	534.0	97.0	18.0	51
520.0	524.3	529.7	541.3	542.3	536.9	534.0	91.0	20.0	52
523.0	527.2	531.7	546.0	545.1	539.0	535.0	95.0	22.0	53
524.0	528.3	533.8	546.0	549.9	542.6	537.0	102.0	22.0	54
526.0	527.2	534.5	549.3	554.8	545.6	539.0	115.0	21.0	55
524.0	528.4	533.7	546.2	556.6	547.6	541.0	119.0	19.0	56
522.0	526.4	530.8	544.3	552.4	544.1	538.0	119.0	17.0	57
520.0	526.3	531.0	539.6	546.8	543.9	538.0	117.0	17.0	58
521.0	524.3	529.9	538.8	543.9	543.0	538.0	112.0	17.0	59
522.0	522.4	528.1	537.6	541.7	540.6	539.0	97.0	20.0	60
523.0	524.3	530.1	540.1	539.7	539.3	536.0	89.0	18.0	61
522.0	526.4	530.3	537.1	541.5	538.6	536.0	87.0	18.0	62
521.0	526.4	532.2	539.5	540.1	537.6	535.0	86.0	16.0	63
521.0	526.5	534.6	540.7	539.9	538.1	536.0	85.0	16.0	64
521.0	525.5	533.8	543.3	540.7	537.2	533.0	86.0	16.0	65
522.0	525.5	534.6	541.4	542.6	537.5	534.0	86.0	15.0	66
522.0	527.4	534.8	543.3	542.7	538.1	534.0	84.0	15.0	67
523.0	526.3	534.5	543.3	541.8	537.2	532.0	84.0	17.0	68
521.0	525.5	532.6	541.9	542.3	536.0	532.0	85.0	16.0	69
525.0	525.3	533.5	544.6	544.8	538.2	532.0	91.0	16.0	70
523.0	524.4	533.6	544.8	542.2	537.6	534.0	93.0	16.0	71
525.0	526.3	532.7	541.8	543.1	536.9	534.0	87.0	16.0	72
524.0	526.2	530.7	541.4	544.0	536.7	530.0	86.0	20.0	73
524.0	525.4	533.6	545.2	547.2	539.4	535.0	92.0	22.0	74
524.0	527.4	533.7	547.6	550.8	539.4	533.0	101.0	19.0	75
525.0	526.3	533.5	549.1	553.7	542.8	538.0	116.0	19.0	76
524.0	524.2	533.4	543.0	551.3	541.7	538.0	117.0	18.0	77
523.0	523.2	532.5	539.6	548.7	543.0	539.0	113.0	18.0	78
524.0	524.2	529.7	538.3	547.2	542.7	538.0	108.0	18.0	79
524.0	524.2	530.2	538.9	544.1	544.0	539.0	109.0	16.0	80
523.0	525.2	527.2	535.8	540.6	538.9	534.0	97.0	17.0	81
522.0	522.5	532.1	535.9	540.0	537.7	534.0	84.0	17.0	82
521.0	524.4	530.2	535.8	536.9	535.8	532.0	84.0	16.0	83
520.0	523.6	531.9	535.3	535.8	535.8	533.0	84.0	16.0	84
522.0	525.4	530.0	539.0	539.0	536.1	533.0	85.0	16.0	85
524.0	528.3	530.2	540.9	538.5	534.1	530.0	84.0	16.0	86
522.0	527.4	532.1	540.2	540.2	535.0	532.0	84.0	16.0	87
521.0	525.5	533.9	539.8	539.7	535.6	532.0	85.0	17.0	88
521.0	526.3	531.7	540.2	539.1	533.0	529.0	90.0	17.0	89
525.0	526.3	533.7	543.0	541.5	534.8	532.0	89.0	17.0	90
526.0	528.3	531.8	546.2	543.1	537.6	533.0	91.0	18.0	91
525.0	526.2	533.5	543.6	544.2	535.2	532.0	89.0	18.0	92
525.0	528.4	534.6	547.3	545.2	537.3	534.0	100.0	20.0	93
524.0	527.3	536.5	548.4	548.4	538.9	534.0	106.0	22.0	94
524.0	524.3	532.3	546.7	548.1	540.0	535.0	109.0	22.0	95
526.0	527.3	535.4	549.5	553.1	543.4	538.0	119.0	21.0	96

523.0	526.4	533.6	544.7	553.4	544.6	538.0	119.0	19.0	97
522.0	525.4	529.8	540.6	551.2	544.2	538.0	112.0	17.0	98
523.0	525.2	528.8	539.1	546.6	542.4	536.0	110.0	17.0	99
523.0	524.3	530.1	537.9	544.3	544.0	539.0	110.0	17.0	100

MOLE FRACTIONS C4, H2, C3, C2

136.	811.	14.	0.	1
133.	805.	18.	0.	2
135.	802.	17.	0.	3
151.	773.	21.	0.	4
121.	827.	15.	0.	5
129.	811.	17.	0.	6
126.	831.	13.	0.	7
133.	800.	20.	0.	8
128.	814.	16.	0.	9
133.	811.	15.	0.	10
143.	794.	18.	0.	11
127.	812.	19.	0.	12
154.	753.	24.	0.	13
129.	836.	10.	0.	14
135.	808.	18.	0.	15
136.	789.	19.	0.	16
123.	838.	10.	0.	17
142.	796.	18.	0.	18

SEP 23 FITTED CONTROL MATRICES

MATRIX A (COLUMNS)

.1871E+00	.2559E+00	-.7925E-01	.5104E-01	-.3824E-01	.5256E-02	.1604E-01
-.9739E-01	.4330E+00	.2346E+00	-.1120E+00	.4683E-01	-.3535E-01	-.3182E-01
.5139E-01	-.1110E+00	.5639E+00	.2412E+00	-.1313E+00	.1342E-01	.8155E-02
-.4127E-01	.7539E-01	-.1528E+00	.8150E+00	.2857E+00	-.1357E+00	-.9017E-01
.3884E-01	-.6659E-01	.1121E+00	-.2380E+00	.9144E+00	.4639E+00	.1723E+00
-.4325E-01	.7236E-01	-.1146E+00	.2072E+00	-.3897E+00	.6470E+00	.8338E+00
.2504E-01	-.4169E-01	.6527E-01	-.1149E+00	.2002E+00	-.2542E+00	-.2464E+00

MATRIX B(COLUMNS)

.1957E-01	.5133E-01	.1292E+00	.4321E+00	.6755E+00	.4900E+00	.4212E+00
-.9986E-02	-.2444E-01	-.4145E-01	-.9468E-01	-.1045E+00	-.4814E-01	-.3151E-01

MATRIX L (ROWS)

.1268E-01	.3750E-01	.1175E+00	.3419E+00	.3538E+00	.5323E-01	.1509E-01
-.2804E-01	-.6498E-01	-.1044E+00	.3107E-01	.8942E-01	-.1183E+00	.3623E-01

MATRIX K (COLUMNS)

.3927E+00	-.2191E-02	.1797E-02	-.3747E-02	.3318E-02	.9506E-03	-.2082E-02
-.2191E-02	.4264E+00	-.2066E-02	.5469E-02	-.5616E-02	-.2651E-02	.3253E-02
.1797E-02	-.2066E-02	.4498E+00	-.1124E-01	.5323E-02	.2252E-02	-.6828E-02
-.3747E-02	.5469E-02	-.1124E-01	.5082E+00	-.1028E-01	-.1437E-01	.4750E-02
.3318E-02	-.5616E-02	.5323E-02	-.1028E-01	.5391E+00	.2378E-01	-.2014E-01
.9506E-03	-.2651E-02	.2252E-02	-.1437E-01	.2378E-01	.4787E+00	.8641E-01
-.2082E-02	.3253E-02	-.6828E-02	.4750E-02	-.2014E-01	.8641E-01	.4809E+00

OPERATING TEMP PROFILE

.5229E+03	.5266E+03	.5335E+03	.5417E+03	.5436E+03	.5387E+03	.5364E+03

MATRIX HI (ROWS)

.1638E-02	.5577E-02	.1202E-01	.2299E-01	.1728E-01	.5750E-02	-.2627E-03
.2186E-02	.5048E-02	.1468E-01	.3375E-01	.3656E-01	.1039E-01	.4950E-03
.6542E-03	.1625E-02	.2950E-02	.4184E-02	.3743E-02	.1411E-02	.2341E-04

MATRIX CI (COL 1 +COL 2)

.6873E-01	.9864E-01	.2850E-01	-.2359E-01	-.3374E-01	-.9767E-02

Typical Correlation Matrices (R) for Parameter Estimates

26 May Data (linearisation about average profile, Figure 17)

$$R = \begin{array}{c} \\ k/k_o \\ \\ \lambda_o \end{array} \begin{bmatrix} 1.0 & & \\ & & \\ 0.813 & 1.0 & \end{bmatrix}$$

26 May Data (linearisation about steady state, Figure 18)

$$R = \begin{array}{c} \beta_1 \\ \beta_2 \\ \beta_3 \end{array} \begin{bmatrix} 1.0 & & \\ -.895 & 1.0 & \\ -.817 & .986 & 1.0 \end{bmatrix}$$

$\beta_1 = 2\ k/k_o$

$\beta_2 = 2\ k/k_o - \lambda_o$

$\beta_3 = \alpha$

23 September Data (linearisation about average profile, Figure 20)

$$R = \begin{array}{c} k/k_o \\ \lambda_o \\ D_{er} \end{array} \begin{bmatrix} 1.0 & & \\ .029 & 1.0 & \\ .355 & -.026 & 1.0 \end{bmatrix}$$